A COMPARISON STUDY OF THE PROTEINS AND EXTRACELLULAR VESICLES SECRETED BY UVEAL MELANOMA CELLS

Thesis submitted in accordance with the requirements of the University of Liverpool for the degree of Doctor of Philosophy

by

SAMUEL J. PRENDERGAST

February 2020

ACKNOWLEDGEMENTS

First and foremost, the highest praise and gratitude goes to Abby for her support and patience during this period of our lives together. You have been an absolute rock for me during this PhD and in particular throughout my write up and revisions. You have supported me, encouraged me, complained with me, rejoiced with me and cried with me. I love you and cannot wait to continue with the next phase of our lives together. I would also like to thank my family for their boundless love and support. In particular my parents Claire and Michael, who have been there for me through all the highs and lows of my life. I love you both and cannot thank you enough for all you do for me.

A big thank you goes to my supervisors, Professor Sarah Coupland and Dr Helen Kalirai for their help and guidance through this PhD. You have taught me so much over the years and your patience has been unending. I'm sure I have not been the easiest student to work with and I am very grateful to both of you for having the strength to put up with me. I would also like to thank the rest of the LOORG group; it has been a difficult four years and your collective support, empathy and comedy have made it far easier.

Many other members of the University of Liverpool have helped with this research and deserve thanks: Mr Simon Bidolph for his help with histological staining, Miss Alison Becket for her training and support with transmission electron microscopy, Dr Deborah Simpson and Professor Rob Beynon for their help and support with the LC-MS/MS and proteomic analysis, Dr Dean Hammond for his help with the bioinformatic analyses of the data and Professor Azzam Taktak for his help with the statistical analyses.

Thank you all.

FUNDING DECLARATION

This research was funded by the Pathological Society, with additional funding from the Eye Tumour Research Fund and the North West Cancer Research Centre towards equipment and allowing this work to be presented at the 2015 NCRI conference and the 2016 and 2017 Ocular Oncology Group meetings.

ABSTRACT

Uveal melanoma (UM) is the most common intraocular malignancy in adults and approximately 50% of UM patients will develop refractory metastases. Metastatic UM (MUM) commonly involves the liver, yet the mechanism of this progression is still poorly understood. The research herein studies the level and pattern of hepatic fibrosis in MUM and investigates the biological functions and signalling pathways associated with the UM secreted proteome and the proteome of extracellular vesicles (EVs) released by UM.

Histological and immunohistochemical analysis of MUM samples demonstrated fibrotic extracellular matrix (ECM) deposition in 100% of cases and this was concomitant with hepatic stellate cell (HSC) activation in 86% of cases. Neither the pattern nor the extent of fibrosis were associated with any assessed genetic feature of the tumour. The research presented compared the secreted proteome of normal choroidal melanocytes (NCM) with that of patient-derived UM cells at high or low risk of metastatic progression. This highlighted an association between UM secreted proteins and cell growth, adhesion and migration. Pathway analysis identified mTOR, Rho GTPase and HSC activation signalling through the UM secretome. Further analysis suggested that these functions/pathways were upregulated in UM compared with NCMs and in HR-UM compared with LR-UM. As a large number of proteins in the UM secretome were predicted to be of EV origin, methods were developed for the isolation and characterisation of UM small exosome-like EVs. These EVs were in the size range of exosomes and demonstrated the characteristic 'cup-shaped' morphology. UM EV proteomes were associated with mTOR, Rho GTPase and integrin signalling, similar to results presented earlier in this Thesis. Analysis suggested that these functions/pathways were downregulated in MUM compared with PUM and were upregulated in *GNA11*-mutant UM EVs compared with those from *GNAQ*-mutant UM.

The research herein provides the rationale for further investigation into UM EV signalling and its role in promoting metastatic progression. The roles of mTOR, Rho GTPase and integrin signalling networks have previously shown importance in UM. The present research suggests that these mechanisms may be governed through intercellular signalling via secreted proteins and EVs.

CONTENTS

LIST OF TABLES

LIST OF FIGURES

Figure 4.7. The top 15 canonical signalling pathways associated with the 539-protein dataset (inverse log10 p-values ≥2) and differentially expressed between the uveal melanoma and normal choroidal melanocyte secretomes (z-scores ≥2 or ≤-2)

Figure 4.8. The ten most differentially expressed Disease and Bio Functions associated with the 539-protein dataset (z-scores ≥2 or ≤-2; inverse log10 p-values ≥2) between the secretomes of uveal melanoma at high and low risk of metastasis

Figure 4.9. The most differentially expressed canonical pathways associated with the 539-protein dataset (z-scores ≥2 or ≤-2; inverse log10 p-values ≥2) between the secretomes of uveal melanoma at high and low risk of metastasis

Figure 4.10. The most differentially expressed Diseases and Bio Functions associated with the 758-protein dataset (z-scores ≥2 or ≤-2; inverse log10 p-values ≥2) between uveal melanoma and normal choroidal melanocyte secretomes

Figure 4.11. The ten Diseases and Bio Functions showing the highest association with the 758-protein dataset, when comparing the uveal melanoma and normal choroidal melanocyte secretomes

Figure 4.12. The top canonical pathways associated with the 758-protein dataset (inverse log10 p-values ≥2) and differentially between the uveal melanoma and normal choroidal melanocyte secretomes (z-score ≥2 or ≤-2)

Figure 4.13. The ten canonical pathways with the highest association to the 758-protein dataset when comparing the uveal melanoma and normal choroidal melanocyte secretomes

Figure 4.14. The fifteen Diseases and Bio Functions with the highest association to the 758-protein dataset when comparing the secretome of uveal melanoma at high and low risk of metastasis

representative of n = 5; remaining CD63 blots represent n = 3; all other blots were performed only once n = 1

Figure 6.1. (A) Mean normalised abundance values of UM exosomal proteins were ranked and plotted in ascending order, each point represents a single protein. All analyses are scaled to the same axis limits for number of proteins and for abundance, to aid comparison between samples. (B) The mean normalised abundance was standardised and pairwise comparisons was performed displaying comparative plots, histograms demonstrating normality and Pearson's statistic of correlation (X92.1 in this panel represent the 92.1 cell line)

Figure 6.2. Hierarchical clustering of UM exosomal proteomic profiles, comparing six UM cell lines each with three biological replicates. Normalised protein abundances were log transformed and plotted with the R package "pheatmap"

Figure 6.3. Gene ontology term clustering assessed with the online freeware ReviGO. Colour indicates the GOrilla generated q-value; size indicates the frequency of the gene ontology term in the underlying gene ontology annotation database (bubbles of more general terms are larger)

Figure 6.4. The Disease and Bio Functions most associated with the uveal melanoma extracellular vesicle proteome (inverse log10 p-values ≥2)

Figure 6.5. The Canonical Pathways most associated with the uveal melanoma extracellular vesicle proteome (inverse log10 p-values ≥2)

Figure 6.6. The upstream regulators most associated with the uveal melanoma extracellular vesicle proteome (inverse log10 p-values ≥2)

Figure 6.7. The disease and bio functions most differentially associated between the extracellular vesicle proteomes from metastatic and primary uveal melanoma cell lines (inverse log10 p-values ≥2; z-scores ≥2 or ≤-2)

Figure 6.8. The canonical pathways most differentially associated between the extracellular vesicle proteomes from metastatic and primary uveal melanoma cell lines (inverse log10 p-values ≥2; z-scores ≥2 or ≤-2)

Figure 6.9. The upstream regulators most differentially associated between the extracellular vesicle proteomes from metastatic and primary uveal melanoma cell lines (inverse log10 p-values ≥2; z-scores ≥2 or ≤-2)

Figure 6.10. The 20 most differentially associated disease and bio functions between the extracellular vesicle proteomes from GNA11-mutant and GNAQ-mutant uveal melanoma (inverse log10 p-values ≥2; z-scores ≥2 or ≤-2)

Figure 6.11. The 20 most differentially associated disease and bio functions between the extracellular vesicle proteomes from GNA11-mutant and GNAQ-mutant uveal melanoma (inverse log10 p-values ≥2; z-scores ≥2 or ≤-2). The categories “Infectious disease” and “Infectious disease, organismal injury” were removed for this analysis.

Figure 6.12. The 20 most differentially associated canonical pathways between the extracellular vesicle proteomes from GNA11-mutant and GNAQ-mutant uveal melanoma (inverse log10 p-values ≥2; z-scores ≥2 or ≤-2)

Figure 6.13. The 20 most differentially associated upstream regulators between the extracellular vesicle proteomes from GNA11-mutant and GNAQ-mutant uveal melanoma (inverse log10 p-values ≥2; z-scores ≥2 or ≤-2)

Figure 6.14. The overlap between the proteomic profiles of the predicted extracellular vesicle fraction of the secretome and of isolated extracellular vesicles.

Figure 6.15. The 20 most differentially associated canonical pathways between the UM secretome and uveal melanoma extracellular vesicles

Figure 6.16. Schematic overview of the mTOR signalling pathway associated with the uveal melanoma extracellular vesicle proteome. Those molecules apparent in the proteome are

highlighted pink; the density of the red colour indicates the relative abundance in the dataset

Figure 6.17. The Rho Family GTPase signalling pathway associated with the uveal melanoma extracellular vesicle proteome. Those molecules apparent in the proteome are highlighted pink; the density of the red colour indicates the relative abundance in the dataset

Figure 6 18. The primary network of signalling pathways potentiated by extracellular vesicles from uveal melanoma.

LIST OF ABBREVIATIONS

AB	Apoptotic body
AC	Affinity capture
AFM	Atomic force microscopy
AMOTL2	Angiomotin like 2
ANXA2	Annexin A2
ARF6	ADP-ribosylation factor 6
BAP1	BRCA1-associated protein 1 gene
CAF	Cancer associated fibroblast
CANX	Calnexin
CD163	Cluster differentiation 163
CD3	Cluster differentiation 3
CD4	Cluster differentiation 4
CD63	Cluster differentiation 63
CD68	Cluster differentiation 68
CD8	Cluster differentiation 8
CD81	Cluster differentiation 81
CD9	Cluster differentiation 9
CDC42	Cell division control protein 42 homolog
CDK5	Cell division protein kinase 5
CLIC	Chloride intracellular channel
CLL	Chronic lymphocytic leukemia
COMS	Collective ocular melanoma study
DLS	Dynamic light scattering
DNA	Deoxyribonucleic acid
DTT	Dithiothreitol
ECM	Extracellular matrix
EDTA	Ethylenediaminetetraacetic acid
EE	Early endosome
EGF	Epidermal growth factor
EGF	epidermal growth factor
EGFR	epidermal growth factor receptor
EIF1AX	Eukaryotic translation initiation factor 1A, X-chromosomal
EIF2	Eukaryotic translation initiation 2
eIF4	Eukaryotic translation initiation 4
ERBB2	Human homologue of avian erythroblastosis oncogene B
ERK	Extracellular-signal-regulated kinase
EV	Extracellular vesicle
FABP3	Fatty acid binding protein 3
FGF2	Fibroblast growth factor 2
FISH	Fluorescence in situ hybridisation
FOXM1	Forkhead box protein M1

GEEC	Glycosylphosphotidylinositol-anchored protein enriched compartments
GNA11	Guanine nucleotide-binding protein subunit alpha-11
GNA12	G Protein Subunit Alpha 12
GNAQ	Guanine nucleotide-binding protein subunit alpha-Q
GO	Gene ontology
GP6	Glycoprotein VI
GRAF1	GTPase regulator associated with focal adhesion kinase 1
GTP	Guanosine triphosphate
HIF1A	hypoxia inducible factor 1 alpha
HR	High risk
HSC	Hepatic stellate cell
HSP 27	Heat shock protein 27
HSP90	Heat shock protein 90
HSP90B1	Heat Shock Protein 90 Beta Family Member 1
IAC	Immunoaffinity capture
IGF-1	Insulin-like growth factor 1
IL-6	Interleukin 6
IL-8	Interleukin 8
ILK	Integrin-linked protein kinase
ILV	Intraluminal vesicle
IPA	Ingenuity pathway analysis
LBD	Largest basal diameter
LC-MS/MS	Liquid chromatography tandem mass spectrometry
LDL	Low-density lipoprotein
LE	Late endosome
LOORG	Liverpool ocular oncology group
LR	Low risk
LXR	Liver X receptor
MAPK	Mitogen-activated protein kinase
MEK	MAPK/ERK kinase
MHC	Major histocompatability
MITF	Melanogenesis associated transcription factor
MLPA	Multiplex ligation probe amplification
MMP12	Matrix metalloprotease
mRNA	Messenger ribonucleic acid
MSA	Microsatellite analysis
MSA	Mass spectrometry
mTOR	Mammalian target of rapamycin
mTORC1	Mammalian target of rapamycin complex 1
mTORC2	Mammalian target of rapamycin complex 2
MUM	Metastatic uveal melanoma
MV	Microvesicle
MVB	Multivesicular body

MYC	Myelocytomatosis protein
NCM	Normal choroidal melanocyte
NF-kB	Nuclear factor kappa-light-chain-enhancer of activated B cells
NN	Neural network
NRF2	Nuclear factor (erythroid-derived 2)-like 2
NTA	Nanoparticle tracking analysis
OOB	Ocular oncology biobank
p70S6K	Ribosomal protein S6 kinase beta-1
PAGE	Polyacrylamide gel electrophoresis
PAS	Periodic acid Schiff
PBR	Proton beam radiation
PDGF	Platelet-derived growth factor
PGR	progesterone receptor
PI3K	Phosphatidylinositol-4,5-bisphosphate 3-kinase
PP	Polymeric precipitation
PPARα	Peroxisome proliferator-activated receptor alpha
PTEN	Phosphatase and tensin homolog
PUM	Primary uveal melanoma
PWM	Position weighted matrices
Rac1	Ras-related C3 botulinum toxin substrate 1
RAF	Rapidly accelerated fibrosarcoma protein
RhoA	Ras homolog gene family, member A
RhoGDI	Rho GDP-dissociation inhibitor
RLUH	Royal Liverpool university hospital
ROS	Reactive oxygen species
RPMI	Roswell park memorial institute medium
RXR	Retinoid X receptor
SDS	Sodium dodecyl sulphate
SE	Size exclusion
SEM	Scanning electron microscopy
SF3B1	Splicing factor 3B subunit 1
SILAC	Stable isotope labelling of amino acids in cell culture
SMARCA4	SWI/SNF Related, Matrix Associated, Actin Dependent Regulator Of Chromatin, Subfamily A, Member 4
SPDEF	SAM pointed domain-containing Ets transcription factor
STR	Short Tandem Repeat
SYVN1	Synovial 1
TAZ	Tafazzin
TBS	Tris buffered saline
TEM	Transmission electron microscopy
TFA	Trifluoroacetic acid
TFEB	Transcription factor EB
TGFβ1	Transforming growth factor beta
TNM	Tumour-node-metastasis

TPI1	Triosephosphate isomerase
TRIO	Triple functional domain protein
tRNA	Transfer riboxynucleic acid
TSG101	Tumour suppressor gene 101
UC	Differential ultracentrifugation
UM	Uveal melanoma
v/v	volume per volume
w/v	weight per volume
YAP	Yes-associated protein
αSMA	Alpha smooth muscle actin

CHAPTER 1: INTRODUCTION

1.1. Uveal melanoma epidemiology and incidence

The uveal tract is the middle layer of the eye and is comprised of the choroid, ciliary body and iris in one continuous structure (Millodot, 2014) (Figure 1.1). Within the uveal tract are stromal melanocytes (Cummings, 2013), which are thought to undergo malignant transformation to give rise to uveal melanoma (UM). Greater than 90% of all UM occur in the choroid, the remainder arising in the iris or ciliary body (Coupland, Lake and Damato, 2014).

UM is the most common intraocular malignancy in adults (Coupland, Lake and Damato, 2014); the reported incidence of UM varies around the world, most estimates suggest between three and ten persons per million per year (Singh, Turell and Topham, 2011). In 2012, Keenan *et al.,* reported that the national incidence in England had remained steady over the prior decade, with estimates of ten persons per million per year (Keenan, Yeates and Goldacre, 2012).

UM is more prevalent in Caucasians (Singh, Turell and Topham, 2011) with significant risk factors including fair skin, light eye colour, cutaneous freckles and a propensity to sunburn, among others (Nayman *et al.*, 2017). Unlike cutaneous melanoma, however, UM does not appear to be associated with an ultra-violet (UV) induced mutational signature (De Lange *et al.*, 2015). UM has a peak incidence between 60 and 80 years of age (Keenan, Yeates and Goldacre, 2012). Recent reports have indicated a rare familial predisposition to UM (Canning and Hungerford, 1988), which is linked to germ-line BRCA1-associated protein 1 gene (*BAP1)* mutations (Abdel-Rahman *et al.*, 2011); the role of *BAP1* in UM is discussed in more detail in Section 1.8.2.

(A)

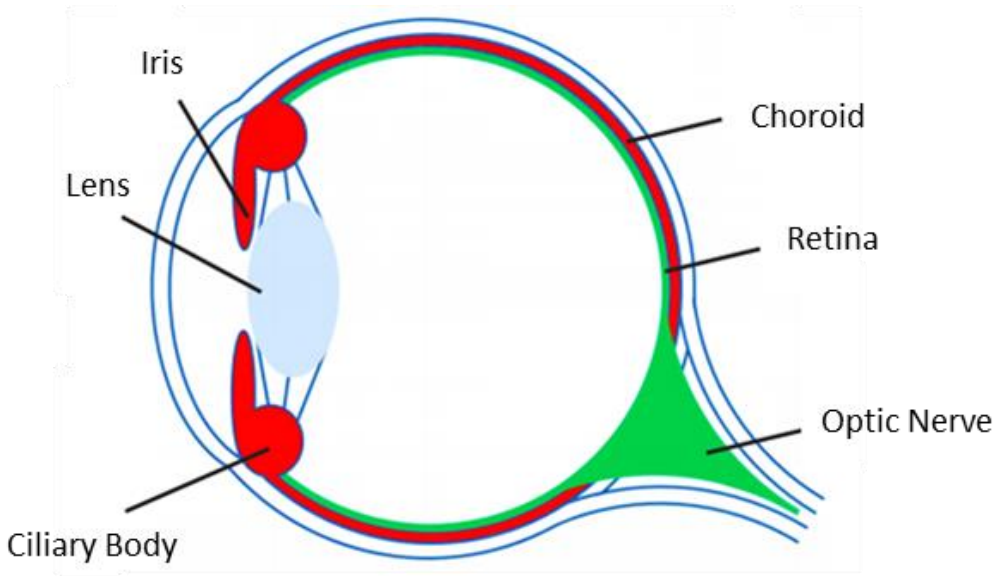

(B)

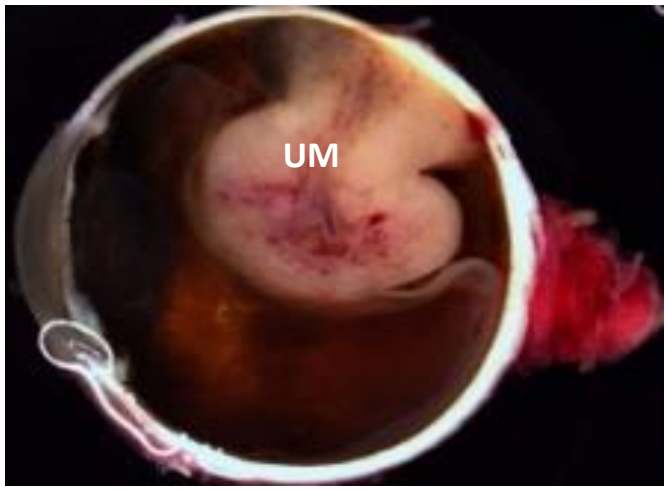

Figure 1.1. Schematic representation of the structure of the uvea (red) in the human eye (A) and a macroscopic photograph of an enucleated eye with a mushroom-shaped melanoma arising from the choroid (B)

UM, uveal melanoma (Courtesy of Prof. S Coupland).

1.2. Diagnosis of uveal melanoma

The diagnosis of UM is often difficult: the tumour presents without major symptoms in approximately 30% of patients, and an additional 20% of symptomatic patients report delayed diagnosis (Damato, 2001). Early stage tumours are most commonly noticed when they arise in the iris as they present with a discolouring or deforming of the pupil. However, as iris melanomas represent <5% of UM (Shields *et al.*, 2012), most early-stage UM are detected during routine eye checks (Damato, 2001). The diagnosis of UM often depends on tumour location: those developing in the anterior or posterior segments of the eye are easier to detect than those arising within the ciliary body (Damato, 2001). Larger UM cause symptoms such as blurred vision, photopsia, central shadow in the visual field, 'floaters' and metamorphosia (Ah-Fat and Damato, 1998).

1.3. Treatment of Primary uveal melanoma

Treatment choices for primary UM (PUM) have remained consistent for many years due to their effectiveness; treatments include radiotherapy (brachytherapy or proton beam), local tumour resection, endoresection or enucleation (i.e. removal of the eye) with prosthesis fitting. The choice of treatment is dependent on the location and size of the UM, as well as the patients' preferences.

Brachytherapy was first performed for UM treatment by Moore in 1930 and involved implanting a radon "seed" into the tumour (Moore, 1930). The treatment has evolved and now involves attaching a small disc shaped irradiation source (either iodine-125 or ruthenium) to the outside of the eye (sclera) adjacent to where the internal tumour is located. Ruthenium plaques are now the most widely employed treatment of UM (Simpson *et al.*, 2014). This low energy radiation allows for localised treatment of the UM, yet as the

radiation emanates from the plaque it can also affect the surrounding normal ocular tissue. Loss of vision is a common post-treatment side effect when treating juxta-foveal PUM and tumours occurring close to the optic disc. This loss of vision is thought to be predominantly due to foveal radiation retinopathy and, while a variety of 'notched' plaques have been developed to try to limit this effect, it represents a major limitation of brachytherapy in these patients (Cruess *et al.*, 1984).

Proton beam radiotherapy (PBR) is reported to have several advantages over brachytherapy, including the specificity at which the dose can be delivered, the homogeneity of the dose and limited effect on surrounding normal ocular and periocular tissue (Damato *et al.*, 2005). PBR employs the radioactive properties of protons by aiming a collimated beam through the pupil towards the tumour. The radiotherapy is not discharged until the point at which the protons slow down and stop, known as the 'Bragg Peak', which can be manipulated to be directly in the tumour. PBR is a slightly more aggressive treatment than plaque radiotherapy and can be more effective against the PUM; however, as the radiation also has to go through the front of the eye several additional side effects are associated with this treatment including dry eye, loss of eyelashes, corneal neovascularisation and, possibly later in life, glaucoma and cataracts (Damato, 2012a).

Endoresection was originally described by Damato *et al*., in 1998 and is a method of surgically removing the PUM while conserving the eye. Briefly, after total vitrectomy the retina is separated above the tumour, the UM is then surgically removed along with immediately adjacent normal choroid to reduce the risk of recurrence and the retina is re-attached. If histology of the removed tumour reveals a higher chance of recurrence, brachytherapy may also be applied post operatively (Damato *et al.*, 1998). Endoresection is

a useful alternative to radiotherapy for tumours close to the optic nerve or fovea and also has a reduced risk of neovascular glaucoma (Cassoux *et al.*, 2013).

Local resection (also termed exoresection or lamellar sclera-uvectomy) was first described by Damato and Foulds (Damato and Foulds, 1996), and is undertaken in only a few ocular oncology centres. It involves creating a lamellar flap in the sclera above the location of the tumour, removing the tumour and replacing the flap and placing a ruthenium plaque. This is often the surgery of choice by UM patients who wish to preserve the eye, and in cases where the tumour is anterior to the equator (Damato, 2012b). It must be noted, however, that the operation is performed under hypotension, and therefore can only be undertaken in fit patients.

For larger PUM, or for tumours involving the ciliary body, “enucleation” (removal of the eye) is the most common treatment. Although it is the more radical procedure, enucleation is a well-established surgical procedure and is associated with very few post-operative complications. Following enucleation, the affected orbit is fitted with a prosthesis and the extraocular muscles reattached, allowing often for a good cosmetic result. Reports concerning the mental wellbeing of monocular patients include self-reported depression, a need for professional counselling, loss of self-esteem, and decreased participation in social events (Coday *et al.*, 2002; Hope-Stone *et al.*, 2015).

1.4. Local recurrence of uveal melanoma

Current conservative treatments for the control of local UM can be considered successful due to reduced rates of local recurrence. A recent meta-analysis demonstrated limited local recurrence rates with both brachytherapy (weighted average of 4.0–9.6%) and PBR (weighted average of 4.2%) (Chang and McCannel, 2013). Endoresection alone also demonstrated effective local control (4.6%) (Chang and McCannel, 2013).

1.5. Metastatic risk in uveal melanoma

Despite the success of local UM control, approximately 50% of UM patients progress to develop metastatic disease (Coupland *et al.*, 2013). Due to the absence of lymphatic vessels within the eye, UM disseminate haematogeneously (Wöll, Bedikian and Legha, 1999). UM preferentially metastasises to the liver (>90% of cases); however, co-presentation can often occur in other tissues including the lung (~24%) and bone (~16%) (Coupland *et al.*, 2013). UM metastases often present as multiple deposits in the liver rather than a single mass. The risk of patients developing metastatic disease is associated with several clinical, histological and genetic features as outlined below.

1.6. Clinical features associated with metastatic risk of uveal melanoma

Kujala *et al*., developed a tumour staging system for UM based on the existing tumour-node-metastasis (TNM) staging used for cancers (Kujala *et al.*, 2013). Presentation of tumour cells in the lymph nodes does not commonly occur in UM due to the absence of lymphatic drainage in the eye (Jovanovic *et al.*, 2013), and so the use of the "N" for UM is inappropriate. The study investigated the largest basal diameter (LBD) of the tumours, the rate of ciliary body involvement (CBI) and the rate of extraocular extension (EOE) of 8,736 patients. Ciliary body involvement and EOE strongly correlated with an increased TNM

stage (Kujala *et al.*, 2013). Yet the factor most highly correlated with an increased risk of metastasis was tumour LBD (Kujala *et al.*, 2013). Due to delays in the detection of PUM (Damato *et al.*, 1998), the LBD could inferably indicate that the tumour had been growing for a greater length of time before diagnosis or that it was a more aggressive, faster growing tumour.

1.7. Histomorphological features associated with metastatic risk of uveal melanoma

UM demonstrate distinct growth patterns and cell populations, with the two most common being epithelioid and spindle cell types (Fig. 1.2.) (McLean, Zimmerman and Evans, 1978). McLean et al., investigated 105 cases of UM and were able to separate the tumours into three groups based on tumour cell population and tumour characteristics *in situ*. The presence of a significant proportion of UM cells with epithelioid morphology is characteristic of a more aggressive PUM; whereas, PUM with a dominance of spindle cells tend to have a better prognosis (McLean, Zimmerman and Evans, 1978).

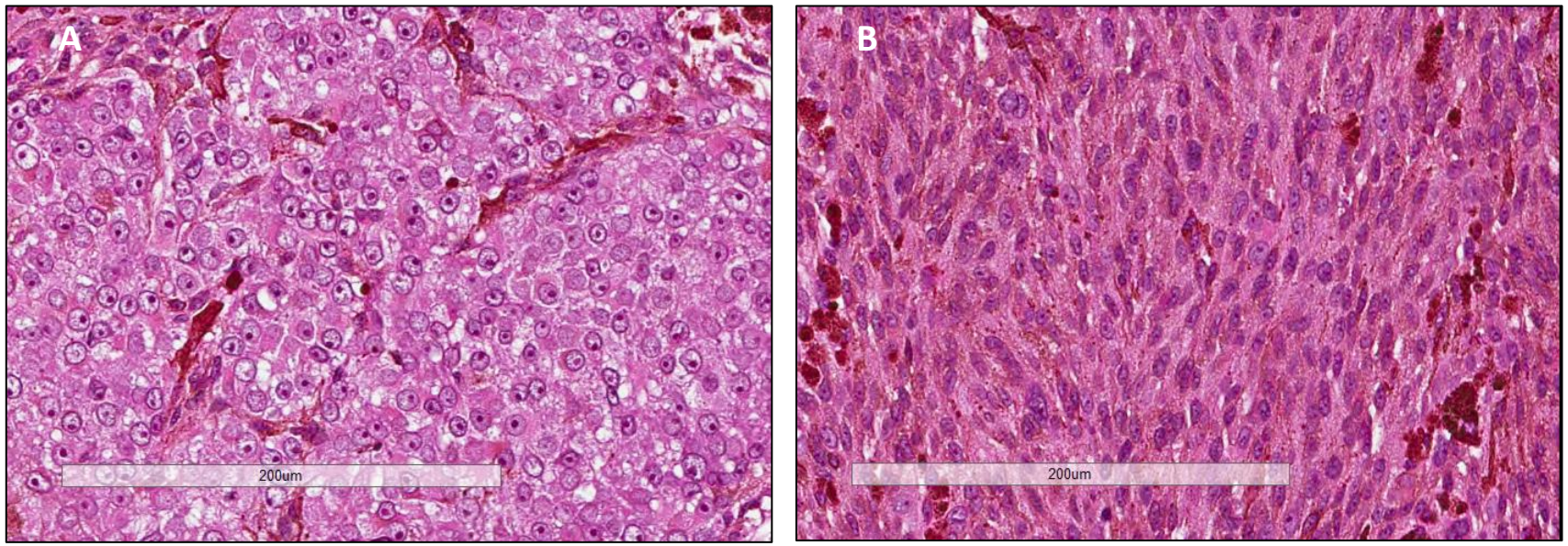

Figure 1.2. Haematoxylin and eosin staining of uveal melanoma tumours, demonstrating their different cell morphologies: A) epithelioid, B) spindle

In 1992 Folberg *et al*., identified distinct morphologic patterns of tumour vasculature in UM (Folberg *et al.*, 1992), which could be demonstrated with a modified Periodic Acid-Schiff (PAS) reaction, viewed with a green narrow band pass filter. In this study, UM patients were split into two groups; (1) those tumours from patients who survived at least 15 years without metastatic progression following enucleation, and (2) tumours from patients who died from metastatic UM. The presence of at least one closed connective-tissue loop identified in the extracellular matrix of UM was associated with metastatic death of the patient, and was considered to be a marker of tumour progression and metastasis (Folberg *et al.*, 1992). These features – highlighted by positive staining with PAS – were thought to show vascular neogenesis within the tumour; however, it was later suggested that these features were formed by the UM cells themselves, in a process known as vasculogenic mimicry (Lin *et al.*, 2005). In conjunction with the presence or dominance of an epithelioid cell type, this morphological feature may be an indication of UM cell de-differentiation.

Lattman *et al*., demonstrated that UM with a high mitotic count also have an increased metastatic risk (Lattman *et al.*, 1995). Mitotic rate corresponds to the high cell proliferation rate in the tumour. Mitotic rate can also be determined using immunohistochemical markers, such as Ki-67, proliferating cell nuclear antigen (PCNA) (Mooy *et al.*, 1990; Pe'er *et al.*, 1994) and Ser10 (PHH3) (Angi *et al.*, 2011).

1.8. Genetic features of uveal melanoma tumours associated with metastatic risk

1.8.1. Chromosomal alterations in uveal melanoma

Specific and repetitive patterns of genetic abnormalities were identified in PUM in the late 1980's, originally with standard karyotype analysis (Griffin, Long and Schachat, 1988; Horsman *et al.*, 1990). Of these patterns, the most conspicuous is the complete loss of one copy of chromosome 3 (termed monosomy 3 [M3]), shown by Prescher *et al*., in 1996 to be linked to disease-specific mortality (Prescher *et al.*, 1996). Gains in chromosome 8q have also been associated with reduced survival time (Sisley *et al.*, 1997) and specifically 8q gain in conjunction with M3 (Damato *et al.*, 2007; Damato and Coupland, 2009; Cassoux *et al.*, 2014). Studies have further investigated this link and demonstrated three prognostic groups; both chromosome 3 and 8q normal conferring favourable outcome, either chromosome 3 or 8q abnormal causing increased risk of metastasis and both chromosome 3 and 8q abnormal with further increased risk of metastatic progression (Caines *et al.*, 2015). These patterns of alterations have been confirmed by several groups using several different techniques, such as comparative genomic hybridisation (Cassoux *et al.*, 2014), multiplex ligation-dependent probe amplification (MLPA) (Damato *et al.*, 2009), microsatellite analysis (MSA) (Tschentscher *et al.*, 2000) and fluorescence in situ hybridisation (FISH) (Sisley *et al.*, 1997).

1.8.2. Common mutations in uveal melanoma

GNAQ/GNA11

The most common genetic alterations in PUM (found in ~84% of cases) are mutually exclusive mutations in one of two large GTPases of the Gαq family; either guanine nucleotide-binding protein subunit alpha-Q (*GNAQ*) or guanine nucleotide-binding protein subunit alpha-11 (*GNA11*). Although there is little evidence linking these to clinical outcome, they have been shown to be initiating mutations in the majority of PUM cases (Van Raamsdonk *et al.*, 2009, 2010). Mutations in these genes follow similar patterns, the most common for both being substitution mutations in exons 5 and 4 affecting amino acids Q209 or R183 respectively. This similarity in mutations correlates with the highly comparable homology between the GNAQ and GNA11 proteins of ~90% (Shoushtari and Carvajal, 2014). Both *GNAQ* and *GNA11* mutations are activating mutations and cause ERK phosphorylation through the MAP-kinase pathway (Van Raamsdonk *et al.*, 2009) (Figure 1.3.). *GNA11* mutations in UM have been reported to correlate with a more aggressive tumour compared to *GNAQ* mutated tumours (Dono *et al.*, 2014).

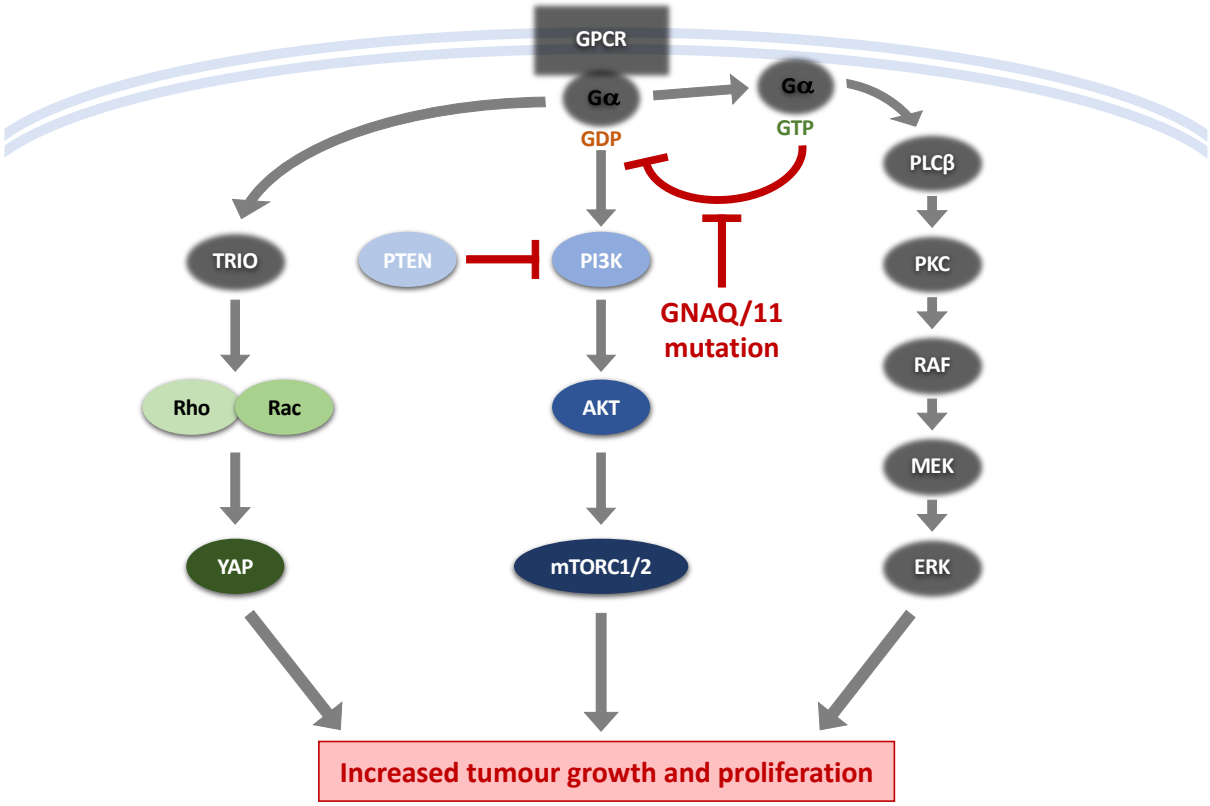

Figure 1.3. Signalling pathways downstream of aberrant GNAQ/11 activation. Adapted from (Patel *et al.*, 2011) and (Feng *et al.*, 2014).

AKT, protein kinase B; ERK, extracellular-signal-regulated kinase; GPCR, G-protein coupled receptor; mTORC1/2, mammalian target of rapamycin complex 1 or 2; PKC, protein kinase C; PLCβ, phospholipase c beta; PTEN, phosphatase and tensin homolog; Rac, Ras-related C3 botulinum toxin substrate; RAF, Rapidly Accelerated Fibrosarcoma protein; Rho, Ras homolog gene family; YAP, yes-associated protein

Mutations in *GNAQ* or *GNA11* cause the G-protein alpha subunits of currently unspecified GTPases to be constitutively active, stimulating downstream pathways (Shoushtari and Carvajal, 2014) such as RAF/MEK/ERK pathway (Weber *et al.*, 2003), TRIO (Feng *et al.*, 2014) and PLCβ (Chua *et al.*, 2017), which in turn stimulates many biological processes such as proliferation, apoptosis, differentiation, inflammation and cell cycle progression (Figure 1.2).

BAP1

The *BAP1* gene encodes the BAP1 protein, a member of the ubiquitin C-terminal hydrolase subfamily of deubiquitylating enzymes. *BAP1* mutations were originally identified using massively parallel exome sequencing coupled with Sanger re-sequencing (Harbour *et al.*, 2010). In patients with M3 UM, the loss of one copy of the chromosome causes any mutations in *BAP1* at the 3p21.1 locus on the remaining chromosome copy to be exposed (Harbour *et al.*, 2010). *BAP1* mutations are associated with loss of nuclear BAP1 protein expression (Harbour *et al.*, 2010; Kalirai *et al.*, 2014; Song *et al.*, 2017; Farquhar *et al.*, 2018; Szalai *et al.*, 2018) and inactivating mutations in the *BAP1* gene, concomitant with M3, have been shown to correlate with increased metastasis and reduced survival in UM (Abdel-Rahman *et al.*, 2011; Kalirai *et al.*, 2014; Koopmans *et al.*, 2014). Absence of nuclear BAP1 protein was also reported in 10/13 (77%) disomy 3 (D3) UM patients who had unexpected metastatic relapse (Kalirai *et al.*, 2014; Koopmans *et al.*, 2014), suggesting that absent nuclear BAP1 protein is a survival predictor for patients with UM, independent of chromosome 3 status. It has been proposed that *BAP1* acts within the melanocytic lineage as a regulator of differentiation and that the absence of BAP1 through inactivating mutations and M3 allows de-differentiation of the neoplastic melanocytes into cells more likely to metastasise (Matatall *et al.*, 2013), further implicating its role in UM metastatic progression.

EIF1AX

The *EIF1AX* gene encodes the eukaryotic translation initiation protein factor EIF1AX (Krishnamoorthy *et al.*, 2019). The EIF1AX protein is an essential component in the recruitment and assembly of the pre-initiation complex 43S (Krishnamoorthy *et al.*, 2019). Mutations in the *EIF1AX* gene were shown through exome sequencing to be present in 48% of D3 PUM, only 5.7% of M3 UM and 8% of tumours with partial losses on chromosome 3 (Martin *et al.*, 2013), suggesting that this mutation was associated with a good outcome. This was also supported by the data of Ewens *et al*., who demonstrated *EIF1AX* mutations in 16% of PUMs; 61% of UM without *EIF1AX* mutations metastasised compared to 12% of tumours containing the mutation (Ewens *et al.*, 2014). These findings also correlate with the findings of Dono *et al*., in 2014; in which, *EIF1AX* mutations occur almost exclusively in D3 UM (Dono *et al.*, 2014).

SF3B1

SF3B1 (splicing factor 3B subunit 1) is a protein involved in the alternative splicing of mRNA, generating multiple transcript variants of a gene that give rise to different protein isoforms. Mutations in the *SF3B1* gene seem to occur most frequently as somatic point mutations at the Arginine-625 position (Te Raa *et al.*, 2015). These mutations have been shown to affect the DNA damage response, increasing the baseline activity of the process (Te Raa *et al.*, 2015). Previously described in myelodysplastic syndromes (Dey *et al.*, 2012), chronic lymphocytic leukaemia (CLL) (Wang *et al.*, 2011) and breast cancer (Muzny *et al.*, 2012) as being linked with poor prognosis, *SF3B1* mutations were originally thought to be associated with a favourable outcome in UM. In 2013, Martin *et al*., showed 29% of D3 UM had *SF3B1* mutations, where only 5.7% of M3 UM had the mutation (Martin *et al.*, 2013). This was corroborated by Yavuzyigitoglu *et al*., in 2016; however, their results showed that *SF3B1*

mutations in D3 PUM conferred an increased risk of developing later metastases (Yavuzyigitoglu *et al.*, 2016).

1.9. Prognostication of uveal melanoma and the likelihood of metastatic progression

Prognostication of UM is extremely useful to identify patients at higher risk of metastatic development who may then be followed-up and screened for metastatic disease more frequently. By detecting metastasis earlier, UM patients may be more suitable for liver resection or entered into clinical trials. Prognostication also allows reassurance of patients at low risk of metastasis. After removal of the tumour or if a small tumour biopsy is taken, the tissue can be analysed for histological features of PUM and genetic alterations, which together with clinical features, give an indication of the risk of the patient developing metastases.

At the Royal Liverpool University Hospital, a personalised prognostication algorithm has been developed, which integrates clinical, histomorphological and genetic data from PUM patients to generate personalised prognostic curves compared with an age and gender-matched healthy individual (Eleuteri *et al.*, 2007). The prognostication tool incorporates data such as age, tumour size, CBI, EOE, epithelioid cell presence, closed PAS positive loops, mitotic count, chromosome 3 and chromosome 8q status (Deparis *et al.*, 2016).

Expanding on work originally performed by Tschentscher *et al*., in 2003, a method based on gene expression profiling was developed by Onken *et al*., in 2004 utilising the amplification or deletion of well-characterised genes with distinct patterns (Tschentscher *et al.*, 2000; Onken *et al.*, 2004). The 62 differentially expressed genes have since been reduced to a

panel of 15; 12 discriminating genes and 3 housekeeping genes, collectively capable of discriminating between PUM at low risk (Class 1) and high risk (Class 2) of developing metastases. This is now available as a commercial test, Decision Dx UM, provided by Castle Biosciences (http://castlebiosciences.com/tests/uveal-melanoma/).

1.10. Treatment of metastatic uveal melanoma

A Collaborative Ocular Melanoma Study (COMS) showed that the 5 and 10-year cumulative metastatic rates for patients with UM were 25% and 34% respectively. Of the patients with metastatic disease, 80% died within the first year of a metastatic diagnosis, 92% within the first two years (Diener-West *et al.*, 2005).

Where microscopically complete resection is possible, surgical removal of metastatic UM (MUM) in the liver confers a postoperative survival of 27 months as compared with 14 months when MUM is non-resectable due to multiple deposits in the liver. For MUM where resection is not an option, current courses of chemotherapy include treatment with cisplatin, dacarbazine and fotemustine; yet none have shown any significant increase in patient survival (Augsburger, Corrêa and Shaikh, 2009). Recent clinical trials have focused on targeted therapies e.g. MEK inhibitors (Gilbert, 2014), chemoembolization (Patel *et al.*, 2005) and isolated hepatic perfusion (Olofsson *et al.*, 2014) among others.

1.11. The metastatic niche

The mechanism of UM metastatic progression to the liver is still poorly understood. However, liver metastasis has been investigated in other cancers and it is well established that the microenvironment in the liver is modulated during the metastatic process (Vidal-Vanaclocha, 2008). This modulation during metastatic development has been shown

previously in the literature to include features such as increased invasion of bone marrow-derived macrophages in the liver (Costa-Silva *et al.*, 2015), local upregulation of proinflammatory factors (Brodt, 2016), increased production of fibronectin by resident liver fibroblasts (Costa-Silva *et al.*, 2015), and the increased deposition of multiple extracellular matrix (ECM) products (van Huizen *et al.*, 2019). Taken collectively these features highlight one of the most common characteristics of liver metastasis, an increase in the local fibrotic environment at the metastatic niche (Lee *et al.*, 2019).

It has been shown that this modulation may occur prior to cancer cell "seeding" via tumour-metastatic niche communication through the secretion of signalling proteins into the bloodstream, both exogenously and via extracellular vesicles (Costa-Silva *et al.*, 2015). These proteins/vesicles are thought to travel haematogenously to the metastatic site and prepare the metastatic niche, generating a more accepting microenvironment for the tumour (Xiaogang Wang *et al.*, 2015).

1.12. Cancer secretome

The term “secretome” was originally introduced in a genome-wide study of secreted proteins in bacteria (Tjalsma *et al.*, 2000) and describes the whole range of organic molecules and inorganic compounds secreted by cells/tissue into their local environment. The major components of the secretome from mammalian cells are lipids, genetic materials and proteins; the profiles of which can be altered in illness/disease. Most, if not all, cells in the human body engage in communication via protein signalling, whether that is by secretion of signalling proteins, receipt of proteins secreted by other cells or both (Halban and Irminger, 1994). As such, the most well studied component of the cancer secretome is the protein content, which has been widely investigated for its potential in biomarker discovery and the elucidation of intercellular signalling pathways (Makridakis *et al.*, 2010; Piersma *et al.*, 2010). Research investigating cancer biomarkers has gradually increased since the late 80’s and is becoming ever more useful with calls for less invasive procedures in the clinic and the potential for “liquid biopsies” to identify biomarkers of disease progression and/or response to treatment in bodily fluids (Ludwig and Weinstein, 2005). The relevance of proteomic research over genetic material was reinforced in 2009 when de Sousa Abreu *et al*., published data showing that the relationship between mRNA and protein expression may not always be constant (de Sousa Abreu *et al.*, 2009).

Proteins released by cancer cells into their local environment form the proteomic aspect of the cancer secretome and can act either locally, through autocrine or paracrine signalling and may also induce distal or systemic signalling by entering the bloodstream. The latter has generated an increased interest in interrogating the plasma or serum of cancer patients for potential blood borne cancer biomarkers (Hanash, Pitteri and Faca, 2008). Proteins secreted by cancer cells may be vastly important in tumour progression and play a key role in areas such as cancer cell proliferation/clonal expansion (Sporn and Todaro, 1980),

epithelial to mesenchymal transition (L. Li *et al.*, 2015), angiogenesis (Carmeliet, 2005), matrix remodelling (Oskarsson, 2013), immune system manipulation (De Visser, Eichten and Coussens, 2006) and stromal cell manipulation (De Wever and Mareel, 2003).

Early stage MUM is often not detectable by current, clinically used screening techniques due to their low sensitivity and MUMs proclivity for miliary presentation. This suggests that MUM may be present for a longer amount of time and is likely to present with increased tumour burden upon detection (Eskelin *et al.*, 1999; Borthwick *et al.*, 2011). This has led to the increased popularity of biomarker research becoming a focal point in UM research and highlighted the need to find sensitive indicators of metastatic spread in UM patients prior to clinically detectable presentation.

Several groups have also investigated the proteomic profile of UM. In 2003, Missotten *et al.,* demonstrated that eyes with UM could be distinguished from healthy eyes through proteomic analysis of the aqueous humour, suggesting that two unidentified proteins were capable of accurate distinction in 89% of cases when used in combination (Missotten *et al.*, 2003). Zuidervaart *et al.,* performed similar analysis on UM cell lines in 2006 and established a panel of 24 proteins differentially expressed between primary and metastatic derived lines; these including eight with known functions in cell proliferation and migration (Zuidervaart *et al.*, 2006). Pardo *et al.,* investigated the proteomic profile of the secretome of UM cell lines, again highlighting an abundance of proteins linked with adhesion and migration, in particular components modulating the ECM (Pardo *et al.*, 2007). The authors suggested that the proteins cathepsin D, syntenin and gp100 represented potential biomarkers of UM metastatic potential. The proteomic profiles of PUM samples classified as either D3 or M3 identified differential expression of several proteins, highlighting that low-to-negative HSP-27 (heat shock protein 27) correlated strongly with M3, a known

predictor of metastatic progression (Coupland *et al.*, 2010). Linge *et al.,* identified 14 proteins differentially expressed in PUM tissue from patients who developed metastases compared with PUM tissue from patients who did not develop metastases in the >7-year follow-up (Linge *et al.*, 2012). They suggested that Fatty Acid Binding Protein 3 (FABP3) and Triosephosphate isomerase 1 (TPI1) may be involved in the metastatic phenotype of UM. Proteins linked to adhesion and cytoskeletal remodelling were also identified as differentially expressed, such as upregulation of vimentin and F-actin capping protein subunit alpha-1, and downregulation of tubulin alpha-1B chain and tubulin beta chain. Eukaryotic translation initiation factor 2 subunit 1 (EIF2S1) was also shown to be downregulated in MUM (Linge *et al.*, 2012). Proteomic analysis of UM by Crabb *et al.,* identified a panel of 31 proteins differentially expressed in metastatic and non-metastatic PUM samples (Crabb *et al.*, 2015). Their data again highlighted the differential expression of HSP-27 and suggested that collagen alpha-3(VI) and heat shock protein beta-1 allowed accurate prediction of metastatic potential. This work highlighted the complexity of cultured cancer cell secretomes and the availability of novel data within this field of study; 68% of their total protein cohort had, at that time, not previously been linked to cancer.

1.13. Extracellular vesicles

Extracellular vesicles (EV) are small membranous structures released by all cells in the human body (Yáñez-Mó *et al.*, 2015). Research into EVs has increased rapidly over the past decade as evidence of their involvement in numerous diseases continues to grow (Antonyak and Cerione, 2015). In particular, the EV subpopulation exosomes is receiving increased attention (Figure 1.5.).

The pleiotropic roles of EVs in physiology and pathology suggest a wealth of possibilities for their use in a clinical setting (van der Pol *et al.*, 2012). In cancer it is common to see

upregulation in EV cargo specific to the cancer type or stage. The availability of this cargo in liquid biopsy-derived EVs highlights the potential for their use as biomarkers for the diagnosis and prognostication of cancer from non-invasive patient samples (Katsuda, Kosaka and Ochiya, 2014; Halvaei *et al.*, 2018). As the levels of any specific exosomal cargo may represent the presence or stage of a disease, similarly, they can also act as markers of treatment efficacy and disease regression (Mitchell *et al.*, 2009).

Importantly, EVs facilitate intercellular signalling (Camussi *et al.*, 2010), carrying biologically active cargo from one cell to another and stimulating signalling pathways which may promote disease progression. Due to this mechanism, perturbation of these pathways represents a potential avenue for novel therapeutic targeting (Zhang *et al.*, 2007). Some EVs are capable of housing therapeutic drugs and can deliver these across biological membranes (Ha, Yang and Nadithe, 2016). Certain EVs have also demonstrated organotropic targeting, dependent on the integrin protein composition on the exosome surface; this could allow targeted delivery of internal cargo and/or therapeutics (Hoshino *et al.*, 2015).

In order to allow for their role in the intercellular transmission of biologically active materials, EVs need to be secreted by their cell of origin into the surrounding extracellular fluid. As such EVs form a major part of the tissue/cell secretome.

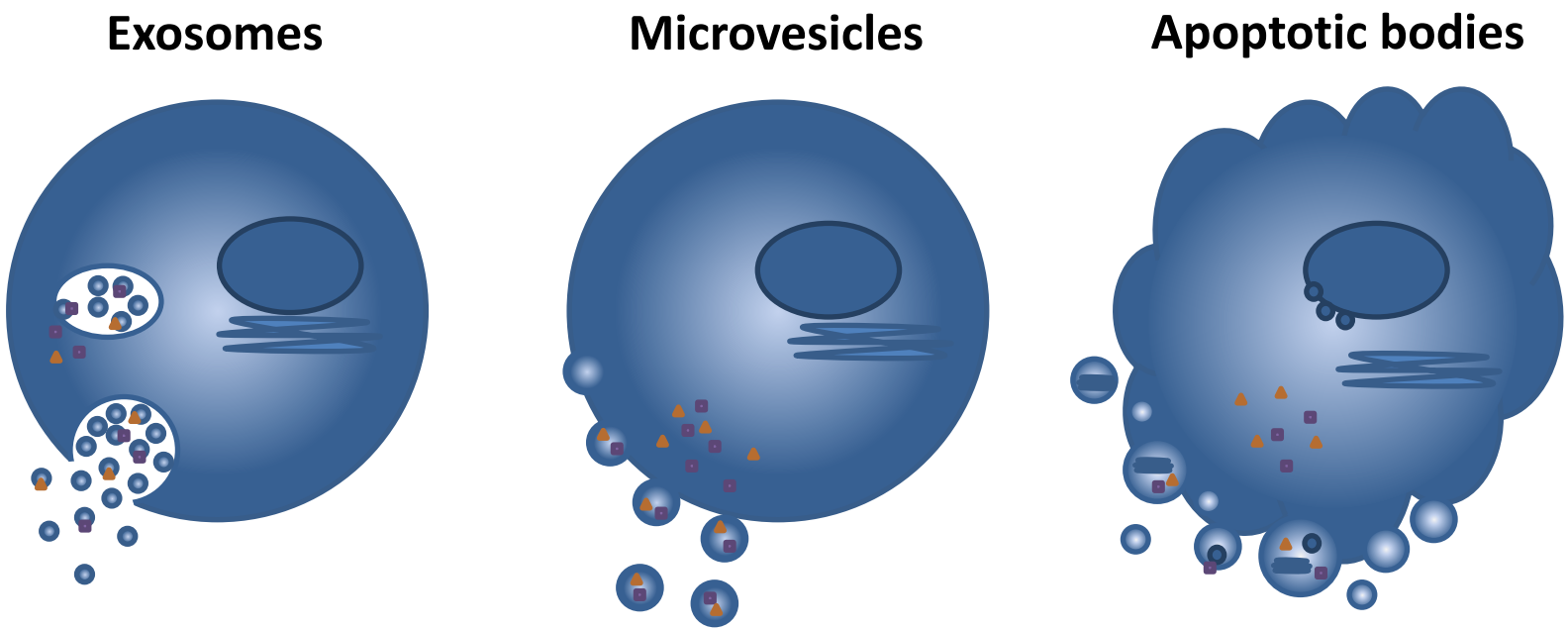

Figure 1.4. The three main types of extracellular vesicles and their mechanism of release. Exosomes are released from multivesicular bodies within the cell upon their fusion with the cell surface membrane; microvesicles form at the cell surface through direct budding from the surface membrane; apoptotic bodies form during programmed cell death through apoptotic blebbing

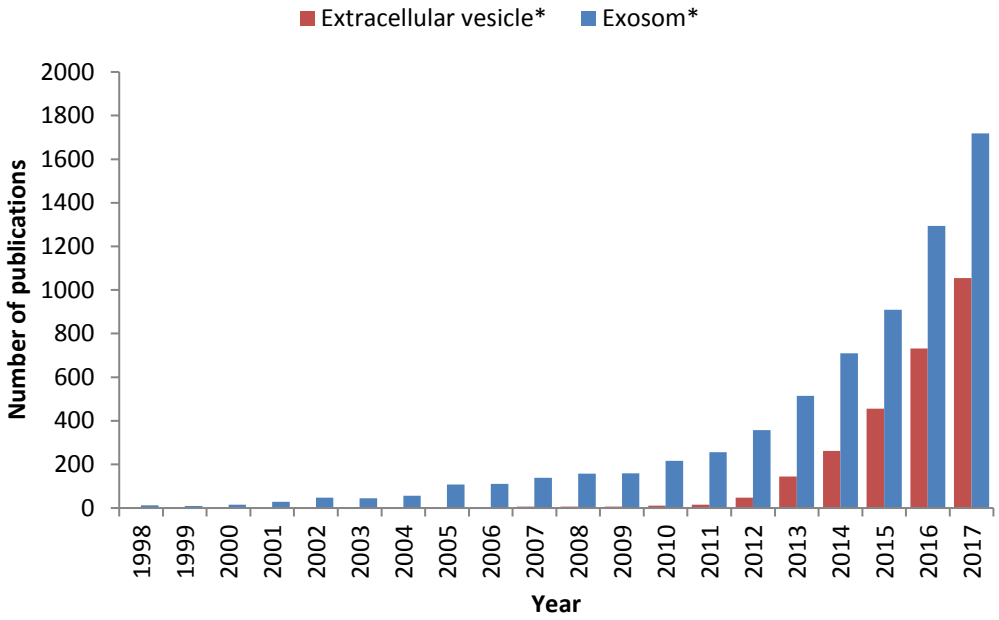

Figure 1.5. The number of publications on Pubmed per year containing the words 'extracellular vesicles' or 'exosomes' in the title

(Search for "Extracellular vesicle" included terms "extracellular vesicle" or "extracellular vesicles"; the search for "Exosom*" included terms "exosom", "exosoma", "exosomal", "exosomal14", "exosomal18s", "exosomally", "exosomalmir" "exosomas", "exosomatic", "exosome", "exosome'", "exosome's", "exosomecontaining", "exosomederived", "exosomeencapsulated", "exosomemediated", "exosomes", "exosomes'", "exosomesagainst", "exosomesthesia", "exosomesyncytiotrophoblast", "exosomic", "exosomics", "exosomopathies", "exosomopathy" or "exosomse"*

EVs are commonly split into three categories based on their size, morphology and mechanism of biogenesis: apoptotic bodies, microvesicles and exosomes. While EV categories are defined by their distinct biogenesis pathways, the biophysical characteristics used to differentiate EV subtypes commonly overlap between categories (Willms *et al.*, 2018). As such, current methods for the isolation/enrichment of EV subtypes remain imperfect. It is now commonly assumed that research involving the enrichment/isolation of EV subtypes is investigating heterogenous populations of vesicles (Raposo and Stoorvogel, 2013). As the biogenesis of EV population remains distinct, the mechanisms and typical biophysical characteristics are defined below; however, the references applied to the functions of these subtypes can be assumed to refer to a heterogenous population of vesicles differentiated primarily by one physical feature, often vesicle size.

1.13.1. Apoptotic bodies

Apoptotic bodies (ABs) are formed by stressed cells undergoing programmed cell death during adverse conditions and range from 800-5000 nm diameter (Crescitelli *et al.*, 2013). ABs form through "blebbing" of the cellular membrane of cells undergoing apoptosis. While the exact mechanisms governing apoptotic body formation are elusive, the current paradigm suggests that this is mediated by actin-myosin remodelling through Rho-associated protein kinase 1 (ROCK1), LIM domain kinase 1 (LIMK1), myosin light chain kinase (MLCK), and P21-activated kinase (PAK2) activity (Coleman *et al.*, 2001). AB formation is thought to occur through three distinct membrane protrusions during apoptotic blebbing: microtubule spikes (Moss *et al.*, 2006), apoptopodia (Ivan K H Poon *et al.*, 2014), and beaded apoptopodia (Atkin-Smith *et al.*, 2015).

Due to the large size of ABs they can often be characterized by their containment of intracellular organelles (Taylor, Cullen and Martin, 2008) and can be isolated from cultured

cells, tissue and bodily fluids by differential centrifugation (Atkin-Smith *et al.*, 2017). ABs are thought to provide "homing signals" for phagocytes, stimulating the recruitment of macrophages and the subsequent efferocytosis of the apoptotic cell (Ivan K.H. Poon *et al.*, 2014). ABs have been shown to possess distinct protein and RNA profiles from other EVs (Crescitelli *et al.*, 2013).

1.13.2. Microvesicles

Microvesicles (MVs) — also known as shedding MVs, microparticles or ectosomes — are smaller membranous vesicles generated by the outward budding and fission of the membrane at the cell surface (Raposo and Stoorvogel, 2013). They are commonly reported to have a diameter between 100–1000 nm (Raposo and Stoorvogel, 2013). The mechanism of MV assembly, budding and release into the extracellular space is not completely understood. It is thought to involve distinct changes in the local lipid and protein composition of the plasma membrane and cytoskeletal remodelling through GTPase signalling (Tricarico, Clancy and D'Souza-Schorey, 2017).

The proteins regulating MV biogenesis were reviewed and described by Taylor and Bebawy in 2019 (Taylor and Bebawy, 2019). They highlighted the loss of phospholipid asymmetry in the plasma membrane as one of the primary stages of MV biogenesis. Inactivation of 'flippase' and concomitant activation of 'floppase' and 'scramblase' through Ca2+ mobilization promotes random distribution of phospholipids and loss of anionic charge on the inner membrane leaflet. This promotes cleavage of cytoskeletal proteins anchoring the membrane. Areas of membrane detachment are subject to intracellular hydrostatic pressure, modulation of contractile proteins, and changes in membrane curvature resulting in membrane bleb formation. Recruitment of other proteins such as the endosomal sorting complexes required for transport (ESCRT) machinery and/or neutral sphingomyelinase

leads to scission of the vesicle's neck and MV release into the extracellular environment .(Taylor and Bebawy, 2019).

Microvesicles have received less interest in the literature than exosomes; and as previously stated, in research in which MV have been “isolated” it can be assumed that samples contain heterogenous populations of vesicles. That said, MV have described roles in coagulation (Del Conde *et al.*, 2005), immune modulation (Huber *et al.*, 2005), inflammation (Hulsmans and Holvoet, 2013), cancer (Pap, Pállinger and Falus, 2011) and when separated by size, MVs are known to possess distinct protein cargo to other EV subtypes (Tucher *et al.*, 2018).

1.13.3. Exosomes

Exosomes are the smallest member of the EV family, ranging from 50-120nm in diameter (Xu *et al.*, 2016). They are spherical vesicles consisting of a lipid bilayer membrane enveloping biologically active cargo and are produced in multivesicular bodies at the later stage of the endosomal cycle. Exosomes were originally reported in 1981 as a method of membrane protein exfoliation (Trams *et al.*, 1981) and later in 1987 by Johnstone *et al.,* as a method of changing the membrane protein composition of during maturation of reticulocytes (Johnstone *et al.*, 1987).

The first description of exosomes regarded the “shedding” of 5’nucleotidase along with increased amounts of specific lipids and fatty acids (Trams *et al.*, 1981). They have since been shown to house specifically enriched proteins (Schey, Luther and Rose, 2015), lipids (Lydic *et al.*, 2015) and genetic materials (Valadi *et al.*, 2007; Rodríguez *et al.*, 2015; Sato-Kuwabara *et al.*, 2015).

The current dominant hypothesis is that exosomes are formed in the lumen of the early endosome (Théry, Zitvogel and Amigorena, 2002). Initially a section of cell membrane is internalised at the cell surface due to ligand-receptor binding. Internal budding at these cell surface receptors can occur through several pathways, the canonical pathway being clathrin-dependent endocytosis, in which a stimulated receptor is thought to be recruited to specific clathrin rich domains. Invagination within the cell membrane due to loss of lipid membrane asymmetry causes clathrin-coated pits to form, with any receptor-ligand complex engaged inside. The recruitment of proteins such as dynamin and endophilin causes the pit to deepen and eventually pinch off to create an intracellular vesicle (Mousavi *et al.*, 2004). This forms a compartment within the cell known as the early endosome. As the early endosome matures, budding occurs from the surface generating vesicles within the internal lumen (Huotari and Helenius, 2011). A driving mechanism in this process involves the ESCRT machinery, which consists of four protein complexes; ESCRT-0, -I, -II, -III and the Vps4 complex (Henne, Stenmark and Emr, 2013).

Other non-canonical methods of exosome formation have also been documented in the literature. The clathrin-independent pathway involves caveolin rich lipid rafts, which are internalised when bound to a receptor-ligand complex (Sandvig *et al.*, 2011). Other pathways include the involvement of either flotillin, which has proposed roles in endocytosis, endosomal sorting and exosome biogenesis (Meister and Tikkanen, 2014); GRAF1 mediated CLIC/GEEC endocytosis (Lundmark *et al.*, 2008), Arf6 endocytosis (Ghossoub *et al.*, 2014) or macropinocytosis (Doherty and Mcmahon, 2009)

During this stage the ESCRT machinery is thought to aid the selective enrichment of biologically active cargo through recruitment of proteins into the intraluminal vesicles (ILVs). Alternatively, CD63, CD81 and HSC70 have all been identified as ESCRT-independent

mechanisms of protein loading into ILVs (Kowal, Tkach and Thery, 2014). Furthermore, it has been shown that exosomal proteins are commonly ubiquitinated and ubiquitination has been proposed as a canonical mechanism by which proteins are targeted to exosomal loading (Buschow *et al.*, 2005). Studies have also suggested that ubiquitination of recombinant proteins allowed directed loading and exosomal secretion of the synthesised product (Cheng and Schorey, 2016). Sumoylation of miRNA sequence motifs is thought to preferentially select for miRNA loading into ILVs (Villarroya-Beltri *et al.*, 2013), prior to exosome secretion.

Once these ILVs are formed, the ILV-containing endosome is commonly referred to as a multivesicular body (MVB). MVB trafficking to the cell surface prior to release of the ILVs is modulated by the Rab GTPases Rab27, Rab11 and Rab35 (Blanc and Vidal, 2018). Rab11 and Rab35 mediated exosomal release is primarily associated with vesicles formed in an ESCRT-independent manner. Whereas Rab27 mediates the release of MVBs containing vesicles generated through an ESCRT-dependent formation (Blanc and Vidal, 2018). Fusion of the MVB with the cell surface membrane allows the extracellular release of the ILVs as exosomes. This fusion is mediated by soluble NSF-attachment protein receptor complexes (SNARE) (Zylbersztejn and Galli, 2011).

1.13.4. Techniques for the isolation of UM EVs

Several techniques exist for the isolation/enrichment of exosomes and many more are being developed in the literature every year. The more common techniques employed in the literature are comprehensively reviewed by (Konoshenko *et al.*, 2018). These methods rely on specific physical or biological properties of exosomes; this can be the presence of surface proteins and immuno-affinity capture (Greening *et al.*, 2015), enrichment due to the buoyant density of the particle (Théry *et al.*, 2006) or enrichment due to the size of the

EVs (Cheruvanky *et al.*, 2007); each of these techniques comes with its own benefits and limitation.

Polymeric precipitation (PP) allows for quick and simple enrichment of EVs from culture media or biological fluid yet does very little to distinguish between the enriched EV, protein complexes, lipoproteins or larger protein aggregates (Kanchi Ravi, Khosroheidari and DiStefano, 2015). Size exclusion techniques (SE), such as chromatography columns or sequential filtration, allows for EV isolation with similar speed and simplicity as PP and has reduced contamination from non-exosomal proteins yet can still contain larger protein aggregates and other EV types (Böing *et al.*, 2014). Affinity capture (AC) employs biochemical properties of the exosomes to bind and hold them while eluting all other elements in the starting sample. The properties used can include the biochemistry of the lipid bilayer membrane of the exosomes (Nakai *et al.*, 2016) but most commonly employ antibodies specific to proteins suggested to be enriched on their surface (Clayton *et al.*, 2001; Théry *et al.*, 2006). Currently, however, no definitive exosome marker exists for affinity capture (Kowal *et al.*, 2016), and recent studies have shown that proteins commonly used for the immunoaffinity isolation of exosomes, such as CD63 and CD9, can also be present on all other EVs (Kowal *et al.*, 2016). Therefore, while AC offers reduced contamination from protein aggregates, it does not specifically isolate exosomes. Moreover, it has also been shown that isolation of exosomes with this method may select for subpopulations within a sample (Kowal *et al.*, 2016). This could potentially be beneficial if the protein presentation of subpopulations was known and the investigator was only concerned with a specific population; however, without certainty that the populations are known, this could create an unintended bias in sample population and affect downstream analyses. Differential ultracentrifugation (UC) is the most commonly described technique (P. Li *et al.*, 2017) involving the centrifugation of samples at incrementally increasing speeds

to pellet and remove particles of higher buoyant density from the supernatant, eventually pelleting the exosomes and removing the supernatant, containing soluble proteins. UC presents fewer contaminating protein aggregates than PP and SE yet is a lengthy and laborious protocol (P. Li *et al.*, 2017). UC requires specialised equipment and also suffers from contamination problems; it has been shown to co-enrich high density lipoproteins (Yuana *et al.*, 2014) and other small vesicles (Kowal *et al.*, 2016). Nevertheless, UC is the most well validated and most referenced method for isolating exosomes. Each of these methods can be combined in different orders or have added filtration or sucrose cushion/gradient steps; however, each additional step is often employed at the expense of EV yield. As no definitive method for the isolation of pure exosomes is currently available (Kowal *et al.*, 2016), the method(s) employed must be tailored to suit the primary research question.

Table 1.1. The pros and cons of various literature-reported techniques for the isolation/enrichment of exosomes.

	Polymer Precipitation (PP)	**Size exclusion (SE)**	**Ultracentrifugation (UC)**	**Immuno-affinity capture (IAC)**
Benefits	• Speed of protocol, • Technical simplicity • Low start-up cost	• Speed of protocol • Technical simplicity • Fewer contaminants that PP • Low start-up cost	• Fewer protein contaminants that PP and SE • Well validated • Customisable • Wash steps can reduce protein contaminants	• Speed of protocol • Technical simplicity
Drawbacks	• Co-enriches protein aggregates/complexes and other similar sized vesicles • Often requires combination with other purification techniques	• Co-enriches protein aggregates/complexes and other similar sized vesicles • Filtration may induce shear-stress	• Laborious and time consuming • Co-enriches large protein aggregates/complexes, other similar sized vesicles lipoproteins • Requires specialized equipment	• No definitive exosome marker exists • Co-enriches other vesicles with similar protein presentation • Inherent bias for sub-populations • High start-up cost

1.13.5. Characterisation of EVs

There are many methods available for the characterisation of EVs isolated from bodily fluids or cell culture media. These techniques commonly focus on the qualitative or quantitative analysis of EV size, morphology and protein presentation.

EV size is often measured by techniques employing dynamic light scattering (DLS) or nanoparticle tracking analysis (NTA), a more recent strategy employs resistive pulse sensing (RPS). DLS is a technique for measuring the size distribution of particles in a suspension. A laser is shone through a sample and any particle in the path of the laser causes the light to be scattered in all directions. The intensity of the scattered light is recorded and expressed as a function of time and the size of the particle can be calculated through fluctuations of the light intensity due to Brownian motion (Szatanek *et al.*, 2017). NTA works in a very similar manner to DLS; however, the scattered light is recorded with a highly sensitive camera and the recording is analysed by tracking the displacement of each particle and plotting the motion as a function of time. This can be used to calculate the size distribution of particles in a sample using the Stokes-Einstein equation (Szatanek *et al.*, 2017). A potential benefit of NTA compared with DLS is the ability of the camera to detect fluorescence; combined with the application of fluorescently tagged antibodies, NTA would allow subpopulations of EV's within a sample to be identified by differential presentation of surface proteins. It should be noted, however, that both DLS and NTA suffer from a similar caveat; larger particles and particles with a higher refractive index would scatter more light and "outshine" smaller particles, limiting their detection, this could bias size distribution in a polydisperse sample towards those larger particles and those with higher refractive indices (Szatanek *et al.*, 2017). RPS employs a "size-tunable" polyurethane membrane for quantitative measuring of nano- and micro-particles. A transient change in the ionic current

across the membrane is detected as particles traverse the pores, this is denoted as a blockade event, the magnitude of which is indicative of particle size (Vogel *et al.*, 2011).

Vesicle diameter has long been considered a differentiator of EV subtype (György *et al.*, 2011); however, more recent studies have shown that the size ranges of EV subtypes likely overlap, and any method of isolation relying solely on vesicle diameter is likely to produce samples of heterogeneous vesicles (Willms *et al.*, 2018).

EV morphology can be assessed by several methods of microscopy, these allow visualisation and measurement of their size and include transmission electron microscopy (TEM) (Théry *et al.*, 2006), scanning electron microscopy (SEM) and atomic force microscopy (AFM) (Sharma *et al.*, 2010). In TEM, samples are fixed, adsorbed onto a microscopy grid, dehydrated and stained with an optically opaque substance; samples are often embedded to improve contrast. Electrons are passed through the sample, detected and magnified. Stains more readily adhere to the background and deflect more electrons than the sample, allowing greater resolution of the sample compared with the background (Szatanek *et al.*, 2017). SEM involves fixing and dehydrating a sample, adsorbing the sample onto a microscopy grid and scanning the sample with a narrow beam of electrons. The backscattered electrons emitted from the sample surface are then detected (Fischer *et al.*, 2012). In AFM, a sample's surface is probed with a fine tip attached to a cantilever; interaction forces between the surface and the tip cause deflection of the cantilever, which is recorded by a photodiode detector system (Szatanek *et al.*, 2017). These methods provide high-resolution, high-magnification images, visualisation of sample morphology and size along with information about surface topography and composition. Immuno-labelling of EV surface proteins with gold tagged antibodies allows the detection of specific proteins on the surface of EVs (Szatanek *et al.*, 2017). It is worth noting that the size and

morphology of EVs can be altered during the extensive multistep process and sample dehydration involved in these methods, and so they can only be assumed to give relative size quantification. Progress has been made in the mitigation of these effects through the alteration of the methods; such as the use of cryo-vitrification of EVs instead of dehydration and fixation prior to electron microscopy (Cizmar and Yuana, 2017).

Analysis of protein cargo is a common method used to characterise EVs and there have been several proteins suggested to be specific for EV subtypes. Among others, proteins previously thought to be specific for exosomes include CD63, CD9, CD81 and ANXA2 (Théry *et al.*, 2006). Immunolabelling can be employed with several techniques such as flow cytometry (Pospichalova *et al.*, 2015), electron microscopy (Théry *et al.*, 2006), NTA (Dragovic *et al.*, 2011) and western blotting (Théry *et al.*, 2006). Due to the distinct mechanisms of biogenesis of EV subtypes, certain proteins are often enriched on the surface or in the lumen of EVs; the presence of which is indicative of subtypes within a sample (Raposo and Stoorvogel, 2013). These include proteins involved in membrane fusion dynamics and intracellular transport (e.g. Rab GTPases, annexins, flotillin), endosomal maturation and the biogenesis of MVBs (Alix, TSG101), and transmembrane proteins such as major histocompatibility complex class I and II, heat shock proteins (hsc70 and 90), integrins and tetraspanins (e.g. CD63, CD9 and CD81) (Simons and Raposo, 2009; Simpson *et al.*, 2009; Mathivanan, Ji and Simpson, 2010). It has been shown, however, that several of the proteins previously suggested as specific markers of EV subtypes, such as exosomes, are apparent on multiple vesicle types (Kowal *et al.*, 2016) and so may not represent definitive markers.

1.13.6. Intracellular communication and manipulation of the microenvironment by extracellular vesicle

Once released into the surrounding extracellular milieu, EVs are free to interact with other local cells or to enter the blood stream and affect more distal cells. Several methods of EV uptake have been described in the literature and were reviewed in detail by Mulcahy *et al.,* (Mulcahy, Pink and Carter, 2014). Mechanisms of uptake include membrane fusion, caveolin-mediated endocytosis, micropinocytosis, lipid raft-mediated endocytosis, clathrin mediated endocytosis and phagocytosis (Mulcahy, Pink and Carter, 2014).

The mechanism of exosomal genesis governs the protein composition and content of the vesicle thereby affecting its involvement in communication and signalling. Hoshino *et al.,* showed that integrin composition on the surface of exosomes determine organotropic metastasis (Hoshino *et al.*, 2015). Exosomes have also been shown to manipulate the immune system with roles in; macrophage polarization (Jang *et al.*, 2013), suppression of the adaptive immune response (Barros *et al.*, 2018), angiogenesis (Mineo *et al.*, 2012) education and mobilisation of bone marrow derived cells (Peinado *et al.*, 2012).

Exosomes have been shown to play a pivotal role in metastatic spread, facilitating pro-metastatic processes such as inflammation (Hiratsuka *et al.*, 2008), stromal cell activation/recruitment (Costa-Silva *et al.*, 2015; Paggetti *et al.*, 2015), upregulation of cancer cell chemo-attractants (Kaplan *et al.*, 2005), angiogenesis (Mineo *et al.*, 2012) and matrix manipulation (Erler *et al.*, 2009). These processes have been demonstrated in the target organs of breast (Fong *et al.*, 2015), pancreatic (Costa-Silva *et al.*, 2015), cutaneous melanoma (Hood, San and Wickline, 2011; García-Silva and Peinado, 2016), prostate (Sánchez *et al.*, 2016) and colorectal cancers (Ji *et al.*, 2013) among others.

1.13.7. Extracellular vesicles in uveal melanoma

A limited amount of research has explored the role of EVs in UM. Two of the three papers identified focused on the miRNA content of the EVs and only one paper investigated the protein content of UM EVs.

The first paper investigating UM EVs was published in 2014 by Eldh *et al.,* and described exosome-like EVs isolated by differential ultracentrifugation from local liver perfusates in patients with MUM (Eldh *et al.*, 2014). The EVs were approximately 50 nm in diameter by transmission electron microscopy (TEM) and shown to be positive for CD63 by immune-gold labelling, and CD63, CD9 and CD81 by flow cytometry, following immunoprecipitation on anti-CD63 coated latex beads. EVs were considered of UM origin due to positivity for Melan-A when assessed by western blot. Patients with UM were shown to have significantly more EVs in peripheral blood plasma than healthy controls, according to the total protein content of vesicles isolated per mL of plasma. Functional analysis of a specific cluster of miRNAs derived from isolated EVs suggested their involvement in various cancer related signalling pathways, including “Hedgehog signalling”, “Focal Adhesion” and “mTOR” signalling, each of which has previously been suggested as a potential pharmacological target in UM treatment (Ho *et al.*, 2012; Duan *et al.*, 2014; Faingold *et al.*, 2014).

In 2015, Ragusa *et al.,* isolated small EVs – considered exosomes – from the aqueous humor of patients with primary UM (Ragusa *et al.*, 2015). Small EVs were isolated by differential centrifugation, filtration and subsequent ultracentrifugation. The EVs had a diameter of 100 nm when measured by dynamic light scattering and showed presentation of CD9, CD63 and CD81 by flow cytometry following adsorption onto aldehyde/sulphate latex beads. A cohort of 179 miRNAs were detected in the vitreous humour derived EVs from a TaqMan low-density array of 754 miRNAs profiled. The authors identified miRNAs 146a, 21, 34a and

618 as significantly differentially expressed between the EVs isolated from healthy control patients and patients with UM. They suggested that exosomal mir-146a in patient serum could act as a diagnostic biomarker of UM and possibly discriminate between UM and cutaneous melanoma.

Recently in 2019, Surman *et al.,* (Surman *et al.*, 2019) isolated larger EVs – described as ectosomes – from the UM cell line Mel202. EVs were isolated by differential centrifugation from cell culture media and characterised for morphology, size and purity by TEM. Size analysis of electron micrographs determined a mean vesicle diameter of 317 nm. Proteomic analysis identified 949 proteins. While the primary focus of the paper was the investigation of the glycosylation pattern of the UM ectosomal proteome, functional enrichment highlighted processes and functions associated with cell–cell adhesion; including adherens junctions (11.1%), focal adhesion (15%), or cadherin-binding activity (11.1%).

1.14. Proteomics

Proteins are the major regulators and effectors of most signalling pathways within a cell. The dysregulation of protein expression or signalling can result in a variety of physiological disorders such as cancer; conversely, the inhibition or activation of specific proteins within a signalling pathway can help treat disease and/or alleviate symptoms (Downward, 2003). Identification, quantification and characterization of the total protein content of a cell or cellular system is of the greatest importance when investigating the function and physiology of that system (Schmidt, Forne and Imhof, 2014).

The term ‘proteomics’ describes the large-scale study of a system of proteins. Due to their influence in health and disease, the proteins present in specific tissues, organisms, cells or

bodily fluids are often investigated for their abundance, function and any modification therein (Mallick and Kuster, 2010).

Proteomic research often follows a similar workflow; however, depending on the biological question and the complexity of the sample, steps in the process can often change (Mallick and Kuster, 2010). Common workflows start with the cells, tissues or biological fluid to be investigated. The proteins are extracted in the cleanest way possible for their downstream processing and analysis. The proteins are digested to generate peptide fragments, which is often done enzymatically. The peptides are separated electrophoretically, chromatographically, or through a combination of the two, and their mass spectrum is analysed (Di Girolamo *et al.*, 2013).

Mass spectrometry (MS) involves generating gas-phase ions of the sample peptides and separating these ions by their mass-to-charge ratios via a magnetic or electric field produced by a mass analyser. The separated ions are detected as electrical charge, generating signals proportional to the abundance of each species. MS analysis is often performed in tandem, where separated ions are subsequently fired into collision chambers generating multiple ion fragments; analysis of the fragments in the second-stage mass analyser allows more accurate structural predictions of the parent ion(Di Girolamo *et al.*, 2013). The resulting data allows predictive identification of the peptides, and through this predictive reassembly of the peptides into proteins. With the list of proteins identified and their relative or absolute quantities calculated (depending on the method chosen), further functional and bioinformatic analysis can be performed (Schmidt, Forne and Imhof, 2014).

1.14.1. Bioinformatics

Bioinformatics represents a subset of statistical analyses focused on discerning the underlying patterns within 'omics data (genomic, proteomic, lipidomic data etc.) and represents the translational application of computer science, mathematics and statistics to the understanding of biological systems (Rothberg, Merriman and Higgs, 2012). Within proteomic studies, bioinformatic analyses can be crudely separated into two categories, predictive and investigative bioinformatics.

Predictive bioinformatics concerns the comparison of a given proteomic dataset with known protein networks. Common examples include gene ontology (GO) term identification and enrichment which can allow ranking, clustering and comparison of "biological processes", "molecular functions" or "cellular components". Pathway analysis allows identification of specific signalling pathways, the proteins involved and where they sit in the signalling network, it also has the benefit of predicting upstream regulators of the signalling networks (Schmidt, Forne and Imhof, 2014).

Investigative bioinformatics attempts to graphically visualise patterns in the dataset as a whole. Common methods include hierarchical clustering and principal component analysis (Adachi, 2017).

1.14.2. Protein identification and quantitation

A frequently used approach to protein identification involves database searching (Cottrell, 2011). The basic principal involves cross-referencing the spectra of peptides in an experimental dataset with theoretical spectra generated *in silico* from protein sequences in a given database and applying a scoring model, such as cross correlation scoring (SEQUEST)

(Eng, McCormack and Yates, 1994), hypergeometric scoring (X!Tandem) (Craig and Beavis, 2004), Poisson scoring (OMSSA) (Geer *et al.*, 2004), or probability based scoring (MASCOT) (Perkins *et al.*, 1999). As these methods are based on empirical data previously generated and assessed, they are extremely robust. However, their ability can be limited when assessing proteins that harbour specifically challenging characteristics, splice variants, previously unidentified proteins, or proteins containing unknown posttranslational modifications (Lubec and Afjehi-Sadat, 2007).

1.14.3. Predicting protein secretion mechanisms

The protein content of the secretome can be subcategorised based on a variety of secretory mechanisms; these include classical secretion, non-classical secretion (Nickel and Seedorf, 2008) and secretion via EVs, such as exosomes (Raposo and Stoorvogel, 2013).

Several software packages and algorithm-based methods for predicting the mechanism of secretion have been developed and published. In order to identify classical or non-classical secretory mechanisms, these software packages interrogate different protein features, including the primary amino acid sequence, in order to predict the likelihood that a protein enters a secretory pathway (https://omictools.com/secretome-analysis-category).

Sequence alignment is a method of comparing an experimentally resolved sequence of nucleotides (DNA or RNA) or amino acids (protein) with a reference sequence to identify regions of similarity that may suggest shared function, structure or evolution. Programs such as 'Signal-BLAST' employ sequence alignment and predict the presence of a signal peptide (Frank and Sippl, 2008).

Position weighted matrices (PWM) allow for the inclusion of probability at each point in a sequence motif based on the previous sequence alignments, increasing both the sensitivity and the precision of the prediction. The signal peptide prediction software PrediSi uses a method based on a position weighted matrix approach (Hiller *et al.*, 2004).

Machine learning algorithms involve the design of a program, which improves its performance based on previous results and experience, and can employ multiple algorithms, including sequence alignment, consensus sequence or PWM (Swan *et al.*, 2013). 'SignalP' and 'SecretomeP' both employ neural networks to separate proteins in multidimensional space. They assess proteins for features such as cleavage site, signal peptide and/or transmembrane domains using multiple methods such as sequence alignment and hidden Markov models (Nielsen *et al.*, 1997).

Secretion through EVs can be interrogated in a similar way, as prediction of non-classical secretion of a protein encompasses secretion via EVs. Other methods include the cross referencing of a protein's designated identifier (such as UniProtKB accession number) with databases of identifiers known to be found in EVs, such as vesiclepedia or exocarta (Mathivanan and Simpson, 2009; Kalra *et al.*, 2012). As these databases are publicly curated, this method may be more liberal in its approach.

1.14.4. Interrogating the functionality of the secretome

Several software packages which interrogate transcriptomic and proteomic datasets have previously been reported in the literature. These software packages predict protein-protein interactions, signal transduction pathways, molecular networks and biological processes associated with a given dataset (Hu *et al.*, 2011). Example software packages include REACTOME, DAVID, STRING, PANTHER and Ingenuity Pathway Analysis (IPA). REACTOME is

a software package which predicts and maps cellular functions such as signal transduction (Fabregat *et al.*, 2018). DAVID is another program which reduces dimensionality of a given dataset, grouping proteins by functional relationship through GO term enrichment (Huang, Sherman and Lempicki, 2009a, 2009b); the STRING program maps known protein-protein interactions associated with the dataset and predicts functional enrichment (Szklarczyk *et al.*, 2017). PANTHER classifies and clusters proteins/genes for the prediction of molecular functions, biological process and pathways associated with the dataset (Mi, Muruganujan and Thomas, 2013). QIAGEN IPA combines statistical association of proteins/genes in the dataset with those in known signalling pathways and biological function, with causal relationship analysis and directionality of activation (Krämer *et al.*, 2014).

1.15. Scope and aims of this thesis

The risk of liver metastasis in UM patients can be stratified based on clinical, histomorphological and genetic characteristics of the tumour, allowing classification of the patients into groups at either low- or high-risk of progressing to metastatic disease. The biological process by which PUM metastasises is still poorly understood.

This thesis hypothesises that factors secreted by UM cells drive metastasis through the autocrine promotion of molecular mechanisms which encourage tumour dissemination. Furthermore, it hypothesises that secreted factors can influence other cells in the tumour microenvironment; in particular, priming the metastatic niche.

As UM metastasis most commonly involves the liver, Chapter 3 investigates the fibrotic response in the liver of patients with MUM and aims to identify any correlation between markers of fibrosis and clinical and histological features.

Since UM dissemination occurs solely haematogenously, previous work in LOORG investigated the presence of potential biomarkers in the secretome of cells isolated from PUM samples and grown in short term 2D culture. Using this dataset, Chapter 4 investigates the differences in proteomic profiles of the PUM secretome by challenging the dataset with a series of bioinformatic analyses. The aim of the chapter was to elucidate any auto/para/endocrine signalling mechanisms dictated by those proteins secreted by PUM into their local environment and to assess how they may aid PUM progression and/or affect the patients' risk of metastatic spread of UM.

Chapter 5 details the selection and optimisation of methods for the isolation, characterisation and analysis of UM EVs.

Chapter 6 investigates the role of EVs in UM by analysing the differences in proteomic profile between EVs isolated from a panel of distinct UM cell lines.

Chapter 7 brings together the findings of each chapter, collectively discussing consistent themes in the results relative to the current literature. It examines the possible implications of the research to the wider scientific community and suggests possible future research that could come as a result of the conclusions drawn herein.

CHAPTER 2: MATERIALS AND METHODS

2.1. Microtomy and slide preparation

Sections were prepared from formalin-fixed paraffin-embedded (FFPE) MUM tissue samples with a microtome set to a thickness of 4 μm. These were adhered to Xtra-adhesive™ slides (Leica biosystems, Milton Keynes, UK) for immunohistochemistry and Superfrost™ slides (VWR, Lutterworth, UK) for haematoxylin and eosin (H&E) staining, by floatation on water. Slides were subsequently dried overnight at 45-50^{o}C.

2.2. Slide preparation for histological stains

Slides were deparaffinised through three 10-minute incubations in xylene and brought to water through sequential 1-minute incubations in ethanol at 100%, 90%, 70% and 50% concentration, followed by a 1-minute incubation in distilled water (ethanol dilutions were in distilled water).

2.3. Haematoxylin and eosin staining

Following preparation, slides were incubated in Harris haematoxylin (Leica, UK; catalogue number: 3801560) for 3 minutes and washed with running tap water until the water runs clear. The slides were then differentiated in 0.25% acid alcohol (HCl in 90% ethanol). Slides were washed in tap water for 1 minute and blued in scotts tap water for 1 minute. Slides were washed in running tap water until the water ran clear. Slides were then incubated in 95% ethanol for 1 minute before incubation in Eosin staining solution (Leica, UK; catalogue number: 3801600) for 45 seconds. Slides were then dehydrated in 95% ethanol for 1 minute and 100% ethanol twice for 1 minute each time, followed by two incubations in xylene for two minutes each time. Slides were then mounted in DPX (Leica, UK; catalogue number: 3808601ES) before cover slipping.

2.4. Gomori trichrome staining of uveal melanoma liver metastases

Gomori trichrome staining was performed according to the manufacturer's instructions (Leica). Briefly, the slides were subjected to secondary fixation with Bouin's fixative for 1 hour at 56 °C and subsequently rinsed in running tap water for 3-5 minutes (until the yellow colouring was removed). Slides were placed in Weigert's Iron Haematoxylin stain for 10 minutes (the working Weigert's haematoxylin solution was a combination of equal parts Weigert's solution A and Weigert's solution B, provided by the supplier and made <1 hour prior to staining). Sections were rinsed in running tap water for 5-10 minutes until the water ran clear and subsequently incubated in the Gomori's trichrome green stain for 15 minutes. Slides were incubated in 1% Acetic Acid Solution for 1 minute and immediately rinsed in distilled water for 30 seconds. The slides were then dehydrated in 95% ethanol for 1 minute followed by two 1-minute incubations in 100% ethanol. Sections were cleared through three 1-minute incubations in xylene and mounted in DPX resinous mounting media (Fisher Scientific, Loughborough UK).

2.5. Immunohistochemical staining of uveal melanoma liver metastases

Dewaxing and antigen retrieval were performed using the Dako PT Link. IHC was performed using the Dako Autostainer Plus system and Envision^{TM} FLEX Kit according to the manufacturers' instructions (Dako UK Ltd, Cambridgeshire, UK). Antigen retrieval was performed at high pH (pH 9.0) at 96°C for 20 minutes and the slides then incubated in FLEX wash buffer for 5 minutes. Using the ready to use reagents in the Dako Envision^{TM} FLEX Kit, slides were blocked for endogenous peroxide for 5 minutes followed by three sequential wash steps with 1x FLEX wash buffer. Samples were then incubated with the primary antibody for 30 minutes and subsequently washed three times with 1x FLEX wash buffer. Depending on the host of the primary antibody, mouse/rabbit linker was added, and slides

were incubated for 15 minutes. Slides were washed with 1x FLEX buffer and incubated in horseradish peroxidase for 20 minutes.

Positive staining was detected by 30 minutes incubation with AEC peroxidase substrate (3-amino-9-ethylcarbazole, Vector Labs, Peterborough, UK). Slides were counterstained with Mayers haematoxylin (VWR) for 10 seconds, washed in running tap water and then blued in Scott's tap water (Leica) for 30 seconds before mounting with Aquatex aqueous mounting medium (Merck Millipore, Nottingham, UK).

2.6. Histological assessment of uveal melanoma metastases

UM liver metastases were assessed for tumour stage according to criteria detailed by Grossniklaus in their 2013 paper (Grossniklaus, 2013)*;* for dominant cell type (Epithelioid or spindle), degree of pigmentation (mild/moderate/strong), necrosis (absent [N]/present [Y]), and growth pattern (Infiltrative/nodular) through examination of archival H&E stained slides of the samples.

2.7. Culture of primary uveal melanoma cells from patient tumours

Following research ethics committee approval (HRA REC Ref 11/NW/0568), fresh PUM specimens of consenting patients undergoing surgical removal as treatment were obtained from the Liverpool Ocular Oncology Biobank (HRA REC Ref 16/NW/0380).

Primary UM cell culture was performed by Dr Martina Angi as previously published (Angi *et al.*, 2016). For each UM sample, a single cell suspension was obtained by mincing the tissue, followed by incubation with 500 U/mL of type I collagenase (Sigma-Aldrich Company Ltd, Dorset, UK) at 37°C for approximately 1 hr, with occasional agitation of the solution. Single cells were recovered by centrifugation (250 × g for 2 min) and re-suspended in primary

culture medium (1:1 αMEM (Life Technologies Ltd, Paisley, UK): Quantum 3-21, (PAA Laboratories Ltd, UK), 10% fetal bovine serum, plus antibiotics and 2 mM L-Glutamine). The cells were seeded into two 75 cm2 tissue culture flasks (Falcon, VWR international, Leicestershire, UK) and grown to approximately 75–80% confluence.

2.8. Culture of primary normal choroidal melanocytes from post-mortem human eyes

The culture and characterisation of normal choroidal melanocytes (NCM) was performed by Dr Michele Madigan as previously published (Angi *et al.*, 2016). NCM were isolated, with consent, from post-mortem human eyes after a delay of less than 18 hours, from the Lions New South Wales Eye Bank. The study was performed with approval from the University of Sydney and University of New South Wales Human Research Ethics Committee. NCM were isolated and grown in melanocyte growth medium as previously described (Lai *et al.*, 2007). Briefly, the choroid of the posterior chamber was isolated from the vitreous, retina and sclera through a combination of incubation with 0.25% trypsin for 1 hr at 37^{o}C and excision with a dissecting microscope. Choroidal samples were disaggregated with 0.25% trypsin solution at 4°C overnight followed by 37°C for 1 hr, then with 400 U/ml collagenase in F12 medium with 10% FBS at 37°C for 3 hr. Released cells were collected each hour during the incubation and cultured in melanocyte growth medium (MGM) [Ham's F12 supplemented with 10% heat inactivated fetal bovine serum (FBS), 2 mM L-glutamine, 50 IU/ml penicillin/50 µg/ml streptomycin and 10 ng/ml cholera toxin (Sigma Chemical Co., St. Louis, MO), 100 nM PMA (phorbol 12-myristate 13-acetate) and 0.1 mM isobutylmethylxanthine (IBMX) (Sigma)]. Contaminant cells were eliminated by adding the selective cytotoxic agent, geneticin, when necessary. Cells were passaged by detaching with 0.25% trypsin/0.1% EDTA for 2 min and centrifugation at 290x *g*, resuspended in MGM and sub-cultured in 25 cm^2 flasks. Passage 1–3 melanocytes were used for all experiments.

Immunofluorescence staining was performed on a subset of each NCM culture grown in 8-well chamber slides. Cells in chamber slides were fixed in 2% paraformaldehyde in PBS (pH 7.4) for 20 min at RT, rinsed in PBS and blocked in 5% BSA prior to immunofluorescence staining.

2.9. Secretome collection and preparation from cultured primary cells

Secretomes from PUM cultures were collected as previously published by Dr Martina Angi (Angi *et al.*, 2016). PUM and NCM cell monolayers were rinsed three times with 10 mL of PBS, incubated with 10mL of serum free medium (SFM; phenol-red free αMEM, Life Technologies Ltd) for 1 hr, and rinsed once again with fresh SFM. Cells were then incubated with 8 mL of SFM for 48 hr, and the conditioned medium at the end of the incubation period was defined as the secretome. UM secretomes were aliquoted and stored at −80°C until further analysis.

2.10. Liquid chromatography tandem mass spectrometry of uveal melanoma and normal choroidal melanocyte secretomes

All proteomic analyses of the PUM and NCM secretome samples were conducted together, once the collection of all samples had been completed. A standard Bradford assay was employed to determine the total protein content of each UM secretome sample. UM secretomes were adsorbed onto StrataClean™ beads (Stratagene®, Hycor Biomedical Ltd., Edinburgh, UK), to concentrate the protein prior to proteome analysis (McLean *et al.*, 2007). The beads were re-suspended in 80 µL of 25 mM ammonium bicarbonate with 5 µL of 1%$_{(w/v)}$ Rapigest (Waters, Hertfordshire, UK). The samples were heated at 80°C for 10 min, reduced with the addition of 5 µL of 60 mM DTT and subsequently heated at 60°C for 10 min. Samples were cooled prior to alkylation with 5 µL of 180 mM iodoacetamide and incubation at RT for 30 min in the dark. Porcine trypsin (sequencing grade, Sigma) (1 µg)

was added to digest the proteins and the samples were incubated at 37°C overnight on a rotary mixer. Peptide digests were then acidified by the addition of 1 µL of trifluoroacetic acid (TFA) and incubated at 37°C for 45 min. Samples were then centrifuged at 17,000 × *g* for 30 min and the supernatants were transferred to 0.5 mL low-bind tubes and further centrifuged (17,000 × *g* for 30 min). 10 µL of each peptide mixture was prepared for nano LC-MS/MS.

Digests (2 µL) from each sample were loaded onto a trap column (Acclaim PepMap 100, 2 cm × 75 µm inner diameter, C18, 3 µm, 100 Å) at 5 µl min^{-1} with an aqueous solution containing 0.1%$_{(v/v)}$ TFA and 2%(v/v) acetonitrile. After 3 min, the trap column was set in-line with an analytical column (Easy-Spray PepMap® RSLC 50 cm × 75 µm inner diameter, C18, 2 µm, 100 Å) (Dionex). Peptides were loaded in 0.1%(v/v) formic acid and eluted with a linear 95 min gradient of 3.8 – 40% buffer B (HPLC grade acetonitrile 80%(v/v) with 0.1%(v/v) formic acid) at 300 nl min^{-1}, followed by a 5 min washing step at 99% solvent B and a 15 min equilibration step at 3.8% solvent B. All peptide separations were carried out using an Ultimate 3000 nano system (Dionex/Thermo Fisher Scientific). The column was operated at a constant temperature of 35°C and the LC system coupled to a Q-Exactive mass spectrometer (Thermo Fisher Scientific). The Q-Exactive was operated in data-dependent mode with survey scans acquired at a resolution of 70,000 at m/z 200. Up to the top 10 most abundant isotope patterns, with charge states +2, +3 and/or +4 from the survey scan, were selected with an isolation window of 2.0 Th for fragmentation by higher energy collisional dissociation, with normalized collision energies of 30. The maximum ion injection times for the survey scan and the MS/MS scans were 250 and 100 ms, respectively, and the ion target value was set to $1x10^6$ for survey scans and $1x10^5$ for the MS/MS scans. Repetitive sequencing of peptides was minimized through dynamic exclusion of the sequenced peptides for 20 sec (Hammond *et al.*, 2016).

2.11. Fasta file generation

The protein accession numbers generated by the Progenesis software were exported and multiple, secondary accession numbers were removed to leave only primary accession numbers. These were then uploaded into Uniprot (www.uniprot.org) to generate primary amino acid sequences for each protein, which display the peptide sequence as amino-acid single letter code. Gene ontology information about "cellular component" and "subcellular location" were also recorded (Ashburner *et al.*, 2000).

2.12. Assessing the likelihood of "classical secretion" of a protein

Classical secretion was predicted with the online freeware "SignalP" (described in Chapter 4). Amino acid sequences were uploaded manually into the online software "SignalP v4.0" with default settings selected for eukaryote analysis with a default D-score cut-off for optimised correlation in both the presence and absence of transmembrane segments (TM-regions) in the dataset (D-scores above 0.5 when TM-regions are present and 0.45 when absent suggest probable secretion). The method was set to allow inclusion of TM-regions and output was selected to be short and non-graphical.

2.13. Assessing the likelihood of "non-classical" secretion of a protein

Primary sequences were uploaded into "SecretomeP v2.0" to generate individual predictions of the likelihood of non-classical protein secretion. Mammalian analysis was performed with a Neural Network score (NN-score) cut-off of 0.6 as suggested by the developers. Proteins were identified as 'non-classically' secreted when the Neural network-(NN) score exceeded the threshold and no signal peptide was present.

2.14. Assessing the likelihood of the secretion of identified proteins via extracellular vesicles

The “Exocarta v5.0 (2015)” protein/mRNA dataset was downloaded from the website (www.exocarta.org/download). The list was initially filtered to remove mRNA data and non-human data leaving only a list of proteins reported in the scientific literature to be found in humans. The ENTREZ gene ID’s were uploaded into “Uniprot” to generate the corresponding accession numbers. Using Excel each protein accession number from the experimental dataset was cross- referenced with the generated accession numbers of proteins remaining in the exocarta list with the function {=IF((COUNTIF([Exocarta accession list],[experimental protein accession]))>0,”YES”,”no”)}. The exocarta prediction method was also strengthened by cross-referencing the experimental dataset with the Uniprot output using a substring text search in the “GO ontology column” for *“exosome”* [=IF(COUNTA([cells containing each secretion prediction *(binary output)*])>0,”YES”,”no”)].

2.15. Comparative analysis of the primary uveal melanoma proteomic secretome

Protein abundances were grouped by disease state into four groups: (1) high risk UM (HR-UM); (2) low-risk UM (LR-UM); (3) total UM (UM); (4) normal choroidal melanocytes (NCM). Samples were stratified into metastatic risk groups based on their chromosome 3 status: loss of one copy of chromosome 3 (M3) was deemed high risk, where no loss of chromosome 3 (D3) was considered low risk of metastatic progression. The average normalised abundance for each protein was calculated with Microsoft Excel. Mann-Whitney U tests were performed between select groups (UM versus NCM, HR UM versus LR UM) using SPSS software (v.24; IBM – New York, USA). This allowed experimental fold changes with associated statistical significance to be determined between disease states and for upload into the pathway analysis software.

2.16. Pathway analysis of proteomic datasets

Data were analysed using QIAGEN's Ingenuity® Pathway Analysis (IPA®, QIAGEN Redwood City, www.qiagen.com/ingenuity). Each of the core analyses were performed using the same settings shown in Figures 2.1. and 2.2. The "ingenuity knowledgebase" was used as the reference set and relationships to consider was set to "direct relationships" only. The Networks tab was altered to exclude endogenous chemicals or casual networks, default settings of 35 molecules per network and 25 networks per analysis were employed. The data sources tab was set to all, confidence options were set to "Experimentally observed" and species was limited to "Human" only, applying stringent filters. "Tissues and Cell Lines" and "Mutation" tabs were set to "All" and relaxed filters were applied. There was no cut off used for either fold change or p-value.

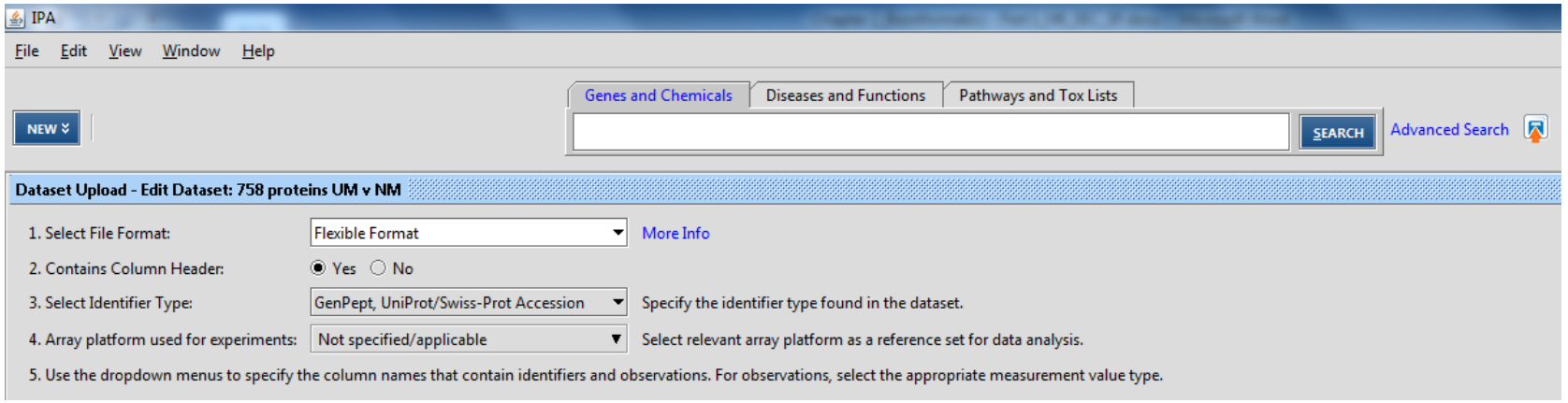

Figure 2.1. Ingenuity Pathway Analysis (IPA) settings for 'Dataset upload' of the proteomic datasets

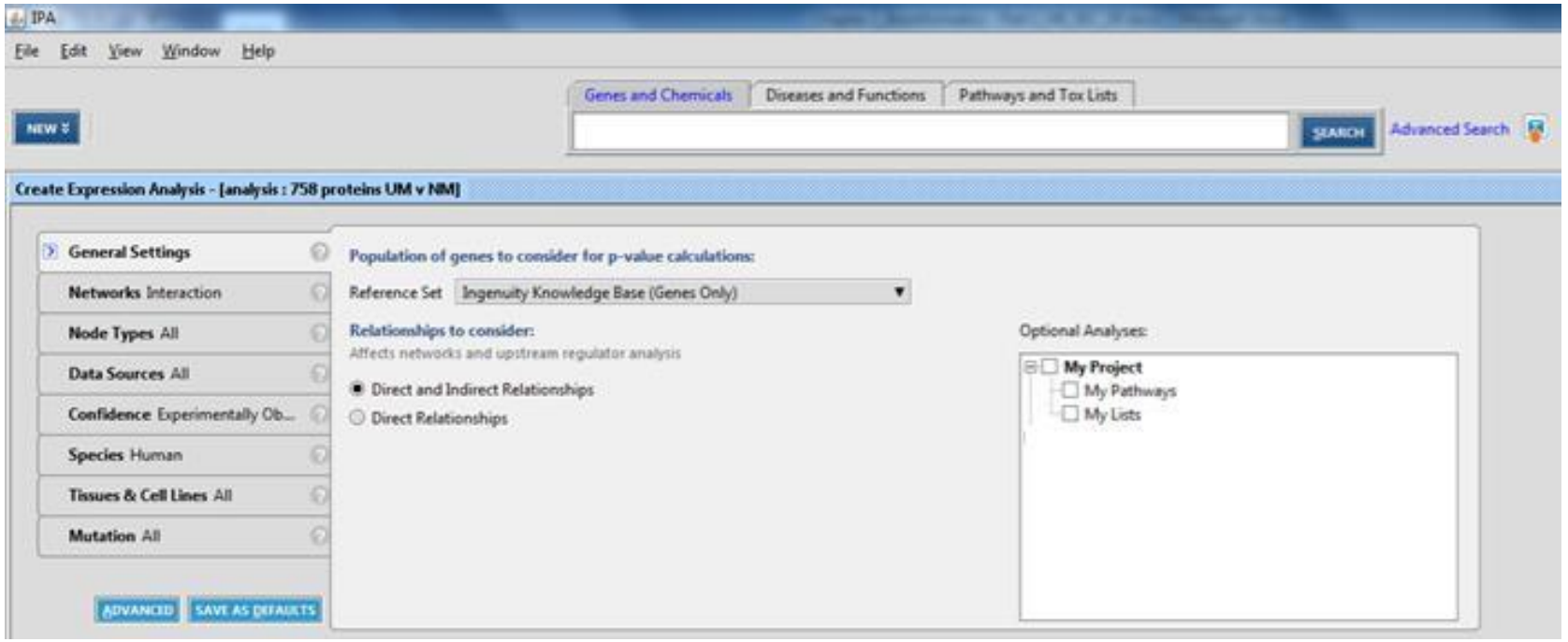

Figure 2.2. Ingenuity Pathway Analysis (IPA) settings for (A) 'Dataset upload' and (B) 'Core Analysis' of the proteomic datasets

2.17. Uveal melanoma cell line culture and secretome collection for extracellular vesicle isolation

UM cell lines (92.1, Mel270, MP41, OMM1, OMM2.3, OMM2.5) were cultured in RPMI 1640 (Thermo Fisher Scientific, UK) containing 10% (v/v) fetal bovine serum (Labtech, Heathfield, UK) and 2 mM L-glutamine (Thermo Fisher Scientific, UK) in a humidified atmosphere at 37°C, 5% CO_2. At ~50% confluence (around 3 days after seeding) the growth media was removed and the cells were washed three times with serum-free, phenol-red-free RPMI 1640 (Thermo Fisher Scientific, UK), incubating the wash steps for 30 seconds, 5 minutes and 20 minutes respectively. After the final wash, the media was removed and the cells were incubated for 48 hours in serum-free, phenol-red-free RPMI with L-glutamine. After 48 hours, the cell-conditioned media was collected and centrifuged at 300x *g* for 5 minutes (to remove non-adherent or dead cells), followed by 2000x *g* for 20 minutes (to remove large cellular debris and large apoptotic bodies). The supernatants were then frozen at -80^{o}C and stored prior to UC. All UM cell lines were STR profiled by members of LOORG at the University of Liverpool and matched known profiles (Amirouchene-Angelozzi *et al.*, 2014; Jager *et al.*, 2016). All cell lines were also routinely assessed for mycoplasma contamination by members of the University of Liverpool and shown to be mycoplasma free.

2.18. Ultracentrifugation of uveal melanoma cell line secretome for the enrichment of uveal melanoma extracellular vesicles

Frozen samples were thawed in a water bath set to 37^{o}C and vortexed for ~60s to loosen aggregated EV and reduce EV retention in the storage vessels (Zhou *et al.*, 2006). A 600 µL aliquot of "Pre-ultracentrifuged (UC) culture supernatant" was taken for size distribution analysis. The method of UC employed was adapted from Théry *et al*., with some modifications (Théry *et al.*, 2006). Supernatant samples were pipetted into Ultra Clear UC

tubes (Beckman Coulter, United States) and submitted to UC in a Beckman coulter SW 40 Ti Swinging-Bucket Rotor (Beckman Coulter, United States) at 10,000x *g* for 45 minutes to remove MVs and small ABs; the pellet was discarded and the supernatants were submitted to 100,000x *g* for 90 minutes to pellet remaining EV. The supernatant was discarded, the remaining pellet was resuspended in 14 mL PBS (Fisher Scientific - UK Ltd, UK) to solubilise any co-precipitated protein aggregates and this was subjected to a further 90-minute centrifugation at 100,000x *g.* The remaining pellets were resuspended in <100 µL PBS for further analysis. Enriched EV samples were frozen and stored at -80^{o}C prior to downstream analyses. Upon thawing, samples were once more vortexed for ~60s to loosen aggregated EVs and reduce EV retention in the storage vessels.

2.19. Nanoparticle tracking analysis of enriched uveal melanoma extracellular vesicles

Thawed EV samples were diluted to their "pre-UC" concentration in PBS and a ~600 µL aliquot was injected into the viewing chamber of a Nanosight – NS300 (Malvern, UK) for nanoparticle tracking analysis. The samples were recorded five times for 60 seconds each recording with the camera level set to 14 and the focus set manually to reduce 'halos'; the chamber temperature was set to 22^{o}C for each assessment. Between samples the chamber was washed with PBS until there were no particles detectable at camera level 16.

When processing the recordings of each sample, the detection threshold was established to incorporate each visible particle while minimising inappropriate detection of "halos"; this was consistent between samples and set at level 5.

The above process was also conducted for aliquots of "pre-UC conditioned media", for comparison of size distribution with the corresponding final EV isolation.

2.20. Transmission electron microscopy of uveal melanoma extracellular vesicles

For the visualisation of single EV, 5µl of each sample was adsorbed onto formvar/carbon coated 200 mesh copper grids (Agar Scientific, UK) by incubating at room temperature for 20 minutes. Surplus sample was removed by passing the grid on Whatman blotting paper (VWR, UK) and the grids were then rinsed twice with PBS and fixed with PBS containing 1% glutaraldehyde (Sigma Aldrich, UK) for 5 minutes at room temperature. Following fixation in glutaraldehyde the grids were washed seven times with distilled water, each wash lasting 2 minutes. The grids were then incubated for 5 minutes on 1% uranyl acetate (pH 7) (Sigma Aldrich, UK), followed by 10 minutes in 5% uranyl acetate/2% methylcellulose (Sigma Aldrich, UK) on ice (steps with uranyl acetate are carried out in the dark). The surplus methyl cellulose was removed through the grid gates by passing them across Whatman blotting paper. Each of the above steps were performed by resting/suspending the grid, face down, on a "bead" of solution on parafilm. Images were taken with a FEI 120kV Tecnai G2 Spirit BioTWIN Transmission electron microscope (FEI, United States).

2.21. Western blotting of lysed uveal melanoma extracellular vesicles and uveal melanoma whole cell lysates

Cell lysates were generated by washing sub confluent cell cultures with PBS and incubating on ice in a "1x lysis buffer" containing 1% (w/v) sodium dodecylsulphate (SDS) (Fisher Scientific, UK), 5 mM ethylenediaminetetraacetic acid (EDTA) (Sigma Aldrich, UK), 50 mM Tris HCl (Fisher Scientific, UK) and 1% (v/v) glycerol, and 1x halt protease inhibitor cocktail (Thermo Fisher Scientific, UK) at pH 6.8. After 20 minutes incubation on ice, the cells were scraped from the culture flask into the lysis buffer, collected, boiled at 90 ^{o}C for 10 minutes and sonicated in a water bath on high for 10 minutes (30 seconds on, 30 seconds off

repeated). Lysates were then centrifuged at 15,000x *g* at 4 ^{o}C for 10 minutes and the supernatant was decanted.

Protein quantitation of whole cell lysate samples was achieved with the DC (detergent compatible) protein assay (Bio-Rad, UK; catalogue number: 5000116), according to the manufacturer's instructions. The working reagent was produced by diluting reagent S in reagent A at a 1:50 ratio. Samples were added to a 96-well plate (Greiner, UK) at 5 µL per well, followed by 25 µL per well of the working reagent and 200 µL per well of reagent B. Additional wells were also processed with a serial dilution of bovine serum albumin (BSA) (Sigma, UK) at known concentrations. The plate was gently agitated for 5 seconds to ensure thorough mixing and incubated for 15 minutes before the absorbance was read at 750 nm. The absorbance measurements for the serial dilution of BSA were used to calculate the protein concentration of the cell lysate samples.

EV lysates were generated by adding a "10x lysis buffer" (to a final concentration of 1X) containing 10% (w/v) SDS, 50 mM EDTA, 500 mM Tris HCl and 1x halt protease inhibitor cocktail at pH 6.8 to suspended EV samples. Whole cell and EV lysate samples were aliquoted and frozen at -20 ^{o}C until use.

Whole cell and EV lysates were thawed on ice prior to western blotting and then boiled at 95 ^{o}C for 10 minutes in a SDS sample buffer containing 50 mM Tris/HCl (pH 7.5) (Fisher Scientific, UK), 4% SDS containing 0.01% Bromophenol Blue (Sigma Aldrich, UK) and 5% β-mercaptoethanol (Sigma Aldrich, UK) to reduce and further denature the proteins.

Western blots were conducted in denaturing and reducing conditions. SDS-PAGE gels were made in house at 12% (v/v) acrylamide (National Diagnostics™, United Stated) in 1x

Protogel resolving buffer (National Diagnostics™, United Stated) diluted in distilled water. The gel was polymerised by adding ammonium persulfate at a final concentration of 0.3% (w/v) (Sigma Aldrich, UK), and TEMED at a final concentration of 0.15% (v/v) (Sigma Aldrich, UK). This was overlaid with water during polymerisation, after which the stacking gel was formed with 5% acrylamide (w/v) (National Diagnostics™, United Stated) in 1x Protogel stacking buffer (National Diagnostics™, United Stated), polymerised with ammonium persulfate at a final concentration of 0.3% (w/v) (Sigma Aldrich, UK), and TEMED at a final concentration of 0.15% (v/v) (Sigma Aldrich, UK).

Reduced and denatured samples were loaded alongside a BLUeye Pre-Stained Protein Ladder 10-245kDa (Geneflow, UK). Whole cell lysates were all loaded at 10 µg per lane, EV lysates were loaded at 10 $x10^6$ lysed EVs per lane (determined by NTA).

Electrophoresis was run in 25 mM Tris base (Fisher Scientific, UK) containing 192 mM glycine (Fisher Scientific, UK) and 0.1% (w/v) SDS for approximately 1 hour at a constant 50mA. Protein was then transferred from the gel to PVDF western blotting membrane (0.22 µm pore size; Sigma Aldrich, UK) at 400mA for 1 hour in a 25 mM Tris base, 192 mM glycine (Fisher Scientific, UK) buffer.

After protein transfer, the membrane was blocked in 2.5% marvel milk powder (Tesco, UK) in Tris-buffered saline (TBS), containing 200 mM Tris base and 1.2 M glycine at pH 7.4. The blot was then washed with TBS containing 0.1% tween-20 (TBS-T) and incubated with primary antibodies overnight.

The blot was washed with TBS-T five times and incubated with the HRP-tagged secondary antibody for 1 hour before another five washes in TBS-T. The membrane was then

incubated with the enhanced chemiluminescence western blot detection kit ‘SuperSignal West Pico Plus’ (Thermofisher Scientific, UK) according to the manufacturer’s instructions. The membrane was removed from incubation and any excess detection solution was allowed to drain off. The membrane was then placed between two clear plastic sheets and worked with a roller to remove any air bubbles. The chemiluminescence was then imaged with the GeneGnome XRQ imaging system.

2.22. Liquid chromatography tandem mass spectrometry of enriched uveal melanoma extracellular vesicles

EV pellets were submitted for processing and LC-MS/MS in triplicate. All steps of LC-MS/MS and protein identification/quantitation were performed by Dr Deborah Simpson in collaboration with the Centre for Proteome Research at the University of Liverpool. Each pellet was re-suspended in 25 µL of PBS, 20 µL of 50 mM ammonium bicarbonate and 5 µL of 1%(w/v) Rapigest (Waters, UK) was added and the samples were heated at 80°C for 10 min. Samples were reduced, with the addition of 5 µL of 60 mM DTT and heated at 60°C for 10 min. They were then cooled prior to the addition of 5 µL of 180 mM iodoacetamide and incubation at RT for 30 min in the dark. Porcine trypsin (sequencing grade; Sigma, UK) (1 µg) was added and the sample was incubated at 37°C overnight on a rotary mixer. The samples were acidified by the addition of 1 µL trifluoroacetic acid (TFA), followed by incubation at 37°C for 45 min. Samples were centrifuged at 17,000× *g* for 30 min and the clarified supernatants were transferred to 0.5 mL lobind tubes, centrifuged once more at 17,000× *g* for 30 min and. 10 µL of each peptide mixture was prepared for nano LC-MS/MS. Digests from each sample were loaded onto a trap column (Acclaim PepMap 100, 2 cm × 75 µm inner diameter, C18, 3 µm, 100 Å) at 5 µl min−1 with an aqueous solution containing 0.1%(v/v) TFA and 2%(v/v) acetonitrile. After 3 min, the trap column was set in-line with an analytical column (Easy-Spray PepMap® RSLC 50 cm × 75 µm inner diameter, C18, 2 µm, 100 Å) (Dionex, UK).

Peptides were loaded in 0.1% (v/v) formic acid and eluted with a linear gradient of 3.8 – 40% buffer B (HPLC-grade acetonitrile 80% (v/v) with 0.1% (v/v) formic acid) over 95 minutes at 300 nl/minute, followed by a washing step (5 min at 99% solvent B) and an equilibration step (15 minutes at 3.8% solvent). All peptide separations were carried out using an Ultimate 3000 nano system (Dionex/Thermo Fisher Scientific, UK). The column was

operated at a constant temperature of 35°C and the LC system coupled to a Q-Exactive mass spectrometer (Thermo Fisher Scientific).

The Q-Exactive was operated in data-dependent mode with survey scans acquired at a resolution of 70,000 at m/z 200. Up to the top 10 most abundant isotope patterns with charge states +2, +3 and/or +4 from the survey scan were selected with an isolation window of 2.0 Th for fragmentation by higher energy collisional dissociation with normalized collision energies of 30. The maximum ion injection times for the survey scan and the MS/MS scans were 250 and 100 ms, respectively, and the ion target value was set to $1x10^6$ for survey scans and $1x10^5$ for the MS/MS scans. Repetitive sequencing of peptides was minimized through dynamic exclusion of the sequenced peptides for 20 sec (Hammond *et al.*, 2016).

2.23. Protein identification and quantitation

Protein identification and quantification of raw mass spectral data files were processed using Progenesis-QI (v2; Nonlinear Dynamics) to determine total protein abundances. All raw files were initially automatically aligned to a pooled sample file. This aggregated spectral map contains MS features from all aligned runs enabling maximal protein identification across all samples. Data were then separated into the experimental sample groups of biological triplicates for each cell line; Mel270, 92.1, MP41, OMM1, OMM2.3 and OMM2.5.

An aggregate peak list file (.mgf format) containing only MS data relating to peptides ranked 1 – 5, was then searched against a human reviewed UniProt database using the Mascot search engine (version 2.6.1; Matrix Science, UK). A precursor ion tolerance of 10ppm and a fragment ion tolerance of 0.01Da were used, with carbamidomethylation of

cysteine set as a fixed modification and oxidation of methionine as a variable modification. Trypsin was the specified enzyme and one missed cleavage was allowed. The peptide matches in Mascot were set to a 1% false discovery rate before being re-imported into Progenesis and UniProt accession numbers being assigned to peptides.

Progenesis QI also allowed the quantitation of normalized relative protein abundance by averaging the individual abundances of each unique peptide for each protein and applying a global scaling factor across sample runs between cell line groups. This was used to calculate the average abundance for each protein in each sample run. These were used to create an average normalized relative abundance for each cell line and each sample group (primary uveal melanoma, PUM; metastatic uveal melanoma MUM; Guanine nucleotide-binding protein G(q) subunit alpha mutants, *GNAQ*-mutants; and Guanine nucleotide-binding protein G subunit alpha-11 mutants, *GNA11* mutants).

The resultant dataset was filtered to include only proteins identified with three or more unique peptides. The filtered dataset was used for all further downstream analyses.

2.24. Assessing the comparability of the uveal melanoma extracellular vesicles proteome

The mean log10 abundance values of each protein were ranked in ascending order and plotted for each cell line. The scales were standardised for ease of comparison. Pairwise comparison was also performed with the R package “pairs.panel”. This provided a visual overview of the descriptive statistics for each proteome.

2.25. Functional enrichment and gene-ontology analysis of the uveal melanoma extracellular vesicles proteome

The accession numbers of the proteins in the dataset were analysed with the online software Gorilla (Eden *et al.*, 2009) to assess the presence of enriched gene-ontology (GO) terms associated with the proteins present in UM EV. Uniprot accession IDs were uploaded to the online freeware as directed. The organism was set to Homo sapien, running mode was set to “single ranked list of genes” and ontology requested was set to “All”. Clustering of the enriched GO terms was assessed and visualised with the online freeware ReviGO clustering (Supek *et al.*, 2011).

2.26. Comparing the proteomes of the uveal melanoma secretome with that of uveal melanoma extracellular vesicles

The datasets from Chapter 4 and Chapter 6 were compared to evaluate the statistical likelihood of their overlap using the hypergeometric probability assessment originally described by Gonin *et al.,* and employed according to Kim *et al.,* (Gonin, 1936; Kim *et al.*, 2001).

Significantly associated pathways were compared with Microsoft Excel () using the data output from Ingenuity Pathway Analysis (Qiagen). Association values representing Fisher right-tailed exact assessment were compared and ordered by the magnitude of difference. This was done for ‘canonical signalling pathways’, ‘disease and biological function’ and for predicted ‘upstream regulators’.

CHAPTER 3: HISTOLOGICAL AND IMMUNOHISTOCHEMICAL ANALYSIS OF HUMAN UVEAL MELANOMA METASTASES IN THE LIVER

3.1. Introduction

As discussed above, UM is known to preferentially metastasise to the liver in around half of all patients diagnosed with this disease (Coupland *et al.*, 2013). The risk of metastatic spread is associated with genetic changes occurring in the PUM. In particular, the loss of one copy of chromosome 3, copy number variations causing gains in 8q, loss in 1p, 6q and 8p, and loss of nuclear translocation of the deubiquitinase BAP1 through mutations in the *BAP1* gene (Ewens *et al.*, 2013; Cassoux *et al.*, 2014; Kalirai *et al.*, 2014).

Although the molecular mechanisms by which PUM cells escape the eye and spread to the liver are unclear, there are data suggesting that PUM cells with increased c-MET expression more readily invade the microvasculature, aiding systemic spread (Hendrix *et al.*, 1998) preferentially to the liver due to chemokine signalling through constitutive expression of CXCR4 (Li, Alizadeh and Niederkorn, 2008). Once in the liver, single UM cells are thought to give rise to MUM lesions in either nodular or infiltrative patterns (Grossniklaus, 2013). In the infiltrative growth pattern, the UM cells may metastasize to the sinusoidal spaces in the parenchyma of the hepatic lobule (Grossniklaus *et al.*, 2016). Here the UM cells draw nutrition from the blood in the sinusoidal space and seem to replace or destroy local hepatocytes. This type of growth pattern is often termed ‘miliary’ presentation, where metastases present as multiple submillimetre sized lesions, and is associated with a poorer prognosis (Mariani *et al.*, 2009).

In the nodular growth pattern, the circulating UM cells seed in the periportal area of the hepatic triad, where they draw nutrition from the blood supply in the portal venules

(Grossniklaus *et al.*, 2016). As they grow, the MUM lesions efface local hepatocytes, forming larger more distinct tumours than the infiltrative growth pattern. Nodular MUM lesions are often surgically resectable, which is known to positively influence prognosis (Mariani *et al.*, 2009).

Once MUM is established in the liver, if surgical resection is not possible due to the presence of multiple metastatic deposits, MUM is invariably fatal (Frenkel *et al.*, 2009). The one-year survival of patients with metastases is reported to be around 15%, with a reported median survival ranging from 4 to 15 months (Carvajal *et al.*, 2017). Currently there is a lack of alternative effective treatment options for these patients, which have previously been based around those therapies effective in cutaneous melanoma.

The characteristic progression of UM to the liver has been investigated due to its frequency and fatality; however, the number of studies remains small. MUM in the liver has previously been shown to present with distinct features such as frequent miliary presentation (Carvajal *et al.*, 2017), consistent chromosomal copy number variations of chromosomes 3 and 8q as noted in the PUM (McCarthy *et al.*, 2016) as well as increased collagen deposition at the metastatic site (Grossniklaus, 2013). An increase in the production of ECM components, such as collagen, is associated with the inflammatory response fibrosis (Friedman, 2004), a feature known to impact cancer progression (Cox and Erler, 2014). Fibrosis is a dynamic healing process involving many cellular mechanisms and is characterised by increased ECM deposition (Friedman, 2004), decreased ECM turnover (Lu *et al.*, 2011) and gross remodelling of normal cellular architecture (Mormone, George and Nieto, 2011). Fibrosis in the liver occurs most often in response to cellular stress; such as, physical injury, local infection, alcohol/drug abuse (Friedman, 2004) or cancer (Whatcott *et al.*, 2015). Increasing evidence suggests an involvement of fibrosis in both primary liver

cancer (Affo, Yu and Schwabe, 2017) and the metastatic spread of other cancers to the liver (Kondo *et al.*, 2016).

Cancer has also been considered an aberrant healing process, resulting in modulation of ECM composition (Schäfer and Werner, 2008). While the physiological composition of the ECM is generated by a complex dialogue involving multiple cell types (Frantz, Stewart and Weaver, 2010), a major cell type in the regulation of ECM composition in cancer pathology are cancer-associated-fibroblasts (CAFs) (Karagiannis *et al.*, 2012). Tumour cells are thought to activate local normal fibroblasts through the secretion of a variety of cytokines and growth factors. This includes transforming growth factor beta-1 (TGFβ1), epidermal growth factor (EGF), platelet derived growth factor (PDGF) and fibroblast growth factor 2 (FGF2), among others (Räsänen and Vaheri, 2010). TGFβ1 is derived from both paracrine and autocrine sources and is the most potent fibrogenic cytokine in the liver (Breitkopf *et al.*, 2006; Inagaki and Okazaki, 2007). Quiescent hepatic stellate cells (HSC) reside in the perisinusoidal space of the liver, where upon activation through external stimuli act in a wound healing mechanism, causing fibrogenesis and the formation of scar tissue in the liver (Eng and Friedman, 2000). They can be induced by TGFβ1 to transdifferentiate into myofibroblasts (activated stellate cells) that secrete ECM products (Tsuchida and Friedman, 2017). Once activated, myofibroblast cells have increased motility to allow migration to the site of injury/infection (Tsuchida and Friedman, 2017). This motility is achieved by increasing the expression of the contractile cytoskeletal protein α-smooth muscle actin (αSMA) (Shi and Rockey, 2010). The expression αSMA defines the activated phenotype of HSCs (Rockey *et al.*, 1992). Activation of resident HSCs and the increased deposition of ECM products are hallmarks of fibrosis in the liver.

Fibrosis has been described in several cancer types and the role of CAFs has been linked to local progression and metastatic risk in breast cancer (Oza and Boyd, 1993), pancreatic cancer (Bolm *et al.*, 2017), melanoma (Flach *et al.*, 2011), colorectal cancer (Mukaida and Sasaki, 2016), lung cancer (L. Wang *et al.*, 2017) and liver cancer (Affo, Yu and Schwabe, 2017). A fibrotic response has also previously been demonstrated in MUM (Grossniklaus, 2013). The authors examined the metastases of 10 patients who had died from MUM in the liver; they evaluated tumour stage and proposed a model for UM metastatic progression. Their research concluded that dormant UM micrometastases in the liver require HSC activation to provide structural support for tumour progression prior to vascularity (Grossniklaus, 2013). Previously, in 1996, Daniels *et al*., had demonstrated that UM cells are capable of producing collagen VI (Daniels *et al.*, 1996), an ECM component associated with the recruitment of endothelial cells and neovascularisation (Karousou *et al.*, 2014).

The research by Grossniklaus and by Daniels *et al*., (Daniels *et al.*, 1996; Grossniklaus, 2013) highlights the limited knowledge we have of the fibrotic response in the liver to MUM, and no further examination in the literature exists. While a distinct pattern of fibrosis in MUM was reported by Grossniklaus (Grossniklaus, 2013), the cause or influence of this phenomenon remains unexamined. There has also been no investigation into the relationship between the pattern/extent of fibrosis in MUM and the clinical and genetic characteristics of the tumour. Due to the influence that a fibrotic environment can have on the effectiveness of chemotherapeutics, a prediction of local fibrotic response in MUM based on other clinical or genetic features could affect treatment decisions and potentially predict response rate to therapy.

In this Chapter, I hypothesise that hepatic fibrosis plays an important role in UM metastatic progression in the liver and that the presence or extent of fibrosis may be associated with clinical or genetic characteristics of the tumour.

The aims of this chapter were to (1) investigate the prevalence and pattern of ECM deposition and αSMA expression in UM liver metastases; (2) investigate the relationship between these markers of fibrosis and several tumour characteristics i.e. growth pattern, degree of pigmentation, and common clinical and genetic features of the MUM.

3.2. Materials and Methods

3.2.1. Samples

This study was approved by the Health Research Authority (REC Ref 11/NW/0759) and conducted in accordance with the Declaration of Helsinki. Archival formalin-fixed, paraffin-embedded specimens of hepatic MUM were provided by the Ocular Oncology Biobank (OOB) (REC Ref. 16/NW/0380). Samples originated from (1) 19 patients who had undergone local resection of their liver metastases and 2 patients who had percutaneous fine needle biopsies at Aintree University Hospital between 2005 and 2016; and (2) the dissections of the liver metastases of 9 patients, taken during the autopsy (Queen Alexandra Hospital Portsmouth).

Using a standard protocol, sections of each sample were prepared on glass slides by members of the Liverpool Ocular Oncology Research Group (LOORG) or by members of the Royal Liverpool University Hospital (RLUH) Pathology department. Sections were cut to a thickness of 4 μm, adhered to Xtra™ adhesive microscope slides (Leica) by floatation and dried overnight at 56 ^{o}C.

3.2.2. Slide Preparation for Staining

Slides were prepared for staining as described in section 2.2

3.2.3. Gomori Trichrome Staining

Gomori Trichrome staining was employed to highlight ECM deposition in the UM liver metastases. Gomori trichrome staining was performed by a Senior Pathologist of the Royal

Liverpool and Broadgreen University Hospitals NHS Trust. Gomori trichrome staining was performed as described in section 2.4

3.2.4. Alpha Smooth Muscle Actin staining

Samples were stained by immunohistochemistry (IHC) for alpha-smooth muscle actin (αSMA) to highlight the involvement of activated HSCs (resident fibroblasts in the liver). Antigen retrieval and IHC were performed using the Dako PT Link, Autostainer Plus systems and Envision^{TM} FLEX Kit, respectively, as described in section 2.5; both methods were performed according to the manufacturers' instructions (Dako UK Ltd, Cambridgeshire, UK). The primary antibody for αSMA (Dako, UK) was used at a dilution of 1:600.

3.2.5. Assessment of Tumour Characteristics

UM liver metastases were assessed for tumour stage according to criteria detailed by Grossniklaus in 2013 (Grossniklaus, 2013); for dominant cell type (epithelioid or spindle), degree of pigmentation (mild/moderate/severe), necrosis (absent [N]/present [Y]), and growth pattern (infiltrative/nodular) through examination of archival haematoxylin and eosin (H&E) stained slides of the samples. This was performed in triplicate by the author and two senior consultant histopathologists. In the case of inconsistent scoring, a consensus was reached by re-evaluation of all scorers. H&E staining was performed as described in section 2.3.

3.2.6. Staining of Immune Cells

Staining for the presence of immune cells in UM liver metastases has previously been carried out by (Krishna *et al.*, 2017), looking at CD68 (cluster differentiation 68), CD163,

CD3, CD4 and CD8. Staining was performed as described in section 2.5 with appropriate antibodies as follows. CD68PG (mouse anti-human PG-M1, M0876; Dako) and CD163 (mouse anti-human, NCL-L-CD163; Leica Biosystems, Newcastle Upon Tyne, UK) allowed the identification of macrophages. Immunostaining of T cells was performed with antibodies against: CD3 (polyclonal rabbit anti-human, ready to use, IR503; Dako), CD4 (monoclonal mouse anti-human, NCL-L-CD4–368; Leica Biosystems), and CD8 (monoclonal mouse anti-human, M7103; Dako). The dilutions of the antibodies used are provided in Table 3.1.

Table 3.1. Antibodies used to detect immune cells present in hepatic MUM

Antigen	Dilution factor	Supplier (catalogue code)
CD68PG	1:200	Dako, UK (M0876)
CD163	1:400	Leica Biosystems, UK (CD163-L-CE)
CD3	1:20	Dako, UK (IR503)
CD4	1:20	LeicaBiosystems, UK (CD4-368-L-CE-H)
CD8	1:200	Dako, UK (M7103)

CD, cluster differentiation

3.2.7. Scoring and statistical analyses

The level of immunohistochemical staining for CD68PG, CD163, CD3, CD4 and CD8 was scored from 0–3 (0, absent; 1, mild; 2, moderate; 3, heavy) as previously described in the manuscript (Krishna *et al.*, 2017). Slides stained for αSMA were scored 0–1 (0, absent; 1, present), and intratumoural and peritumoural fibrosis was assessed by Gomori trichrome staining and scored from 0–3 (0, absent; 1, mild; 2, moderate; 3, severe). Other clinical, histological and genetic data pertaining to the tumour samples were provided in a pseudonymised form by the Ocular Oncology Biobank.

All statistical analyses were performed using the SPSS software (version 24; IBM, New York, US). Due to imbalances in samples sizes and measurement types Mann Whitney U test was employed for statistical comparison.

3.3. Results

Table 3.2. Patient demographics of the experimental cohort

Total patients [n (%)]	30
Male	18 (60)
Female	12 (40)
Age at primary management [years]	
Median	57
Range	32-78

n, number of patients

Staining and analyses were performed on UM liver metastases from 30 patients consisting of 12 females and 18 males. The median age at presentation with PUM was 57 years (range = 32–78 years) (Table 3.2.).

Clinical data for the PUM was available in 21 patients who went on to develop hepatic MUM. The median largest basal diameter (LBD) was 16.6 mm (range = 11.0–19.6 mm) with a median height of 8.3 mm (range = 2.4–14.7 mm). Epithelioid cells were present in 84% of the PUM cases with defined cell type (n = 16/19). Ciliary body involvement was noted in 29% of tumours (n = 6/21) and 14% presented with extraocular extension (n = 3/21). Mitotic count was recorded in 18/21 cases and the median was 7 mitotic figures per 40 high power fields (range = 2–52).

Where chromosome 3 data were available, chromosome 3 loss was reported in the PUM of 18/19 patients, and one patient was D3. Chromosome 3 status of the PUM is reported to be

representative of the MUM (McCarthy *et al.*, 2016). The status of other common genomic aberrations in UM are detailed in Table 3.3.

Of the 30 MUM cases analysed, 19 were tumour surgical resections from the liver, two were hepatic laparoscopic biopsies, and 9 were hepatic lesions collected post-mortem. 57% presented with an infiltrative growth pattern (n = 17/30), with the remaining samples demonstrating nodular growth (n = 13/30). The dominant cell type in the hepatic MUM was epithelioid, occurring in 77% of cases (n = 23/30) and pigmentation was present in 70% (n = 21/30) (Table 3.4). Nuclear BAP1 negativity associated with metastatic spread was observed in 81% (n = 17/21) samples analysed. At the time of data analysis 20 patients had subsequently died of metastatic melanoma and a single patient had died from sepsis.

Table 3.3. The genetic profile of the sample cohort.

Patient Sample	Chr1	Chr3	Chr6p	Chr6q	Chr8p	Chr8q
MUM 1	-	L	-	-	-	-
MUM 2	-	L	-	-	-	-
MUM 3	-	L	-	-	-	-
MUM 4	-	L	-	-	-	-
MUM 5	-	L	-	-	-	-
MUM 6	-	L	-	-	-	-
MUM 7	-	-	-	-	-	-
MUM 8	-	L	-	-	-	-
MUM 9	-	-	-	-	-	-
MUM 10	-	L	-	-	-	-
MUM 11	N	L	N	N	L	G
MUM 12	L	L	N	N	N	U
MUM 13	N	L	N	L	L	G
MUM 14	N	L	G	L	N	G
MUM 15	L	L	U	N	N	G
MUM 16	N	L	U	N	L	G
MUM 17	N	L	N	N	N	G
MUM 18	L	N	G	-	-	G
MUM 19	-	L	-	-	-	-
MUM 20	-	L	-	-	-	-
MUM 21	N	L	G	N	L	G
MUM 22	-	-	-	-	-	-

MUM 23	-	-	-	-	-	-
MUM 24	-	-	-	-	-	-
MUM 25	-	-	-	-	-	-
MUM 26	-	-	-	-	-	-
MUM 27	-	-	-	-	-	-
MUM 28	-	-	-	-	-	-
MUM 29	-	-	-	-	-	-
MUM 30	-	-	-	-	-	-

Copy number variation of chromosomes were assessed in the primary uveal melanoma by multiplex ligation-dependent probe amplification, fluorescence in situ hybridization, or microsatellite analysis

Chr, chromosome; G, gain; L, loss; N, normal;

U, undefined/not defined/inconclusive; -, not performed

Table 3.4. Clinical and histological data from the 30 analysed MUM samples.

Case number	Gender	Age at PM	Sample type	Stage*	Growth pattern (nodular/infiltrative)	Dominant cell type	Degree of Pigmentation	Necrosis present	Nuclear BAP1 present
MUM 1	M	63	Resection	3	Infiltrative	Epithelioid	Mild	N	N
MUM 2	M	54	Resection	3	Nodular	Epithelioid	Heavy	N	Y
MUM 3	F	57	Resection	3	Nodular	Epithelioid	None	N	N
MUM 4	F	39	Resection	2	Nodular	Epithelioid	Mild	N	N
MUM 5	F	56	Resection	3	Nodular	Spindle	Moderate	Y	N
MUM 6	F	69	Resection	3	Infiltrative	Epithelioid	None	Y	N
MUM 7	F	38	Resection	3	Nodular	Epithelioid	None	Y	Y
MUM 8	F	64	Resection	3	Infiltrative	Epithelioid	Mild	Y	N
MUM 9	M	54	Resection	3	Infiltrative	Spindle	Moderate	Y	Y
MUM 10	M	66	Resection	3	Nodular	Epithelioid	None	Y	N
MUM 11	NR	NR	Resection	3	Nodular	Epithelioid	None	N	N

MUM 12	NR	NR	Resection	3	Infiltrative	Epithelioid	Heavy	N	N
MUM 13	M	67	Resection	3	Infiltrative	Epithelioid	None	Y	N
MUM 14	F	53	Resection	3	Nodular	Epithelioid	Mild	N	N
MUM 15	F	54	Resection	3	Infiltrative	Spindle	Moderate	N	N
MUM 16	M	47	Biopsy	3	Infiltrative	Epithelioid	Moderate	N	N
MUM 17	M	45	Resection	3	Infiltrative	Epithelioid	Heavy	N	N
MUM 18	M	46	Resection	3	Nodular	Spindle	None	N	Y
MUM 19	NR	NR	Resection	3	Infiltrative	Epithelioid	None	N	N
MUM 20	M	39	Resection	3	Nodular	Spindle	None	N	Y
MUM 21	F	78	Biopsy	3	Nodular	Epithelioid	Mild	N	N
MUM 22	M	75	Autopsy	3	Nodular	Epithelioid	Moderate	Y	NA
MUM 23	M	NR	Autopsy	3	Infiltrative	Epithelioid	Moderate	N	NA
MUM 24	F	NR	Autopsy	3	Infiltrative	Epithelioid	Heavy	N	NA
MUM 25	M	NR	Autopsy	3	Infiltrative	Epithelioid	Moderate	N	NA
MUM 26	F	62	Autopsy	3	Infiltrative	Epithelioid	Mild	Y	NA

MUM 27	M	64	Autopsy	3	Infiltrative	Epithelioid	Heavy	N	NA
MUM 28	F	NR	Autopsy	3	Nodular	Spindle	Moderate	Y	NA
MUM 29	M	66	Autopsy	3	Infiltrative	Epithelioid	Moderate	Y	NA
MUM 30	M	NR	Autopsy	3	Infiltrative	Spindle	Heavy	Y	NA

* Staging according to Grossniklaus, 2013 (Grossniklaus, 2013); # BAP1 positivity assessed by immunohistochemistry

F, female; M, male; MUM, metastatic uveal melanoma; N, not present; NA, not assessed; PM, primary management; Y, present

.

3.3.1. Gomori Trichrome Staining

The Gomori trichrome staining demonstrated positive hepatic fibrosis in all samples of UM metastasis, which was present in an intratumoural pattern (Figure 3.1.) and/or peri-tumourally (Figure 3.2.). Intratumoral fibrosis was present in all samples except one (patient sample MUM 2) and varied in severity (Figure 3.1.); seven patients were assessed to have mild intratumoural fibrosis, 13 demonstrated moderate fibrosis, and 9 presented with heavy intratumoural fibrosis. Frequently, the intratumoural fibrosis demonstrated a striking loop morphology in sections of the tumour (Figure 3.3.). Peritumoural fibrosis was present in 16 of 26 MUM with six samples demonstrating extensive collagen deposition around the tumour (Figure 3.3.).

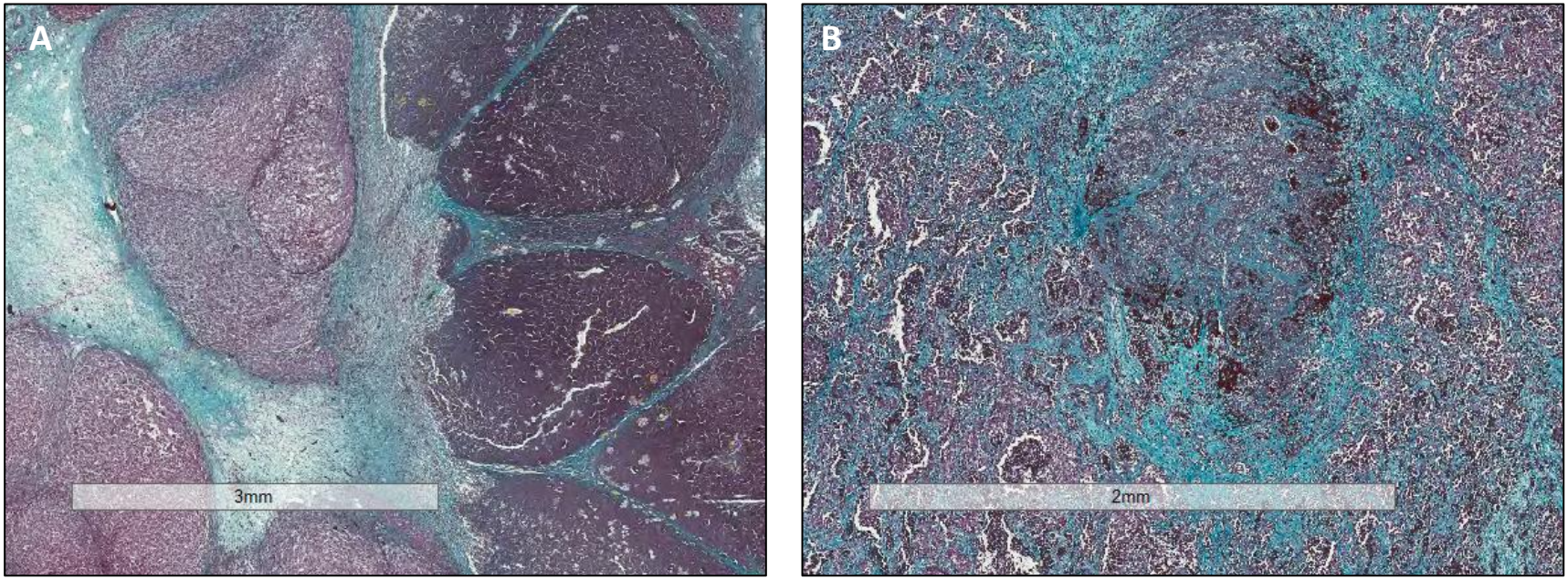

Figure 3.1. Intratumoural extracellular matrix deposition demonstrated the presence of extensive fibrosis in metastatic uveal melanoma of the liver when stained with Gomori trichrome stain. Scale bars represent 3 mm (A) and 2 mm (B)

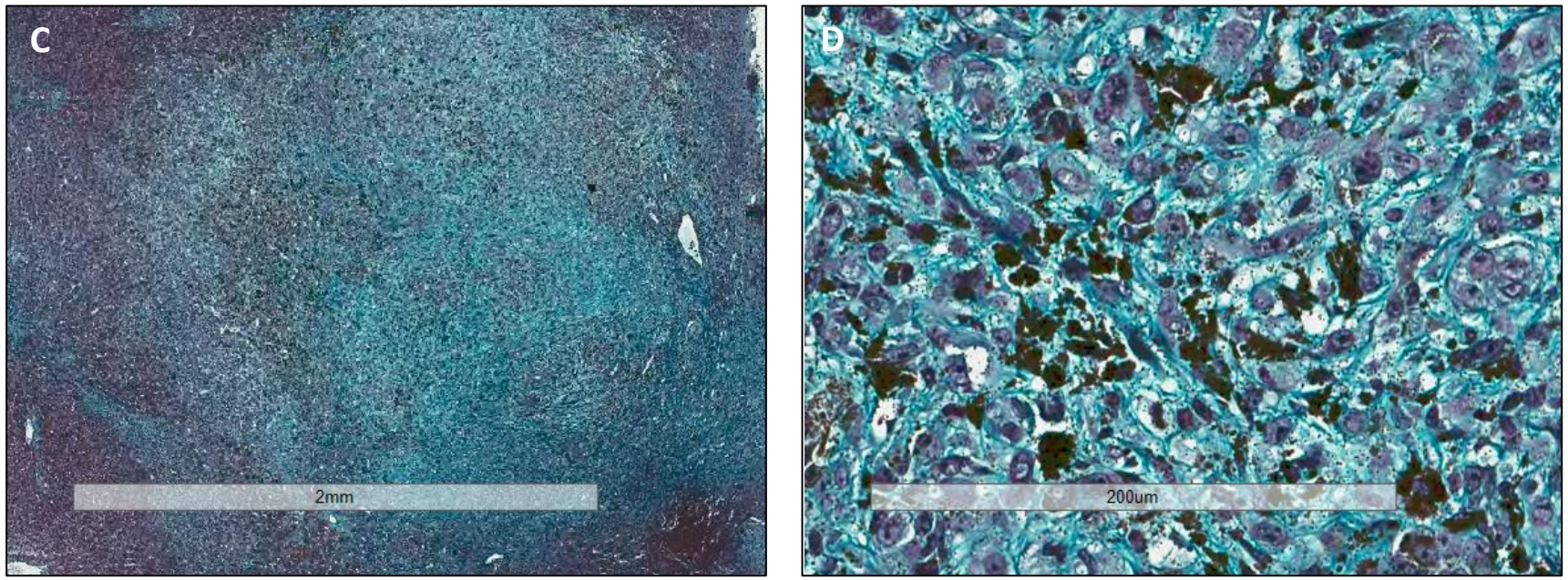

Figure 3.1. (continued) Intratumoural extracellular matrix deposition demonstrated the presence of extensive fibrosis in metastatic uveal melanoma of the liver when stained with Gomori trichrome stain. Scale bars represent 2 mm (C) and 200 µm (D)

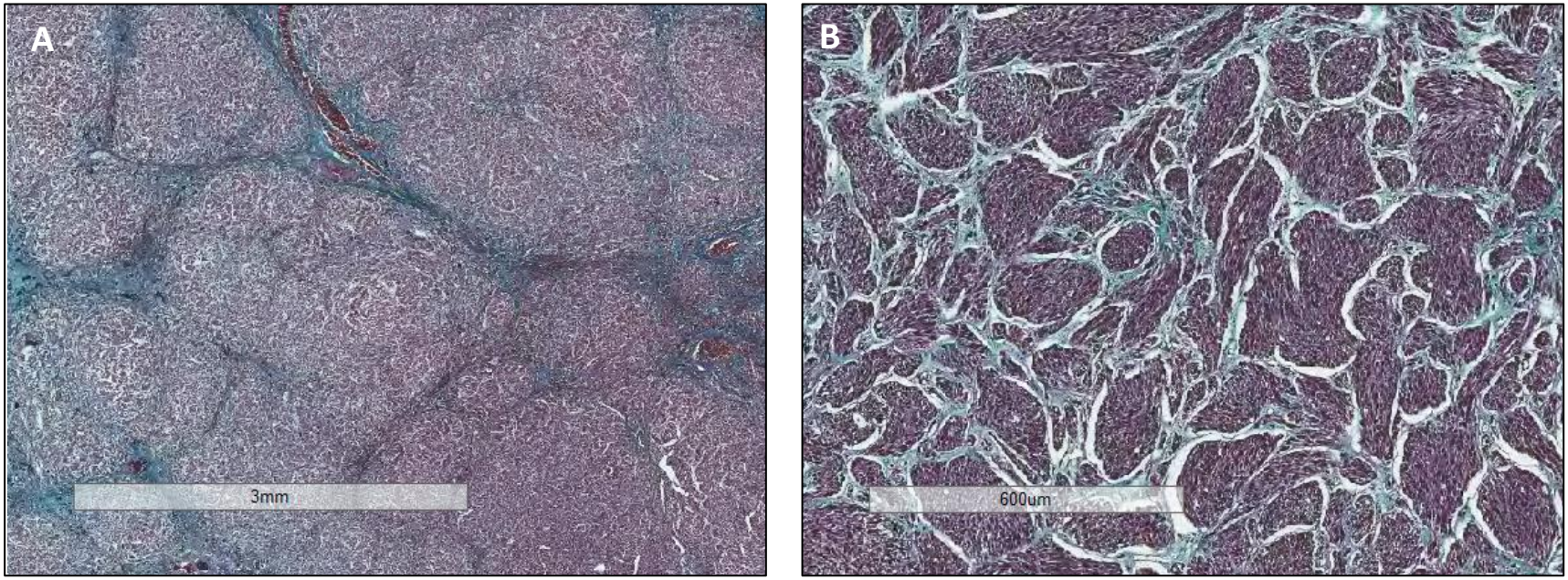

Figure 3.2. Nodular pattern of intratumoural extracellular matrix deposition in metastatic uveal melanoma when stained with Gomori trichrome staining.

Scale bars represent 3 mm (A) and 600 µm (B)

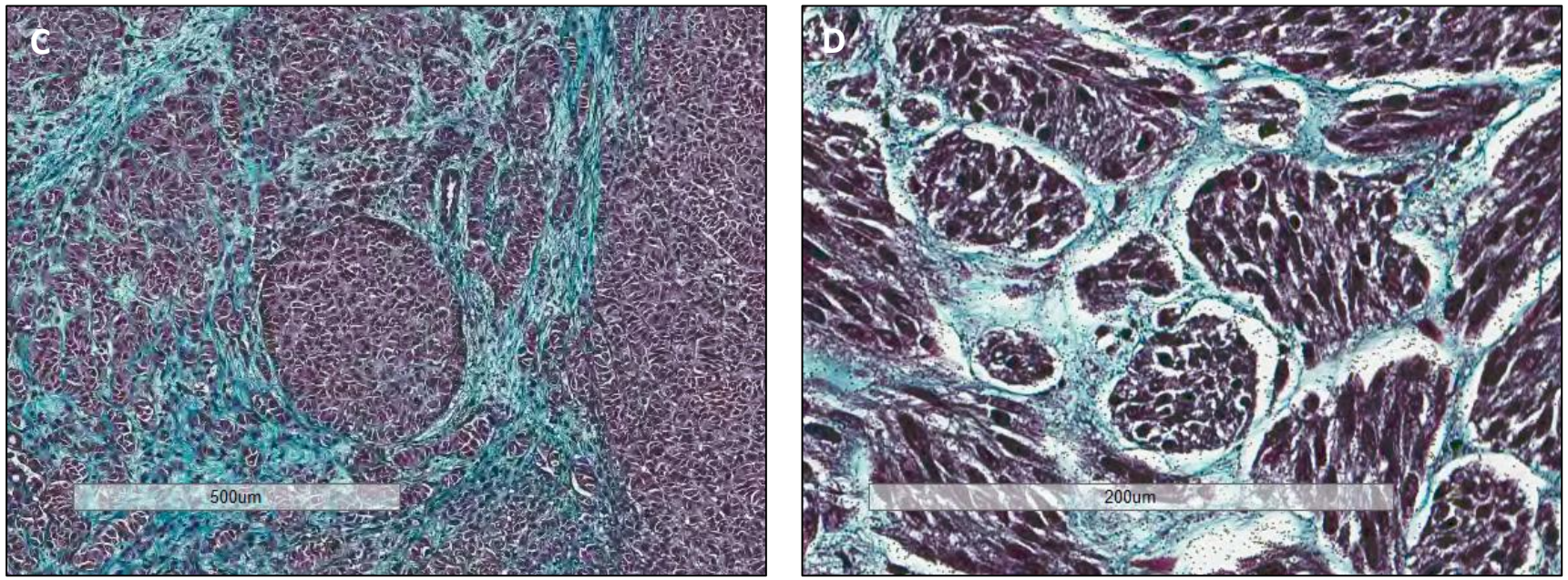

Figure 3.2. (continued) Nodular pattern of intratumoural extracellular matrix deposition in metastatic uveal melanoma when stained with Gomori trichrome staining. Scale bars represent 500 µm (C) and 200 µm (D)

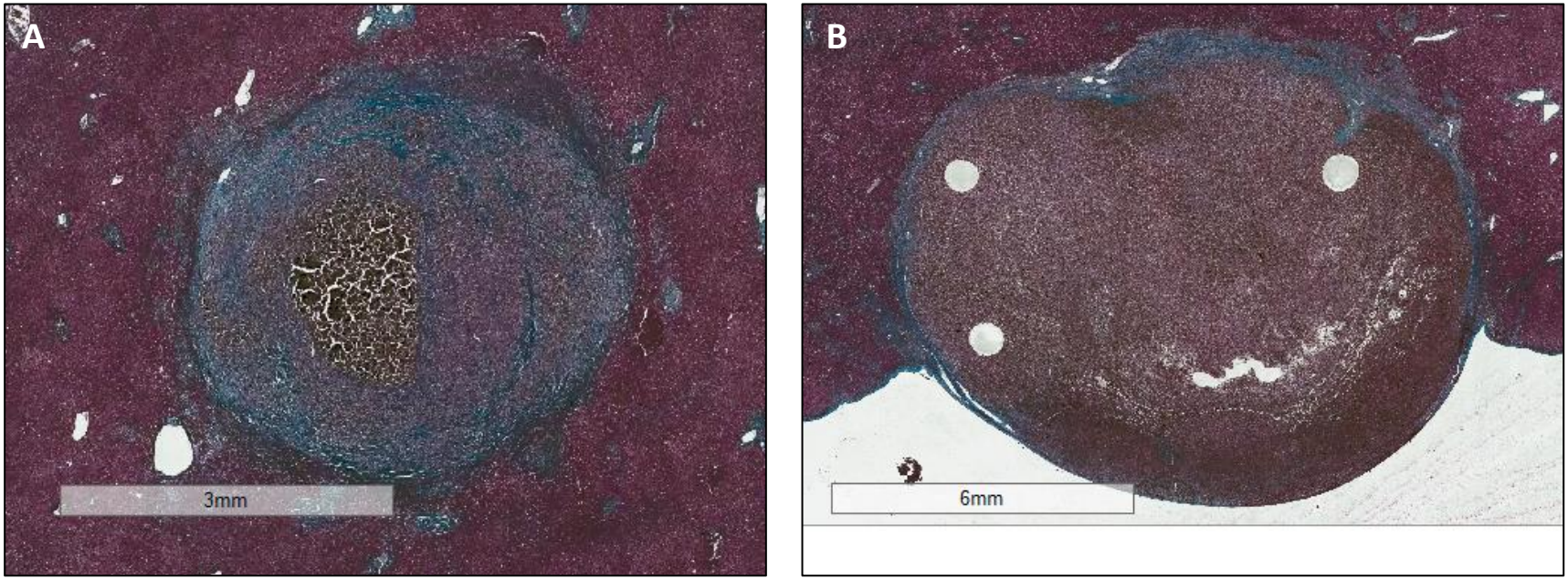

Figure 3.3. Peritumoural fibrotic environment around metastatic uveal melanoma in the liver demonstrated by increase extracellular matrix deposition by Gomori trichrome staining. Scale bars represent 3 mm (A) and 6 mm (B)

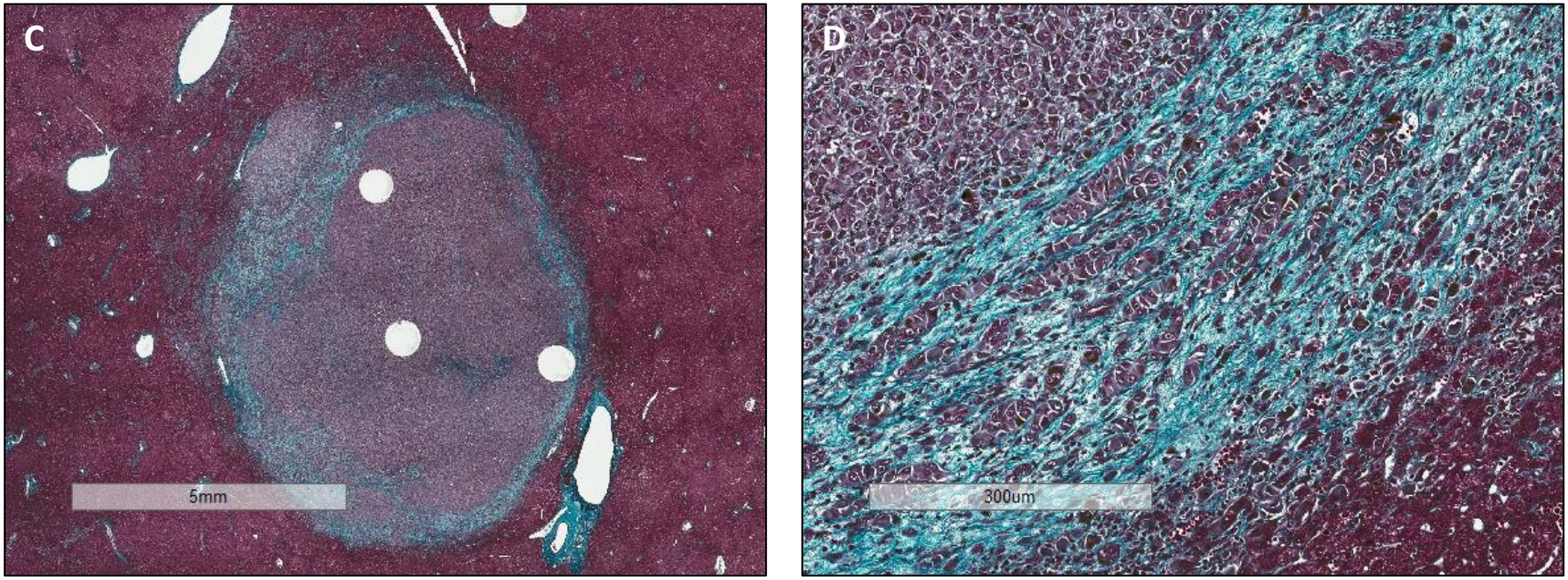

Figure 3.3. (continued) Peritumoural fibrotic environment around metastatic uveal melanoma in the liver demonstrated by increase extracellular matrix deposition by Gomori trichrome staining. Scale bars represent 5 mm (C) and 300 µm (D)

3.3.2. Alpha-Smooth Muscle Actin Staining

Positive immunohistochemical staining for αSMA was present intra and/or peri-tumourally in all cases. Similar to the Gomori trichrome staining of ECM components in hepatic MUM, αSMA staining demonstrated distinct yet varied patterns in the MUM lesions.

Intratumoural αSMA positive staining was demonstrated in 77% of cases (n = 23/30) and often presented as looping/nodular structures in the lesion (Figure 3.3.). Tumour adjacent αSMA positive staining was visible in 63% of cases where this could be assessed (n = 15/24) and often presented as peri-tumoural border staining around the MUM (Figure 3.4.).

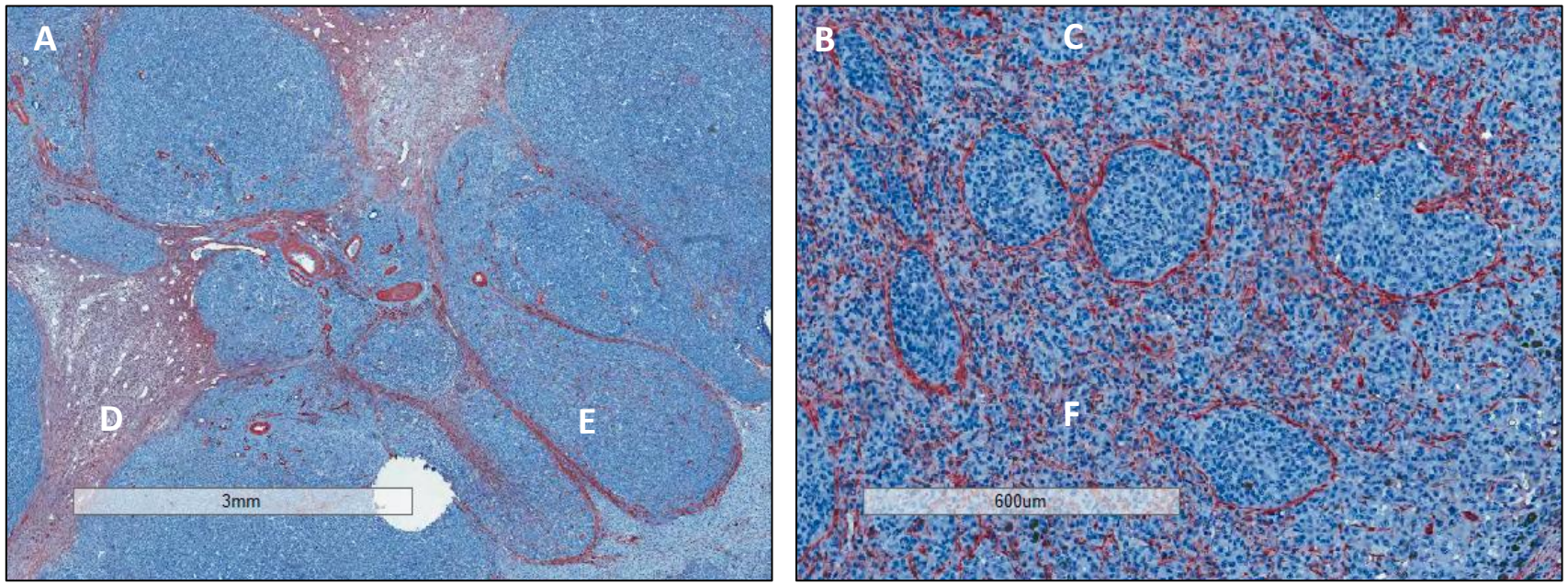

Figure 3.4. (A-D) Intratumoural alpha smooth muscle actin staining highlighted the presence of activated stellate cells in metastatic uveal melanoma and their frequent presentation in a looping formation; (E) Positive control in colon tissue; (F) IgG negative control in colon tissue. Scale bars represent 3 mm (A) and 600 µm (B)

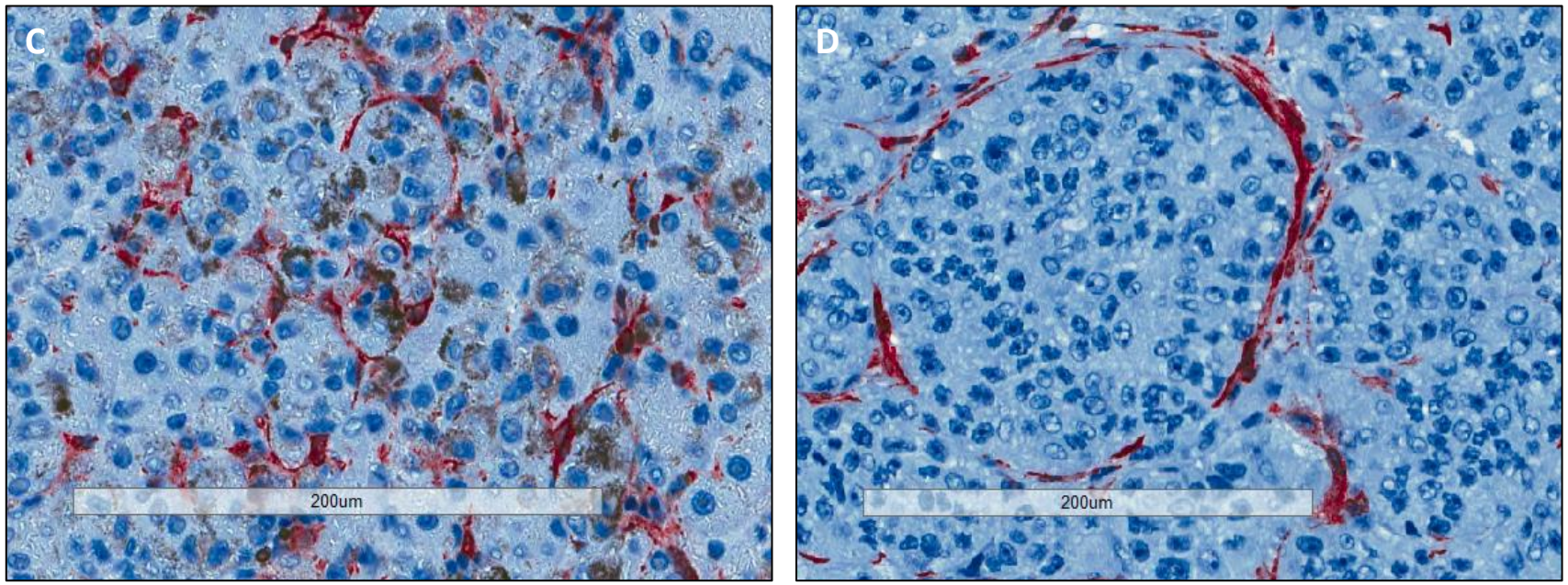

Figure 3.4. (continued) (A-D) Intratumoural alpha smooth muscle actin staining highlighted the presence of activated stellate cells in metastatic uveal melanoma and their frequent presentation in a looping formation; (E) Positive control in colon tissue; (F) IgG negative control in colon tissue. Scale bars represent 200 µm (A) and 200 µm (B)

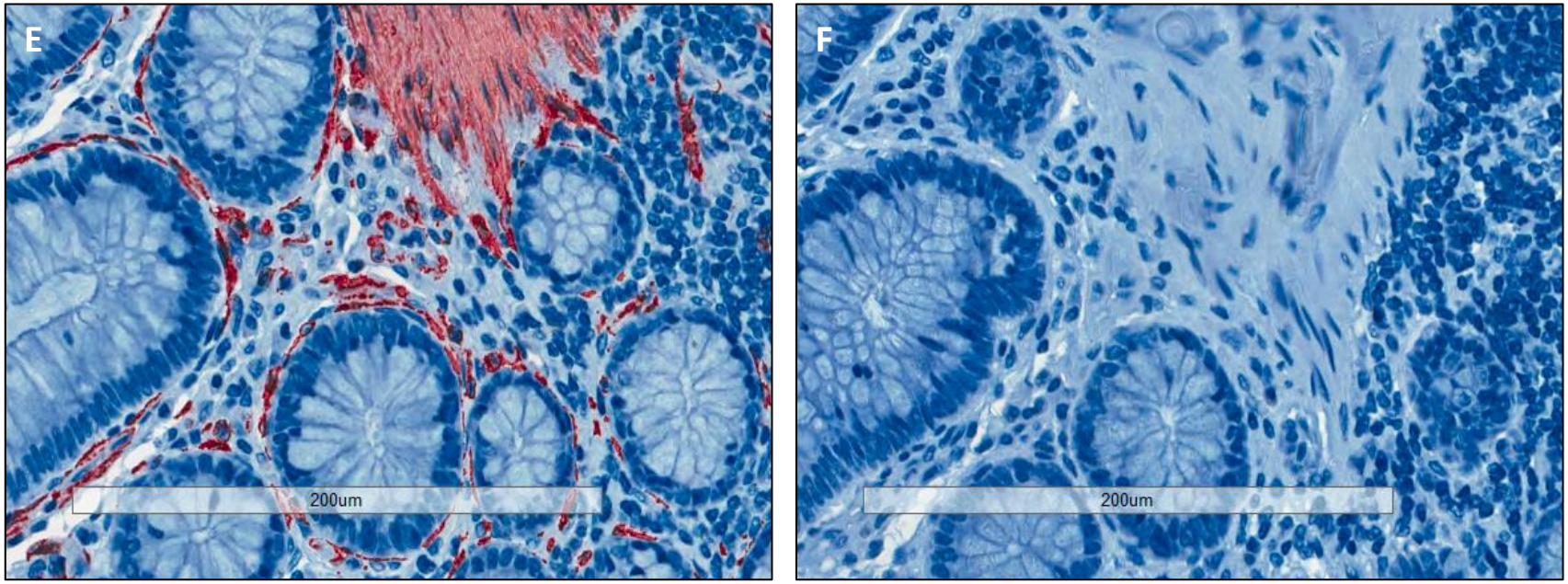

Figure 3.4. (continued) (A-D) Intratumoural alpha smooth muscle actin staining highlighted the presence of activated stellate cells in metastatic uveal melanoma and their frequent presentation in a looping formation; (E) Positive control in colon tissue; (F) IgG negative control in colon tissue. Scale bars represent 200 μm.

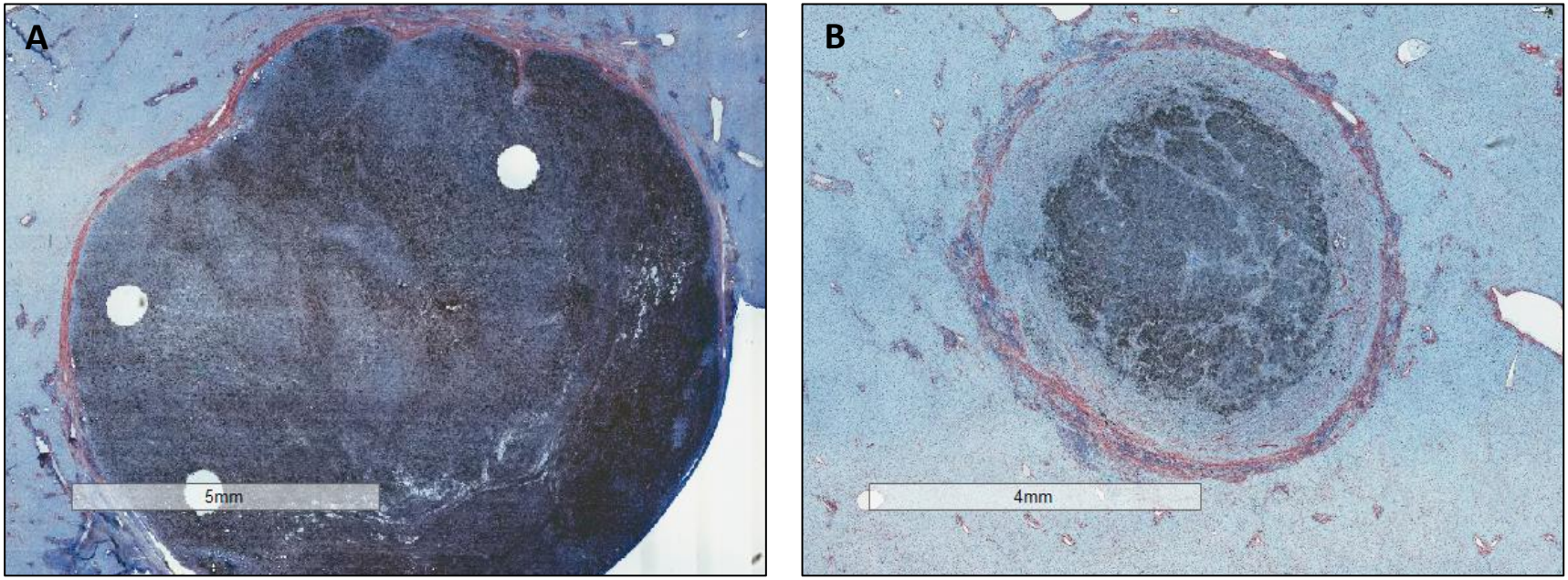

Figure 3.5. Peritumoural alpha smooth muscle actin staining demonstrating the activation of stellate cells at the peripheral edge of the metastatic uveal melanoma. Scale bars represent 5 mm (A) and 4 mm (B)

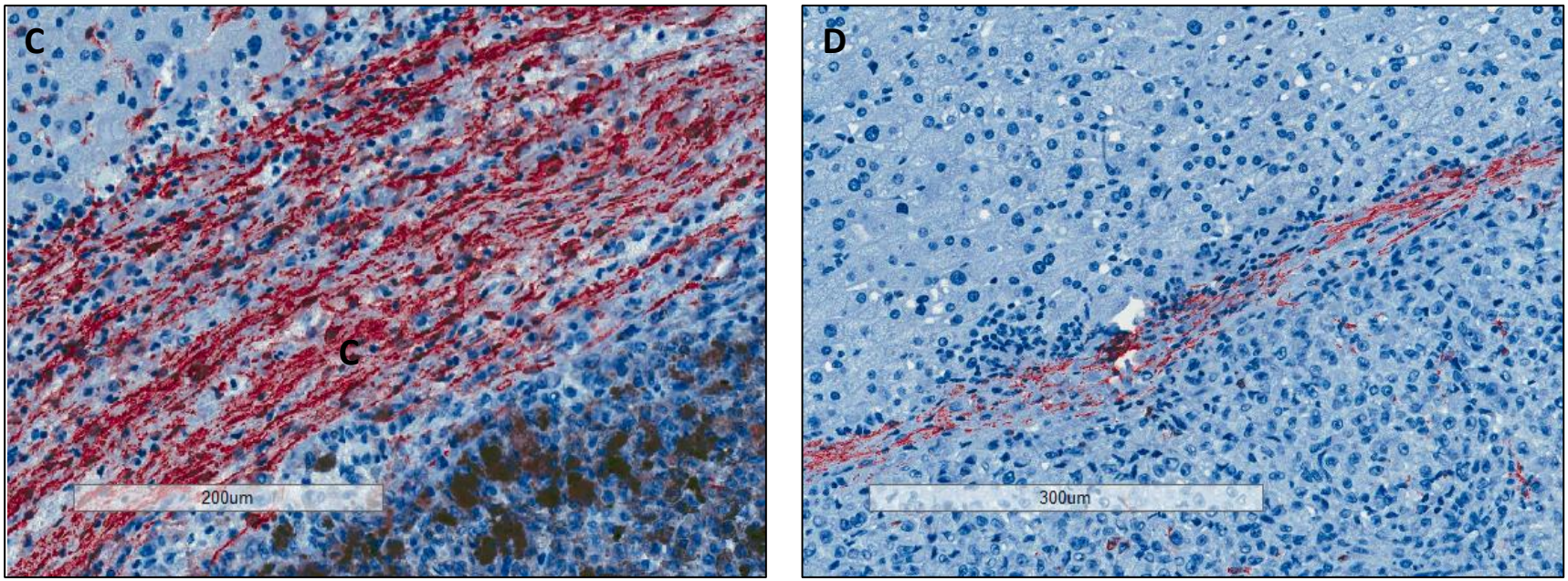

Figure 3.5. Peritumoural alpha smooth muscle actin staining demonstrating the activation of stellate cells at the peripheral edge of the metastatic uveal melanoma. Scale bars represent 200 µm (C) and 300 µm (D)

3.3.3. Correlative Analyses

In the current study, the histological and immunohistochemical staining patterns of MUM in the liver were assessed and compared with other tumour characteristics. This was performed to investigate the relationship between cellular characteristics of the MUM and more macroscopic behaviours of the MUM, such as growth pattern and fibrotic response.

The growth pattern of the hepatic MUM seemed to follow the expected relationship when compared with the pattern of ECM deposition, with nodular tumours demonstrating slightly higher tendency to present with peritumoural ECM deposition and infiltrative tumours demonstrating slightly higher intratumoural ECM deposition; however, these relationships were not statistically significant (Mann-Whitney U, $p \geq 0.05$).

Hepatic MUM with a higher degree of pigmentation were more likely to present as infiltrative disseminated lesions ($U = 61$, $p = 0.036$; 2-tailed exact) while nodular growth pattern was associated with an increase in macrophage infiltration ($U = 65.5$, $p = 0.044$; 2-tailed exact).

To assess if the presence of activated HSCs was associated with increased ECM deposition at the metastatic site, Mann-Whitney U assessments were performed and a cut off of $p \leq 0.05$ allowed rejection of the null hypothesis. Intratumoural αSMA positivity was not associated with the level of in intratumoural ECM deposition; however, greater ECM deposition around the periphery of the tumour was associated with the presence of αSMA positivity at the tumour edge ($U = 55$, $p = 0.038$; 2-tailed exact).

Comparison between the degree of pigmentation and the presence of intratumoural αSMA positive cells suggested that HSC activity was less likely in MUM displaying increased pigmentation (U = 33, p = 0.048, 2-tailed exact).

The fibrotic markers were also compared in relation to genetic characteristics commonly associated with increased metastatic risk and mortality. Nuclear BAP1 positivity, chromosome 1p loss, chromosome 6p gain and chromosome 8p loss were all assessed against both the pattern of ECM deposition and that of αSMA positivity but demonstrated no statistically significant association (Mann-Whitney U or Chi-square, $p \geq 0.05$)

Similarly, the degree and pattern of immune infiltration in the MUM was compared with the fibrotic markers but demonstrated no statistically significant associations (Mann-Whitney U, $p \geq 0.05$).

3.4. Discussion

In this chapter I demonstrated that a local fibrotic response occurs in the liver of patients with MUM. This is consistent with previous work suggesting an increased deposition of collagen and a recruitment of αSMA positive cells in response to UM metastasis (Grossniklaus, 2013). Distinct patterns of fibrosis were observed in hepatic MUM; presenting as a peritumoural border and/or as intratumoural loops. The data also demonstrate an association between increased peritumoural ECM deposition and αSMA positive cells surrounding the MUM, warranting further investigation of the role of activated HSCs in the peritumoural fibrosis of MUM.

The fibrotic response often resembled late stage hepatic fibrotic/cirrhosis, presenting with a similar morphology to cirrhotic nodules (Figure 3.2.) (Lo and Kim, 2017). This pattern has previously been reported in MUM (Grossniklaus, 2013) and suggests a similarity to aberrant fibrosis and cirrhosis, a known precursor to local malignant progression (La Vecchia *et al.*, 1998). The morphology of the intratumoural fibrosis was also consistent with periodic acid Schiff (PAS) positive loops, known to form in PUM (Folberg *et al.*, 1993). These loops are thought to signify the presence of vascular mimicry and have been associated with increased risk of death due to metastatic progression (Folberg *et al.*, 1993). This poses a difficulty in the interpretation of the MUM presentation; whether this looping pattern of ECM deposition is a consequence of vascular mimicry akin to PUM, whether it is due to the fibrotic response in the liver and similar to cirrhotic nodules, or whether it is a combination of the two. To my knowledge, this cannot currently be determined through any previously described methodology due to the similarities of the two phenomena. Further investigation into the specific molecular profile of these ECM loops in both the PUM and MUM is needed, and assessment into whether vascular mimicry of the PUM is associated with similar behaviour in the MUM.

The deposition of ECM around the peripheral border of the MUM demonstrated association with the concomitant presence of αSMA positive cells and is akin to the recruitment and activation of HSCs (Figures 3.3. and 3.5.) (Tsuchida and Friedman, 2017). This peripheral fibrosis has previously been described in pancreatic cancer and is considered a protective environment that may contribute to the chemoresistance of the tumour (Tanaka and Kano, 2018). It has been shown that fibrotic borders may inhibit the diffusive potential of chemotherapeutics into the tumour due to altered fluid dynamics caused in the interstitial space (Provenzano *et al.*, 2012). The tendency for peripheral fibrotic envelopment of MUM within the liver was demonstrated in 57% of cases at varying degrees and could be linked to the refractory nature of MUM to conventional chemotherapy. While intratumoural ECM deposition was not statistically associated with intratumoural αSMA positivity in this analysis, it has previously been described to involve the recruitment and activation of HSCs (Grossniklaus, 2013). As stated, increased intratumoural ECM deposition often presented in a looping pattern and may perform a similar protective mechanism at a smaller scale.

The research aimed to compare the fibrotic response in hepatic MUM with the genetic profile of the tumour. Common genetic aberrations include complete loss of chromosome 3 (M3), partial loss of chromosomes 1p, 6q and 8p, gains of chromosomes 6p and 8q, and mutations in BAP1 resulting in a loss of nuclear positivity when assessed by IHC (Ewens *et al.*, 2013; Kalirai *et al.*, 2014; Farquhar *et al.*, 2018). Of these, the most influential with regard to metastatic progression are M3 and gains of 8q (Cassoux *et al.*, 2014), yet all samples assessed presented with 8q gains and only one displayed D3. This meant comparison of these characteristics with MUM fibrosis was not possible. Furthermore, only eight of the 31 experimental samples had available genomic data for the chromosomal

copy number aberrations. Repeat analysis with a greater number of samples displaying a variety of genomic profiles would allow a greater insight into these relationships.

MUM in the liver presents with two distinct growth patterns; nodular and infiltrative (Grossniklaus, 2013). Herein, MUM presenting with an infiltrative growth pattern were more likely to possess a higher degree of pigmentation; additionally, the data herein also suggests that HSC activation is less likely in MUM with greater pigmentation. There is little data in the literature regarding the influence of pigmentation on MUM progression and malignancy; yet higher melanin content of cutaneous melanoma metastases has been linked to reduced response to radiotherapy (Brożyna *et al.*, 2016). While pure amelanotic UM are rare, this relationship and its clinical impact requires further investigation.

The chronology of fibrosis and MUM could also be investigated in future research. There is no indication in the present results as to whether the MUM is causing the fibrosis, or whether existing fibrosis in the metastatic niche is adapted by MUM. Kondo *et al.,* demonstrated that the presence of hepatic fibrosis measured by the non-alcoholic fatty liver disease fibrosis score (NFS) pre-operatively at primary surgical resection was significantly related to the rate of hepatic metastasis in patients with colorectal cancer (Kondo *et al.*, 2016). Future work in UM could perform similar analysis to that presented by Kondo *et al.,* 2016; liver fibrosis could be measured at primary diagnosis with the NFS score and the rate of metastatic progression could be assessed. Additionally, the duration of patient survival following initial diagnosis of metastatic progression could be compared to the NFS score to assess whether pre-existing liver fibrosis affects the rate of mortality.

The NFS score could be taken prior to treatment of MUM and the response to chemotherapy measured. Unveiling the relationship between fibrosis and response to

chemotherapy could suggest new treatment options for MUM or impact current treatment choice. The biological characteristics that determine the difference in fibrotic pattern or level could also be investigated further, and whether this is associated with the MUMs response to chemotherapy.

It is not clear whether the ECM deposition is due to the activation of HSCs or if it is a product of the MUM cells present. Clarijs *et al.,* demonstrated that UM cells deposit a multitude of ECM products and that these components can form characteristic arcs and loops in the primary tumour (Clarijs *et al.*, 2005). While this study demonstrated a significant association between concomitant αSMA positivity and increased ECM deposits surrounding the tumour, this was not always the case. Furthermore, intratumoural ECM deposition and αSMA positivity within the tumour were often concomitant but not statistically associated. This ECM deposition in the metastatic lesion requires further investigation and the possibility that UM cells generate the fibrotic environment present in the liver during MUM also needs examining.

It is also worth noting that the cohort of samples analysed may not represent a typical cohort of MUM tumours. The samples assessed were predominantly cases in which the MUM was able to be surgically resected and so available for analysis by IHC. It is frequent in patients with MUM that metastases present as dispersed micrometastases that are not surgically resectable. In these instances, appropriate analyses of the MUM could only be performed post-mortem or in patients where the tumour burden was significant enough for surgical resection.

The process of HSC activation and ECM production in UM could be further interrogated through cellular assays. For example, the ability of the UM secretome to activate HSCs

grown in culture could be investigated. The secretomes of UM cultures could be isolated as previously described (Angi *et al.*, 2016) and used to stimulate cultured human hepatic stellate cells (Hong *et al.*, 2018). Markers of activation such as αSMA (Micallef *et al.*, 2012) or GFAP (Kalluri and Zeisberg, 2006) positivity could be assessed through PCR, IHC or immunofluorescence. Increased cell migration could be assessed through multiple methods, several of which were described by (Hulkower and Herber, 2011), including scratch plate assays, transmembrane "Boyden chamber" assays, microfluidic chamber assays and cell exclusion zone assays. An increase in, or the composition of, the ECM deposition of HSCs could also be investigated as a measure of their activation (Wynn, 2008). Appropriately controlled methods of these kind would allow an understanding of the extent to which secreted proteins from PUM or MUM cells impact the fibrotic environment at the metastatic niche in liver.

3.5. Conclusion

In conclusion, the analysis herein highlights an extensive presence of fibrosis in hepatic MUM and demonstrates two characteristic phenotypes (1) peritumoural fibrosis representing an ECM border around the tumour and (2) intratumoural fibrosis often presenting in a looping pattern. Increased peritumoural ECM deposition was associated with the activation and recruitment of resident HSCs.

The pattern of fibrosis was inconsistent and did not correlate with any common genetic aberrations. The cellular and molecular mechanisms of this fibrotic response, its impact on MUM progression and its relationship with other tumour characteristics require further investigation and repeat analysis with a larger cohort. Nevertheless, the extent and prevalence of fibrosis in MUM suggests an important role in MUM progression and opens

the field for further investigation into the chronology and biology of MUM-associated hepatic fibrosis.

CHAPTER 4: MOLECULAR CHARACTERISATION OF THE UVEAL MELANOMA SECRETOME

4.1. Introduction

The impact UM cells have on their local environment is orchestrated through intercellular signalling via the release of biologically active materials, such as proteins. Chapter 3 highlighted a fibrotic response in MUM in the liver. This chapter investigates the functional enrichment of signalling pathways associated with the UM secreted proteome and discusses these pathways in relation to UM pathology and progression.

Intercellular communication is imperative for the functionality of any multicellular system; and protein secretion/transfer plays an orchestral role in this (Ahmed and Xiang, 2011). Through protein transfer, cancer cells influence the behaviour of neighbouring cells in their microenvironment, at both the primary site and in the metastatic niche (Liotta and Kohn, 2001). Secreted proteins are known to influence many biological functions (Robinson *et al.*, 2019). The effect these secreted proteins have on the hallmarks of cancer have been reviewed by (Patel *et al.*, 2014). The tumour cell secretome can influence a diverse range of functions which can influence cancer progression; such as stromal fibroblast activation (Kuzet and Gaggioli, 2016), immune cell manipulation (Awad *et al.*, 2018), angiogenesis (Yadav *et al.*, 2015) and migration (Mathias *et al.*, 2009).

Several papers have investigated the pathophysiologic potential of specific proteins shown to be secreted by UM cells into their microenvironment. Repp *et al.*, demonstrated that UM cells secrete bioactive macrophage inhibitory factor (MIF) (Repp *et al.*, 2000), which protects the tumour from cytolysis by natural killer (NK) lymphocytes. The authors demonstrated that the secretome of multiple UM cell lines reduced NK cytolysis *in vitro*,

and that this effect could be significantly reduced through targeted depletion of MIF activity (Repp *et al.*, 2000). The secretion of matrix metalloprotease 2 protein (MMP-2) by PUM was shown to correlate with a significantly reduced 5-year survival rate (Väisänen *et al.*, 1999). MMPs act to break down specific ECM products and, in cancer, can influence tumour growth, migration and invasion (Gialeli, Theocharis and Karamanos, 2011). Further research has demonstrated that MMP-9 is also secreted by UM and can be secreted in its active form (Elshaw *et al.*, 2001); however, this did not correlate with invasive potential *in vitro*. Apte et al., demonstrated that UM cells secrete angiostatin (Apte *et al.*, 2001). The authors showed in an *in vivo* UM model that the secretion of angiostatin from the primary tumour in the eye may protect against increased metastatic burden in the liver (Apte *et al.*, 2001). UM cells from choroidal tumours were shown to secrete a variety of cytokines (Enzmann *et al.*, 1998); interleukins 6, 8 and 10, TGFβ-1 and FGF2. The authors highlight that these factors can influence immune suppression, inflammation, angiogenesis and tumour growth. FGF2 was also shown to be produced by UM tumours (Y. Wang *et al.*, 2017). The authors demonstrated that levels of FGF2 in UM were related to an epithelioid cell type and the presence of metastatic spread in patients. Stimulation of UM cells with exogenous FGF2 demonstrated increased tumour growth and metastatic spread *in vivo*, and increased cytoskeletal remodelling and migratory potential *in vitro*. Hepatocyte growth factor (HGF) and vascular endothelial growth factor (VEGF) were also shown to be secreted by UM (Cools-Lartigue *et al.*, 2005), and at increased levels when stimulated with monocyte conditioned media. Whether through autocrine or intercellular signalling, immune infiltration in UM could promote angiogenesis and an invasive phenotype through VEGF and HGF secretion into the microenvironment. Many these proteins shown in the literature to be secreted by UM cells possess roles in the manipulation of the microenvironment, and in the stimulation of inflammatory and fibrotic pathways. In 2007, Pardo *et al.,* investigated the proteomic profile of the secretome of UM cell lines (Pardo *et al.*, 2007), highlighting an

abundance of proteins linked with adhesion, migration and modulation the ECM. The authors suggested that the proteins cathepsin D, syntenin and gp100 represented potential biomarkers of UM metastatic potential.

Chapter 3 investigated the fibrotic profile of hepatic MUM and highlighted extensive and distinct patterns of fibrosis concomitant with MUM. Analysis demonstrated an association between HSCs and the production of peritumoural ECM deposits, as well as an association between pigmentation of the MUM and intratumoural HSC activity. Similar activation of HSCs in response to hepatic metastasis has previously been demonstrated in melanoma, colonic and pancreatic cancer (Olaso *et al.*, 2003; Matsusue *et al.*, 2009; Costa-Silva *et al.*, 2015). While the presence of previously identified proteins in the UM secretome suggest a role in propagating a fibrotic environment, the presence of multiple factors influencing specific pathways or functions could have summative or negatory effects. This chapter interrogates the protein content of the total secretome of 2D-cultured primary UM cells isolated from excised patient tumours. It aims to (1) identify and quantify the totality of proteins secreted by 2D-cultured primary UM cells isolated from excised patient tumours, (2) to characterise these proteins by predicting their secretory mechanisms, (3) to predict the biological processes and signalling pathways associated with the UM proteomic secretome, and (4) to compare these functions and pathways between disease states. The working hypothesis was that proteins secreted by primary UM cells are associated with signalling pathways that promote tumour progression and metastasis, that these pathways are upregulated in UM compared with normal choroidal melanocytes (NCM), and in UM with M3 compared with D3 UM.

The analysis herein interrogates a previously generated dataset of proteins released by PUM incubated for 48 hours in 2D, serum-free culture (Angi *et al.*, 2016). The hypothesis

being that the secretome of UM contains proteins associated with their malignancy, and that the proteins in the secretome of UM at higher risk of metastasis are associated with signalling indicative of a more aggressive phenotype. The analysis employs the freely available software SignalP, SecretomeP and exocarta for the prediction of secretory mechanisms, followed by in-depth pathway analysis with IPA.

4.2. Methods

4.2.1. Proteomic Processing – Generation of the Dataset

The following analyses were performed on a proteomic dataset previously generated from label-free quantitative mass-spectrometry of the conditioned media of 2D short-term cultures.

The cultures included 5 NCM samples and 14 independent PUM samples stratified by chromosome 3 status into 10 UM samples at high risk (HR UM) of developing metastasis (M3) and 4 UM samples at low risk (LR UM) of developing metastasis (D3). The samples were cultured according to the methods in section 2.7. and section 2.8.

The initial dataset was generated by Angi *et al.,* and included the raw spectral data of proteins identified with a 1% false discovery rate (FDR), from 19 cultures (Angi *et al.*, 2016). The methods employed when generating the dataset included a novel, on-bead digestion method followed by a quadrapole, orbitrap LC-MS/MS with a MASCOT search of detected peptides against the UniProtKB/Swiss-Prot database for identification.

Step 1: Ensuring confidence in the dataset

This dataset was filtered to remove any proteins identified with fewer than 3 unique peptides in order to apply a cut off to improve confidence in the identified proteins (Levin, Hradetzky and Bahn, 2011). The resulting dataset was considered to be a confident assessment of the proteins present in the conditioned culture media of primary UM and NCM cultures.

Step 2: Uniprot FASTA-file generation and gene ontology (GO) classifications

The 758-protein dataset was ordered alphanumerically by accession number. Multiple, secondary accession numbers were removed, to leave only primary accession numbers, which were then uploaded into Uniprot (www.uniprot.org). This generated FASTA files for each protein which display the primary peptide sequence as amino-acid single letter code. Gene ontology information about "cellular component" and "subcellular location" were also recorded (Ashburner *et al.*, 2000).

Step 3: Prediction of Classical Secretion

Classical secretion relies on a peptide signal sequence within the transported protein (Schatz and Dobberstein, 1996). This was predicted with the methods in section 2.5.

Step 4: Prediction of Non-classical Secretion

Non-classical secretion can be predicted by interrogating post-translational and localisation aspects of the protein to predict non-signal-peptide-mediated protein secretion (Bendtsen, Jensen, *et al.*, 2004). This was performed according to methods in section 2.6.

Step 5: Prediction of Exosomal Secretion

Secretion via EVs can occur by a variety of routes depending on the vesicle employed (Raposo and Stoorvogel, 2013). The differences between vesicles are discussed in detail in Chapter 1; this chapter focuses on the proteins with predicted exosomal secretion. This can be predicted through the cross interrogation of a given proteomic dataset with a curated database of exosomal proteins. This was undertaken using the methods detailed in section 2.7.

In the instance that a protein was predicted to be secreted by two or more of these methods, characterisation was weighted in favour of (1) classical secretion followed by (2)

non-classical secretion and then (3) exosomal secretion. Employing this method allowed for the filtering of the dataset to leave proteins that have predicted secretory mechanisms, these proteins were considered to represent the “intentionally secreted” dataset.

4.2.2. Predicting the cellular localisation of the identified proteins

The “cellular component” of the proteins was assessed using the online freeware “GOrilla” (Eden *et al.*, 2009). Uniprot accession numbers were uploaded with the organism set to *homo sapien*, the running mode as “Single ranked list of genes”, and ontology set to “Component”.

4.2.3. Differential expression

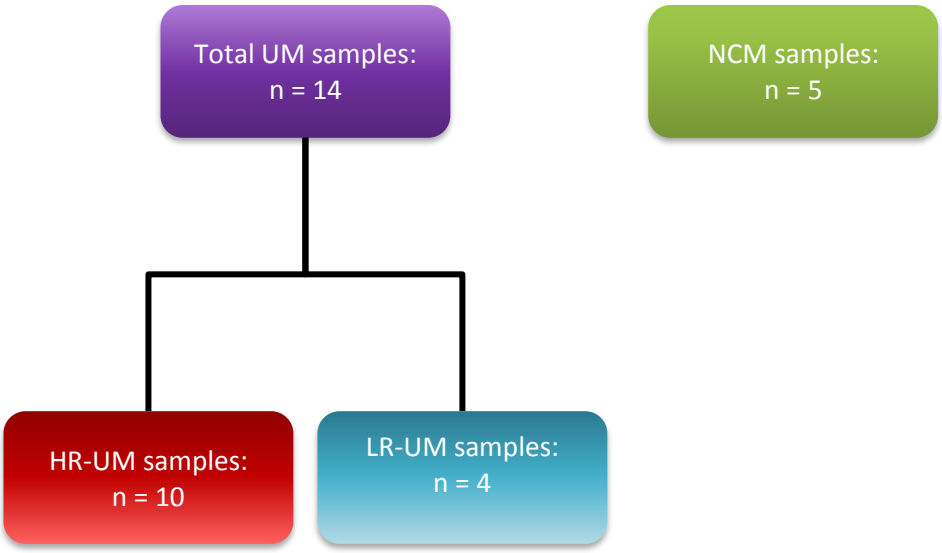

Figure 4.1. Grouping of the samples cultured for comparative analyses.

HR, high risk; LR, low risk; NCM, normal choroidal melanocyte; UM, uveal melanoma

The protein abundances were grouped by disease state: high risk UM (HR-UM), low-risk UM (LR-UM), total UM (UM) and NCM. Samples were stratified into metastatic risk groups based on their chromosome 3 status: loss of chromosome 3 (M3) was deemed high risk, where no loss of chromosome 3 (D3) was considered low risk of metastatic progression. The averages were calculated and Mann-Whitney U tests were performed between select groups (UM versus NM, HR UM versus LR UM) using SPSS software (IBM – New York, USA). This allowed experimental fold changes with associated statistical significance to be determined between disease states and for upload into the pathway analysis software.

4.2.4. Pathway analysis

Data were analysed through the use of QIAGEN's Ingenuity® Pathway Analysis (IPA®, QIAGEN Redwood City, www.qiagen.com/ingenuity) for pathway/network analyses, etc. according to the methods described in section 2.8. A p-value cut off was used to limit the association of functions and pathways to those with an inverse log10 p-value ≥ 2. No cut off was employed for z-score; however, a threshold of ≥ 2 or ≤ -2 was used to determine up/down regulation (colour coding figures: z-score ≥ 2 = orange [upregulation]; z-score ≤ -2 = blue [downregulation])

4.3. Results

The clinical information of the patients with PUM are detailed in Table 4.1. Those of the patient cadavers from which NCM cultures were isolated are detailed in Table 4.2.

Table 4.1. The clinical information of the primary uveal melanoma samples analysed

Sample No.	Age at diagnosis (years)	Sex	LBD (mm)	UH (mm)	CBI	EOE	Cell Type	Loops	Mitotic count / 40 HPF	Chr3 status	Mets risk
1	59	F	15.7	5.2	N	N	SPIN	Y	7	L	HR#
2	58	M	17.6	11.0	N	Y	MIX	N	5	L	HR*
3	61	M	16.3	8.6	N	N	MIX	Y	5	N	LR*
4	64	F	17.4	6.5	N	N	SPIN	N	3	N	LR
5	41	M	12.7	11.6	N	N	MIX	N	3	N	LR
6	77	F	14.7	55.7	N	N	EPI	N	7	L	HR*
7	71	F	13.6	8.0	N	N	MIX	Y	6	L	HR
8	80	F	18.2	12.5	N	Y	MIX	N	1	L	HR
9	51	M	16.2	14.8	Y	N	SPIN	Y	4	N	LR
10	67	M	18.7	12.2	Y	N	MIX	N	2	L	HR*
11	76	F	15.4	7.8	N	N	SPIN	N	7	L	HR
12	71	M	13.0	5.9	N	Y	MIX	N	4	L	HR*
13	65	M	19.2	16.8	Y	N	MIX	Y	1	L	HR
14	77	F	15.2	8.9	N	N	MIX	N	4	L	HR

CBI, ciliary body involvement; Chr3, Chromosome 3; EOE, extraocular extension; EPI, epithelioid cell type; F, Female; G, gain; HPF, high power field; HR, high risk; L, loss; LBD, largest basal diameter; LR, low risk; M, Male; MIX, mixed cell type; N, normal; SPIN, spindle cell type; UH, tumour thickness

*indicates death from metastatic disease; # indicates death from other causes

Table 4.2. The clinical history of the human cadavers from which normal choroidal melanocytes were derived

Sample No.	Age	Sex	Cause of death	Other history
NCM1	63	F	Renal cancer Thyroid disease, hypercholesterolemia,	Thyroid disease, hypercholesterolemia, atherosclerosis
NCM2	39	M	Cardiac arrest	Nil
NCM3	52	M	Pancreatic cancer	Non-insulin dependent diabetes
NCM4	55	M	Cardiac arrest	Nil
NCM5	17	M	Motor vehicle accident	Nil

F, female; M, male; NCM, normal choroidal melanocytes

4.3.1. Analysis of the predicted secretory mechanism of the proteome

The initial protein dataset consisted of 1843 proteins. After filtering the proteins to remove any identified with less than three unique peptides, 758 confidently identified proteins remained for further analysis.

The secretory mechanism of each of the 758 proteins identified in the PUM and NCM cultures were assessed and demonstrated that 29% (220 proteins) of the proteins in the sample were not predicted to be associated with any secretory mechanism. Of the remaining 71% (539) of proteins, 19% (144 proteins) were predicted to be classically secreted, 6% (15 proteins) non-classically secreted and the remaining 46% (379 proteins) were predicted to be secreted via exosomes (Figure 4.2). The GO-annotation of the 379 proteins identified as exosomal were interrogated to identify 'cellular component', proteins were filtered to show those which were identified as 'EV proteins' through exocarta, but not annotated with GO-terms associated with EV biogenesis and release; filtering identified proteins with annotations including the terms 'vesicle', 'exosome', 'endosome' 'membrane', 'cell surface', 'clathrin', 'caveola' and 'lipid raft'. Of the 379 proteins identified as released through EVs, 359 had annotations associated with EV biogenesis and release. The 20 proteins listed on exocarta which do not contain GO-annotation of cellular components related to EV biogenesis and release are listed in Table 4.3.

Table 4.3. The names and accession numbers of proteins identified as secreted via extracellular vesicles that had no cellular component gene ontology annotations associated with the biogenesis or release of extracellular vesicles

Protein Accession Number	Protein Name
P14678	Small nuclear ribonucleoprotein-associated proteins B
O60869	Endothelial differentiation-related factor 1
P09871	Complement C1s subcomponent
Q14103	Heterogeneous nuclear ribonucleoprotein D0
P16401	Histone H1.5
Q07955	Serine/arginine-rich splicing factor 1
Q14847	LIM and SH3 domain protein 1
P42765	3-ketoacyl-CoA thiolase
Q9UNE7	E3 ubiquitin-protein ligase CHIP
Q9Y315	Deoxyribose-phosphate aldolase
Q9NVA2	Septin-11
P15559	NAD(P)H dehydrogenase
Q99436	Proteasome subunit beta type-7
P07311	Acylphosphatase-1
P29218	Inositol monophosphatase 1
Q15370	Elongin-B
P38117	Electron transfer flavoprotein subunit beta
P51452	Dual specificity protein phosphatase 3
O75347	Tubulin-specific chaperone A
O43396	Thioredoxin-like protein 1

When filtered for proteins that are not predicted to be secreted, the dataset consisted of 539 ‘intentionally secreted’ proteins (Figure 4.3.).

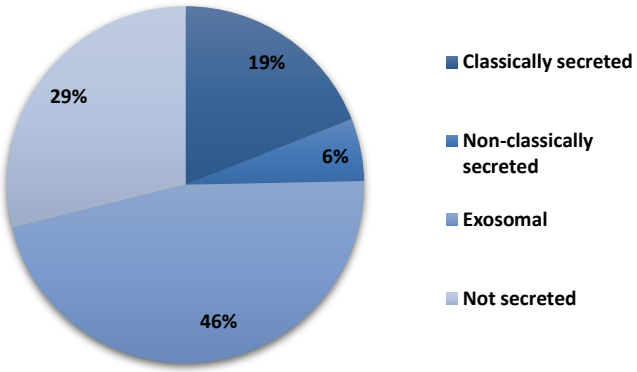

Figure 4.2: The abundance of 758 proteins in the UM and NCM secretome, grouped according to their mechanism of secretion.

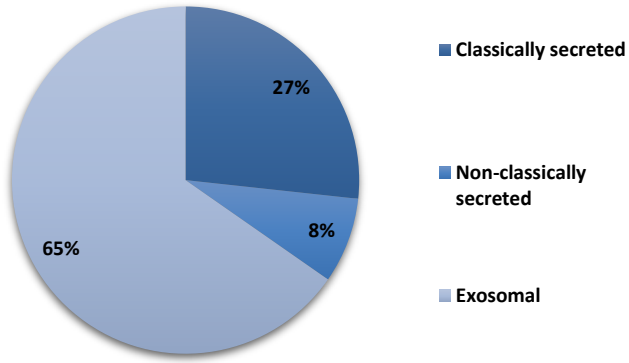

Figure 4.3: The abundance of 539 proteins with predicted secretory mechanisms in the UM and NCM secretome, grouped according to their mechanism of secretion.

4.3.2. Assessing the accession numbers in the dataset

The accession numbers of the 758 proteins identified in the conditioned media of samples from all groups (N=19) were uploaded into IPA. All protein IDs were recognised except for the three proteins listed in Table 4.4.

Table 4.4. Unmapped protein identifiers in the 758-protein dataset

Primary accession number	Uniprot associated protein
Q71DI3	Histone H3.2
P62805	Histone H4
P69905	Haemoglobin subunit alpha

Over-representation of cell death and apoptosis-related proteins/pathways associated with the dataset may indicate proteins "unintentionally" secreted due to protein leakage during cell death. When the 758 protein accession numbers were analysed with IPA, cell death pathways were associated with the dataset, with a p-value of 2.38×10^{-29}, suggesting a reduced cell viability in the culture system; however, as only accession numbers were uploaded, no z-score for the up/downregulation of the pathway was attributable. An association with cellular proliferation was also identified, with a p-value of 3.86×10^{-55}. As the association significance of cellular proliferation was ranked higher in the software than that of cell death, the association of both was assumed to indicate that the data set was representative of a living system. The ranking of the two pathways suggested that the dataset was more representative of secreted proteins involved in proliferation due to cellular viability than protein leakage due to cell death. This corresponds to original analysis on these data by (Angi *et al.*, 2016), who reported that cell viability was ≥95% at 48h during serum free culture. This assessment was made through the employment of methods previously demonstrated by (Villarreal *et al.*, 2013).

4.3.3. Predicting the cellular localisation of the identified proteins

The localisation of the proteins identified in the UM secretome was assessed with the online freeware GOrilla. Enrichment of the gene ontology cellular component information for the dataset was performed and highlighted extracellular secreted proteins and proteins associated with membrane vesicles (Table 4.5.)

Table 4.5. Functionally enriched cellular components predicting the most common cellular location of the proteins in the 758-protein dataset.

GO term	Description	Inverse log10 q-value
GO:0005788	Endoplasmic reticulum lumen	5.65
GO:0044432	Endoplasmic reticulum part	4.41
GO:0031093	Platelet alpha granule lumen	3.36
GO:0030667	Secretory granule membrane	3.21
GO:0031982	Vesicle	3.10
GO:0005576	Extracellular region	2.89
GO:0044421	Extracellular region part	2.84
GO:0005615	Extracellular space	2.64
GO:0044433	Cytoplasmic vesicle part	2.61
GO:0012506	Vesicle membrane	2.58
GO:1903561	Extracellular vesicle	2.56
GO:0043230	Extracellular organelle	2.52
GO:0070062	Extracellular exosome	2.40
GO:0030659	Cytoplasmic vesicle membrane	2.33
GO:0098805	Whole membrane	2.30

4.3.4. Comparing the intentionally secreted proteins of UM with NCM cultures

Initial comparisons of the UM secretome with that of NCM focused on the 539 proteins deemed to be ‘intentionally secreted’; these were examined in 19 samples.

The experimental ratios between the average UM relative abundance (n=14) and the average NCM relative abundance (n=5), the associated Mann-Whitney U values, and the corresponding protein accession numbers were uploaded to IPA. IPA was employed to assess the correlation of the dataset with known 'Disease and Bio Functions', 'Canonical Pathways', and to predict activation z-scores for each function/pathway highlighted. Positive z-scores represent upregulation/activation of the correlated pathway/function, and negative z-scores represent downregulation/inhibition of the pathway/function.

4.3.5. Comparing the intentionally secreted proteins of UM with NCM cultures: Assessing the associated diseases and bio functions

The associated 'Diseases and Bio Function' were filtered to only give functions with a z-score ≥2 or ≤-2, and an inverse log10 p-value ≥2. Two functions predicted to be upregulated in UM compared with NCM were linked to the adhesion and attachment of cells (z-score = 2.41 and 2.28 respectively). The synthesis and metabolism of reactive oxygen species were both predicted to be upregulated by the software in UM compared with NCM (z-score = 2.51 and 2.01, respectively) (Figure 4.4.).

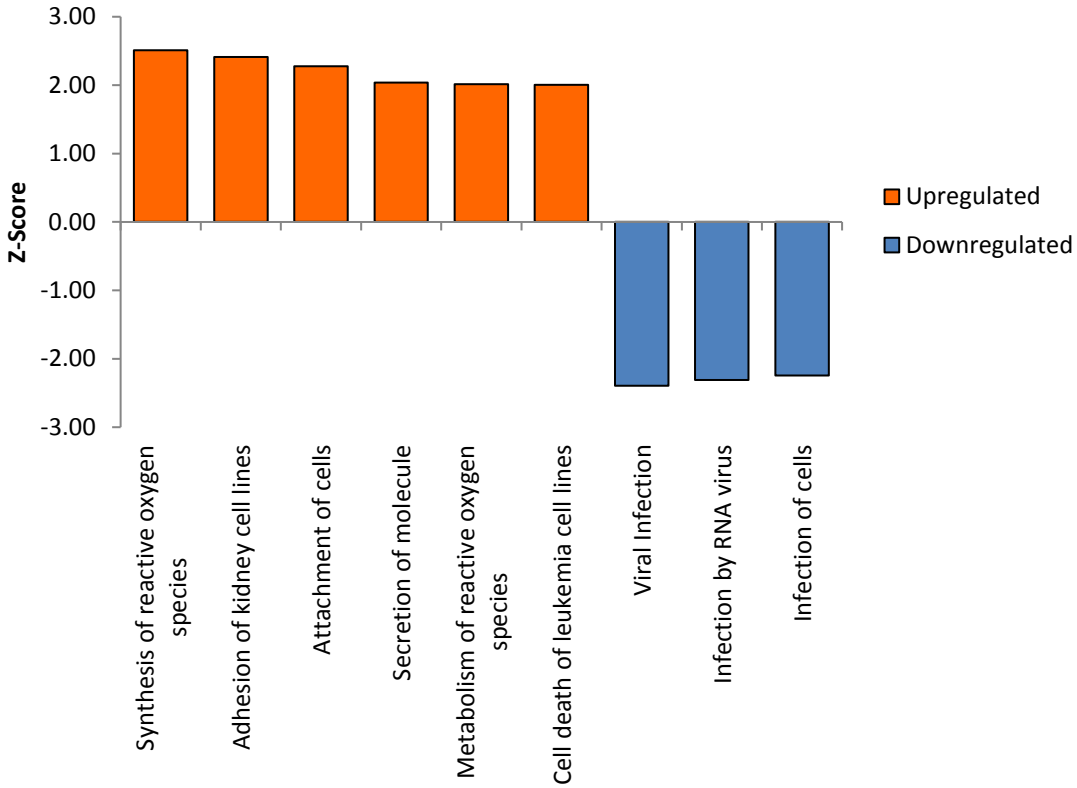

Figure 4.4. Diseases and Bio Functions associated with the 539-protein dataset (inverse log10 p-value ≥ 2) that were differentially expressed between UM and NCM (z-score ≥2 or ≤-2)

As z-scores ≥2 or ≤-2 were infrequent, the associated functions were expressed in the order of their association score (inverse log10 p-value). Cell movement, migration and invasion dominated the top ten associated functions (6/10 functions) (Figure 4.5.). Cell death and apoptosis were also apparent in the dataset (inverse log10 p-values = 27.9 and 25.6 respectively); interestingly, while the associated z-scores were below the cut off (z-scores ≥2 or ≤-2), they were both positive (z-score = 1.08 and 0.71 respectively), suggesting the possibility of a slight increase in cell death and apoptosis in UM compared with NCM.

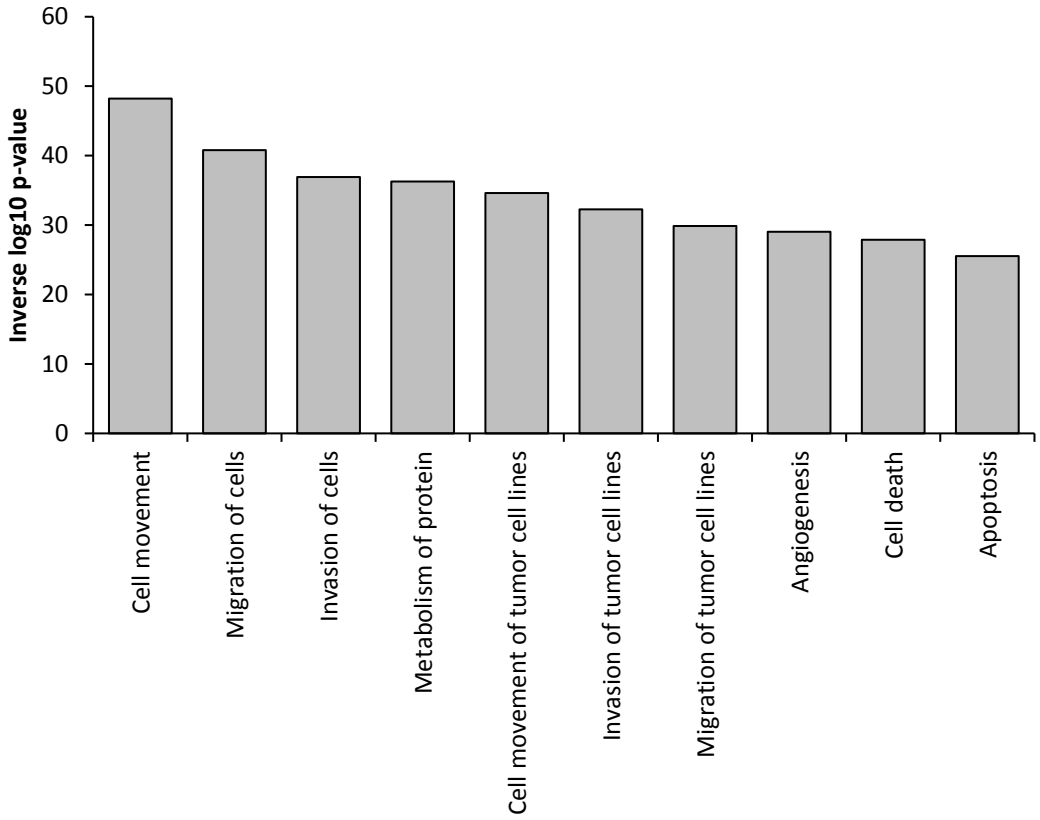

Figure 4.5. The ten Diseases and Bio Functions showing the highest association with the 539-protein dataset, when comparing the uveal melanoma and normal choroidal melanocyte secretomes

4.3.6. Comparing the intentionally secreted proteins of UM with NCM cultures: Assessing the associated top canonical pathways

IPA analysis highlighted 'top canonical pathways' associated with the proteins in the dataset and attributed z-scores to those pathways, where possible. When the data set was filtered for pathways with an inverse log10 p-value ≥2 and a z-score ≥2 or ≤-2, upregulated pathways included GP6 signalling, agrin neuromuscular junction signalling, and LXR/RXR activation (z-score = 3.3, 2.2 and 2.1, respectively) (Figure 4.6.).

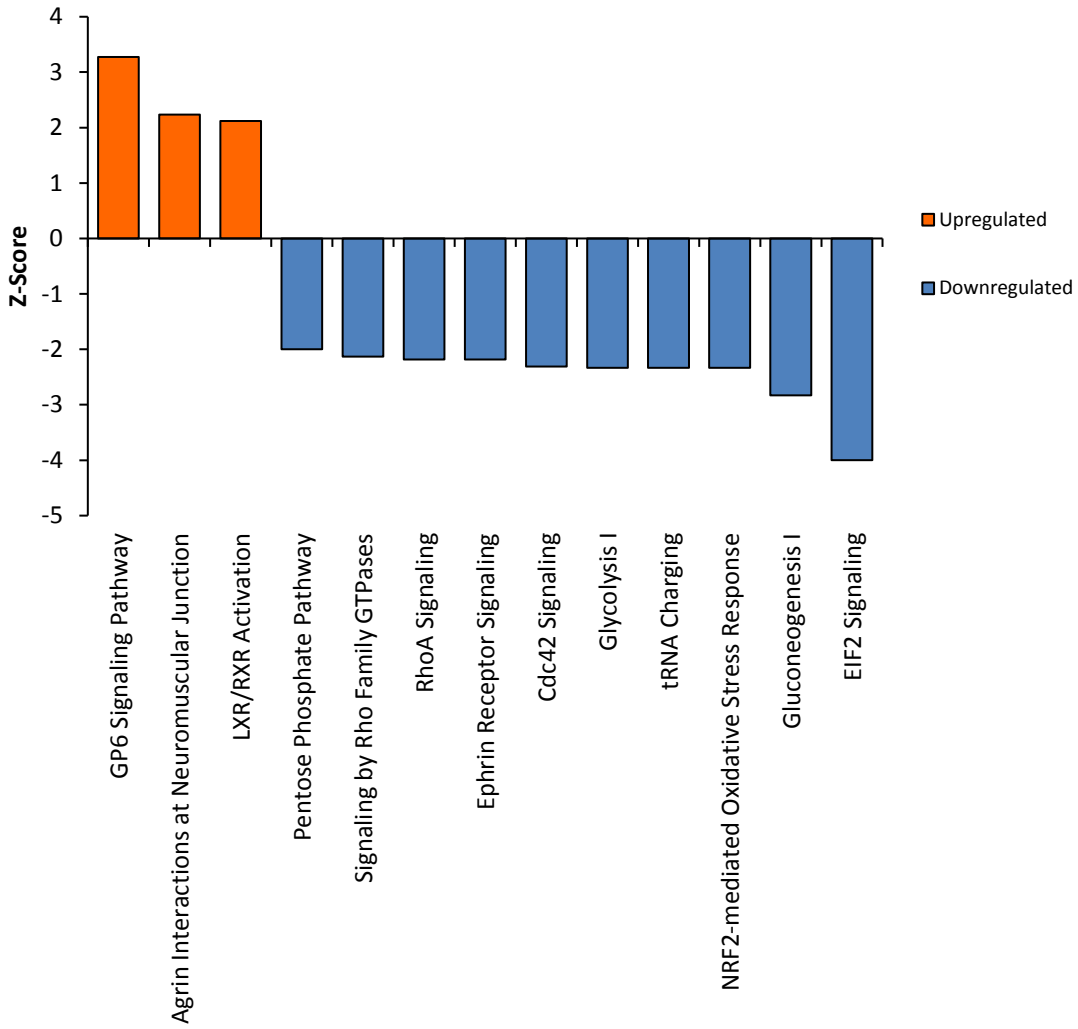

Figure 4.6. The top canonical pathways associated with the 539-protein dataset (inverse log10 p-values ≥2) and differentially expressed between the uveal melanoma and normal choroidal melanocyte secretomes (z-scores ≥2 or ≤-2)

As z-scores were again infrequent, pathways were ranked by association score to highlight what pathways dominated the secretome signalling, regardless of directionality. 'Top canonical pathway' analysis revealed that 11 of the top 15 pathways most statistically associated with the dataset were related to mTOR and GTPase signalling with inverse log10 p-values ranging from 7.37 to 20.7. Hepatic fibrosis and HSC activation was the third most correlated pathway with an inverse log10 p-value of 12.7, which is of interest due to the propensity of UM to metastasise to the liver, and Leukocyte Extravasation signalling also correlated with an inverse log10 p-value of 9.7 (Figure 4.7.).

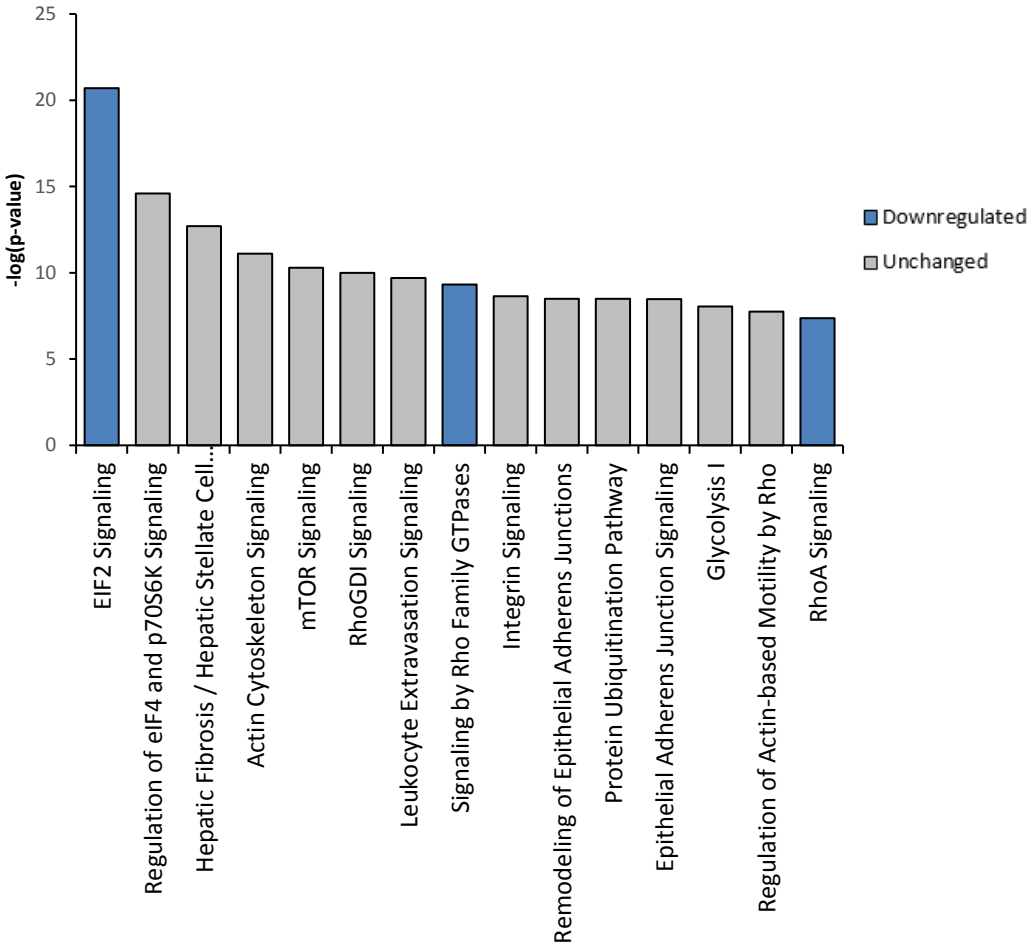

Figure 4.7. The top 15 canonical signalling pathways associated with the 539-protein dataset (inverse log10 p-values ≥2) and differentially expressed between the uveal melanoma and normal choroidal melanocyte secretomes (z-scores ≥2 or ≤-2)

4.3.7. Comparing the intentionally secreted proteins of HR-UM with LR-UM cultures: Assessing the associated diseases and bio functions

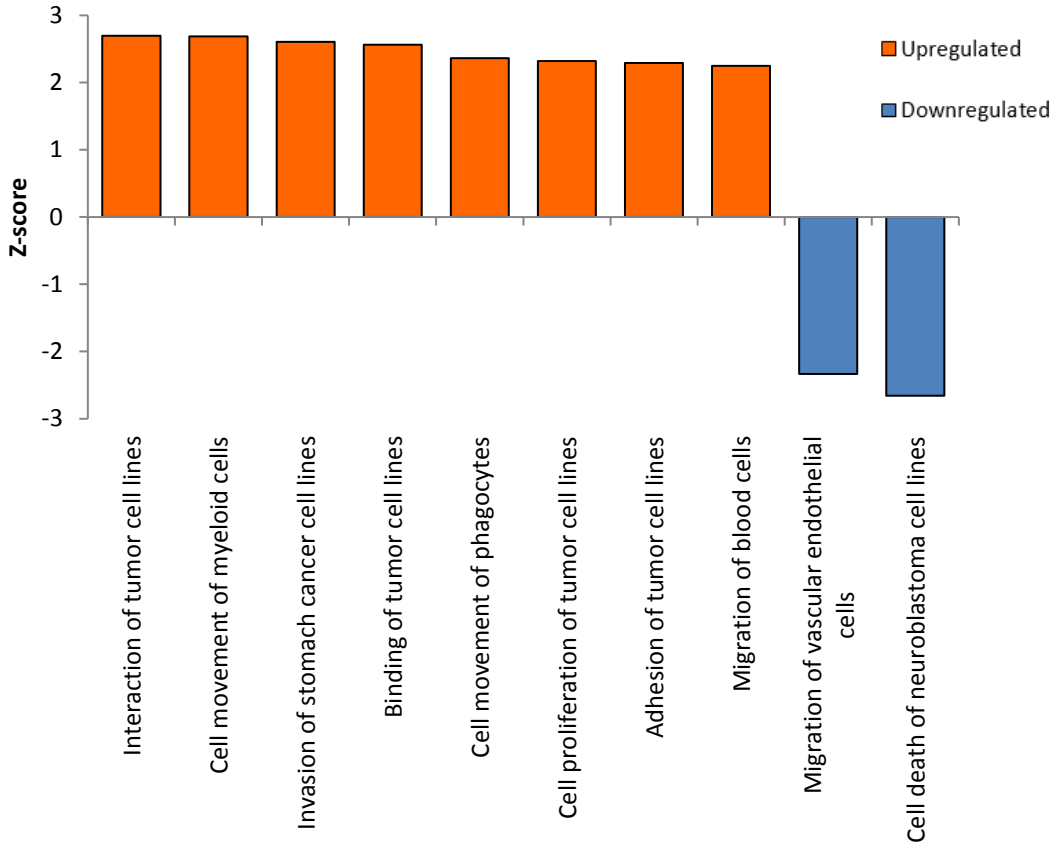

Figure 4.8. The ten most differentially expressed Disease and Bio Functions associated with the 539-protein dataset (z-scores ≥2 or ≤-2; inverse log10 p-values ≥2) between the secretomes of uveal melanoma at high and low risk of metastasis

When comparing HR-UM with LR-UM, functions linked with adhesion and migration were frequently upregulated (6 of the 10 most differentially expressed functions); interestingly however, one migration related pathway (migration of vascular endothelial cells) was predicted to be downregulated. Cell proliferation was shown to be upregulated (z-score = 2.32), likewise cell death was downregulated (z-score = -2.66) (Figure 4.8).

4.3.8. Comparing the intentionally secreted proteins of HR-UM with LR-UM cultures: Assessing the associated top canonical pathways

Comparing HR-UM with LR-UM revealed differentially associated pathways related to an upregulation in inflammation (NFkB signalling, IL-6 signalling), and signalling associated immune cell health, activation and migration (Agrin, IL-6 and leukocyte extravasation); downregulation of PTEN and EIF2 signalling was also observed (Figure 4.9.).

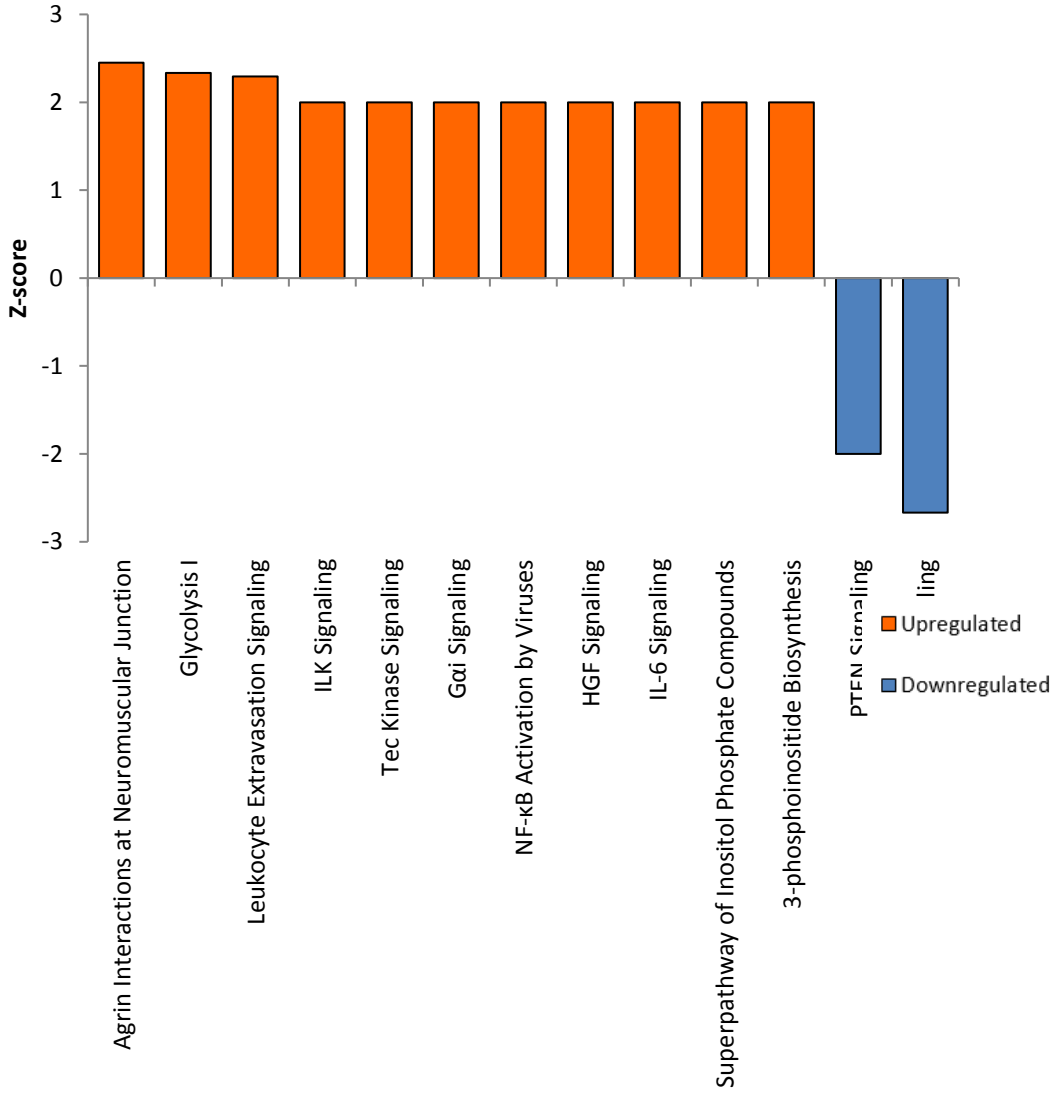

Figure 4.9. The most differentially expressed canonical pathways associated with the 539-protein dataset (z-scores ≥2 or ≤-2; inverse log10 p-values ≥2) between the secretomes of uveal melanoma at high and low risk of metastasis

4.3.9. Comparing the total secretomes of UM and NCM: 758-protein dataset

The method employed for establishing a dataset of 539 'intentionally secreted' proteins was reliant on algorithms which predict secretory mechanisms based on experimentally observed data of proteins previously reported in the literature. As studies into the contents of tissue secretomes and exosomes are consistently revealing new insights, and as this dataset represents the first study interrogating the proteome of the UM secretome, it was decided that all confidently identified proteins (the 758 protein dataset) would be included in all further analysis.

The following analyses interrogate the 758-protein total secretome dataset, containing proteins confidently identified with ≥3 unique peptides, in 19 samples. Again, the experimental ratios between the average UM relative abundance (n=14) and the average NCM relative abundance (n=5), the associated Mann-Whitney U values, and the corresponding protein accession numbers were uploaded to IPA to assess the correlation of the dataset with known 'Disease and Bio Functions' and 'Canonical pathways', and to predict z-scores for each function/pathway.

4.3.10. Comparing the total secretomes of UM and NCM: Assessing the associated Disease and Bio Functions of the 758-protein dataset

When analysing the 758-protein data set, cell death, apoptosis and necrosis were apparent in the disease and bio-functions, with p-values of 1.41×10^{-21}, 1.18×10^{-19} and 1.24×10^{-21}, respectively. Activation z-scores for cell death, apoptosis and necrosis were -1.212, -1.565 and -0.845; while below the cut-off, this could signify slight downregulation in cell death in

the UM secretome compared with NCM. Additionally, cell viability and cell survival were predicted to be associated with the dataset and upregulated in UM compared with NCM (z-scores = 4.552 and 5.538, respectively) (Figure 4.10.).

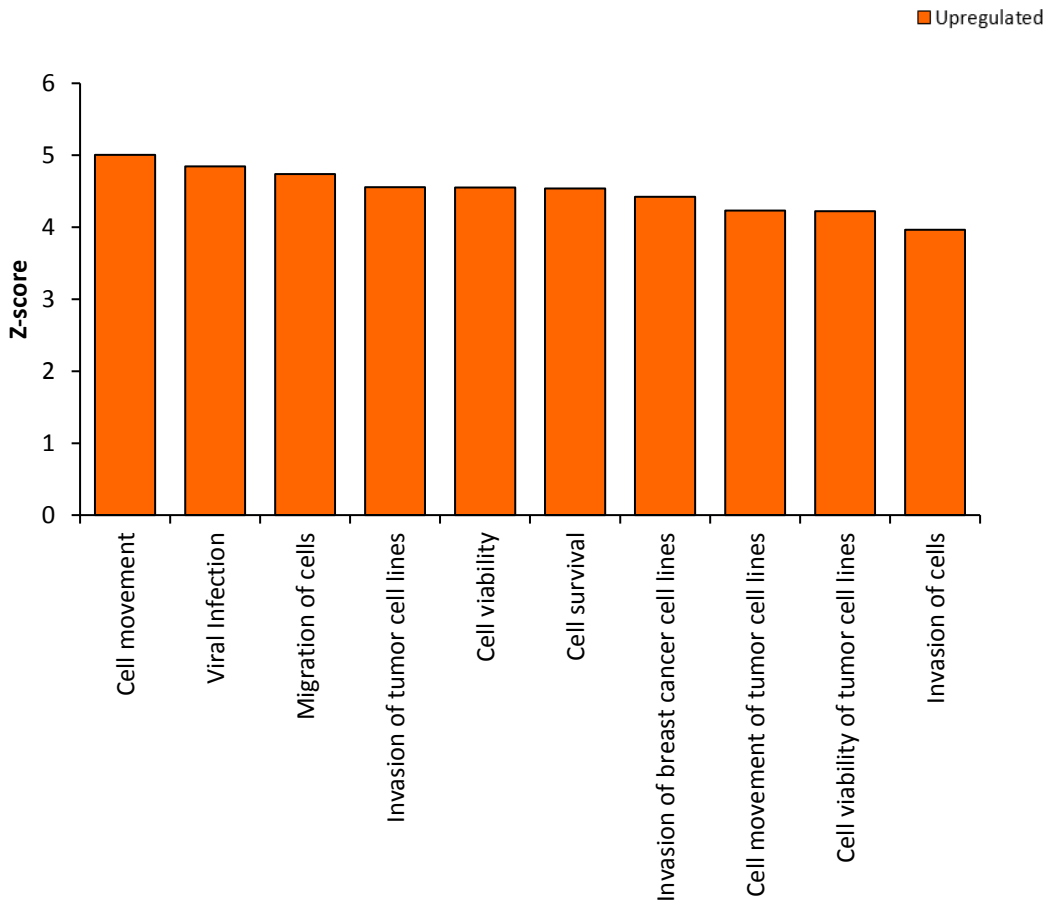

Figure 4.10. The most differentially expressed Diseases and Bio Functions associated with the 758-protein dataset (z-scores ≥2 or ≤-2; inverse log10 p-values ≥2) between uveal melanoma and normal choroidal melanocyte secretomes

Of the 10 'Disease and Bio Functions' with the highest predicted activation (z-score greater than 2), the majority of functions suggested a malignant phenotype; cell movement, invasion and migration were all predicted to be upregulated in UM compared with NCM, with z-scores between 3.96 and 5.00 (Figure 4.10). When the functions were ordered by

association statistic, increased malignancy was apparent in the functions highlighted; an upregulation of invasive and migratory processes dominated the top ten associated functions; the top six associated functions each possess z-scores >2 and collectively suggest an upregulation of a migratory and invasive phenotype in UM compared with NCM (Figure 4.11).

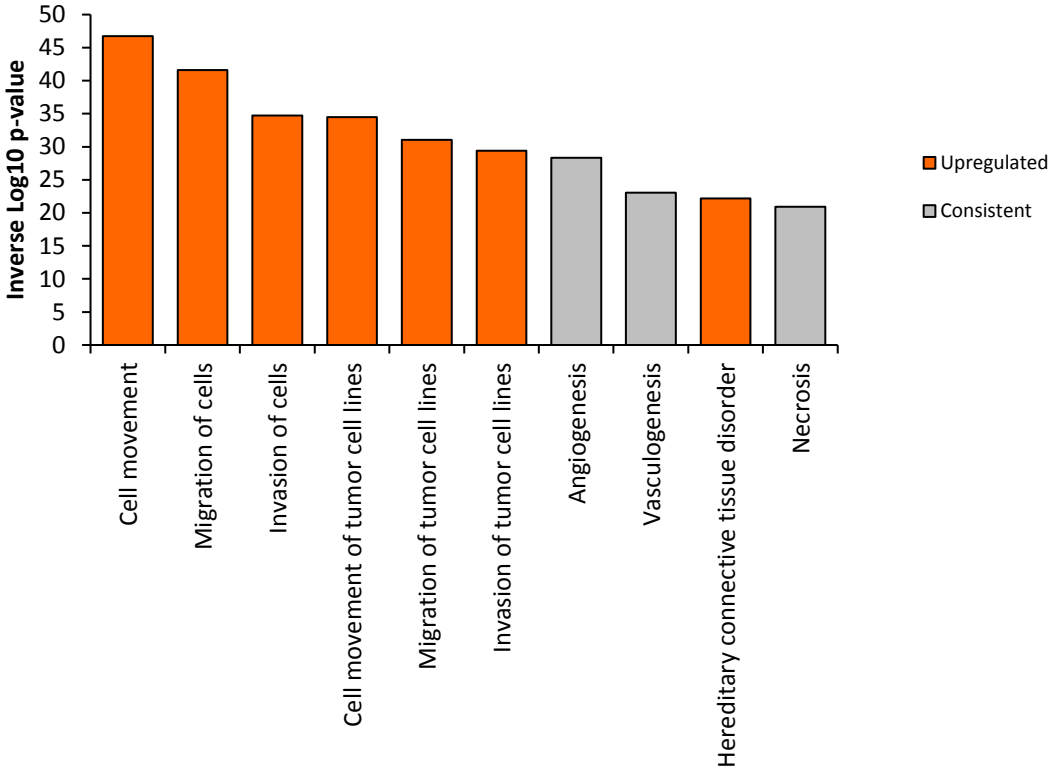

Figure 4.11. The ten Diseases and Bio Functions showing the highest association with the 758-protein dataset, when comparing the uveal melanoma and normal choroidal melanocyte secretomes

4.3.11. Comparing the total secretomes of UM and NCM: Canonical pathways associated with the 758-protein dataset

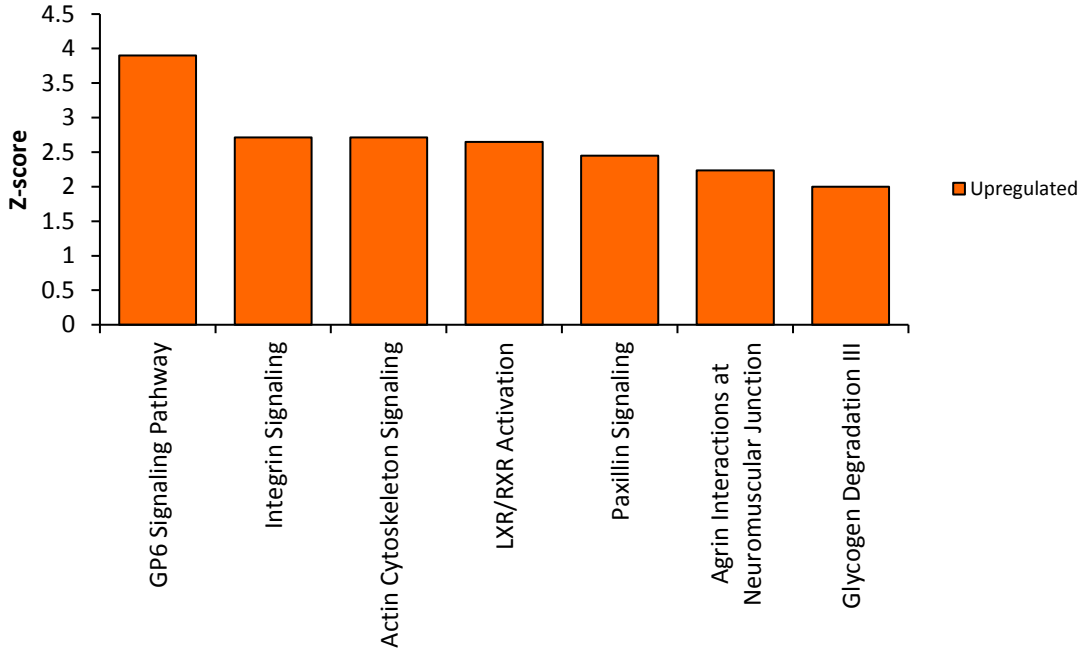

Figure 4.12. The top canonical pathways associated with the 758-protein dataset (inverse log10 p-values ≥2) and differentially between the uveal melanoma and normal choroidal melanocyte secretomes (z-score ≥2 or ≤-2)

Top canonical pathway analysis of the 758-protein data set revealed similar pathways to that of the 539-protein data set. GP6, LXR/RXR and agrin signalling were predicted to be upregulated, similar to the 539-protein dataset (z-score = 3.9, 2.6 and 2.2 respectively) (Figure 4.11). Other upregulated pathways were integrin signalling (z-score = 2.7), actin cytoskeleton signalling (z-score = 2.7) and paxillin signalling (z-score = 2.4) (Figure 4.12.). Glycogenolysis was also associated with the dataset and was suggested to be upregulated in UM compared with NCM (z-score = 2.00) (Figure 4.12.).

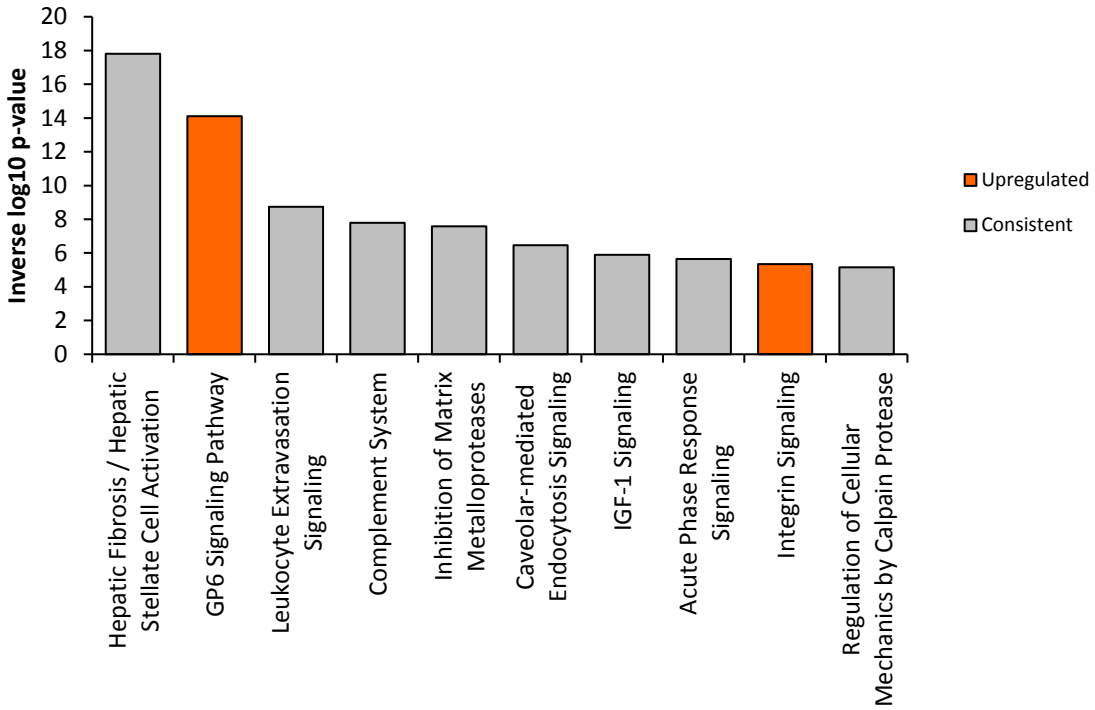

Figure 4.13. The ten canonical pathways with the highest association to the 758-protein dataset when comparing the uveal melanoma and normal choroidal melanocyte secretomes

Several pathways showed high association with the 758-protein data set with z-scores below the cut off (Figure 4.13). Hepatic fibrosis showed the greatest association with the data set (inverse log10 p-value = 17.8). Several other associated pathways suggested a migratory phenotype, with signalling linked to extravasation, matrix metalloprotease inhibition, integrin signalling and the regulation of cellular mechanics (inverse log10 p-values = 8.74, 7.59, 5.35 and 5.16, respectively).

4.3.12. Comparing the total secretomes of HR-UM with LR-UM: Assessing the associated Disease and Bio Functions of the 758-protein dataset

HR-UM samples displayed a downregulation in pathways associated with cell death when compared with LR-UM. Of the 16 functions predicted to be downregulated, ten were related to cell death and had z-scores between -2.04 and -9.93. Conversely, 'Cell survival' and 'Cell viability' were upregulated in HR-UM samples compared with LR-UM, predicted z-scores were between 6.31 and 6.17.

There was a pattern of upregulation in pathways associated with invasion and metastasis in HR-UM samples when compared with LR-UM. More than half of the functions predicted to be upregulated were related to invasion and/or migration (75/138 functions; z-score = 2.01–6.08).

Collectively, these proliferative and migratory pathways suggest a malignant phenotype was promoted by the HR-UM secretome; 14 of the top 15 associated functions support proliferation and metastatic progression (Figure 4.14.).

There were also two upregulated functions associated with fibrosis, 'Cell proliferation of fibroblasts' and 'Cell movement of fibroblasts' with z-scores of 2.33 and 2.81, respectively. Taken collectively with other potentially related, upregulated functions such as 'Organization of cytoskeleton' (z-score = 4.53), this suggests that HR-UM possesses increased potential to stimulate fibrosis via secreted proteins.

Protein turnover was predicted to be upregulated in the HR-UM secretome compared to LR-UM; 'Catabolism of protein' (z-score = 3.40), 'Metabolism of protein' (z-score = 3.29) and 'Proteolysis' (z-score = 2.68) demonstrating upregulation.

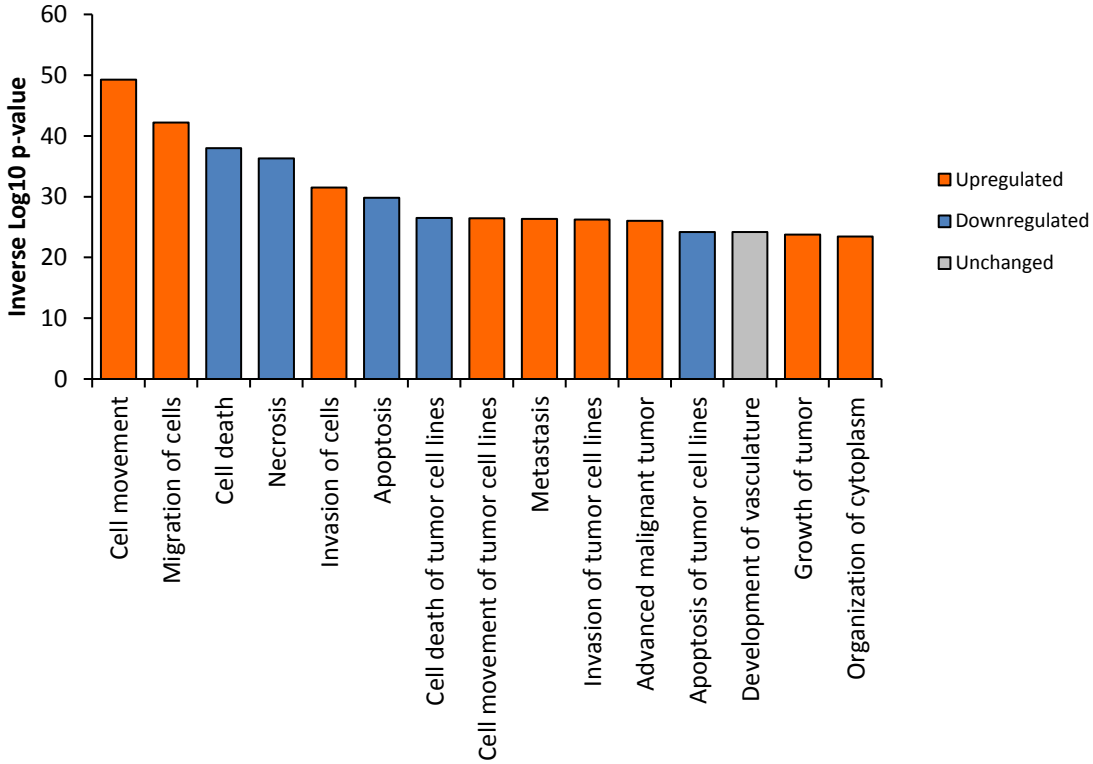

Figure 4.14. The fifteen Diseases and Bio Functions with the highest association to the 758-protein dataset when comparing the secretome of uveal melanoma at high and low risk of metastasis

4.3.13. Comparing the total secretomes of HR-UM with LR-UM: Assessing the canonical pathways associated with the 758-protein dataset

When arranged by z-score, there is a striking pattern of pathways linked with migration or motility; of the 16 pathways predicted to be upregulated or downregulated, 14 pathways have links with cytoskeletal modulation, migration, adhesion or invasion (z-scores = -2.14–4.12) (Figure 4.15.). This suggests that an enhanced migratory phenotype is observed in HR-UM compared with LR-UM.

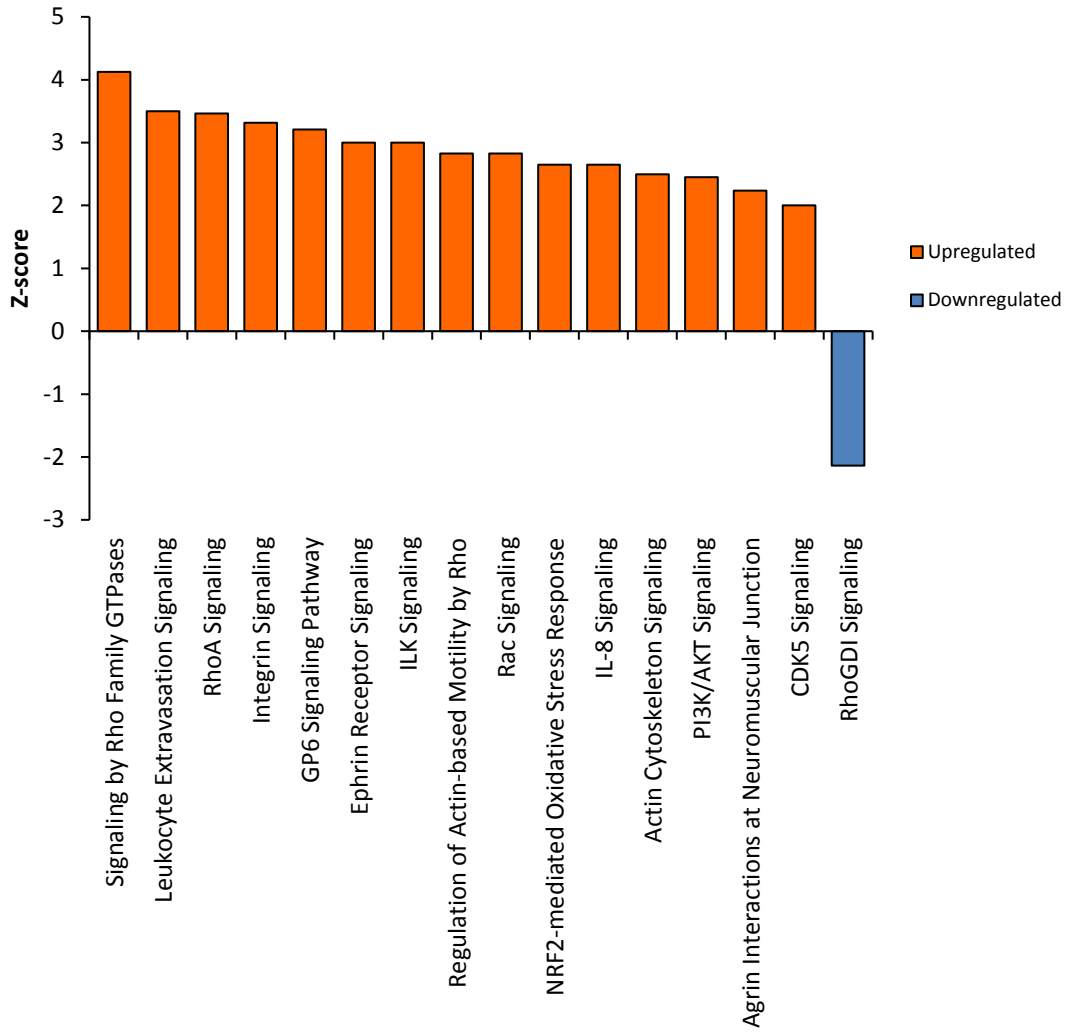

Figure 4.15. The top canonical pathways associated with the 758-protein dataset (inverse log10 p-values ≥2) most differentially expressed (z-scores ≥2 or ≤-2) between the secretomes of uveal melanoma at high and low risk of metastasis

When ordered by statistical association, hepatic fibrosis/HSC activation was the pathway with the highest predicted association (inverse log10 p-value = 10.7) but had no predicted z-score for activation or inhibition. Of the 15 highest associated canonical pathways, 10 could be linked to cytoskeletal remodelling, invasion and migration (Figure 4.16).

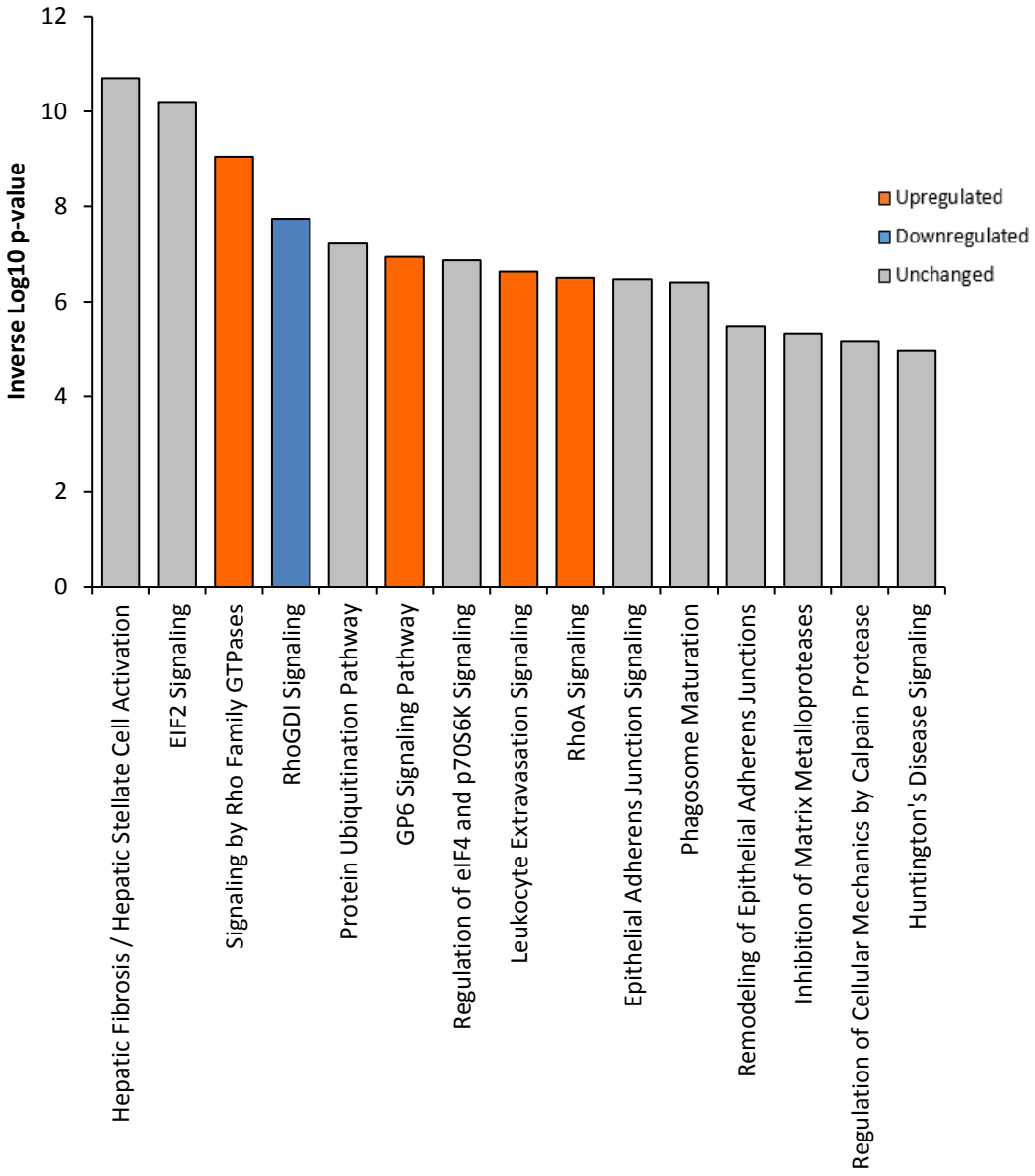

Figure 4.16. The fifteen canonical pathways with the highest association to the 758-protein dataset when comparing the secretomes of uveal melanoma at high and low risk of metastasis

4.3.14. Proteins in the 758-dataset with potential significance to primary tumour development and metastatic progression

The UM samples were sub-grouped into 'total UM' (HR-UM and LR-UM) for comparison with NCM individually. Proteins differentially expressed in both the total UM group when compared with NCM were identified to highlight their potential importance in UM development. This grouping is detailed in Table 4.6. There were 326 proteins identified with greater than 2-fold differential expression; 131 were upregulated, the majority of which were classically or non-classically secreted (77%) and 186 were downregulated, the majority of which were exosomal (51%).

Proteins with potential importance to metastatic progression were also identified by comparing the HR-UM group and the combined LR-UM and NCM groups, 142 proteins were differentially expressed greater than 2-fold, 65 of which were upregulated and 77 were down-regulated. There were 32 exosomal proteins present in this dataset; 15 up-regulated and 17 down-regulated.

Table 4.6. The distribution of differentially expressed proteins when assessing UM development or metastatic risk

Comparison		Differentially expressed proteins		
Group 1	**Group 2**	**Total**	**Upregulated**	**Downregulated**
HR-UM & LR-UM	NCM	326	131	186
HR-UM	NCM & LR-UM	142	65	77

HR, high risk; LR, low risk; UM, uveal melanoma

4.4. Discussion

All cells release biologically active material into their local environment, and the primary effectors of intercellular signalling in mammalian cells are proteins (Lodish *et al.,* 2000). Secreted proteins can facilitate cellular communication in autocrine, juxtacrine, paracrine and endocrine signalling (Lodish *et al.,* 2000).

It is hypothesised that the proteins in the UM secretome are associated with specific intercellular signalling pathways that may be linked with manipulation of the local microenvironment and with education of the premetastatic niche. The research herein aimed to investigate this through a series of comparative analyses, assessing the differences between cultured NCM and primary UM samples, as well as between samples from patients at high risk of metastatic progression and patients at lower risk of metastatic progression.

To the authors knowledge, this research represents the most comprehensive study of the UM secretome to date: of an initial dataset of 1843 proteins identified in all samples with a 1% FDR cut-off, 758 proteins were confidently identified with 3 or more unique peptides, and 539 had predicted secretory pathways (Figure 4.2.). Furthermore, to the authors knowledge, this is first study to comparatively analyse secretomes from short-term 2D cultures of cells isolated from PUM with that of NCM control cells.

Using a variety of freeware and publicly curated databases, this research demonstrates that a large number of proteins in the UM secretome possess predicted secretory mechanisms. Furthermore, our work demonstrates that a strikingly large proportion of the proteins in the UM secretome have been previously been shown in the literature to be of EV origin (Figure 4.2.) (Keerthikumar *et al.*, 2016). Of the 379 proteins identified as secreted via EVs,

only 20 were highlighted via interrogation of Exocarta but not through interrogation of GO cellular component annotation, suggesting that both methods of prediction are appropriate.

The importance of EVs in cancer pathology is gaining increased interest due to their pleiotropism through the transfer of biologically-active signalling molecules (Meehan and Vella, 2016). Previous research by Eldh *et al.,* investigated the miRNA content of small EVs – considered exosomes – isolated from the liver perfusate of patients with MUM (Eldh *et al.*, 2014). The authors analysed the miRNAs against a panel of 88 cancer-related miRNAs, identifying 73 miRNAs in the samples. The authors performed functional analysis of the miRNAs and, similar to the research presented in this chapter, identified cancer related pathways including melanoma and highlighted focal adhesion and mTOR signalling.

In 2015, Ragusa *et al.,* isolated small EVs – considered exosomes – from the aqueous humor of patients with PUM (Ragusa *et al.*, 2015). They identified 179 micro-RNAs, 32 of which were differentially expressed between sample groups. Functional enrichment or functional studies were not performed on the micro-RNAs identified; however, the authors highlighted a role of the candidate micro-RNA mir-146a in immune suppression.

Recently, Surman *et al.,* isolated larger EVs (MVs – termed ectosomes by the authors) from the UM cell line Mel202 (Surman *et al.*, 2019). The research identified 949 proteins and again, similar to the research presented herein, highlighted processes and functions associated with cellular adhesion; including adherens junctions (11.1%), focal adhesion (15%), or cadherin-binding activity (11.1%).

Of importance in UM is that the protein content of small exosome-like EVs has not been studied to date. This forms the principle aims of Chapters 5 and 6, which demonstrate the ability to isolate and characterise EVs from UM cell lines and then perform in-depth proteomic profiling and functional enrichment on the isolated EVs.

Cell death pathways were monitored throughout our analyses. High association with cell-death/apoptosis could suggest that the secretome dataset contains large amounts of protein that could be unintentionally released through protein leakage during cell death. Analysis of the proteins suggested that, while present, cell death signalling was not overrepresented in the dataset. This corroborates with our reported >95% viability of UM cells in culture system when assessed by trypan blue staining (Angi *et al.*, 2016). When the dataset was filtered to show only proteins with secretory pathways (539 protein dataset), cell death and apoptosis processes were both highly represented (Figure 4.5.). However, when comparing the secretome of UM samples with NCM, and the HR-UM secretome with that of LR-UM, the predicted activation/inhibition of the cell death and apoptosis processes was below the cut-off value for differential expression of (z-score ≥2 or ≤-2) (Figure 4.5.). When considering the 758 protein dataset, several processes associated with cell death were downregulated in UM compared with NCM, and in HR-UM compared with LR-UM (z-score ≤ -2), while cell viability pathways were upregulated (z score ≥ 2) (Figures 4.10. and 4.14.). Both resistance to cell death and sustained proliferative signalling were highlighted as hallmarks of cancer by Hannahan and Weinberg (Hanahan and Weinberg, 2011). The comparative difference between HR-UM and LR-UM could be explained by the relationship between proliferation kinetics and clinical outcome. This can be explained by the association between higher mitotic count in PUM with higher metastatic risk and mortality (Lattman *et al.*, 1995).

Cellular component analysis highlighted compartments associated with extracellular and vesicular secretion (Table 4.4.). However, cellular components related to the endoplasmic reticulum (ER) were dominantly associated. ER stress is known to influence both the secretory phenotype (Pluquet, Pourtier and Abbadie, 2015) and the level of EV secretion (Keerthikumar *et al.*, 2016). While this could suggest that the serum free culture conditions may be affecting the analysis, it has also been demonstrated that ER stress is associated with dedifferentiation (Ulianich *et al.*, 2008), a known aspect of tumourigenesis. ER stress is also commonly associated with exosome biology and autophagy (Baixauli, López-Otín and Mittelbrunn, 2014); in UM, upregulation of the latter has been linked with early metastasis and reduced survival (Giatromanolaki *et al.*, 2011).

Throughout these analyses, a similar pattern of canonical signalling pathway activation was represented. This pattern included pathways associated with mTOR signalling, RhoA/RhoGTPase signalling, actin remodelling, and adhesion molecule signalling (such as integrin, paxillin integrin-like-kinase (ILK), ephrin and agrin).

The present analyses identified a consistent recurrence of mTOR and mTOR related networks in the pathways associated with the UM secretome (Figures 4.6, 4.7, 4.9 and 4.16). The mTOR protein (mechanistic target of rapamycin) is a serine/threonine protein kinase in the PI3K-related kinase family of proteins and forms the catalytic subunit of two protein complexes, MTORC1 (mTOR complex 1) and MTORC2 (mTOR complex 2) (Saxton and Sabatini, 2017). MTORC1 plays a role in the promotion of mRNA translation and protein synthesis (Saxton and Sabatini, 2017), nucleotide and lipid synthesis (Laplante and Sabatini, 2009; Valvezan *et al.*, 2017), and the inhibition of protein turnover and autophagy (Paquette, El-Houjeiri and Pause, 2018). MTORC2 has reported functions in cell survival and reduced apoptosis (Zou *et al.*, 2015), promotion of cell cycle progression (B. W. Chen *et al.*,

2015), cytoskeletal remodelling (Jacinto *et al.*, 2004), and cell migration (Li *et al.*, 2012). When considering the total secretome, these mTOR pathways were most associated when comparing the HR-UM with LR-UM secretomes (Figure 4.16.).

In 2010, Pópulo *et al.,* highlighted extensive activity of the mTOR pathway in UM through immunohistochemical analysis of PUM samples (Pópulo *et al.*, 2010). They demonstrated phosphorylation of mTOR (Ser2448) in 76% of cases and phosphorylation of the downstream targets of MTORC1 signalling S6 (Ser235/S236) and 4EBP1 (Thr37/46) in 43% and 76% of cases, respectively. However, they suggested that the phosphorylation of S6 was lower in UM than in conjunctival melanoma, and that this could be due to increased expression of PTEN which downregulates this pathway. Similar research was conducted in 2014, when Amirouchene-Angelozzi *et al.,* showed the importance of mTORC1 signalling in a panel of genetically representative UM cell lines and patient-derived xenografts. They demonstrated activation of the mTORC1 pathway at levels similar to cell lines with mutations causing constitutive activation of PI3KCA, a kinase upstream of mTORC1. They demonstrated reduced tumour burden *in vivo* in response to MTORC1 inhibition and highlighted the potential of therapeutically targeting this pathway in UM (Amirouchene-Angelozzi *et al.*, 2014). MTORC2 activity has received less attention in UM. In 2012, Ho *et al.,* demonstrated the efficacy of a novel ATP-competitive pan-mTOR inhibitor and showed effective inhibition of AKT phosphorylation, thought to be through MTORC2 inhibition (Ho *et al.*, 2012). They also showed inhibition of S6K phosphorylation through MTORC1 inhibition. Interestingly, the authors demonstrated time-dependent rescue of AKT phosphorylation after MTORC2 inhibition; however, they noted that this was not due to ineffective inhibition of MTORC2.

RhoGTPases are small GTP (guanosine triphosphate) binding proteins and members of the Ras superfamily. Like Ras, Rho cycles between an inactive and active state, dependent on GDP (guanosine diphosphate) and GTP binding respectively (Bishop and Hall, 2000). Rho GTPase related pathways were highlighted throughout these analyses (Figures 4.6., 4.7., 4.15., 4.16.) and were among the most differentially expressed pathways between the HR-UM and LR-UM secretomes (Figure 4.15.). RhoA signalling is known to be activated downstream of the MTORC2 phosphorylation and has also been shown to have a role in cancer motility and migration due to its influence on cytoskeletal remodelling (Jacinto *et al.*, 2004; Gulhati *et al.*, 2011). Both mTOR and RhoA are responsive to multiple, distinct incoming signals. It has been demonstrated in UM that RhoA can act downstream of GPCRs (such as GNAQ/11) and TRIO, stimulating the nuclear translocation of the YAP/TAZ (Feng *et al.*, 2014). YAP/TAZ signalling is involved in cellular response to the mechanical properties of the ECM and cell shape/geometry (Dupont *et al.*, 2011). Adding to the complexity of this signalling network, YAP nuclear translocation is thought to be promoted by MTORC2 inhibition of AMOTL2 (Artinian *et al.*, 2015).

In this research, pathways associated with cellular adhesion were also highly associated and differentially expressed between groups. Integrin, paxillin and agrin signalling were among the most upregulated pathways in the UM secretome compared with NCM secretome (Figure 4.12.). Integrin, ILK, ephrin and agrin signalling were among the most upregulated pathways in the HR-UM secretome compared with the LR-UM secretome (Figure 4.15.).

Integrins are evolutionarily conserved cell adhesion receptors that act as functional links between the ECM and the cytoskeleton (Johnson *et al.*, 2009; Barczyk, Carracedo and Gullberg, 2010). Their role in cancer and the implications of targeting them therapeutically were extensively review by Desgrosellier and Cheresh in 2010 (Desgrosellier and Cheresh,

2010), where the authors highlighted the role of integrins in metastatic progression of several types of cancer. Elshaw *et al.,* investigated the involvement of integrins in the invasive potential of UM and ocular melanocytes (Elshaw *et al.*, 2001). The laminin binding integrins α6β1 were expressed in epithelioid cell UM, yet not in NCM or in those UM with spindle morphology, suggesting the presence of these integrins may be indicative of a worse prognosis and invasive potential (Elshaw *et al.*, 2001). The integrin composition of EVs secreted from tumours is thought to influence organotropic metastasis, as demonstrated by (Hoshino *et al.*, 2015). The authors highlighted the presence of several integrins on EVs secreted by MUM cells; namely, integrins α1, 2, 3, 4, 6 and V, and β1, 3 and 5. Moreover, they suggested that integrins αV and β5, both found on MUM EVs, allowed preferential binding to Kupffer cells, mediating liver tropism. Herein, the integrins αV, α3 and β1 were identified in the UM and NCM secretomes. All three were significantly upregulated in UM compared with NCM and integrin αV was upregulated in HR-UM compared with LR-UM.

Paxillin is thought to be involved in regulation of Rho GTPase signalling and actin remodelling (Chen *et al.*, 2005), while agrin is a laminin-binding protein that promotes YAP nuclear translocation and HIPPO-pathway signalling, facilitating YAP-regulated mechanotransduction in response to changes in the ECM (Chakraborty *et al.*, 2017). Paxillin was not identified in the dataset. Agrin was identified and significantly upregulated in UM compared with NCM more than 8-fold ($p < 0.05$; 2-tailed Mann-Whitney U) but was not differentially expressed between HR-UM and LR-UM.

Collectively, the mTOR and Rho GTPase signalling, actin dynamics, and adhesion signalling all link with the cell's reciprocal relationship to its surrounding ECM (Boyle and Samuel, 2016). Remodelling of the actin cytoskeleton in response to external mechanical stimuli is

governed by a complex feedback loop involving Rho GTPase signalling, integrins and cell adhesion dynamics among other processes associated with mTOR signalling (Boyle and Samuel, 2016). Highly invasive UM cells are known to generate multiple ECM products, such as laminin (Chen *et al.*, 2001), collagen IV (Hao *et al.*, 2003), collagen VI (Daniels *et al.*, 1996), and fibronectin (Lin *et al.*, 2005).

Manipulation of the ECM in UM is also associated with a process termed vasculogenic mimicry, a known prognostic factor in UM (Folberg *et al.*, 1992). ECM remodelling is known to occur in other cancers and fibrotic diseases and can aid tumourigenesis, progression and metastasis (Cox and Erler, 2011; Pickup, Mouw and Weaver, 2014) . Butcher et al., reviewed the effect of ECM stiffness on cellular mechanoreciprocity in breast cancer, reporting that a stiffer matrix conferred increased proliferation and favoured cell-cell junction and polarity disruption (Butcher, Alliston and Weaver, 2009). Breast cancer cells have been shown to generate a desmoplastic microenvironment and 'stiffer' ECM in both the tumour and the surrounding cells (Acerbi *et al.*, 2015), which has been linked to increased metastatic potential (Provenzano *et al.*, 2008). Interestingly, higher numbers of infiltrating macrophages, which is a known indicator of worse UM prognosis (Mäkitie *et al.*, 2001), has also been shown to correlate with increased ECM 'stiffness' in breast cancer (Acerbi *et al.*, 2015). In our analysis, leukocyte extravasation signalling was upregulated in HR-UM compared with LR-UM; aberrant leukocyte infiltration has been shown to be a direct trigger for breast tumour invasion and metastasis (Man, 2010).

Previous data in Chapter 3 demonstrated extensive ECM deposition in conjunction with hepatic MUM and showed association between peritumoural ECM deposition and αSMA positive cells at that site, indicative of HSC activity. In this chapter, functional enrichment and pathway analysis suggested an upregulation in 'Hepatic fibrosis/HSC activation'

signalling in UM compared with NCM and in HR-UM compared with LR-UM. Furthermore, pathways governing cell proliferation of fibroblasts and movement of fibroblasts also demonstrated upregulation in HR-UM compared with LR-UM, further qualifying the importance of hepatic myofibroblast activation. Upon investigation of the proteins which overlapped between our dataset and known proteins in the pathway, 4/28 were predicted to be exosomal. These were intercellular adhesion molecule 1 (ICAM1) and three subcomponents of the myosin complex, myosin heavy chain 9 (MYH9), heavy chain 10 (MYH10) and light chain 6 (MYL6). ICAM1 was more than 3-fold higher in the secretome of UM cells compared with NCM cultures ($p < 0.01$; 2-tailed Mann Whitney U). MYH10 was almost three-fold lower in UM than in NCM ($p < 0.01$, 2- tailed Mann Whitney U), MYH9 and MYL6 were not significantly different between groups. This presented an exciting prospect for a role of ICAM1 in the regulation and formation of the 'pre-metastatic niche' via exosomes, as the liver is the main site of metastatic spread in UM, presenting in approximately 90% of cases (Damato, 2010). Interestingly, however, the data suggest that the majority of the overlapping proteins were "products" of 'Hepatic fibrosis/HSC activation' rather than initiating factors. Figure 2.4.1 shows that the majority of the proteins overlapping with the 'Hepatic fibrosis/HSC activation' pathway are actually proteins known to be synthesised by activated HSCs (Figure 2.18).

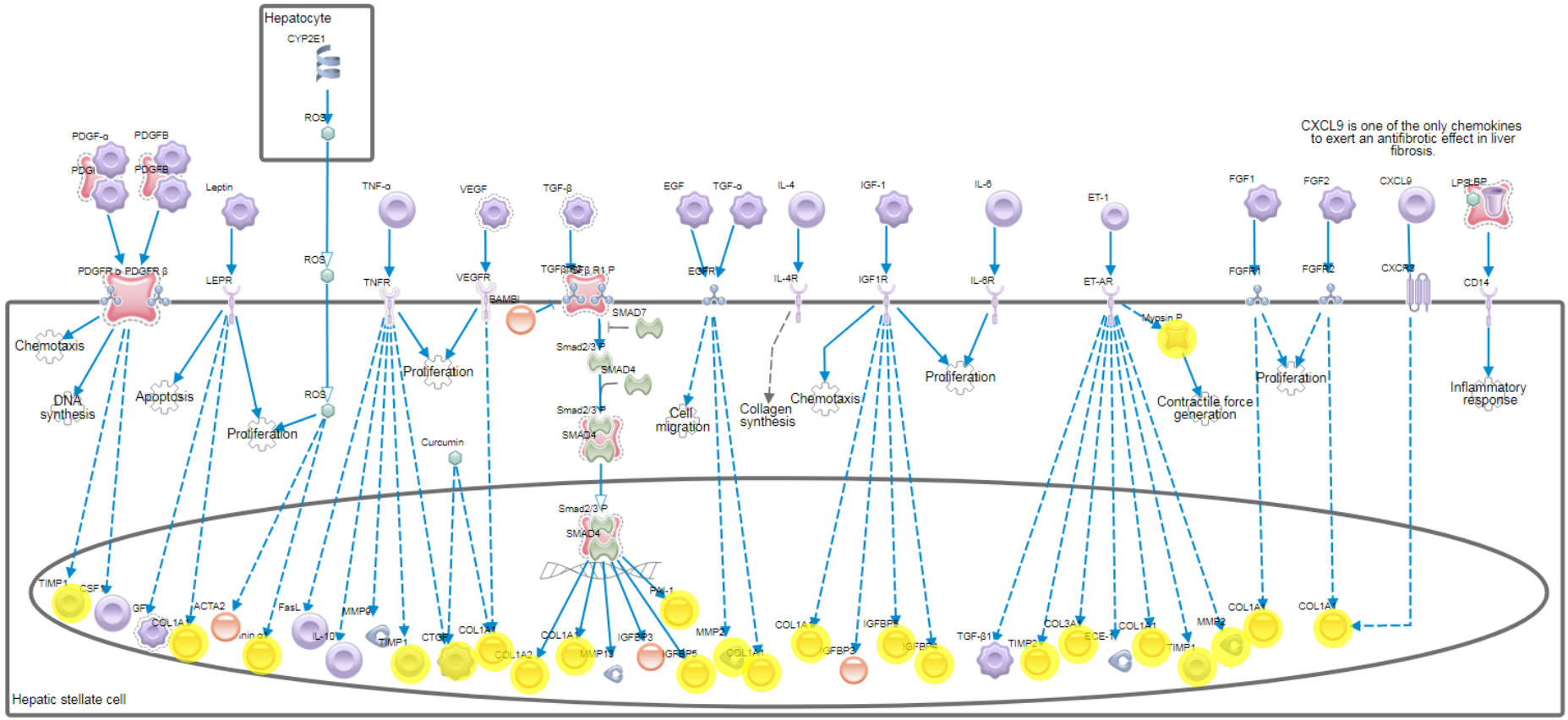

Figure 4.17. (A) Schematic of the early signalling events in hepatic fibrosis/HSC activation signalling pathway with protein present in the UM-NCM comparison dataset highlighted in yellow. Adapted from Ingenuity, Qiagen.

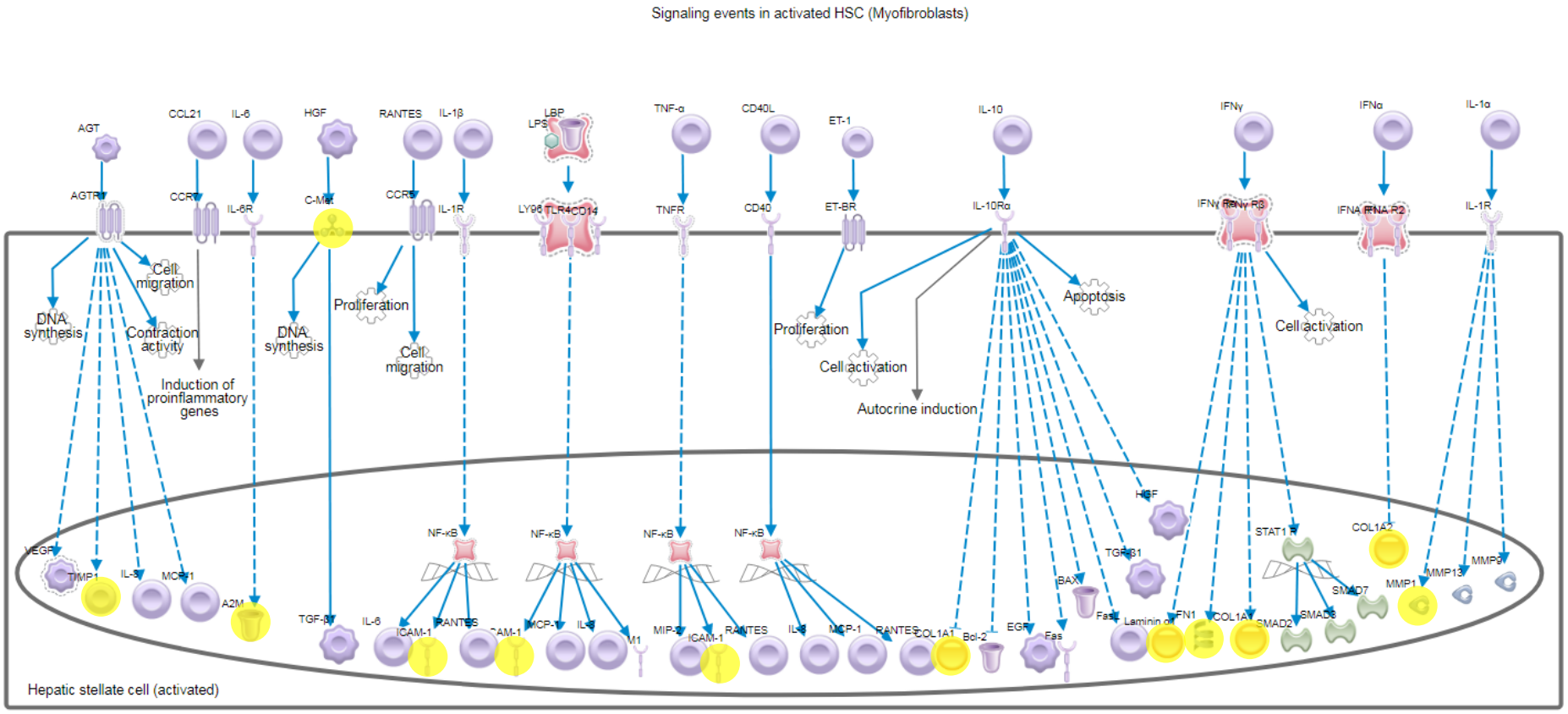

Figure 4.17. (B) Schematic of the signalling pathways in activated HSCs with protein present in the UM-NCM comparison dataset highlighted in yellow. Adapted from Ingenuity, Qiagen.

This highlights that the ability of UM cells to colonise the liver may be due to their production of and adhesion to similar ECM components and/or their ability to influence the behaviour of resident HSCs in the metastatic niche. It is worth noting here that during the culture of the PUM, cells were characterised to ensure that the majority displayed a melanocytic phenotype; however, it remains possible that other cell types were also present (Angi *et al.*, 2016). As tumour associated fibroblasts may be contained in the culture, their deposition of ECM products could affect the secretome profile and therefore the associated signalling through functional enrichment. While the impact of unwanted fibroblasts in the culture should be limited due to their limited representation therein, the possibility of their presence suggests that future research employing a similar model could benefit from further validation of the cellular content of the cultures.

Previous research into proteins secreted by UM cells have highlighted several proteins involved in inflammation, fibrosis and modulation of the ECM. The secretion of multiple factors associated with inflammation, and fibrosis were previously described by (Enzmann *et al.*, 1998). The authors demonstrated the presence of TGFβ-1, FGF2, and interleukins 6, 8 and 10. Interestingly these cytokines were not highlighted in our dataset; however, TGFβ-1 is known as a potent activator of fibroblasts during cancer and can promote cell migration, actin dynamics, adhesion and ECM modulation, all processes frequently highlighted in this research. Cools-Lartigue *et al.,* demonstrated that hepatocyte growth factor (HGF) and vascular endothelial growth factor (VEGF) are secreted by UM cells and their release was upregulated during 2D culture with monocyte conditioned media (Cools-Lartigue *et al.*, 2005). While neither were highlighted in this dataset, the hepatocyte growth factor receptor MET was identified and shown to be two-fold higher in HR-UM compared with both LR-UM and NCM, though not significantly ($p > 0.05$). Väisänen *et al.,* demonstrated the secretion of MMP-2 by UM cells and correlated this with significantly reduced 5-year

survival (Väisänen *et al.*, 1999). MMP-2 was demonstrated in this dataset; however, the levels were lower in UM compared with NCM and similar in HR-UM and LR-UM. MMP-1 and MMP-14 were also expressed in our dataset but were not differentially expressed between groups. In 2000, (Repp *et al.*, 2000)highlighted macrophage inhibitory factor (MIF) in the secretome of a panel of UM cell lines. MIF was shown to protect UM cells from cytolysis by (natural killer) NK lymphocytes. Herein, MIF was demonstrated in the secretome of PUM samples and was more than two-fold higher in HR-UM than in LR-UM ($p = 0.002$); however, MIF was lower in UM than in NCM, though not significantly. In 2007, Pardo *et al.,* investigated the proteomic profile of the secretome of UM cell lines (Pardo *et al.*, 2007), highlighting an abundance of proteins linked with adhesion, migration and modulation of the ECM. The authors suggested that the proteins cathepsin D, syntenin and gp100 represented potential biomarkers of UM metastatic potential gp100 was identified in the current study as PMEL. In contrast to the results presented by Pardo *et al.*, PMEL was over four-fold lower in the UM secretome than that of NCM cultures ($p < 0.01$); furthermore, it was not significantly different between UM metastatic risk groups. Cathepsin-D was identified herein but was not significantly different between groups. Syntenin was not identified in the secretomes analysed.

It should be considered when evaluating the results of these analyses that the methods used to predict the secretory mechanisms of the proteins have inherent limitations. In this research, SignalP was used to interrogate 758 proteins for classical prediction. The reported accuracy of the SignalP prediction software is 93%. While better than the reported accuracy rate of most other freeware designed for this purpose (Bendtsen, Nielsen, *et al.*, 2004), this corresponds to a possible 53 proteins with incorrect associated predictions. SecretomeP boasts a false positive rate <5%; however, its sensitivity is only 40% (Bendtsen, Jensen, *et*

al., 2004). This could be due to the limited training protein dataset for the software containing only 13 proteins that are known to be non-classically secreted. SecretomeP was also assessed on the total proteome with proteins harbouring transmembrane sequences removed, as proteins with transmembrane sequences are known to be secreted via EV secretion. Further predictions were made employing exocarta for proteins secreted via exosomal release. Exocarta is a manually created database, compiling proteins experimentally observed in exosomes; this could, therefore, include falsely identified exosomal proteins. Of note, there are no UM studies or studies in ocular melanocytes included in the Exocarta database to date. Proteins predicted to be secreted via exosomes in the UM and NCM samples could, therefore, be proteins that have not previously been identified as exosomal.

Alongside the methods used for the prediction of secretory mechanisms, there are limitations to pathway/functional enrichment analysis. The majority of functional enrichment tools employ existing databases (e.g. gene ontology [GO]), which limits the identification of associated functions and pathways to those previously examined in the literature. Furthermore, for a given organism with a fully sequenced genome, only a subset of the sequenced genes is functionally annotated and, therefore, contributed to the existing pathway modules (King *et al.*, 2003). This is further compounded by the assumption that the annotations for any given protein are complete; annotations are often manually curated (Gene Ontology Consortium *et al.*, 2013) and in any advancing field of research, annotation may not always be complete. A given gene may also give rise to multiple products through alternate splicing: these products may be non-functional, possess varied functions or even have opposing functions (Graveley, 2001). When considering the final protein product through analysis of peptide fragments, these splice variants and any single nucleotide polymorphisms in the gene may not be detected, and a protein's functionality

may be assumed to be normal. The protein produced may also possess multiple functions depending on subcellular localisation, activation status (e.g. phosphorylation) (Cohen, 2000), and other post-translational modifications. Recently it was reported that, on a total proteome of 530,264 proteins, 87,308 post-translational modifications have been experimentally identified and 234,938 modifications were predicted through similarities in potential/probable modification sites (Khoury, Baliban and Floudas, 2011), highlighting that while an identified protein may be present in the sample, its activity *in situ* cannot be confirmed through this method.

Another primary limitation to this analytical approach is the inherent assumption that each pathway is an isolated unit or module. While this approach allows the simplification of the research question and can be applied in several situations where the pathway is spatially or chemically isolated (Hartwell *et al.*, 1999), it is widely accepted that biological signalling acts as an integrated network with all pathways directly or indirectly linked through multiple signalling mechanisms (García-Campos, Espinal-Enríquez and Hernández-Lemus, 2015).

Functional validation of the major pathways highlighted in the proteomic analyses of the UM secretome could be achieved by inhibition of major components of those pathways. Amirouchene-Angelozzi *et al.,* previously demonstrated that inhibition of mTOR with the small molecule everolimus could induce apoptosis in UM cell lines and inhibit tumour growth in patient derived xenografts (Amirouchene-Angelozzi *et al.*, 2016). However, everolimus is a selective MTORC1 inhibitor. As our results show increased RhoA signalling and pathways associated with motility and migration, it may be more beneficial to inhibit MTORC2 or both mTOR complexes concurrently similar to (Ho *et al.*, 2012). mTOR pathways, as well as RhoA signalling could be inhibited through small molecule, peptide or knock down models of UM and metastatic traits could be assessed; these could include

proliferation, migration or invasion in *in vitro* models, or the rate/level of metastatic progression and tumour growth in animal models. Similar work has previously employed pan-mTOR inhibitors and knockdown models (Pópulo *et al.*, 2010); however, this was in a limited number of different cell lines and could be expanded upon. Knockdown models of RhoA have highlighted it as a possible therapeutic target, demonstrating reduced proliferation and increased apoptosis in an *in vitro* lung cancer model (Liu *et al.*, 2017), and suppressed tumour cell viability, migration, invasion and adhesion of ovarian cancer cells *in vitro* and reduced tumorigenicity in nude mice (Xiaoxia Wang *et al.*, 2015). Conversely, RhoA knockdown in breast cancer has been shown to have no effect on primary tumour formation or proliferation, yet it increased lymph node invasion and metastatic spread (Kalpana *et al.*, 2019).

Comparative analysis of ECM produced by the PUM, in the liver during non-MUM fibrosis and during MUM-associated fibrosis could reveal insights into similarities between PUM and the metastatic niche. This could help improve our understand of the propensity of UM to metastasise to the liver and/or the chronologic relationship between liver fibrosis and MUM, similar to previous work in colorectal cancer (Kondo *et al.*, 2016). UM-induced ECM changes in the PUM could also be compared between groups with different metastatic risk. It has previously been shown in neuroblastoma that a group of patients at 'ultra-high-risk' of tumour progression and reduced survival exists within a high-risk patient cohort and that this can be defined by identifying differential composition of the tumour ECM (Tadeo *et al.*, 2016).

Herein, cadaver derived NCMs and primary UM cells were cultured in a 2D model. It has been suggested that 3D culture systems are more representative of cells *in situ* (Abbott, 2003) and can influence some of the pathways highlighted in the analyses, such as Rho

GTPase signalling (Ridley, 2015), mTOR-S6K signalling (Riedl *et al.*, 2016), fibroblast signalling (Green and Yamada, 2007) and integrin signalling (Yamada, Pankov and Cukierman, 2003). While the results herein represent UM biology previously reported in the literature, and correspond to UM signalling pathways described *in vivo* (Feng *et al.*, 2014) and in patient-derived xenografts (Decaudin *et al.*, 2018), future studies may seek to examine how the UM secretome differs between 2D and 3D culture.

To limit the identification of exogenous proteins from bovine serum, a common additive in cell culture, the culture of UM and NCM cells in this research was performed in serum-free conditions prior to media collection. While this should limit erroneous results due to contaminating bovine proteins, serum levels in cell culture can alter the cells secretory profile (Nonnis *et al.*, 2016). Future studies could consider alternative methods of culture such as SILAC, in which the cells are cultured in media containing amino acids labelled with stable isotopes (Ong *et al.*, 2002). The cells incorporate the “heavy” amino acids into biosynthesised proteins, making them distinguishable from exogenous serum proteins by mass spectrometry.

In this research we were able to compare groups due to multiple samples of each disease state; however, sample distribution may cause bias in the study as the numbers for NCM, LR-UM and HR-UM were 5, 4 and 10 samples, respectively. Within the UM group more than double the number of samples were HR-UM compared with LR-UM. While the repetition in signalling pathways and biofunctions between the UM versus NCM comparison and the HR-UM versus LR-UM comparison may denote similar differences in physiology and pathology with increasing disease state, it suggests that these pathways or functions may be upregulated in those samples at higher risk of metastatic disease compared with both low risk and normal samples. Whilst this could cause some bias in the results, the highest

possible number of samples were included in order to increase the power of the analysis. As HR-UM tumours tend to be larger, samples from these tumours are more readily available for research purposes.

Whilst the methods employed in this chapter may have associated limitations, these are heavily outweighed by the consistency in results throughout this research and the correspondence of these results with similar reports in the UM literature and with other chapters of this thesis.

4.5. Conclusion

The research herein confirmed the hypothesis that the UM secretome contains proteins associated with a more malignant phenotype when compared with NCM, highlighting upregulations in pathways and functions associated with cell motility, migration and invasion. Furthermore, it suggests a possible role of the Rho GTPase and mTOR signalling axes in UM pathology. It suggests that the PUM secretome contains proteins associated with enhanced ECM deposition, and that the signalling pathway involved in this ECM production is similar to that of activated HSCs. The analysis also suggests that a potentially large amount of the UM proteomic secretome is generated through the release of EVs such as exosomes, suggesting that they may play a fundamental role in UM progression.

While the results presented correspond with previous reports, additional functional studies are required to validate these findings in *in vitro* and *in vivo* models and to assess the involvement of proteins in the UM secretome in the signalling pathways which promote local and metastatic progression of UM.

CHAPTER 5: ISOLATION AND CHARACTERISATION OF EXTRACELLULAR VESICLES FROM UM CELL LINES

5.1. Introduction

Chapter 4 identified a large proportion of the UM protein secretome as being secreted via exosomes. UM EVs, described as exosomes, have previously been isolated from liver perfusate and the vitreous humor of UM patients (Eldh *et al.*, 2014; Ragusa *et al.*, 2015) by UC. Their analyses focused on the microRNA content of UM exosomes and, to our knowledge, no study to date has performed in-depth proteomic analysis on small exosome-like EVs released by UM cells.

The first paper investigating UM EVs was published in 2014 by Eldh *et al.,* and described small exosome-like EVs isolated from local liver perfusates in patients with MUM (Eldh *et al.*, 2014). The authors isolated the EVs from plasma, obtained from both the liver perfusate and peripheral heparinised blood of patients with MUM. EVs were isolated by differential UC, at 400 × *g* for 10 minutes, followed by a second centrifugation at 1880 × *g* for 10 minutes. The purified blood plasma was then centrifuged at 29 500 × g for 20 minutes to remove remaining cells and cell debris. The supernatant was filtered through a 0.2 µm filter to remove particles larger than 200 nm. EVs were pelleted from the purified blood plasma by ultracentrifugation at 120 000 × g for 90 minutes and characterised.

The EVs were assessed by transmission electron microscopy (TEM) and shown to be approximately 50 nm in diameter and positive for cluster differentiation 63 (CD63) by immune-gold labelling, and CD63, CD9 and CD81 by flow cytometry following immunoprecipitation on anti-CD63 coated latex beads. EVs were considered of UM origin due to positivity for Melan-A when assessed by western blot.

In 2015, Ragusa *et al.,* isolated small EVs – considered exosomes – from the aqueous humor and serum of patients with PUM (Ragusa *et al.*, 2015). Small EVs were isolated by differential centrifugation, filtration and subsequent UC. Serum was isolated after whole blood was left to stand for 30 minutes at 20°C before being centrifuged at 3000 rpm for 15 minutes at 4°C.The vitreous humor or serum was centrifuged at 300 g to pellet cell debris, and then at 16500 g for 30 minutes, followed by filtration through a 0.2 μm filter. The final supernatant was UC at 120,000 g for 70 minutes to pellet the small EVs. The EVs had a diameter of 100 nm when measured by dynamic light scattering and showed presentation of CD9, CD63 and CD81 by flow cytometry following adsorption onto aldehyde/sulphate latex beads. A cohort of 179 miRNAs were detected in the vitreous humour derived EVs from a TaqMan low-density array of 754 miRNAs profiled. The authors identified miRNAs 146a, 21, 34a and 618 as significantly differentially expressed between the EVs isolated from healthy control patients and patients with UM. They suggested that exosomal mir-146a in patient serum could act as a diagnostic biomarker of UM and possibly discriminate between UM and cutaneous melanoma.

Recently in 2019, Surman *et al.,* isolated larger EVs – described as ectosomes – from the UM cell line Mel202 (Surman *et al.*, 2019). EVs were isolated by differential UC from cell culture media. Growth conditioned media was centrifuged sequentially at 400 ×g for 5 minutes, 4000 ×g for 20 min and 7000 ×g for 20 min all at 4 °C. With each spin, cells and cellular debris were pelleted and discarded. Supernatants were collected for ectosome isolation and centrifuged at 18,000 ×g for 20 min at 4 °C. Pelleted EVs resuspended in ice cold PBS. EVs were characterised for morphology, size and purity by TEM. Size analysis of electron micrographs determined a mean vesicle diameter of 317 nm.

The research by Eldh *et al*., Ragusa *et al.,* and Surman *et al.,* demonstrate the ability to isolate and characterise small and large UM EVs from various biological fluids of patients with UM and from cell cultures. The research herein aimed to isolate and characterise small exosome-like EVs. While several methods exist for the enrichment of small exosome-like EVs (detailed in Chapter 1), many of these methods focus on the identification and analysis of nucleic acids housed in the isolated EVs. The method herein was chosen with a view to the downstream proteomic analysis of the UM EVs isolated. After considering the extent at which the pros and cons of each method would affect these downstream analyses (Table 1.1.), UC was chosen as the most appropriate technique for the enrichment of small exosome-like EVs from the UM secretome for in-depth proteomic analysis. UC would isolate EVs with reduced protein contamination compared with PP and would allow the highest likelihood of encompassing all exosome subtypes in contrast with methods like immune-affinity capture.

This chapter aimed to isolate small exosome-like EVs from UM cell lines and to characterise these samples by size, morphology and protein presentation. For the characterisation of EV samples, nanoparticle tracking analysis was employed for the analysis of particle size distribution and as a measure of sample purity; transmission electron microscopy was used to identify small exosome-like EVs by their characteristic 'cup-shaped' morphology; western blotting was employed to assess the presence and absence of 'canonical exosomal markers' and cellular contaminants respectively.

5.2. Materials and Methods

5.2.1. Culture of uveal melanoma cells and collection of conditioned media

UM cell lines (92.1, Mel270, MP41, OMM1, OMM2.3, OMM2.5) were cultured according to methods Chapter section 2.1. and the conditioned culture media was collected for EV isolation.

5.2.2. Isolation of uveal melanoma extracellular vesicles

UM EVs were isolated with an UC protocol, performed as described in Chapter section 2.10.

5.2.3. Size distribution analysis of uveal melanoma extracellular vesicles by nanoparticle tracking analysis

NTA was performed on the collected UM culture media according to the protocol described in methods sections 2.11. This was also conducted for aliquots of "pre-UC conditioned media", for comparison of size distribution with the corresponding EV isolation.

5.2.4. Morphology characterisation of uveal melanoma extracellular vesicles by transmission electron microscopy

For the visualisation of single UM EVs, samples were subjected to transmission electron microscopy, performed as described in methods section 2.12.

5.2.1. Characterisation of uveal melanoma extracellular vesicle proteins by western blot

Western blotting of UM cell lines and isolated UM EVs was performed as described in methods section 2.13. Primary antibody suppliers and concentrations are detailed in Table 5.1.

Table 5.1. Antibody concentrations and suppliers for use in western blotting

Target	Dilution factor	Supplier	Product code
HSP90 – 90 kDa	1:200	Santa Cruz, US	SC-13119
CANX – 67 kDa	1:1000	Santa Cruz, US	SC-130059
ANXA2 – 32 kDa	1:200	Santa Cruz, US	SC-28385
CD81 – 22 kDa	1:200	Santa Cruz, US	SC-166029
CD63 – 24 kDa	1:200	Santa Cruz, US	sc-5275

5.3. Results

5.3.1. Size distribution and concentration of enriched EVs

UM cell line secretomes were analysed with nanoparticle tracking analysis software before and after the enrichment of EVs (Figure 5.1.). Prior to UC the samples showed relative heterogeneity in diameter; however, the modal peak of each sample was within the size range of exosomes. After UC the heterogeneity was markedly reduced and the area under the curve minimised, suggesting an increase in purity. The modal peaks for EVs enriched from each UM cell line was between 80 – 100 nm diameter, suggesting the protocol was effective at enriching small exosome-like EVs.

	Uveal Melanoma cell line				
	92.1	**Mel270**	**OMM1**	**OMM2.3**	**OMM2.3**
Before UC	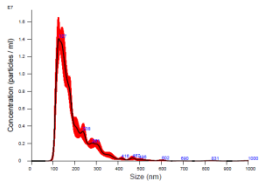	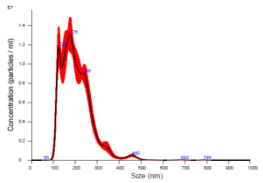	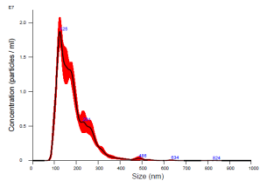	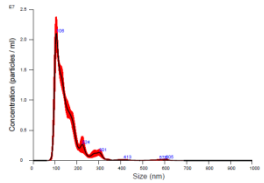	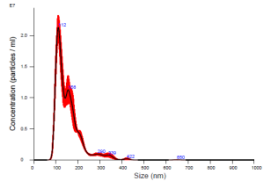
After UC	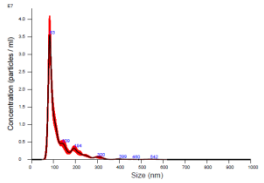	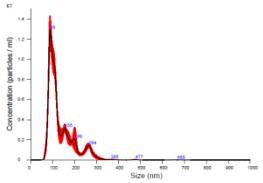	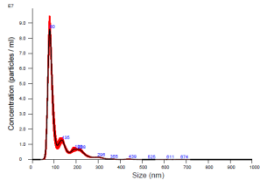	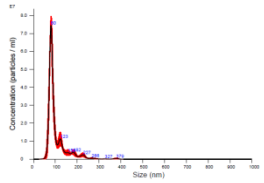	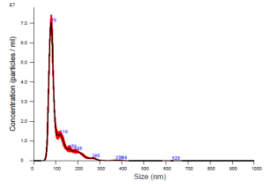
Post-UC concentration (mL^{-1})	$1.33 \times 10^{9} +/- 4.61 \times 10^{7}$	$7.4 \times 10^{8} +/- 1.50 \times 10^{7}$	$3.26 \times 10^{8} +/- 9.64 \times 10^{7}$	$2.21 \times 10^{9} +/- 6.10 \times 10^{7}$	$2.76 \times 10^{9} +/- 5.20 \times 10^{7}$

Figure 5.1. Representative nanoparticle tracking analysis size distribution profiles of cell culture supernatant before and after ultracentrifugation for the enrichment of uveal melanoma cell line extracellular vesicles. Figures show representative profiles from three biological replicates, each with five repeated measurements.

5.3.2. Morphology and purity of enriched EVs

TEM of enriched small EVs from UM cells showed vesicles with a recognisable “cup-shape”, characteristic of exosomes (Figure 5.2.). The isolated EVs had a size similar to that highlighted by the modal peak of the NTA size distribution graphs (Figure 5.1.). The small EVs enriched were consistent with both the size and morphology reported for exosomes, and there was a minimal number of other structures (such as organelles or cellular debris) visible on the electron micrographs (Figure 5.2.).

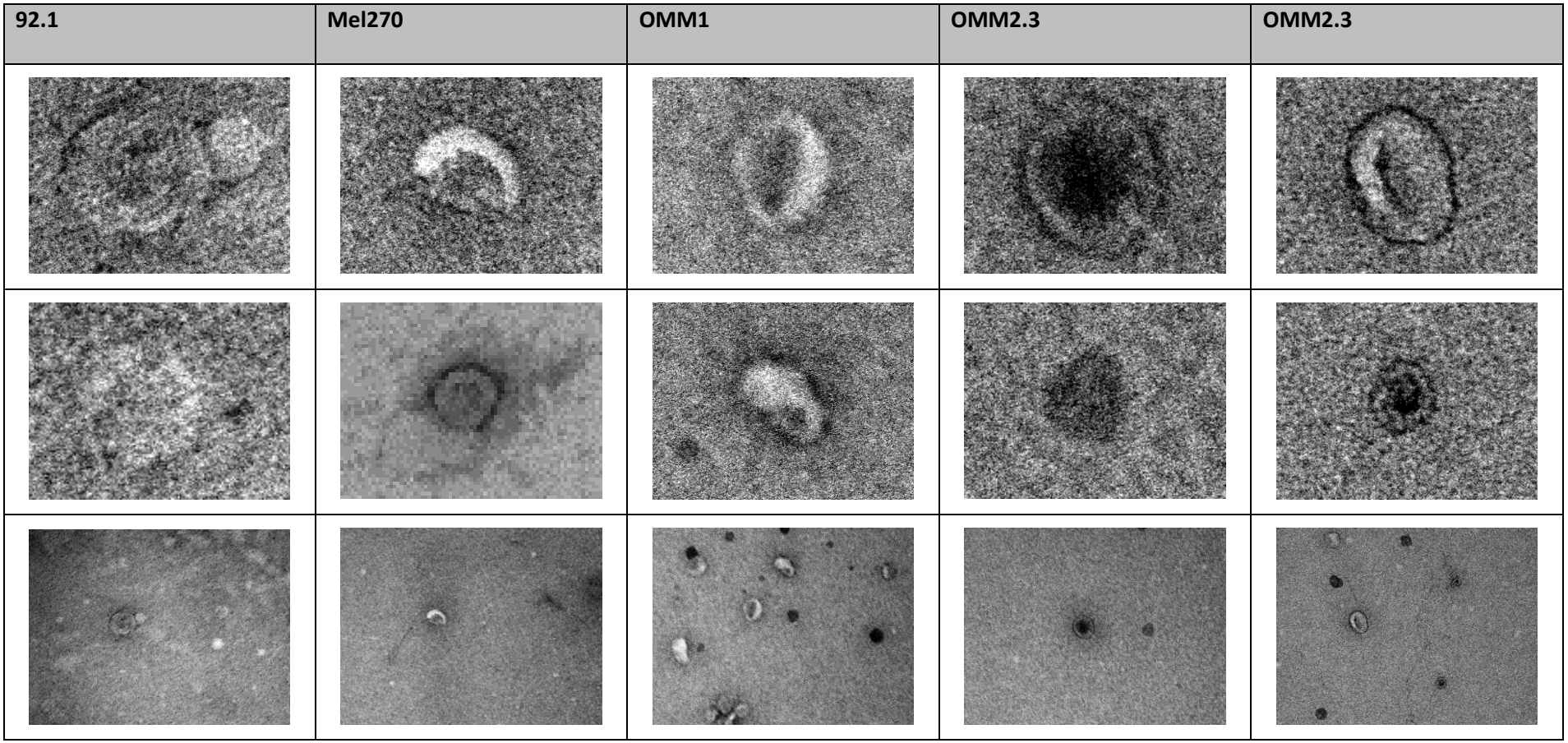

Figure 5.2. Transmission electron microscopy of enriched extracellular vesicles for a panel of uveal melanoma cell lines shows standard “cup” morphology of exosomes. Representative images of two biological replicates, repeated twice for each cell line are shown in rows one and two at 200,000x magnification. The third row displays a wide-field view of vesicles for sample purity at 40,000x magnification.

5.3.3. Protein markers in EVs and sample purity

Whole cell lysates and EV lysates from each UM cell line were subjected to SDS-PAGE and western blotting under denaturing and reducing conditions. They were probed with antibodies for known exosomal proteins (CD63, CD81, ANXA2, HSP90) and proteins that should be absent in EV isolates (CANX). The resultant blots are shown in Figure 5.3.

HSP90 was present in all UM cell lysates and was demonstrated in the EV lysates of 92.1. Mel270 and OMM2.5 cell lines yet was absent in OMM1 and OMM2.3 EV lysates. ANXA2 was present in all UM cell and EV lysates. CD81 demonstrated limited expression in UM cellular lysates but increased expression in matching EV lysates, CD81 was present in OMM1 and OMM2.3 EV lysates at low but visible levels similar to the corresponding cell lysates. CANX was present in all UM cell lysates and at lower levels in the EV lysates of 92.1, Mel270 and OMM1. CANX was absent in the OMM2.3 EV lysate and was expressed at similar levels to the cellular lysate in OMM2.5 cells. CD63 was expressed at varying levels in UM cell lysates. CD63 was consistently difficult to identify by western blot in UM cell lines and was not visible in 92.1 or Mel270 EVs across repeated measures and so was not performed in other UM EVs.

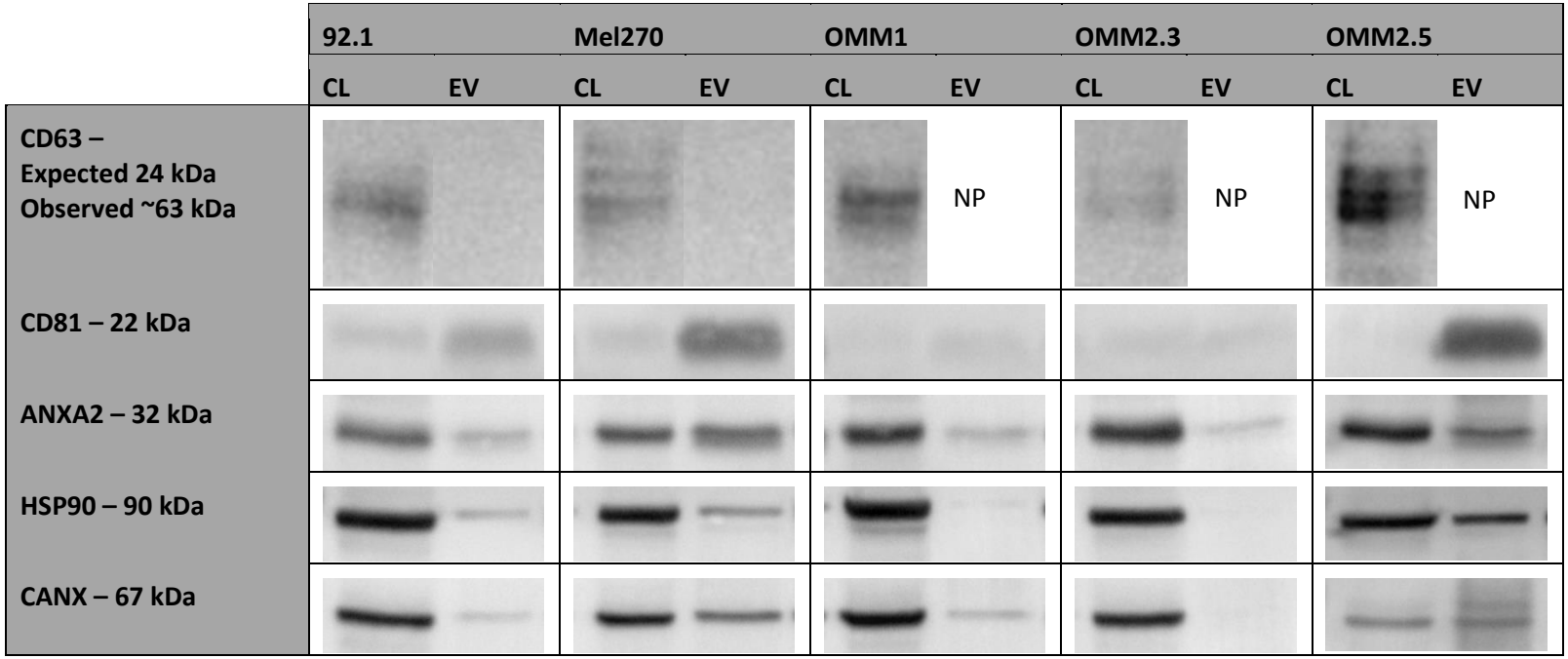

Figure 5.3. Western blotting of proteins commonly enriched in exosomes (CD81, HSP90 and ANXA2) and a negative control protein reported as absent in exosomes (CANX) in cell lysates (CL) and extracellular vesicle lysates (EV) of uveal melanoma cell lines. Cell lines were all loaded at 10 µg per lane; extracellular vesicle loading was standardised by the number of vesicles lysed, at 1 x10^8 EVs per lane. CD63 blots of 92.1 and Mel270 are representative of n = 5; remaining CD63 blots represent n = 3; all other blots were performed only once n = 1.

ANXA2, annexin A2; CANX, calnexin; CD, cluster differentiation; CL, whole cell lysate; EV, extracellular vesicles lysate; HSP90, heat shock protein 90; NP, not performed.

5.4. Discussion

This chapter hypothesised that EVs could be isolated from the conditioned culture media of UM cells grown in short-term 2D culture and that techniques could be employed to select for the enrichment of small exosome-like EVs. This chapter aimed to employ a well-defined UC protocol previously shown to isolate small exosome-like EVs from conditioned culture media of UM cells and other cancer cells. The research aimed to characterise these EVs by their size distribution through NTA, their morphology through TEM imaging and their protein presentation through western blotting. Through these methods, this chapter aimed to demonstrate the presence of small exosome-like EVs in the cultured media of UM cells, with characteristics previously described in the literature as pertaining to exosomes.

Several recent papers have compared techniques for the enrichment of exosomes; often these comparisons focus on exosomal RNA purity/quantity (Taylor, Zacharias and Gercel-Taylor, 2011; Helwa *et al.*, 2017; Tang *et al.*, 2017) and few have focused on proteomic content (Pisitkun, Shen and Knepper, 2004; Tauro *et al.*, 2012). Herein, the choice and optimisation of isolation technique focused on reduced protein contamination while encompassing the total small exosome-like EV population. UC was chosen as the most appropriate method for the isolation of small exosome-like EVs when considering the application of downstream proteomic analysis to the resultant sample. UC represents the most commonly employed technique for the isolation of exosomes (P. Li *et al.*, 2017) and has previously been demonstrated to enrich small exosome-like EVs from UM samples (Eldh *et al.*, 2014; Ragusa *et al.*, 2015). While PP has been shown to produce a higher yield of RNA-containing small exosome-like EVs, UC was shown to present fewer contaminating proteins (Tang *et al.*, 2017). Furthermore, it has been shown that, after pelleting small exosome-like EVs by UC, resuspension in large amounts of PBS prior to another final UC

step can “wash” the sample, reducing any protein contaminants (Théry *et al.*, 2006); hence, this was employed here.

It should be considered, however, that UC protocols pellet EVs of similar densities and it has been demonstrated that multiple EV subpopulations have overlapping buoyant densities. Though characterisation suggests small exosome-like EVs, these samples are likely to contain heterogenous populations (Kowal *et al.*, 2016). A sucrose cushion/gradient can be applied to increase the purity of EVs, further eliminating contaminants with different buoyant densities (Van Deun *et al.*, 2014); however, in my hands this greatly reduced EV yield and a PBS wash step was deemed sufficient.

The EVs in this research demonstrated a size distribution indicative of exosomes (Figure 5.1.). Literature definitions for the size of exosomes differ from suggestions of 20–80 nm (Muller *et al.*, 2014) to those stating 30–200 nm (Garcia-Contreras *et al.*, 2017). The sizing of exosomes is complicated by the fact that most techniques for their isolation do little to differentiate between EV subgroups (Kowal *et al.*, 2016). Therefore, it is well known that available isolation techniques yield heterogenous EV samples (Kowal *et al.*, 2016).

Exosomes are suggested to have a characteristic “cup-shape” morphology when visualised by TEM (Lobb *et al.*, 2015). This is thought to be a consequence of the dehydration process and is not seen in methods where the samples remain hydrated (P. Li *et al.*, 2017). The “cup-shape” morphology can be seen in the EV TEM images (Figure 5.2.) and further qualifies that our samples contain enriched exosome-like small EVs. The change in morphology due to dehydration could affect size determination when visualising exosomes by TEM; therefore, in this research TEM was used simply for confirming “cup-shape” morphology as a characteristic indicator of exosome-like small EVs.

While the UM EV isolates demonstrated the presence of previously reported 'exosome markers' CD81, ANXA2 and HSP90, they were positive for the "negative marker" CANX, and these proteins were at varying levels (Figure 5.3.). Furthermore, the frequently described marker CD63 was difficult to demonstrate in UM cells and was not present in the EV samples tested. The most likely explanation for these results could be the varied protein expression in uveal melanocytes and UM cells compared with previously investigated cells in the literature. To my knowledge, the protein content of UM exosomes has not yet been published. It has previously been demonstrated that populations of EVs devoid of such 'canonical' markers exist (Bobrie *et al.*, 2012; Kowal *et al.*, 2016) and that the levels of these proteins and the level of their enrichment vary drastically between cell lines (Yoshioka *et al.*, 2013). Calnexin is considered a marker of endoplasmic reticulin due to its role as a chaperone in the protein folding process (Williams, 2006); however, it has been shown that calnexin can be found at the cell surface membrane due to continuous changes in its localisation for its lysosomal degradation or recycling (Okazaki *et al.*, 2000). Due to these subcellular locations, the presence of calnexin in the isolated EVs is likely to indicate heterogenous populations of EVs in the samples, through the release of cell surface microvesicles (Haraszti *et al.*, 2016) or the release or subcellular organelles such as the ER in apoptotic bodies during apoptosis (Tucher *et al.*, 2018). Furthermore, Lotvall *et al.,* suggested that research engaging in the study of exosomes should be able to show the enrichment of 'exosomal' proteins and the negative enrichment of 'non-exosomal' proteins when compared with lysates of the cell of origin (Lötvall *et al.*, 2014). However, the protein levels in the EV samples isolated herein were not detectable by common protein quantification methods, and so loading was standardised by vesicle number based on the size distribution and quantification data achieved by NTA. Therefore, it was not possible to appropriately demonstrate the enrichment of these proteins. Regardless, the size

distribution and morphology of the EVs, along with the presence of known exosomal proteins was deemed sufficient to consider the isolation of small exosome like EVs successful. The presence, absence and composition of the protein presentation in EV samples is likely to be specific to the cell type and the enrichment technique employed (Hessvik and Llorente, 2018). Further research is required to define specific markers of UM EV subpopulations.

It has been suggested that UC co-enriches low density lipoproteins (LDLs) due to similar buoyant densities (Sódar *et al.*, 2016). The buoyant density of exosomes ranges between 1.23–1.16 g/L (Théry *et al.*, 2006), while for LDLs it is between 1.019–1.063 (Feingold and Grunfeld, 2000). The errant inclusion of these lipoproteins in the dataset could influence certain downstream analyses such as any proteomic interrogation. LDLs have a reported diameter of 22 – 27.9 nm (Campos *et al.*, 1992). While NTA provided no evidence for LDLs in the size distribution of the isolated EVs (Figure 5.1.), this could be influenced by the lower limit of detection of the Nanosight NS300™, which is approximately 30 nm (Filipe, Hawe and Jiskoot, 2010). However, particles in this size range were not visible when samples were imaged with TEM (Figure 5.2.). Interestingly, LDL recycling and transport pathways are similar to those of exosomal biogenesis; both involving clathrin-mediated endocytosis and endosomal processing (Bissig and Gruenberg, 2013). In future research, the presence of LDLs in the isolated EVs could be assessed through western blot for LDL markers such as apolipoprotein B-100 (Zhang *et al.*, 2008), in order to limit any possible contamination and effects on functional enrichment. Apolipoprotein E was the only LDL identified in the dataset and demonstrated reasonable abundance (240th ranked abundance); however, it showed no significant difference between subgroups and so its impact on the analysis should be limited.

Small exosome-like EVs have previously been isolated in UM models; however, the focus of the downstream analysis was different to the research in this thesis. Eldh *et al.,* and Ragusa *et al.,* previously investigated the levels of micro-RNA in the small exosome-like EVs enriched from isolated liver circulation of patients with MUM and the vitreous humor of patients with PUM, respectively (Eldh *et al.*, 2014; Ragusa *et al.*, 2015). They demonstrated that isolation of small exosome-like EVs from UM cells by UC was effective and that downstream analysis of UM small exosome-like EV micro-RNA was possible. They also demonstrated that protein presentation of common exosomal markers varied between samples, corresponding with the results presented herein. Total proteomic analysis of UM small exosome-like EVs was conducted and is discussed in Chapter 6.

Research by Eldh *et al.,* and Ragusa *et al.,* have analysed EVs in liquid biopsies from patients and so contains EVs released by multiple cell types (Eldh *et al.*, 2014; Ragusa *et al.*, 2015). Eldh *et al.,* also showed small exosome-like EVs by TEM with the 'characteristic cup-shape' and a typical size of 50 nm in EVs isolated by UC from the liver perfusate of patients with MUM (Eldh *et al.*, 2014). Ragusa *et al.,* demonstrated EVs with an average diameter of 100nm (Ragusa *et al.*, 2015). Ragusa *et al.,* demonstrated CD63 and CD81 on the isolated EVs but limited levels of CD9 (Ragusa *et al.*, 2015), while Eldh *et al.,* showed varying levels of each across three separate patient samples (Eldh *et al.*, 2014).

The research herein reports the levels of several EV 'markers' in UM cell line lysates and the corresponding EV samples (Figure 5.3.). Identification of common markers in UM EVs proved difficult. CD63 produced inconsistent bands by western blot in whole cell lysates and was absent in EV lysates. CD63 has historically been used as a canonical exosomal marker due to its enrichment in multivesicular bodies (Piper and Katzmann, 2007). However, recent studies have shown it can be found on multiple vesicle types and can be

absent from small exosome-like vesicles (Kowal *et al.*, 2016). As seen in the western blots presented (Figure 5.3.), CD63 is known to produce a multi-band 'smear' at a higher molecular weight than its reported value (Hikita *et al.*, 2018); it has been suggested that this is due to extensive glycosylation of the protein (Tominaga *et al.*, 2014).

CD81 was expressed at very low levels in cell lysates but was frequently present at high levels in small exosome-like EVs, though it seemed absent in both the cell and EV lysates from OMM1 and OMM2.3 cells (Figure 5.3.). Eldh *et al.,* demonstrated that CD81 levels varied between samples of EVs isolated from the liver perfusate of patients with MUM (Eldh *et al.*, 2014). Ragusa *et al.,* previously showed that CD81 was present on only 32% of EVs isolated from the vitreous humour of patients with PUM (Ragusa *et al.*, 2015). As stated above both the studies of Eldh *et al.,* and Ragusa *et al.,* study used biological fluids likely to contain EVs isolated from multiple cell types. Furthermore, Kowal *et al.,* highlighted the diverse expression profiles of subpopulations within EV isolates, suggesting that 'canonical markers' of exosomes can be both present and absent on vesicles within the same sample (Kowal *et al.*, 2016). Other markers were inconsistently enriched in small exosome-like EVs, sometimes at lower levels than cell lines and sometimes absent. It has been well established that the protein content of vesicles differs between different cell lines (Hessvik and Llorente, 2018). Annexin II has previously been suggested as a marker with low enrichment for exosomes from cell culture supernatant and biological fluids (Théry *et al.*, 2006). Annexin II demonstrated variable levels between cell lines and between EV lysates and whole cell lysates in this study. Annexin II has recently been shown to be expressed on multiple EVs (Kowal *et al.*, 2016). HSP90 has also been suggested as an exosome marker, yet shows varying enrichment in different cell lines (Hosseini-Beheshti *et al.*, 2012). Herein, HSP90 often showed lower levels in EV lysates than in cell lysates and was low in both the cell and EV lysates of OMM1 and OMM2.3 cells. CANX and CYC1, reported as negative

markers of EVs (Lötvall *et al.*, 2014), were found at varying levels in most of the EVs analysed. This could be indicative of cell debris or apoptotic bodies in the EV samples. It should be noted that the EV lysates were loaded at a controlled number of EVs per lane and so the protein content of each EV lysate may vary. Attempts were made to assess the protein content of EV lysates, yet the total protein isolated from large volumes of culture media (>100 mL) was below the limit of detection for several methods applied. This means that the level of protein between cell lysates and EV lysates is not representative of true enrichment as the two sample types are not standardised for protein content.

Although all the samples tested represent small exosome-like EVs of the same cell type, they were isolated from different cell lines with different genetic and phenotypic characteristics, and so display different protein content of common exosome markers. Moreover, the Mel270 cell line was derived from the same patient as the OMM2.3 and OMM2.5 cell lines (Mel270 from the primary tumour and OMM2.3 and OMM2.5 from separate metastatic lesions) and yet all three present different proteomic profiles by western blot. This suggests that proteomic analysis of exosomes and the presence of common exosomal markers will not only differ between different cell types but between samples of the same cell type and patient origin due to differences in the *in situ* physiology, disease state or genetic profile of their cellular origin.

Research in the field of EVs is always conducted with the caveat that the size distributions, buoyant densities, and protein markers of EVs overlap between exosomes, MVs and apoptotic bodies (Kowal *et al.*, 2016), and that subpopulations within the distinct populations of EVs (exosomes, MVs and apoptotic bodies) share some common characteristics (Kowal *et al.*, 2016); therefore, it is acknowledged that where this study

refers to “exosomes”, the interpretation of this wording can be defined as small exosome-like EVs with characteristics indicative of exosomes.

Due to the varied protein expression profile of common exosome ‘markers’ in UM small exosome-like EVs, future research should be performed to identify a panel of EV proteins that differentiate UM exosomes from other EV subpopulations. Further research should be performed employing this panel of differentiating proteins to further optimise isolation protocols in order to reduce the presence of vesicles or debris presenting negative markers of exosomes such as calnexin and cytochrome C1. Unfortunately, this may not be a simple task. Kowal *et al.,* demonstrated the complex presentation of ‘exosome’ markers across various EV subpopulations and further varied presentation across additional subpopulations within those EV types (Kowal *et al.*, 2016). Several methods for the isolation of small exosome like EVs can be combined to improve the EV subpopulation selection. Both Eldh *et al.,* and Ragusa *et al.,* applied a 0.2 µm filter to their EV isolates to exclude larger EVs from the sample (Eldh *et al.*, 2014; Ragusa *et al.*, 2015). Herein, however, this does not appear to have been necessary as the NTA distributions in Figure 5.1. show a size distribution with a modal peak close to 100 nm and only few vesicles/particles with a diameter greater than 200 nm.

As stated earlier, sucrose cushion or density gradient centrifugation has been shown to give the purest exosome population when compared to ultracentrifugation and precipitation-based methods (Van Deun *et al.*, 2014). However, Bobrie *et al.,* suggested that sucrose gradients fail to separate vesicles with small differences in densities, which may use different intracellular machineries for their secretion (Bobrie *et al.*, 2012). The combined suggestions of Kowal *et al.,* and Bobrie *et al.,* could go some way to explaining the complexity in pure exosome isolation, and more needs to be known about the disparate

biogenesis mechanisms of exosome subpopulations before appropriate techniques can be developed for their pure isolation.

The presented methods for the isolation and characterisation of small exosome-like EVs from UM cells could be employed in future research in combination with methods previously applied in Chapter 4 for the collection of conditioned media from primary patient UM cells (Angi *et al.*, 2016). This would allow more clinically applicable analysis of patient samples from a wider cohort. These samples would be less susceptible to genetic drift through long term culture (Torsvik *et al.*, 2014) and should produce EVs more akin to those released *in situ*. EVs from cell lines or primary samples could be isolated and their mRNA or miRNA profiles interrogated similar to Eldh *et al.,* and Ragusa *et al.,* (Eldh *et al.*, 2014; Ragusa *et al.*, 2015). Furthermore lipidomic analysis of small exosome-like EVs from UM cells could be investigated, similar to research into prostate cancer (Brzozowski *et al.*, 2018).

Isolated EVs could be interrogated to assess their role in many steps of UM progression, as EVs have previously been shown to contribute to four of the originally described hallmarks of cancer (Hanahan and Weinberg, 2000) and two of the more recently added hallmarks and enabling characteristics (Hanahan and Weinberg, 2011). These include sustained proliferative signalling, resistance to cell death, induction of angiogenesis, activation of invasion and metastasis, immune evasion/inhibition, and promotion of inflammation (Meehan and Vella, 2016). Koga *et al.,* demonstrated a dose-dependent response in the proliferation of breast cancer cells when challenged with exogenous EVs isolated from the same line (Koga *et al.*, 2005).

The ability of lung cancer derived EVs to promote angiogenesis was demonstrated by Cheng *et al.,* who highlighted this was through reduced expression of lnRNA growth arrest-specific transcript 5 (Cheng *et al.*, 2019). It was previously demonstrated that EVs released by cervical cancer cells contain the protein Survivin (Khan *et al.*, 2011), a protein known to inhibit cell death and apoptosis, promoting metastatic potential (Khan *et al.*, 2009). Migration and invasion was also shown to be promoted in hepatocarcinoma cells through their horizontal transfer of EVs containing CXCR4 (Li *et al.*, 2018). EVs in the serum or plasma of prostate cancer patients inhibit lymphocyte cytotoxic function through the downregulation of the activating cytotoxicity receptor NKG2D on natural killer and CD8+ cells, promoting tumour immune evasion (Lundholm *et al.*, 2014). Hoshino *et al.,* demonstrated the ability of EVs from pancreatic cancer cells to promote pro-inflammatory S100 gene expression through integrin-mediated Src phosphorylation (Hoshino *et al.*, 2015).

The primary consideration when choosing which isolation technique to employ for the isolation of small exosome-like EVs from UM cells was the planned downstream application of in-depth proteomic analysis. The following chapter (Chapter 6) submits the UM small exosome-like EVs, isolated and characterised herein, to liquid chromatography tandem mass spectrometry for in-depth proteomic analysis of their composition and contents. Furthermore, bioinformatic analyses are performed on the resultant spectral data allowing functional enrichment and pathway analysis of the identified proteins. This allows data driven hypothesis generation into signalling pathways and biological processes that UM EVs impact and allows a targeted approach to their research and investigation.

5.5. Conclusion

In conclusion, this chapter demonstrates the successful isolation of small exosome-like EVs UM with the size distribution and morphology indicative of exosomes. The protein presentation in the EV lysates demonstrated the presence of several proteins suggested to be ‘markers’ of exosomes but also the presence of a ‘negative marker’ of exosomes. This presentation was inconsistent between samples. This characterisation was considered to indicate samples of small exosome-like EVs from UM cell lines.

CHAPTER 6: PROTEOMIC ANALYSIS OF EXTRACELLULAR VESICLES FROM UVEAL MELANOMA CELLS

6.1. Introduction

Chapter 5 demonstrated our ability to isolate EVs with a size distribution and morphology indicative of small exosome-like EVs. Previous papers by Eldh *et al.,* and Ragusa *et al.,* demonstrated similar isolation techniques and size distribution of small exosome-like EVs from UM (Eldh *et al.*, 2014; Ragusa *et al.*, 2015). Both papers employed flow cytometry to characterise the presence of 'exosomal' protein markers in UM EVs from primary biological fluids. While this demonstrated the percentage of EVs expressing each protein, it did little to qualify them as 'markers' of UM EVs and investigated no other protein content of the EVs isolated (Eldh *et al.*, 2014; Ragusa *et al.*, 2015). Outside of the percentage presentation of CD63, CD9 and CD81 by flow cytometry, and the presence of MART-1 (aka Melan-A) by western blot, there has been no investigation into the protein content of small exosome-like EVs in UM. As such, no functions have been predicted or attributed to the proteins housed in UM small exosome-like EVs.

The research by Eldh *et al.,* and Ragusa *et al.,* focused primarily on the microRNA content of UM EVs and only discussed their proteomic content in reference to their characterisation (Eldh *et al.*, 2014; Ragusa *et al.*, 2015). However, the application and capabilities of in-depth proteomic research into EVs from other cancers has been extensively reviewed by Rosa-Fernandes *et al.,* in 2017 (Rosa-Fernandes *et al.*, 2017). Many studies have been conducted examining the total proteomic profile of small exosome-like EVs, isolated from cancers of the breast (Clark *et al.*, 2015), pancreas (Costa-Silva *et al.*, 2015), colon (Mathivanan *et al.*, 2010), liver (Qu *et al.*, 2015), bladder (Welton *et al.*, 2010), prostate

(Duijvesz *et al.*, 2013; Fujita *et al.*, 2017), lung (Cheung and Juan, 2017; Wang *et al.*, 2018) and skin (Mears *et al.*, 2004; Lazar *et al.*, 2015), among others.

More recently, Surman *et al.,* investigated the glycoproteome of UM EVs larger than those previously reported, describing them as ectosomes (Surman *et al.*, 2019). They isolated these larger EVs with a modified differential centrifugation protocol and assessed their size and morphology by TEM as previously reported. The authors performed gene-ontology (GO) enrichment on the proteins identified and demonstrated functional enrichment of biological processes associated with RNA processing, translation and protein production, as well as WNT and NF-kB signalling. They highlighted further molecular functions associated with translation, as well as GTPase signalling and manipulation of the cytoskeleton.

While this functional enrichment has been performed on the protein content of larger ectosome-like EVs in UM (Surman *et al.*, 2019), no similar research has been published investigating the proteome of small exosome-like EVs in UM. The research in this chapter investigates the total proteome of small exosome-like EVs from UM cell lines, isolated and characterised with the methods described in Chapter 5. The research hypothesises that small exosome-like EVs isolated from UM cells house proteins associated with the malignant progression and metastatic spread of UM and that the proteomic profile of EVs and signalling profiles conferred by those proteins differ between PUM and MUM derived EVs, and between GNAQ and GNA11 mutant UM cell derived EVs. This chapter aims to submit the isolated EVs to nano liquid chromatography tandem mass spectrometry (nano LC-MS/MS) employing methods similar to those published by Angi *et al.,*(Angi *et al.*, 2016) to generate a sample proteome from the resultant spectral data. It aims to interrogate the resulting proteome with a battery of freeware and proprietary programs to highlight the

functional enrichment of pathways and functions conferred by UM EVs and to compare this with the results demonstrated in Chapter 5.

6.2. Materials and Methods

6.2.1. Cell culture and the isolation of small exosome-like EVs

Six UM cell lines were employed for this research; 92.1, Mel270, MP41, OMM1, OMM2.3 and OMM2.5. Cell lines were cultured and the secretomes were collected for EV isolation according to the methods described in section 2.17.

UM EVs isolation and characterisation was discussed in Chapter 1 and demonstrated in Chapter 5. Isolation employed UC as described in section 2.18. Characterisation for size distribution by nanoparticle tracking analysis, for morphology by TEM and for EV protein presentation by western blot was performed according to sections 2.19., 2.20. and 2.21. respectively. All cell lines were regularly tested for mycoplasma contamination and shown to be negative. STR profiles were assessed and shown to correspond with the literature profiles (Jager *et al.*, 2016).

6.2.2. Processing small exosome-like EVs for nano liquid chromatography tandem mass spectrometry

EV pellets were submitted for processing and nano LC-MS/MS in biological triplicates. All steps of LC-MS/MS and protein identification/quantitation were performed by Dr Deborah Simpson in collaboration with the Centre for Proteome Research at the University of Liverpool. UM EVs were processed and submitted to nano LC-MS/MS according to section 2.22.

6.2.3. Protein identification and quantitation

Protein identification and quantification of raw mass spectral data files were processed according to section 2.23. Data were then separated into the experimental sample groups of triplicates for each cell line; Mel270, 92.1, MP41, OMM1, OMM2.3 and OMM2.5. The

resultant dataset was filtered to include only proteins identified with three or more unique peptides. The filtered dataset was used for all further downstream analyses.

6.2.4. Assessing the proteomic dataset

The mean log10 abundance values of each protein were ranked in ascending order and plotted for each cell line. The scales were standardised for ease of comparison. Pairwise comparison was also performed with the R package "pairs.panel". This provided a visual overview of the descriptive statistics for each proteome.

6.2.5. Gene-ontology enrichment analysis

The accession numbers of the proteins in the dataset were analysed with the online software 'Gorilla' (Eden *et al.*, 2009) to assess the presence of enriched GO terms associated with the proteins present in UM EVs. Clustering of the enriched GO terms was assessed and visualised with the online freeware ReviGO clustering (Supek *et al.*, 2011).

6.2.6. Pathway analysis

In addition to the GO annotation analysis, the canonical pathways and biological functions associated with the dataset were analysed using Qiagen's Ingenuity Pathway Analysis (IPA) (QIAGEN, US) software according to section 2.16. This allowed analysis of the pathways and functions associated with UM-derived small exosome-like EV proteins, and the comparative analysis of these networks between sample groups. The up/downregulation of these pathways and functions were assessed between samples derived from PUM tumours and MUM lesions, and between those samples harbouring *GNAQ* mutations or *GNA11* mutations (Table 6.1). For each protein, the experimental ratios between the means were

compared between groups, and the associated statistical difference between the means of the groups (PUM vs MUM and *GNAQ*-mutant vs *GNA11*-mutant) were calculated in excel (Microsoft, US); p-values were calculated with a 2-way unpaired student's t-test. The accession numbers of the proteins were uploaded into IPA along with the experimental ratios between sample groups and the associated p-values.

Table 6.1. Biological characteristics of the six uveal melanoma cell lines

Cell line	GNAQ/11 mutation	*In situ* tumour site	BAP1 Mutation	Chromosome 3 status	Additional notes
92.1	GNAQ Q209L	Primary (Eye)	WT	D3	
Mel270	GNAQ Q209P	Primary (Eye)	WT	D3[¥]	
MP41	GNA11 Q209L	Primary (Eye)	WT	Loss	Cell line established from patient derived xenograft in mouse
OMM1	GNA11 Q209L	Metastatic (Subcutaneous)	WT	D3	
OMM2.3	GNAQ Q209P	Metastatic (Liver)	WT	D3*	Isolated from the same patient as Mel270 cell line
OMM2.5	GNAQ Q209P	Metastatic (Liver)	WT	ND	Isolated from the same patient as Mel270 and OMM2.3 cell lines

[¥]Primary tumour showed M3 (Jager *et al.*, 2016) but the established cell line showed D3 (White *et al.*, 2006); *White *et al.,* suggested OMM2.3 shows D3 in culture through balanced structural aberrations resulting in a numerical aberration leading to reacquisition of an additional complete copy of chromosome 3 (White *et al.*, 2006). BAP1, BRCA1 associated protein-1; D3, disomy of chromosome 3; GNA11, guanine nucleotide-binding (G protein) α subunit 11; GNAQ, guanine nucleotide-binding (G protein) α subunit q; M3, monosomy of chromosome 3; ND, not defined; WT, wild type

6.2.7. Hierarchical clustering

Hierarchical clustering was performed using the R package “pheatmap”. Due to the vast differences in normalised abundance between the proteins, the dataset was Log10 transformed prior to heatmap clustering.

6.3. Results

6.3.1. Dataset

The proteomic workflow produced the proteomes UM derived small exosome-like EVs that were quantitatively similar, consisting of 2155 proteins (identified with a false discovery rate [FDR] of 1%) and each sample proteome possessing a dynamic range spanning approximately 6 orders of magnitude; 1172 of these proteins were identified as having >2 unique peptides. The ranked value plots of the mean normalized abundance values of the proteomes for each cell line demonstrated comparable profiles between UM cell lines (Figure 6.1.). Pairwise comparison provided a visual overview of the descriptive statistics for each proteome. All UM EV proteome profiles demonstrated normal distribution in their protein abundances and correlative analysis confirmed that the proteomes were statistically comparable (Figure 6.1.). The MP41 small exosome-like EVs proteome consistently demonstrated the lowest correlation statistic with the other proteomes.

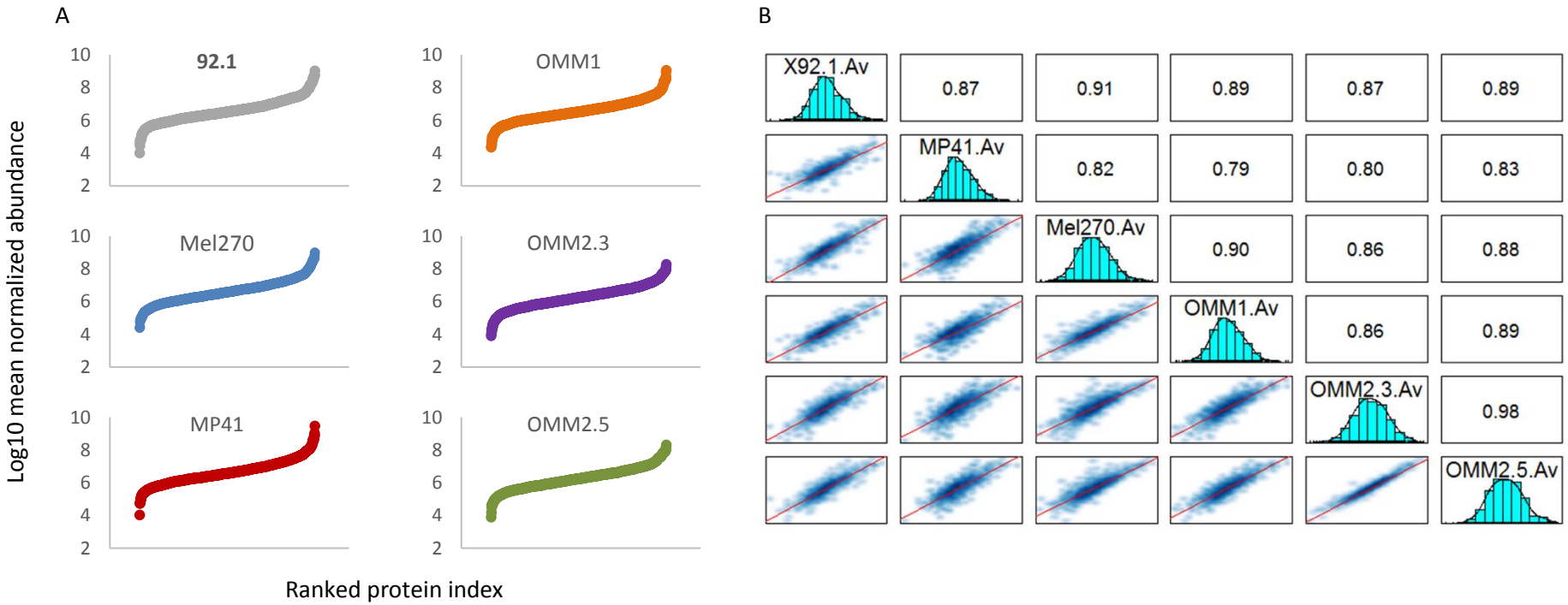

Figure 6.1. (A) Mean normalised abundance values of UM small exosome-like EVs proteins were ranked and plotted in ascending order, each point represents a single protein. All analyses are scaled to the same axis limits for number of proteins and for abundance, to aid comparison between samples. (B) The mean normalised abundance was standardised and pairwise comparisons was performed displaying comparative plots, histograms demonstrating normality and Pearson's statistic of correlation (X92.1 in this panel represent the 92.1 cell line).

6.3.2. Hierarchical clustering

Hierarchical cluster analysis was performed on the three biological replicates of small exosome-like EVs isolated from each cell line (Figure 6.2.). Each cell line replicates were shown to cluster; however, the cell lines did not cluster in any known groups, neither PUM vs MUM nor *GNAQ*-mutant vs *GNA11*-mutant. Small exosome-like EVs from five out of six of the cell lines clustered into PUM or MUM groups; however, Mel270, a cell line derived from PUM clustered with the three MUM cell lines rather than the other PUM cell lines; this was the primary differentiating branch of the clustering.

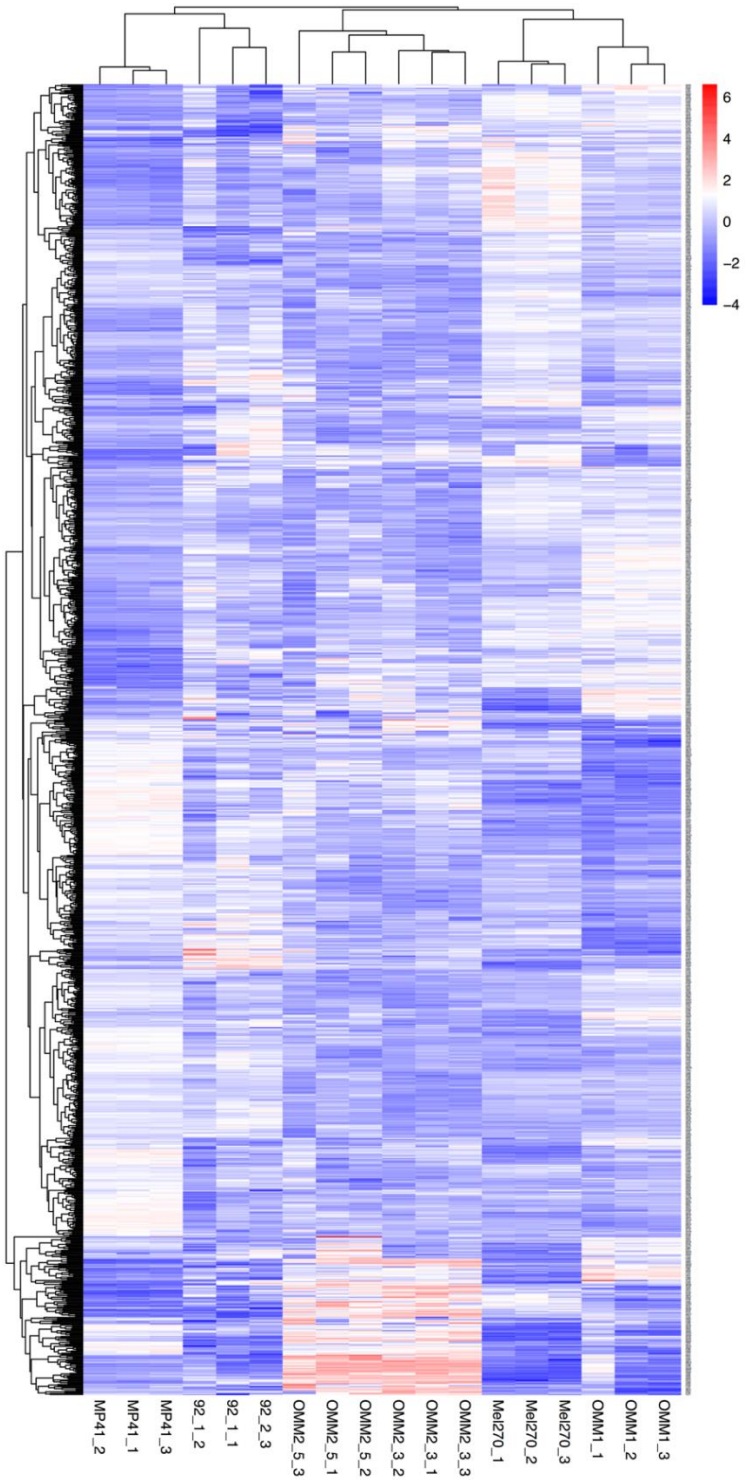

Figure 6.2. Hierarchical clustering of uveal melanoma extracellular vesicles proteomic profiles, comparing six uveal melanoma cell lines each with three biological replicates. Normalised protein abundances were log transformed and plotted with the R package "pheatmap".

6.3.3. Gene-ontology enrichment analysis

GO-annotation of the total proteomic profile of UM EVs revealed functions linked with the regulation of biomolecule localization, transport and EV/exosome signalling, cytoskeleton binding, actin binding, and signal transduction. Collectively these results qualify the analysis of small exosome-like EV content, and suggest they play a role in the regulation of cell morphology.

Table 6.2. Functional enrichment of gene ontology annotation terms associated with the uveal melanoma small exosome-like EV proteome, generated by the online freeware GOrilla

	GO term	Description	FDR q-value
Process	GO:0032879	Regulation of localization	7.08E-06
	GO:0006810	Transport	1.15E-05
	GO:0051234	Establishment of localization	1.92E-05
	GO:0051049	Regulation of transport	2.00E-05
	GO:0065008	Regulation of biological quality	2.19E-05
Function	GO:0023023	MHC protein complex binding	4.35E-05
	GO:0023026	MHC class II protein complex binding	8.69E-05
	GO:0005102	Signalling receptor binding	3.24E-04
	GO:0003779	Actin binding	4.19E-04
	GO:0008092	Cytoskeletal protein binding	9.26E-04
Component	GO:1903561	Extracellular vesicle	3.53E-28
	GO:0070062	Extracellular exosome	6.61E-28
	GO:0043230	Extracellular organelle	7.06E-28
	GO:0044421	Extracellular region part	1.79E-27
	GO:0031982	Vesicle	9.01E-25

FDR, false discovery rate; GO, gene ontology; MHC, major histocompatibility complex

The online freeware ReviGO was employed to allow visualisation of GO-term clustering (Figure 6.3.). Similar to Table 6.2. this demonstrated clustering of terms associated with protein translation, localization, transport and vesicular secretion, signal transduction and manipulation of cytoskeletal processes.

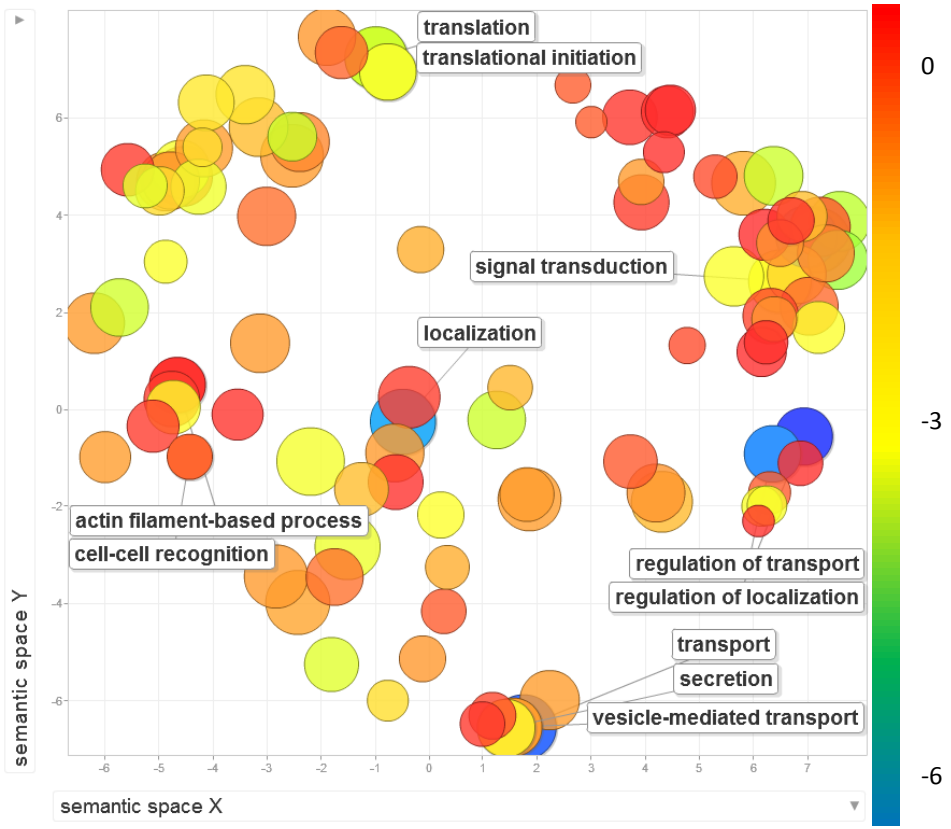

Figure 6.3. Gene ontology term clustering assessed with the online freeware ReviGO. Colour indicates the GOrilla generated q-value; size indicates the frequency of the gene ontology term in the underlying gene ontology annotation database (bubbles of more general terms are larger).

6.3.4. Pathway analysis of the total uveal melanoma extracellular vesicle proteome

The protein accession numbers of the dataset were uploaded to IPA to assess pathways and processes associated with the UM small exosome-like EVs proteome. This allows identification of networks statistically associated with the dataset but provides no information regarding up/downregulation; comparative analysis is required for prediction of the directional regulation.

The biological and functional pathways associated with the UM small exosome-like EV proteome highlighted an association with cell movement and migration, as well as cellular proliferation and protein metabolism. Cell death, apoptosis and necrosis were also associated with the dataset (Figure 6.4.).

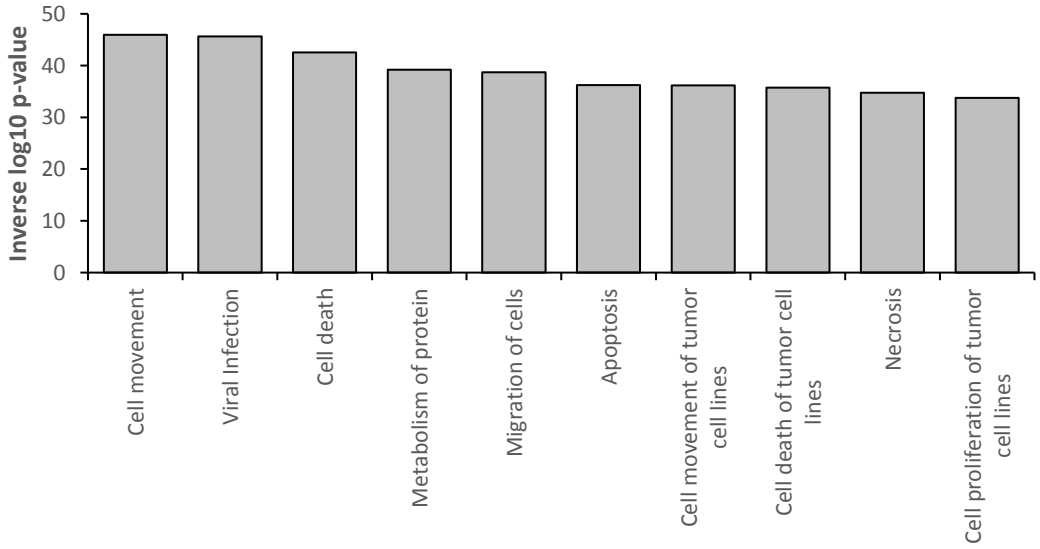

Figure 6.4. The Disease and Bio Functions most associated with the uveal melanoma extracellular vesicle proteome (inverse log10 p-values ≥2)

The top canonical pathways associated with the UM small exosome-like EV proteome highlighted association with two distinct but related groups of signalling pathways. These are a group including EIF2, EIF4/p70S6K, mTOR and Rho family GTPase signalling, and a group with ephrin and integrin signalling (Figure 6.5.).

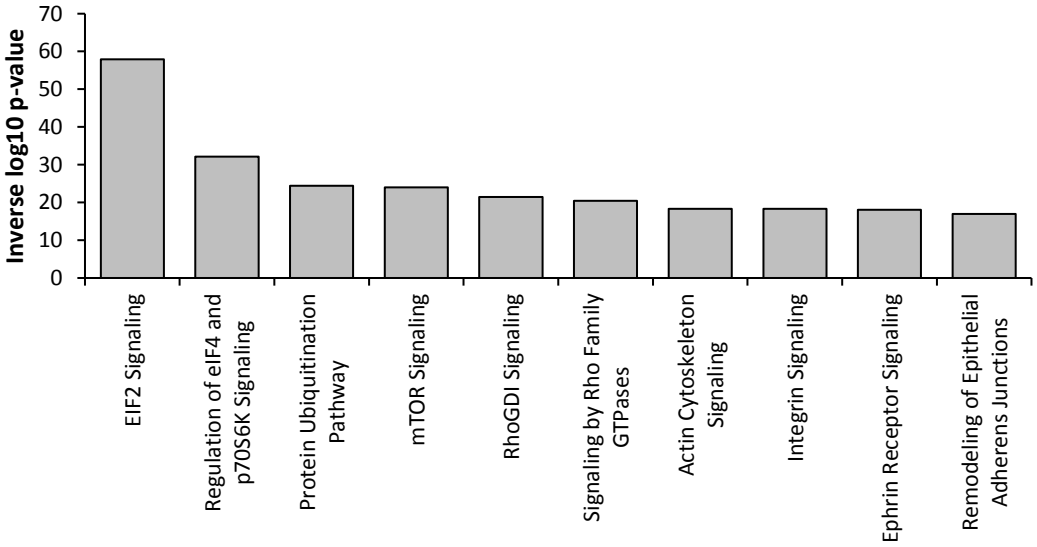

Figure 6.5. The Canonical Pathways most associated with the uveal melanoma extracellular vesicle proteome (inverse log10 p-values ≥2)

The top upstream regulators of the UM small exosome-like EV proteome were predicted with IPA; matrix metalloprotease 12 (MMP12) demonstrated the highest association with the dataset, with an inverse log10 p-value of 39.5. Others of interest included the apoptosis inhibitor Synovial 1 (SYVN1), the proto-oncogene MYC and the micro-RNA mir-122 (Figure 6.6.).

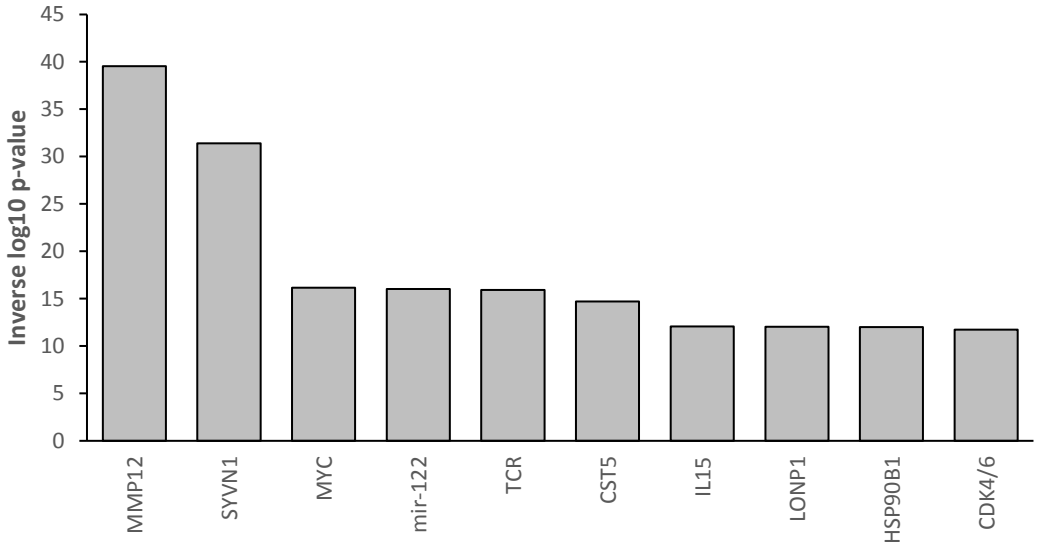

Figure 6.6. The upstream regulators most associated with the uveal melanoma extracellular vesicle proteome (inverse log10 p-values ≥2)

6.3.5. Differential expression of pathways and processes between primary uveal melanoma and metastatic uveal melanoma cell line derived extracellular vesicles

When assessing the differential activation status of biological functions in the MUM small exosome-like EV proteome compared with that of the PUM, necrosis, cell death and apoptosis all appear to be upregulated, while cell viability, survival and cell movement are all downregulated. Viral infection pathways are also downregulated (Figure 6.7.).

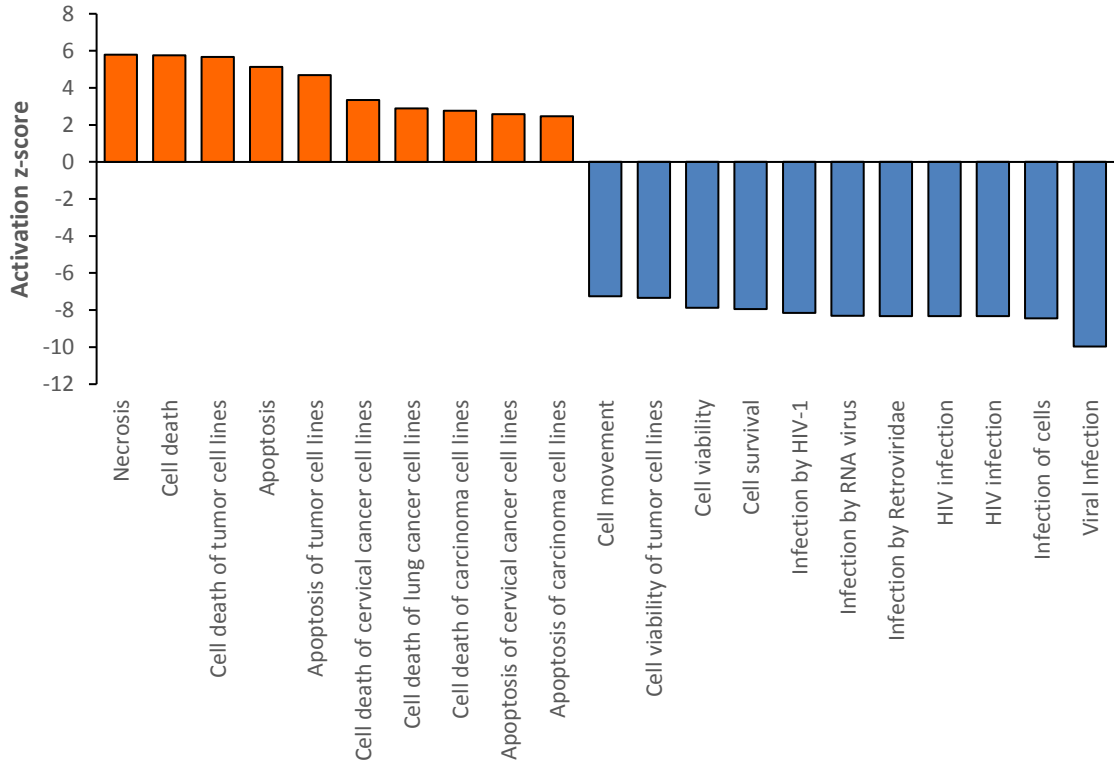

Figure 6.7. The disease and bio functions most differentially associated between the extracellular vesicle proteomes from metastatic and primary uveal melanoma cell lines (inverse log10 p-values ≥2; z-scores ≥2 or ≤-2)

Top canonical pathway analysis revealed an upregulation in vitamin metabolism, PTEN signalling and RhoGDI signalling, and a downregulation in several pathways linked to GTPase signalling, cytoskeletal remodelling, adhesion and cell motility (Figure 6.8.).

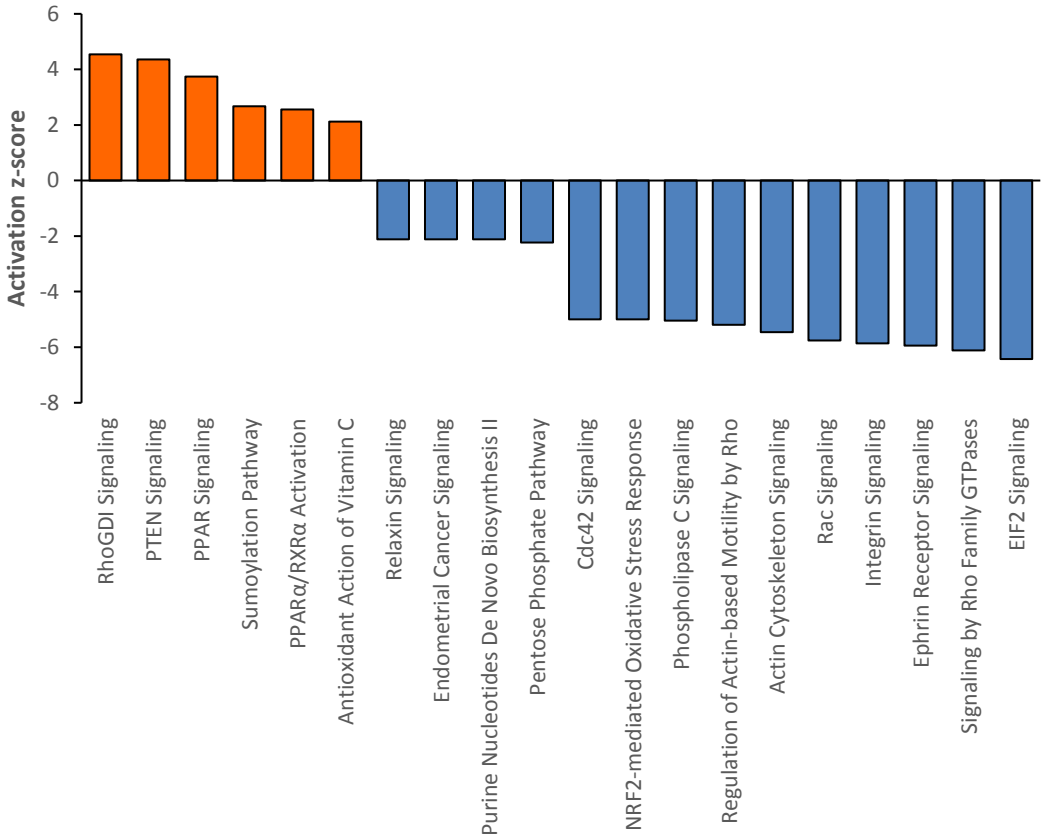

Figure 6.8. The canonical pathways most differentially associated between the extracellular vesicle proteomes from metastatic and primary uveal melanoma cell lines (inverse log10 p-values ≥2; z-scores ≥2 or ≤-2)

Analysis of the upstream regulators differentially expressed in MUM compared with PUM predicted an increase in mir-122, estrogen receptor (ER) and SPDEF (SAM Pointed Domain Containing ETS Transcription Factor). Whereas, MYC (cancer associated myelocytomatosis protein), HIF1A (hypoxia inducible factor 1 alpha), GNA12 (G Protein Subunit Alpha 12), PGR (progesterone receptor), EGF (epidermal growth factor), EGFR (epidermal growth factor receptor), SMARCA4 (SWI/SNF Related, Matrix Associated, Actin Dependent Regulator Of Chromatin, Subfamily A, Member 4), HSP90B1 (Heat Shock Protein 90 Beta Family Member 1) and SYVN1 (Synoviolin 1) were all predicted to be inhibited (Figure 6.9.).

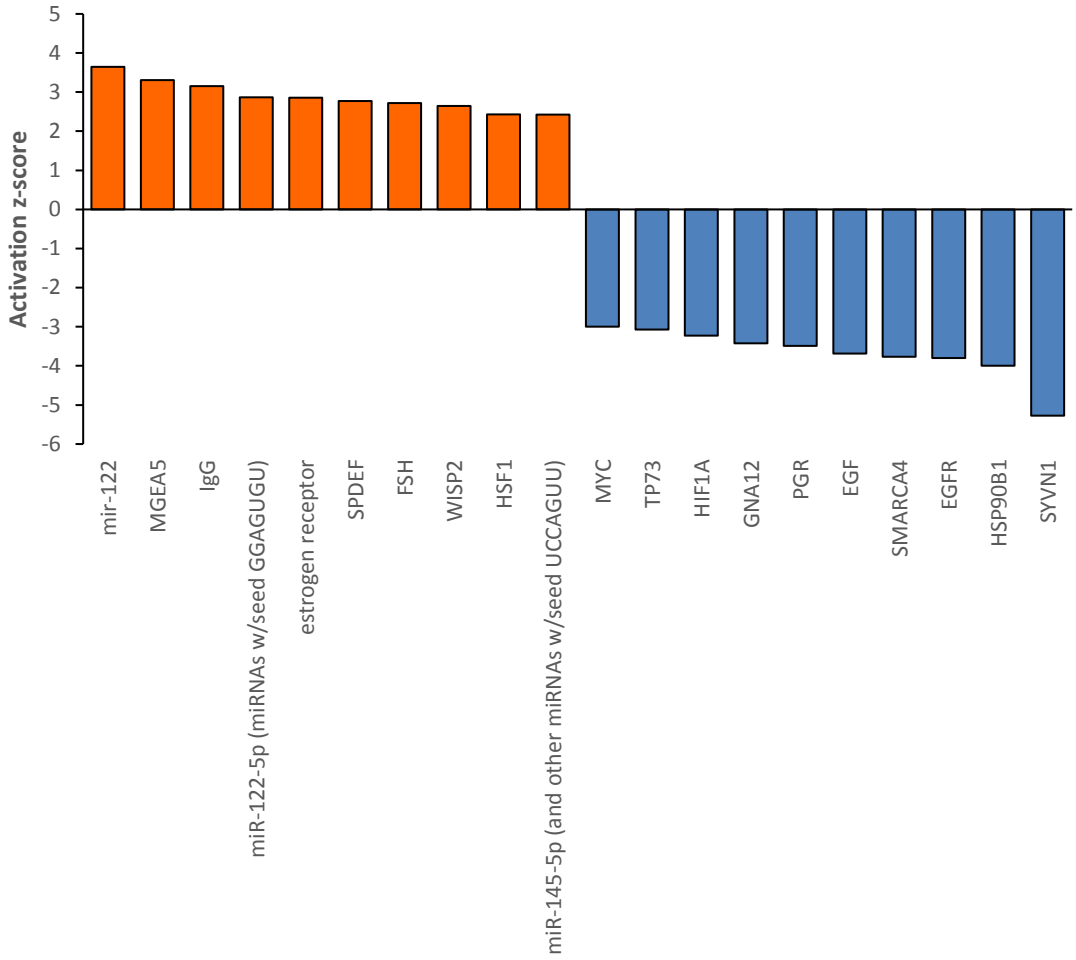

Figure 6.9. The upstream regulators most differentially associated between the extracellular vesicle proteomes from metastatic and primary uveal melanoma cell lines (inverse log10 p-values ≥2; z-scores ≥2 or ≤-2)

6.3.6. Differential expression of pathways and processes between *GNAQ* and *GNA11* mutant uveal melanoma extracellular vesicles

Biological processes that were differentially expressed in the *GNA11*-mutant UM small exosome-like EV proteome compared with that of *GNAQ*-mutant UM were analysed. This

highlighted a reduction in proteins linked with cell death and apoptosis, and an upregulation of proteins associated with cell movement (Figure 6.10.)

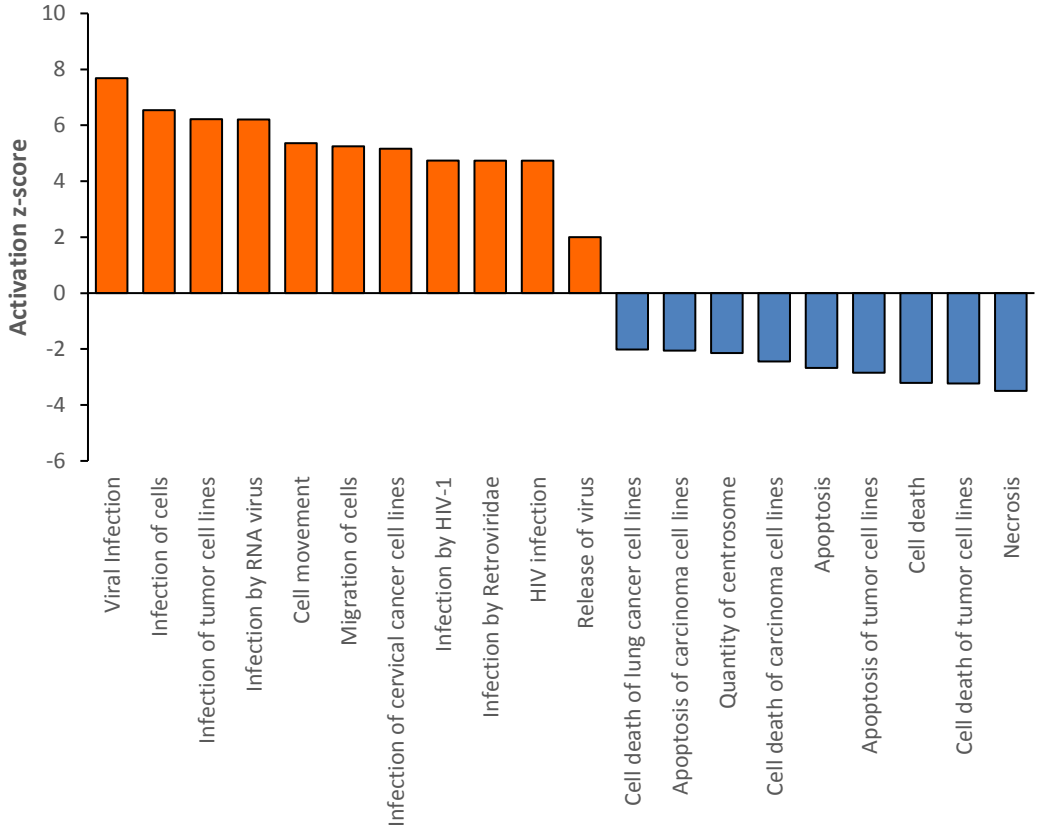

Figure 6.10. The 20 most differentially associated disease and bio functions between the extracellular vesicle proteomes from GNA11-mutant and GNAQ-mutant uveal melanoma (inverse log10 p-values ≥2; z-scores ≥2 or ≤-2)

When assessing the biological processes differentially regulated in the UM small exosome-like EV proteomes, pathways associated with viral infection were dominating those most upregulated. As the viral pathways are known to overlap with those associated with exosomal uptake and release (Nolte-'t Hoen *et al.*, 2016), pathways under the categories "Infectious disease" and "Infectious disease and organismal injury" were

removed to limit this bias and to assess which other pathways were differentially regulated (Figure 6.11.). This demonstrated an upregulation in functions related to cell movement, migration and invasion, and cell survival, viability and proliferation.

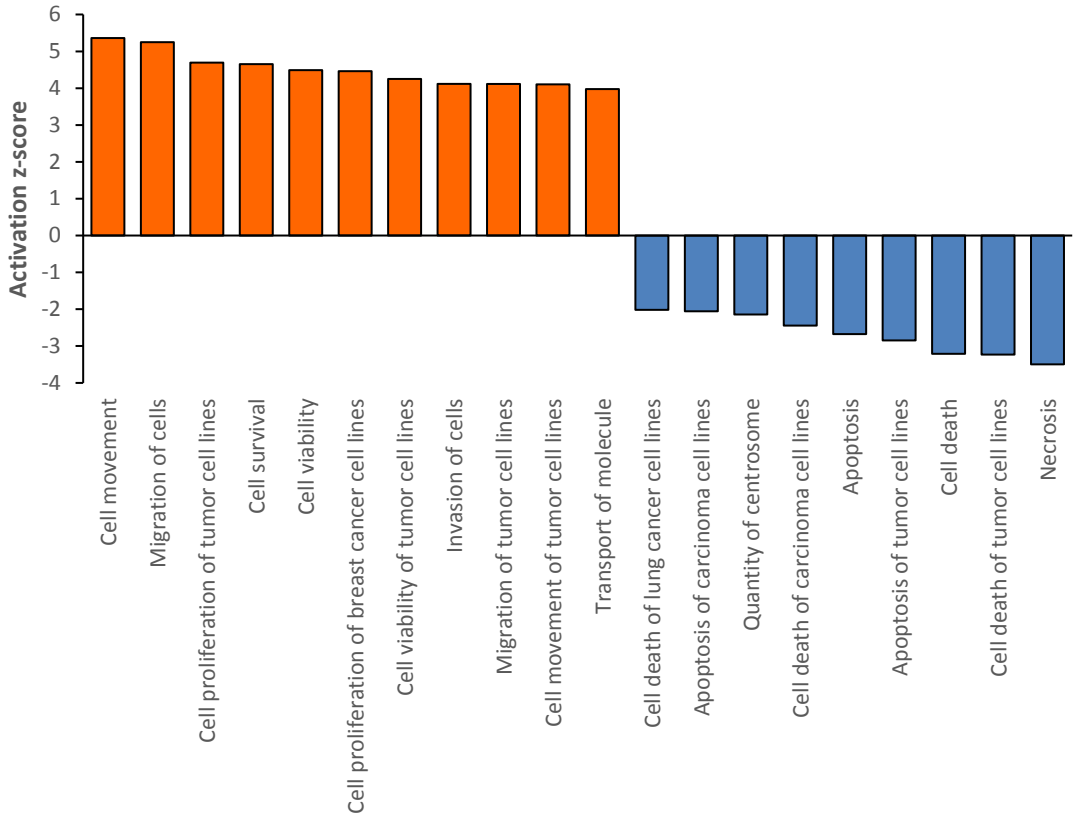

Figure 6.11. The 20 most differentially associated disease and bio functions between the extracellular vesicle proteomes from GNA11-mutant and GNAQ-mutant uveal melanoma (inverse log10 p-values ≥2; z-scores ≥2 or ≤-2). The categories "Infectious disease" and "Infectious disease, organismal injury" were removed for this analysis

The top canonical pathways demonstrating differential expression between the *GNA11*-mutant UM small exosome-like EVs and those of *GNAQ*-mutant UM was an upregulation in GTPase signalling and signalling related to morphology, adhesion and motility. Apoptosis signalling showed downregulation, as did PPARα, HIPPO and PTEN signalling (Figure 6.12.).

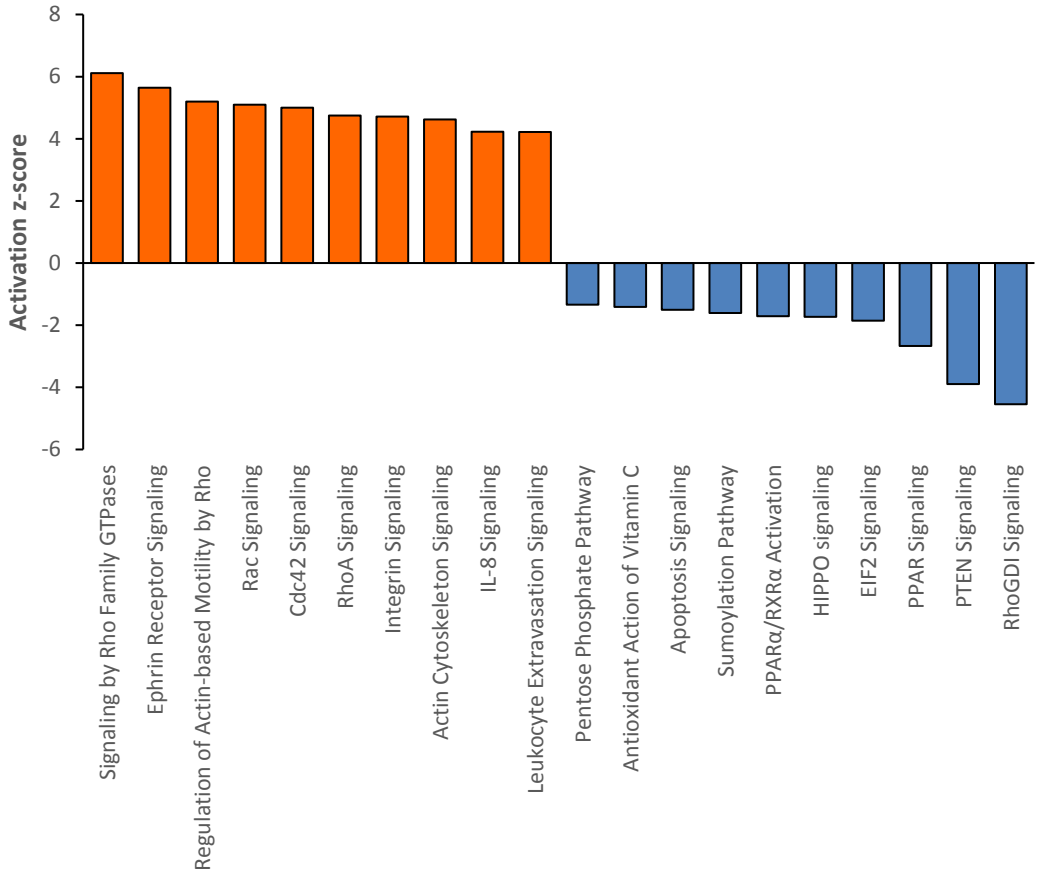

Figure 6.12. The 20 most differentially associated canonical pathways between the extracellular vesicle proteomes from GNA11-mutant and GNAQ-mutant uveal melanoma (inverse log10 p-values ≥2; z-scores ≥2 or ≤-2)

The upstream regulators, differentially expressed in *GNA11*-mutants compared with *GNAQ* mutants, were predicted; activated upstream regulators included the oncogene ERBB2, the transcription factor TFEB, FOXM1, the melanogenesis associated transcription factor MITF, MYC, GNA12 and the transcriptional activator SMARCA4 (Figure 6.13.).

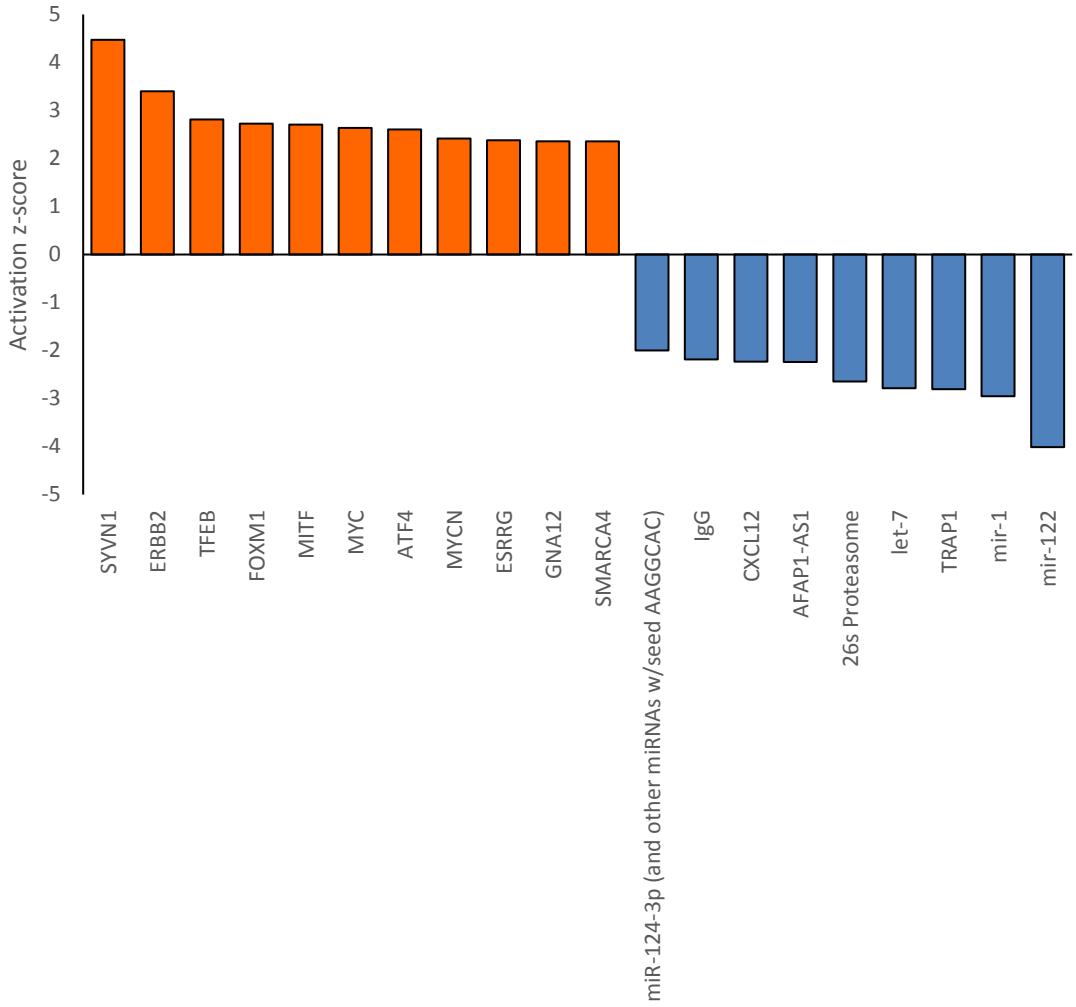

Figure 6.13. The 20 most differentially associated upstream regulators between the extracellular vesicle proteomes from GNA11-mutant and GNAQ-mutant uveal melanoma (inverse log10 p-values ≥2; z-scores ≥2 or ≤-2)

6.3.7. Comparing the uveal melanoma extracellular vesicles proteome with the total secreted proteome

The proteome identified in UM EVs was compared with that of the UM secretome described in Chapter 4. The proteome of the UM EVs highlighted 1172 proteins identified with >2 unique peptides. The proteome of the UM secretome highlighted 758 proteins identified with >2 unique peptides. The two datasets contained 461 proteins that were apparent in both sample types. Employing the UniProt published list of 26,236 proteins identified and reviewed in the total human proteome (Breuza *et al.*, 2016), this allowed statistical evaluation of the probability of overlap between the two datasets using the hypergeometric probability assessment (Gonin, 1936; Kim *et al.*, 2001). This gave a representation factor of 13.6 and a statistically significant overlap between the two proteomes ($p < 0.001$).

The 25 most abundant proteins of each proteome were compared to see which proteins overlapped between the two. Only 5 of the proteins were apparent in both lists; Alpha-enolase, Pyruvate kinase PKM, Cytokeratin-1, Annexin A2 and Peptidyl-prolyl cyc-trans isomerase A (PPIA).

When compared with the proteins in the UM secretome that were predicted to be of EV origin, the proteomic profile of isolated UM EVs demonstrated approximately 3x the number of proteins. The proteome of isolated UM small exosome-like EVs encompassed 82% of the exosomal profile predicted in Chapter 4 (Figure 6.14.) and identified a further 862 proteins. Furthermore, 94% of the proteome of UM EVs has previously been reported to be in EVs isolated from other cell types (Mathivanan and Simpson, 2009).

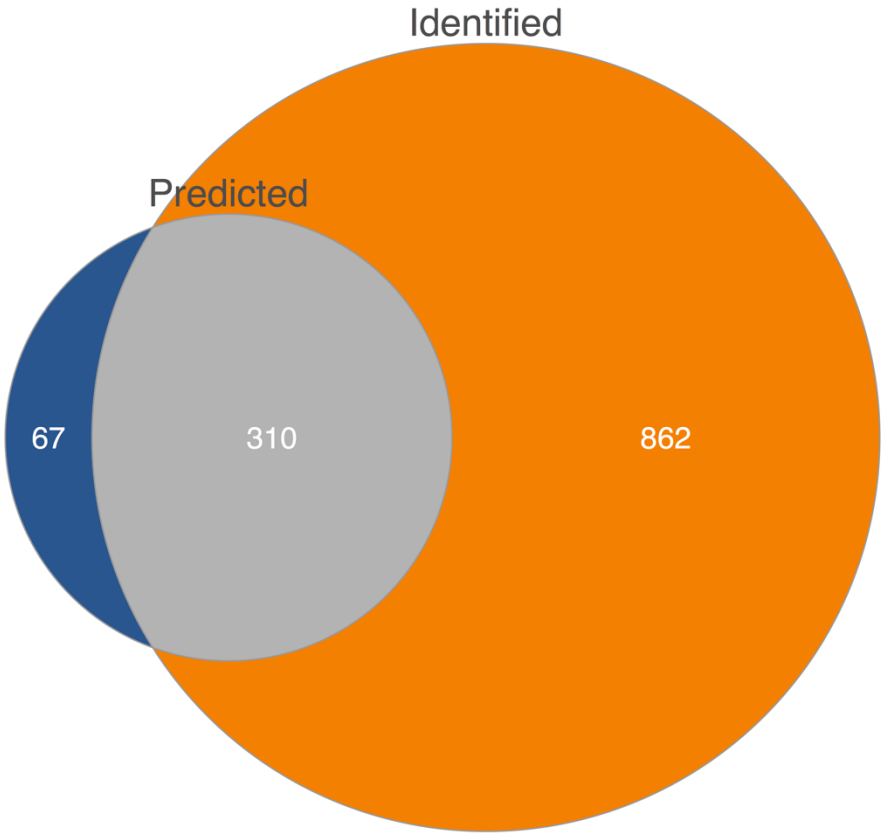

Figure 6.14. The overlap between the proteomic profiles of the predicted extracellular vesicle fraction of the secretome and of isolated extracellular vesicles

Of 255 ‘GO processes’ associated with the UM EV proteome (false discovery rate corrected q-value < 0.01) 25 of these were also associated with the UM secretome (out of a total of 76). However, comparison of the ‘GO functions’ associated with the EV dataset (86 functions) and the secretome (4 functions) revealed only 1 function associated with both, enzyme binding. When comparing the ‘GO compartment’ annotations, 13 of the 32 annotations associated with the secretome were also present in the 81 annotations associated with the UM EV proteome

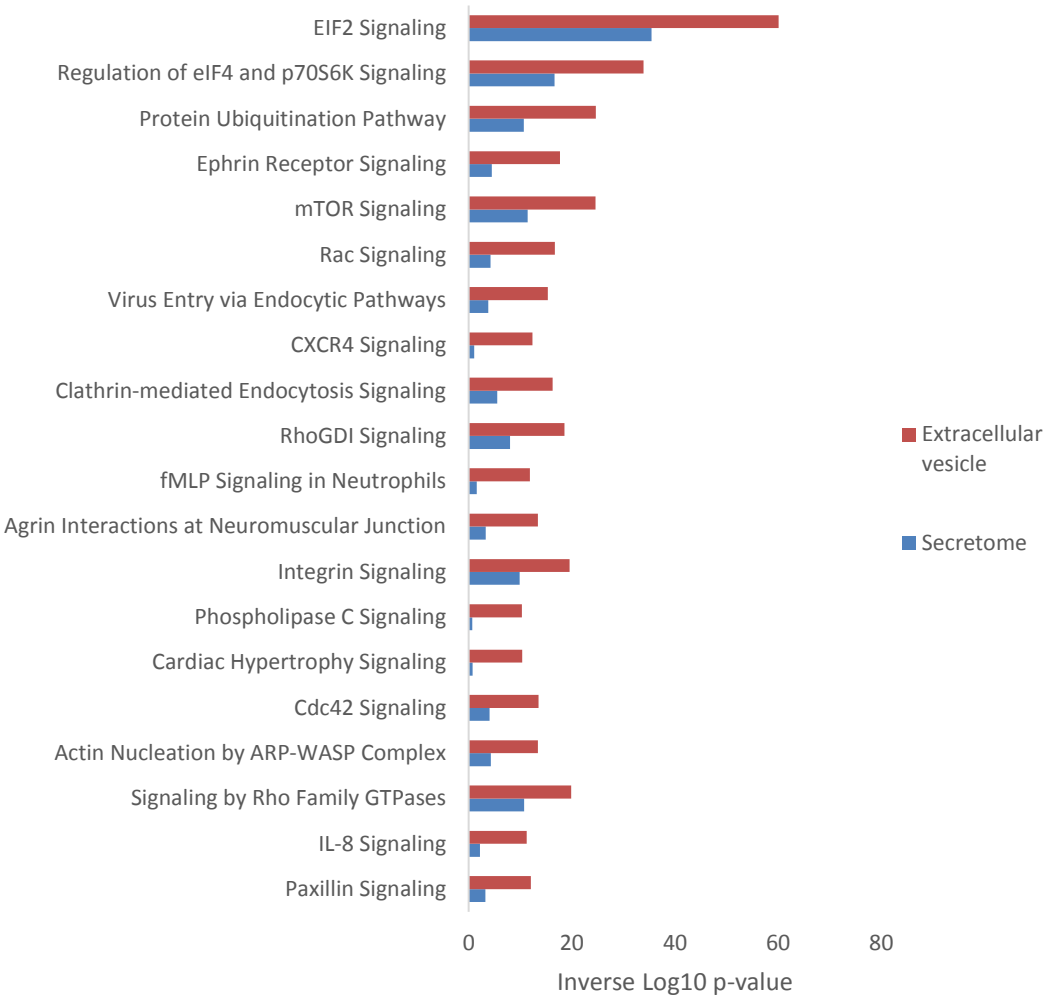

Figure 6.15. The 20 most differentially associated canonical pathways between the UM secretome and uveal melanoma extracellular vesicles

When assessed by IPA, the 20 signalling pathways with the greatest difference in associated between the secretome and UM EVs all demonstrated higher association in UM EVs compared with the secretome (Figure 6.15.). All 20 of these pathways are associated with or regulated by mTOR signalling.

6.4. Discussion

Presented herein is the first in-depth comparison of the proteomes of EVs released by UM cell lines and the functional enrichment of signalling pathways and biological functions associated with these. The research hypothesised that EVs released by UM cells contain proteins associated with the malignant progression of UM, that the signalling pathways associated with this malignancy are upregulated in MUM compared with PUM, that the profile of these pathways may differ between GNAQ/11 mutants. This research suggested that proteins in UM EVs are associated with cellular movement and adhesion through networks such as mTOR, Rho GTPase and integrin signalling pathways; mechanisms commonly associated with malignancy and tumour progression. Contrary to the hypothesis, these pathways and processes were downregulated in MUM compared with PUM. However, these analyses demonstrated they were upregulated in GNA11 mutant UM EVs compared with EVs from GNAQ mutant UM.

The proteomic workflow employed herein generated quantitatively comparable proteomes for each cell line with dynamic ranges spanning six orders of magnitude. The UM EV proteome encompassed 82% of the proteins previously predicted to be exosomal through analysis of the total UM secretome (Angi *et al.*, 2016) and was three-fold larger, containing 1172 confidently identified proteins. The total number of identified proteins was 2155 proteins, with 983 proteins identified by less than 3 unique peptides. While these proteins may be components of the UM EV proteome, for the purpose of this research they were omitted from the analyses to improve the confidence in the results presented.

Hierarchical clustering of the proteomic profiles demonstrated neat clusters within biological triplicates for each cell line. While the three cell lines isolated from one patient also clustered, the total panel of cell lines did not cluster in any known groups based on cell

line characteristics, such as tumour site, G-alpha subunit mutation. This method of analysis relies on commonalities between the values of multiple variables across multiple samples. While the data herein presents >1000 variables (proteins identified), six samples (cell lines) is a limited number for comparison. Increasing the number of samples may generate a different pattern of clustering and is worth investigating in future research.

GO annotation of the UM small exosome-like EV proteome highlighted processes and components associated with EVs and exosomes (Table 6.2.). The high degree of association with exosomal/EV components suggested that the isolation methods were successful in enriching UM EVs from the UM cell secretome. While recent evidence suggests that methods for the isolation of exosomes likely yield heterogenous populations of EVs (Kowal *et al.*, 2016), the GO term 'extracellular exosome' was associated with the UM EV proteome with a corrected p-value of 8.55×10^{-21}. This high level of association could be attributed to an enrichment of exosomes within the EV sample due to the techniques employed and would correspond with the characteristic morphology and size distribution described in Chapter 5.

The analysis herein also enriched the cellular component GO terms 'pigment granule' ($p = \times 10^{-6}$) and 'melanosome' ($p = 7.71 \times 10^{-6}$) confirming the melanocytic origin of the EVs isolated. This method of proteomic analysis and GO term enrichment could therefore be employed to determine cellular origin when isolating/enriching UM EVs from complex samples such as bodily fluids. Previous research by Eldh *et al.,*(Eldh *et al.*, 2014) employed immunoblotting for the MART-1 antigen to establish melanocytic origin of EVs. However, research into MART-1 targeted immunotherapy for the treatment of melanoma suggested that the antigen is not always present on melanoma cells (Sørensen *et al.*, 2009). A more integrated approach employing functional enrichment, such as that described herein, could

be used in conjunction with immunoblotting for MART-1 for a more robust identification of melanocytic origin.

As well as vesicular signalling, GO-annotation highlighted the regulation of localization, transport, biological quality and signalling receptor binding. Taken together with the functions associated with actin binding, this suggests a role of UM EVs in the intercellular regulation of cytoskeletal remodelling and cellular cargo transport. This could be stimulating recipient cells to increase the rate at which they move, degrade, or secrete factors. Alternatively, these functions could represent the localisation and transport of proteins through EV secretion from the donor cell. The association of EV proteins with the modulation of cellular morphology was previously demonstrated by Hood *et al.,* in 2009, who highlighted the ability of cutaneous melanoma derived EVs to influence microtubule number, size and structure in endothelial spheroids (Hood *et al.*, 2009). The authors observed a bi-modal, dose-dependent response in endothelial spheroids. They showed an increase in the size and complexity of nanotubule formation at lower doses; yet produced an increased number of smaller nanotubules at higher doses, generating smaller, more proliferative spheroids. Tunnelling nanotubes are structures involved in the movement and transport of vesicles and organelles (Rustom *et al.*, 2004) which require extensive cytoskeletal remodelling (Gerdes, Bukoreshtliev and Barroso, 2007). This activity has been demonstrated in prostate cancer cells (Vidulescu, Clejan and O'Connor, 2004) known to produce pro-invasive EVs (Chowdhury *et al.*, 2015).

Analysis of the biological functions of the UM EV proteome highlighted a possible function in signalling related to the modulation of cell survival and death. This included 27 individual but overlapping functions associated with cell viability, survival, and death, among others, involving 423 proteins. Cancer derived EVs have been shown to promote cell proliferation

while inhibiting apoptosis in both normal and cancerous cells (Huang *et al.*, 2019). Tumour derived EVs have been shown to modulate cell cycle progression (Atay and Godwin, 2014) and to promote tumour proliferation through upregulation of the PI3K/AKT or MAPK/ERK signalling pathways (Qu *et al.*, 2009; Yang *et al.*, 2013). Zuidervaart *et al.,* demonstrated MAPK/ERK signalling in UM, suggesting its involvement in UM progression (Zuidervaart *et al.*, 2005), and PI3K has been posited to be an effective target for therapeutic intervention in UM when combined with targeting mTOR signalling (Amirouchene-Angelozzi *et al.*, 2016).

Cellular migration processes were strongly associated with the dataset, suggesting that UM EVs may play a role in the early stages of metastatic progression of UM. Cutaneous melanoma EVs have been shown to promote a migratory and metastatic phenotype through autocrine signalling (Lazar *et al.*, 2015). The authors performed functional analysis of the cutaneous melanoma EV proteome and highlighted similar processes and functions to those demonstrated herein, including cytoskeleton reorganisation, cell motility, vesicle and intracellular cascade (Lazar *et al.*, 2015).

Functional enrichment and pathway analyses highlighted a role of mTOR, RhoA and integrin signalling associated with the UM EV proteome. These pathways are known to play key roles in specific behaviours during carcinogenesis and cancer progression and each has been described to have a role in UM.

This analysis highlighted mTOR signalling associated with both the secretome (Chapter 4) and the UM EV proteome. Furthermore, the level of association was shown to be higher in the UM EV proteome (Figure 6.15.). The primary roles of the mTOR protein are executed through the two complexes it forms; MTORC1 and MTORC2. The physiological roles of

MTORC1 involve a role in integrating incoming growth factor and nutrient sensing signals, regulating growth and cell cycle progression (Fingar *et al.*, 2004), and mediating incoming stress and hypoxia signals (Cam *et al.*, 2010; Su and Dai, 2017). MTORC1 is also a known mediator of autophagy (Kim and Guan, 2015), commonly known as a tumour suppressing mechanism (Kung *et al.*, 2011).

Active mTOR signalling has previously been reported in PUM tumours (Pópulo *et al.*, 2010), the authors highlighting a relationship between mTOR and AKT phosphorylation. This association of mTOR pathways with UM corresponds with literature suggesting that pharmacological targeting of mTOR may provide therapeutic benefits in a clinical setting (Amirouchene-Angelozzi *et al.*, 2014). The inhibition of mTOR in UM demonstrated reduced cell growth and viability in 2D culture and reduced tumour growth in patient derived xenografts. Interestingly however, the efficacy of targeting mTOR in 2D culture was shown primarily in PUM cell lines and only few MUM lines, and the PDX models only employed PUM cells (Amirouchene-Angelozzi *et al.*, 2014). These results align with those presented herein, suggesting that mTOR signalling and its influence on migration and invasion may subside once the tumour is established in the metastatic niche. Previous combination therapies have targeted mTOR and demonstrated reasonable efficacy. Carita *et al.,* showed that dual inhibition of PKC and mTORC1 was able to significantly reduce tumour growth *in vivo*, when compared with each monotherapy (Carita *et al.*, 2016), though the results were not seen in all PDXs or in all cell lines *in vitro*. Ho *et al.,* demonstrated that an ATP-competitive pan-mTOR inhibitor was successful in limiting cell cycle progression and inducing apoptosis in GNAQ mutant UM cells when treated in combination with selumetinib (Ho *et al.*, 2012). The induction of apoptosis in the combination therapy was shown to be via inhibition of the MTORC2 complex through siRNA knockdown.

The mTOR signalling network and several known downstream effects are shown in Figure 6.16. Downstream biological effects of upregulated mTOR signalling include the initiation of translation, and remodelling of the actin cytoskeleton, both mechanisms that were associated with the UM EV proteome.

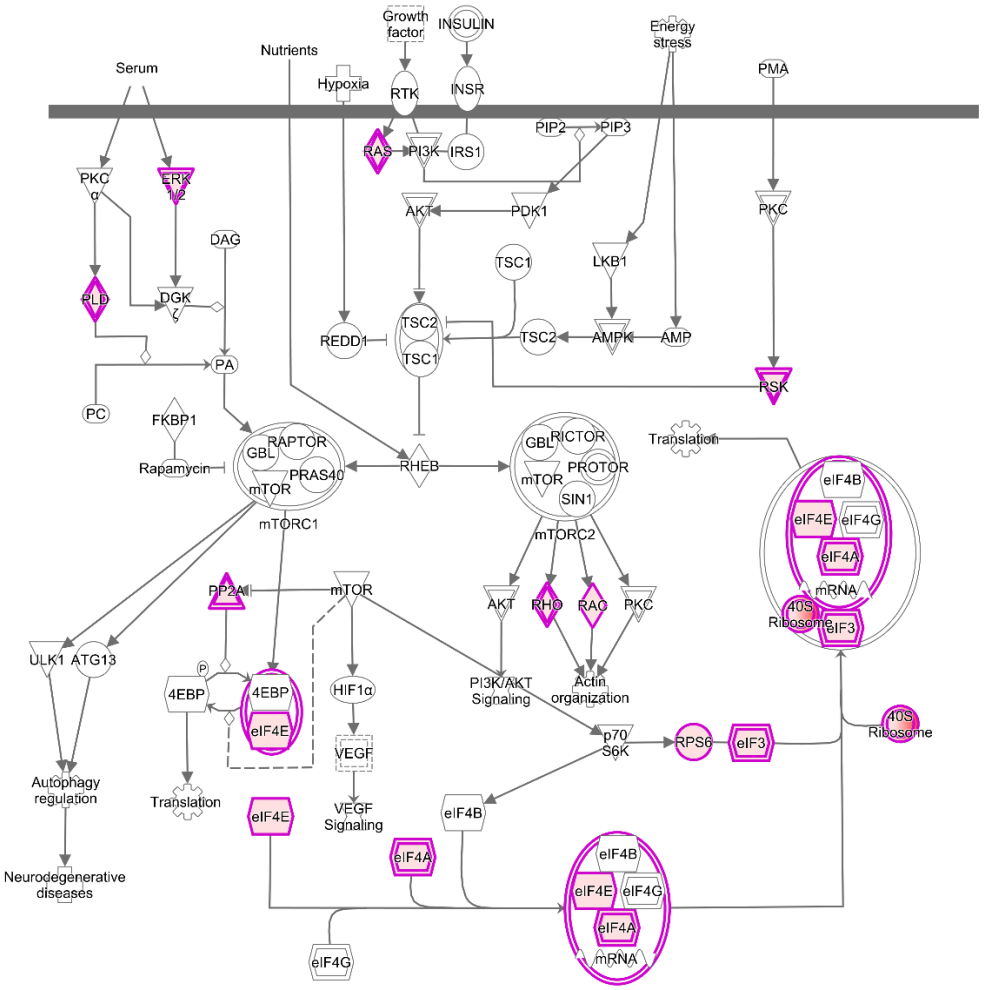

Figure 6.16. Schematic overview of the mTOR signalling pathway associated with the uveal melanoma extracellular vesicle proteome. Those molecules apparent in the proteome are highlighted pink; the density of the red colour indicates the relative abundance in the dataset.

The Rho family of GTPases has a well-established role in remodelling the actin cytoskeleton and regulating cell migration (Hall, 1998) its link with invasion and metastasis in cancer is well documented (Struckhoff, Rana and Worthylake, 2011). However, this mechanism can be inconsistent, as Rodrigues *et al.,* demonstrated that Rho GTPases possess the ability to suppress tumour progression and metastasis in colorectal cancer (Rodrigues *et al.*, 2014). It is thought that the functions of Rho GTPases act in a dynamic balance, and that regulation of Rho proteins can promote both strong focal adhesion through stress fibres and cell motility through membrane ruffling (O'Connor and Chen, 2013). Feng *et al.,* demonstrated TRIO-dependent regulation of the signalling activity of the Rho GTPases, RhoA and Rac1 in cells with activating G protein α-subunit mutation (Feng *et al.*, 2014). They proposed a HIPPO-independent pathway of YAP nuclear localisation and dynamic actin polymerisation downstream of this signalling, suggesting that Rho GTPases play an integral role in orchestrating the downstream effects of GNAQ or GNA11 mutation in UM.

Figure 6.17. highlights the complex signalling network associated with Rho family GTPase activity, compiled in Qiagen's Ingenuity knowledge base. It recognises that Rho family GTPase pathways are downstream of G protein α-subunit signalling, as previously described, and highlights the biological effects of this activity, including cytoskeletal remodelling, adhesion and proliferation; all highlighted in this research.

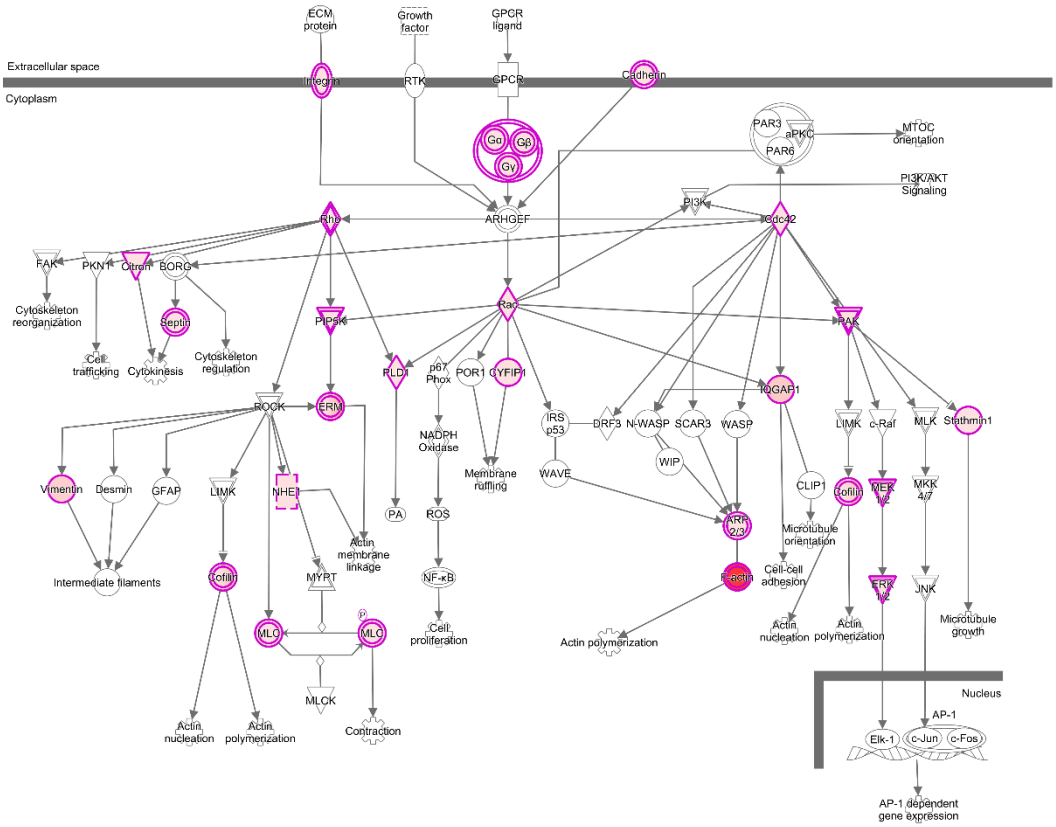

Figure 6.17. The Rho Family GTPase signalling pathway associated with the uveal melanoma extracellular vesicle proteome. Those molecules apparent in the proteome are highlighted pink; the density of the red colour indicates the relative abundance in the dataset.

Integrins are evolutionarily conserved proteins with well-established roles in cell adhesion (Barczyk, Carracedo and Gullberg, 2010). They have demonstrated integral roles in cancer (Desgrosellier and Cheresh, 2010) and have recently been shown to influence many steps in the metastatic progression, including and have recently been shown to influence many steps in the metastatic progression; including migration, invasion, anchorage-independent survival, engagement with cell surface receptors, sensing and remodelling of the tumour stroma, and the acquisition of stem cell-like properties (Hamidi and Ivaska, 2018).

Integrin composition of EVs secreted from the primary tumour is thought to influence organotropic metastasis, as demonstrated by Hoshino *et al.,* in 2016 (Hoshino *et al.*, 2015). The authors highlighted the presence of several integrins on EVs secreted by PUM cells; namely, integrins α1, 2, 3, 4, 6 and V, and β1, 3 and 5. Each of these integrins, with the exception of α4, was identified with the methods presented herein. These are presented in Table 6.3. ranked by average abundance across all samples. Hoshino *et al.,* suggested that integrins αV and β5, both found on in UM EVs, allowed preferential liver tropism through binding to resident Kupffer cells (Hoshino *et al.*, 2015). While integrin αV demonstrated the highest abundance in the UM EVs analysed herein, integrin β5 showed the lowest expression. Elshaw *et al.,* previously demonstrated the involvement of integrins in uveal melanoma and their possible link with poorer prognosis (Elshaw *et al.*, 2001). The authors highlighted the expression of integrin α6β1 in tumours compared with its absence in normal melanocytes, and its differential expression in tumour cells with different cell morphology, a known influencer of prognosis.

Table 6.3. The relative ranking of integrins found in uveal melanoma extracellular vesicles from highest to lowest abundance

Rank*	Integrin
1	αV
2	β1
3	β3
4	α3
5	α2
6	α6
7	α5
8	α1
9	β5

*, Ranking based on average abundance

Additional to the association of integrin signalling networks with both the UM secretome and the UM EV proteome, was the association of ephrin, agrin and paxillin signalling networks. Each of these demonstrated stronger association with the EV proteome in UM when compared with the secretome, suggesting that their signal propagation is heavily mediated through EV transfer.

Ephrin is known to regulate the actin cytoskeleton, modulate adhesion and migration and also negatively regulate ERK/MAPK signalling (Kullander and Klein, 2002). In melanoma models, overexpression of the Ephrin B2 was shown promote actin polymerisation and cause constitutive focal adhesion kinase activity *in vivo*. This caused enhanced preferential integrin-mediated ECM-attachment to laminin and fibronectin. Ephrin B2 overexpression also propagated melanoma-cell migration in Boyden chamber and scratch plate assays *in*

vitro (Meyer *et al.*, 2005). While only ephrin A2 and B4 were identified in the UM EV proteome, the role of these proteins requires further investigation.

Agrin is a protein with an indispensable role in the formation of neuromuscular junctions during embryogenesis (Daniels, 2012). Although, it has previously been suggested that it plays an oncogenic role through its regulation of focal adhesion integrity (Chakraborty *et al.*, 2015). Furthermore, ECM localised Agrin has a role in cellular mechanotransduction, stimulating the transcriptional co-activators YAP/TAZ – a pathway previously demonstrated in UM without reference to the role of Agrin (Feng *et al.*, 2014).

Paxillin has well-established roles in focal adhesion signalling due to its subcellular location at the plasma membrane, actin cytoskeleton interface, where it integrates incoming mechanical and biochemical signals from adhesion dynamics and growth factor stimulation (Turner, 2000; Brown and Turner, 2004). In 2005, Hamamura *et al.,* demonstrated increased phosphorylation of paxillin in melanoma cells expressing the ganglioside GD3 , a molecule associated with transformed/malignant phenotype in melanocytes (Carubia *et al.*, 1984).

RhoGTPase signalling, actin dynamics, mTOR signalling, and focal adhesion, are known to converge in order to facilitate and regulate the cell's relationship with its surrounding ECM (Boyle and Samuel, 2016), allowing tumour invasion, migration and metastasis. Herein, each of these signalling networks were highly associated with the UM EV proteome, suggesting an integral role of UM EVs in the regulation of UM metastatic progression. These pathways and the involvement of the UM EVs in their promotion require further investigation in UM models.

By combining the signalling networks demonstrated in these analyses with information know about them and demonstrated in the literature, a mechanistic network of pathways contributing to UM pathology and progression contributed to by UM EVs is proposed in Figure 6.18.

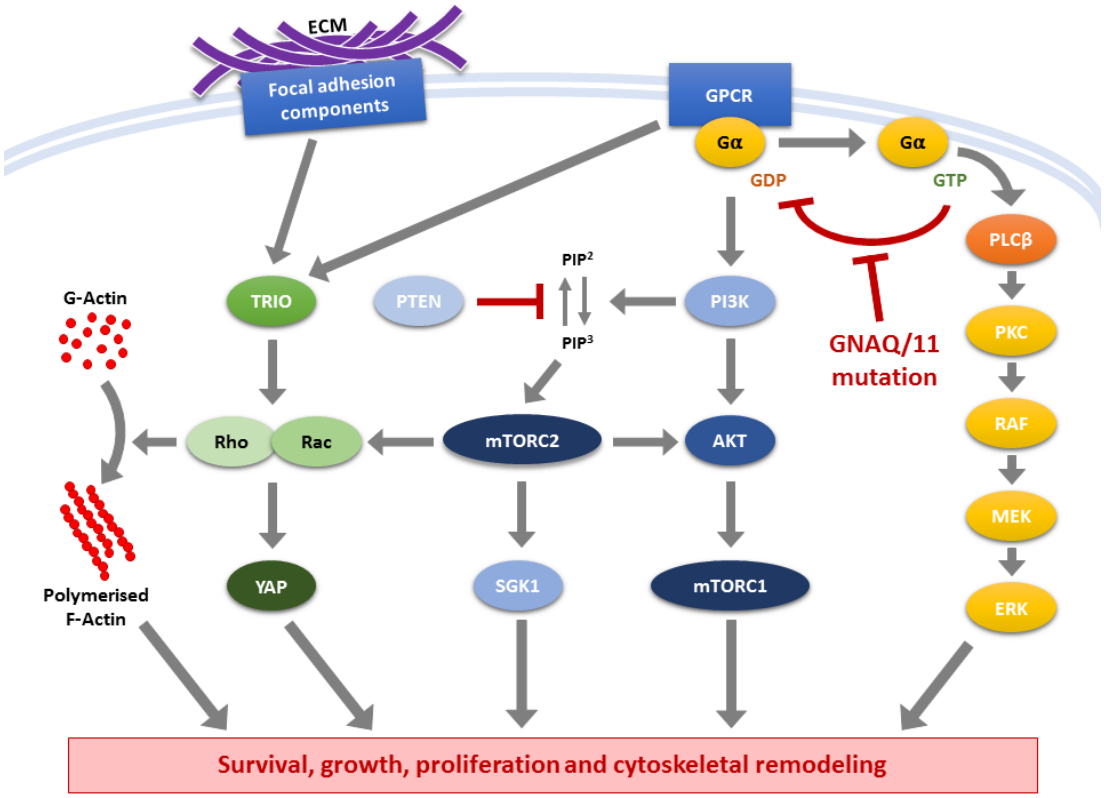

Figure 6.18. The primary network of signalling pathways potentiated by extracellular vesicles from uveal melanoma

AKT, Protein kinase B; ECM, Extracellular matrix; ERK, Extracellular signal-regulated kinase; Gα, Guanine nucleotide binding protein G alpha subunit; GDP, Guanosine diphosphate; GNAQ/11, Guanine nucleotide binding protein G alpha subunit q or 11; GPCR, G-coupled protein receptor; GTP, Guanosine triphosphate; MEK, Mitogen-activated protein kinase kinase; mTORC, mammalian target of rapamycin complex; PI3K, Phosphoinositide 3-kinase; PIP^2, Phosphatidylinositol 4,5-bisphosphate; PIP^3, Phosphatidylinositol (3,4,5)-trisphosphate; PKC, Protein kinase C; PLCβ, Phospholipase C beta; PTEN, Phosphatase and tensin homolog; Rac, Ras-related C3 botulinum toxin substrate; Rho, Ras homolog family member; SGK1, Serine/threonine-protein kinase 1; TRIO, Triple functional domain protein; YAP, yes-associated protein

While these pathways were strongly associated with the UM EV proteome, our research suggests a differential signalling profile of mTOR and Rho Family GTPase signalling between PUM and MUM EVs, inhibition of which could demonstrate different efficacy when targeting the metastatic lesions in the liver compared with the primary tumour in the eye.

The downregulation of these pathways in MUM compared with PUM was contrary to the hypothesis that their up/downregulation would mirror that of pathways demonstrated in HR-UM compared with LR-UM (Angi *et al.*, 2016). This may highlight a difference between PUM and MUM distinct from that between HR and LR UM, as all the cell lines analysed in this chapter display M3, a characteristic which was the primary differentiating characteristic used in Chapter 4 and strongly correlates with increased metastatic potential (Prescher *et al.*, 1996). The downregulation of these pathways may indicate a difference in the physiology of UM tumours depending on their *in situ* location.

While the upregulation of these pathways may aid metastatic dissemination in PUM, it is possible that the profile is altered further once the cells are established in the metastatic niche. Differences in the genetic profile of HR-PUM and LR-PUM are well established (Onken *et al.*, 2004), while both Meir *et al.,* demonstrated the distinct genetic profile between PUM and MUM (Meir *et al.*, 2007). They demonstrated 193 differentially expressed genes in liver MUM compared with PUM, highlighting upregulation of NF-κB and downregulation of CDK4 at both mRNA and protein levels. Differential expression of NF-κB and CDK4 have been shown previously to modulate apoptosis (Karin *et al.*, 2002) and cell cycle regulation (Ekholm and Reed, 2000), respectively. Despite this, a comprehensive analysis comparing matched pairs of primary and metastatic tumours to assess differences

in genetic profile may be warranted, as these differential expressions may differ with inconsistently altered characteristics of UM, such as chromosomal profile.

Further from the comparison of MUM with PUM, we were able to compare EVs isolated from *GNA11*-mutant UM with those from *GNAQ*-mutant UM. GNAQ and GNA11 are highly homologous alpha subunits of heterotrimeric G proteins associated with G-protein coupled receptors. Mutations in *GNAQ* and *GNA11* are considered initiating mutations in UM, occurring mutually exclusively in ~95% of cases (Koopmans *et al.*, 2013). While it has been demonstrated that grouping of UM patients by these mutations does not correlate with survival or metastatic risk (Onken *et al.*, 2008; Koopmans *et al.*, 2013), there is some evidence that GNA11-mutant tumours are linked with a more aggressive phenotype due to its higher frequency in M3 UM (Dono *et al.*, 2014).

The presented research demonstrates that GNA11-mutant UM small exosome-like EVs display a different proteomic signature compared with that of GNAQ-mutant UM. The GNA11-mutant UM small exosome-like EV profile displayed an upregulation in functions and pathways linked with malignant phenotype. Signalling related to multiple Rho GTPases showed upregulation along with focal adhesion signalling mechanisms and actin remodelling. Rho GTPases are known to be activated downstream of GNAQ and GNA11 (Chua *et al.*, 2017) and have been previously demonstrated to modulate actin remodelling through HIPPO-independent pathways (Feng *et al.*, 2014). Interestingly, HIPPO signalling was predicted to be downregulated in GNA11-mutant UM compared with GNAQ-mutant UM. Ephrin-receptor signalling and integrin signalling pathways were associated with the UM EV proteome and the IPA software predicted their upregulation in EVs released by GNA11-mutant UM compared with GNAQ-mutant UM. It has been suggested that ephrin regulates integrin mediated focal adhesion and affects the cytoplasmic levels of GTPases

such as Rho, Rac and Cdc42 (Pasquale, 2005); these GTPases signalling pathways demonstrated association with the UM small exosome-like EV proteome and were predicted to be upregulated in GNA11-mutant small exosome-like EVs compared with GNAQ-mutants.

The difference between PUM and MUM, GNAQ and GNA11, or indeed any subgroup comparison of cell line culture may be limited in its ability to contrast those characteristics *in situ*. Genetic drift of cell line after prolonged culture in 2D models is well established (Torsvik *et al.*, 2014). When examining glioblastoma cells, Torsvig *et al.,* highlighted that this genetic drift often encompasses a loss of primary tumour characteristics and is accompanied with phenotypic changes (Torsvik *et al.*, 2014). Genetic changes have previously been reported in UM cell lines compared with their primary tissues (Amirouchene-Angelozzi *et al.*, 2014; Jager *et al.*, 2016). Of concerning note for the interpretation of this research is the difference between the cell lines Mel270, OMM2.3, OMM2.5 and MP4, and their corresponding primary tumours. Jager *et al.,* demonstrated D3 of the Mel270, OMM2.3 and OMM2.5 cell lines, in contrast to the M3 identified in the primary tumours (Jager *et al.*, 2016). Similarly the MP41 cell line was shown to have M3 in contrast to the D3 identified in the patient derived xenograft from which it was derived (Amirouchene-Angelozzi *et al.*, 2014). Future work should seek to investigate UM EVs in a larger panel of UM cell lines with more genetic diversity or in isolated from a large population of patient primary cultures, as used in Chapter 4.

Significant overlap between the two proteomes ($p < 0.001$) suggests the UM EV proteome extensively contributes to the secretome. When assessing those proteins in the secretome which were predicted to be secreted via EVs, 82% were identified in isolated EVs. While this again highlights extensive overlap, the remaining 18% could have erroneously predicted

secretory mechanism. This discrepancy is not unusual when considering the method of prediction. Manually curated databases may contain incorrect annotations; furthermore, the majority of the proteins in the exocarta database have been identified in EVs from different cell types and pathologies. Proteins identified in the EVs of one cell type may not necessarily be secreted by the same mechanism from other cells and in other diseases. The research presented herein is the first in-depth study of the UM EV proteome.

Of the 25 most abundant proteins in each proteome, only 5 were apparent in both lists; Alpha-enolase, Pyruvate kinase (PKM), Cytokeratin-1, Annexin A2 and Peptidyl-prolyl cyc-trans isomerase A (PPIA). Alpha enolase is a glycolytic enzyme which has been suggested as a prognostic marker in cancer and promotes cell growth migration and invasion (Song *et al.*, 2014). The targeting of alpha enolase in pancreatic cancer has been shown to be effective *in vivo* (Principe *et al.*, 2015). Alpha enolase also demonstrated markedly increased expression in a panel of five malignant melanoma cell lines compared with normal melanocytes (Cecconi *et al.*, 2018). Alpha enolase is a glycolytic enzyme which has been shown to have increased expression in whole cell proteome of PUM samples from patients who progressed to metastasis (Linge *et al.*, 2012). However, it was shown to be downregulated when comparing MUM and PUM cell lines (Zuidervaart *et al.*, 2006). Interestingly, the expression of alpha enolase by was highlighted to be upregulated in the whole cell proteome of a UM cell line with a higher invasive potential compared with that of a UM cell line with a lower invasive potential (Pardo *et al.*, 2006). The role of alpha enolase in UM remains unclear and further research into its importance in UM progression is warranted.

PKM is another glycolytic enzyme and has previously been identified as significantly related to clinical outcome in patients with stage 3 metastatic melanoma (Welinder *et al.*, 2017). A

possible mechanism of this action was proposed by Mortia *et al.,* in 2018, where the authors suggested that increased PKM expression activates glucose catabolism pathways driving tumour cell growth and promoting autophagy and malignancy (Morita *et al.*, 2018).

Cytokeratin-1 was also abundant in both datasets. Cytokeratins have been suggested as tumour markers (Barak *et al.*, 2004) and are thought to influence migration and invasion (Karantza, 2011); however, cytokeratins are known to be common contaminants in MS based proteomic studies (Lyngholm *et al.*, 2011), and so this result may require further investigation before conclusions can be drawn.

Annexin A2 is a member of the annexin calcium-dependent phospholipid-binding protein family and is thought to have a role in endosomal sorting and transport (Morel and Gruenberg, 2009). Proposed relevance of Annexin A2 in cancer has been systematically reviewed by Christensen *et al.,* in 2018. When assessing multiple cancer types, the expression of Annexin A2 was shown to correlate with resistance to treatment, binding to the bone marrow, histological grade and type, TNM-stage and shortened overall survival (Christensen *et al.*, 2018). Over expression of the Annexin 2 receptor demonstrated both increased autophagy and apoptosis in UM (Zhang *et al.*, 2016). The authors highlighted that Annexin 2 receptor-induced autophagy played a protective role against apoptosis in UM. Annexin A2 may also play a role in migration and invasion in liver cancer (Zhang *et al.*, 2013), and its presence in released EVs has been shown to promote angiogenesis in breast cancer (Maji *et al.*, 2016).

PPIA is an enzyme involved in the regulation of intracellular signalling, transcription, inflammation and apoptosis. Its increased expression has been linked with poorer prognosis in liver cancer (Wang *et al.*, 2019). PPIA is also known as cyclophilin-A. The possible roles of

cyclophilin-A in cancer have been reviewed by Lee and Kim, they were shown to include the promotion of growth, increased angiogenesis, resistance to hypoxia, resistance to chemotherapy and promotion of metastatic progression (Lee and Kim, 2010).

UM small exosome-like EV isolates did not contain the common exosomal protein CD63 at levels high enough to be visualised by western blot (Chapter 5). In this research, CD63 was shown to be present in the LC-MS/MS proteome. CD9, a protein commonly extolled as a marker of exosomes, was absent in the LC-MS/MS proteome. As the morphology and size distribution of the EVs isolated are indicative of exosomes, this suggests that CD9 is insufficient as a pan exosome marker for all cell types. However, it is worth noting that these results are in contrast to previous work by Pardo *et al.,* who identified CD9 in the secretome of the 92.1 UM cell line (Pardo *et al.*, 2007). The low level and lack of these proteins suggests that they do not represent sufficient markers of UM exosomes, corroborating literature suggestions that pan-exosome markers are often only present on subpopulations of small EVs (Kowal *et al.*, 2016) and indicating that appropriate markers in UM require further investigation.

UM small exosome-like EVs contained non-exosomal proteins calnexin (CANX) and cytochrome C1 (CYC1). Cell death and apoptosis associated with the dataset could account for this through leakage or release in small apoptotic bodies. Additionally, CANX is known to appear in microvesicles (Haraszti *et al.*, 2016). The literature suggests that currently available approaches for the isolation of exosomes are limited in their ability to provide pure exosomes (P. Li *et al.*, 2017). However, the variability in the levels of these proteins between cell lines could be due to differences in their growth, survival and death profiles in 2D serum-free culture (Hamabe *et al.*, 2000) or simply different physiological levels in different cell lines from different tumours. Additionally, while serum-free culture does not

seem to negatively impact the growth of UM cells in short-term culture, it has been shown that serum free culture conditions can alter the protein composition of EVs in other models (J. Li *et al.*, 2015). Similarly, it has recently been shown that the RNA and protein content of EVs from a 3D culture systems differ from those EVs isolated from 2D culture models (Rocha *et al.*, 2019). Furthermore, the RNA content of EVs from 3D culture systems more closely represents EVs *in vivo* (Thippabhotla, Zhong and He, 2019). Future research could isolate and perform in-depth label free proteomics on UM EVs from cells grown in established 3D models (Valyi-Nagy *et al.*, 2012). This would allow comparison with the proteome presented herein and may give more representative results when interrogated with functional enrichment, as 3D UM models may release EVs more representative of UM *in situ*.

Functional enrichment with the Ingenuity software also allowed prediction of the top upstream regulators associated with the UM EV proteome and its associated highlighted potential roles of Matrix Metallopeptidase 12 (MMP12), synoviolin (SYVN1), MYC and the micro-RNA mir-122 (Figure 5.6.). MMP12 has been shown to correlate with invasive potential in squamous cell carcinoma (Kerkelä *et al.*, 2002), but has also been shown to correlate with reduce vascular invasion in gastric carcinoma (Cheng *et al.*, 2010) and with better prognosis in colorectal carcinoma (Yang *et al.*, 2001). In 2015, Zhang *et al.,* demonstrated increased expression of MMP12 in cutaneous melanoma compared with normal skin, and an association between increased MMP12 expression with invasion and metastasis (Zhang *et al.*, 2015). SYVN1 is known to have anti-apoptotic properties and promote proliferation through regulation of the tumour suppressor p53 (Yamasaki *et al.*, 2007). SYVN1 is also thought to have a role in autophagy, through its relationship with α-1-antitrypsin (Feng *et al.*, 2017). The role of the MYC oncogene in cancer progression has been extensively reviewed by Dang *et al.,*(Dang, 2012). Previous work by Parrella *et al.,* in

2001 described specific amplifications of the MYC oncogene in more than 30% of UM and suggested that this may be due to copy number gains of chromosome 8q (Parrella *et al.*, 2001). The micro-RNA mir-122 is the most abundant in the liver (Hu *et al.*, 2012) and is known to mediate cell motility and invasion by targeting RhoA (Hu *et al.*, 2012). Conversely however, breast cancer secreted mir-122 has also been shown to modulate glucose metabolism within the metastatic niche, propagating metastatic progression (Fong *et al.*, 2015).

Among the upstream regulators predicted by the IPA software were MITF, let-7 and MYC each of which have been linked to cancer pathology or progression. MITF is a known oncogene which is amplified in malignant melanoma (Garraway *et al.*, 2005). MITF is thought to play a role in melanocyte development and survival (Hartman and Czyz, 2015); yet, its overexpression was shown to suppress Rho-GTPase activation and cellular invasion in melanoma (Bianchi-Smiraglia *et al.*, 2017). Let-7 is transcriptionally repressed by MYC (Chang *et al.*, 2008) and has been shown to be upregulated in tumours at higher risk of metastasis (Worley *et al.*, 2008). The *MYC* oncogene codes for the MYC protein and is known to play a role in cell growth and proliferation (Bernard and Eilers, 2006). MYC is thought to play a role in UM proliferation and was suggested as a prognostic marker of UM (Royds *et al.*, 1992). MYC is located on chromosome-8 (Dalla-Favera *et al.*, 1982), which commonly shows additional copies in UM, correlating with reduced survival (Sisley *et al.*, 1997). The inhibition of MYC has been hypothesised to reverse tumorigenesis due to its relationship with cell cycle progression, senescence and apoptosis (Li, Casey and Felsher, 2014); furthermore, it is known to promote integrin-mediated TGFβ signalling, ameliorate Let-7 signalling (Chang *et al.*, 2008), and orchestrate a feedback loop with RhoA that contributes to cytoskeletal remodelling (Bustelo, 2010). Each of these regulators require

further investigation in models of UM, to study how their modulation affects UM pathology and the UM secretome.

The research presented in this chapter lacked an appropriate negative control for comparison against the experimental samples. An example of such a control could be small exosome-like EVs isolated from NCMs as in Chapter 4. Comparison with such a control could demonstrate a difference in the proteomic profiles between small exosome-like EVs isolated from normal choroidal melanocytes and malignantly transformed UM. However, currently NCM cell lines are not available; furthermore, isolated NCMs would require multiple donor eyes for the number of cells required, which is likely to be higher than the number of UM cells as exosomal release is known to be upregulated in cancer (Riches *et al.*, 2014).

It is worth noting that non-exosomal proteins were found in the dataset. This may indicate non-exosomal EVs or proteins released in other forms such as through lysis or cellular debris. To limit the possibility that this release is due to the serum free culture conditions, the research could be repeated with cells grown in conditions including exosome-free serum. Vilas Shelke *et al.,* highlighted the importance of exosome depletion protocols when culturing with fetal bovine serum and concluded that the presence of bovine EVs in cell culture affected the behaviour of cells, such as migration, and that overnight ultracentrifugation was only capable of eliminating 95% of serum EVs (Shelke *et al.*, 2014). Kornilov *et al.,* have since demonstrated an inexpensive filtration method for the removal of EVs from serum (Kornilov *et al.*, 2018). The method maintains the metabolic and proliferative activity of cells compared with those grown in EV-containing serum and reduces ROS production compared with serum-free culture. This could also be implemented in future studies replicating the methods herein.

While the cell lines employed herein are frequently used in UM research, their molecular profile isn't representative of the total population of patients who develop UM and they are considered to have originated from "unusual" tumours (Jager *et al.*, 2016). The MP41 cell line added in this chapter to improve sample size and genetic variation. The MP41 line was described as more appropriately recapitulating the genetic landscape of UM; however, none of the cell lines employed in this research harbour a BAP1 mutation, an event apparent in 47% of UM cases (Koopmans *et al.*, 2014), an even considered an independent marker of metastatic risk (Harbour *et al.*, 2010). A greater number of cell lines or primary sample cultures would allow collection of EVs from a greater cohort of sample types. The research herein compares tumour site and GNAQ/11 mutation; however, comparing wild type with BAP1, EIF1AX or SF3B1 mutations could provide insight into their impact in intercellular signalling through EVs. Similarly, comparison of UM harbouring common genomic aberrations (described in Chapter 1) with normal copy number samples could also highlight interesting biological implications.

While this research represents the first in-depth proteomic analysis of UM EVs and is the first research to propose molecular mechanisms influenced by the proteins un UM EVs, functional validation of the associated pathways is required to confirm their involvement in UM pathology. The influence of UM EVs on the mTORC1 and mTORC2 pathways could be interrogated through exogenous treatment of UM cells with UM EVs. UM EVs could be isolated as described herein and administered in a dose dependent manner to UM culture models. The mTORC1 and mTORC2 pathways could be assessed for upregulation by western blot of downstream protein phosphorylation (Amirouchene-Angelozzi *et al.*, 2014) and inhibited either independently (Amirouchene-Angelozzi *et al.*, 2014; Werfel *et al.*, 2018) or through dual inhibition (Srivastava *et al.*, 2019). Similarly, methods of silencing

RhoA could be employed to assess the importance of RhoA signalling through UM EVs. UM EVs could be then added exogenously to UM cells and downstream outcomes of RhoA activity could be assessed, such as RhoA activity binding, actin dynamics through immunofluorescence, migration and adhesion (Yan *et al.*, 2014; Jatho *et al.*, 2015). Some of these methods would also assess cell migration and adhesion in response to UM EVs. Additionally, several methods for quantifying adhesion have been reviewed by Khalili *et al.,* (Khalili and Ahmad, 2015). The authors described imaging techniques such as polyacrylamide-traction force microscopy and three-dimensional traction force quantification, among others. These could be applied to cultured UM cells in the presence or absence of exogenous UM EV treatment. Collectively these methods could be employed to assess the impact of UM EVs on the pathways highlighted in this research.

6.5. Conclusion

In conclusion, proteomic analyses identified an association between UM small exosome-like EVs and functional pathways related to cell proliferation, adhesion and migration. The functionally enriched pathways were commonly related to mTOR and Rho GTPase signalling. It highlighted increased activation of these pathways in GNA11-mutant UM EVs compared with GNAQ-mutant UM EVs, and downregulation in MUM EVs compared with PUM EVs. These results demonstrate the exciting implication of UM EVs in autocrine or intercellular signalling in UM. The pathways discussed in this chapter require functional validation in relevant UM models.

CHAPTER 7: THESIS SUMMARY AND DISCUSSION

This thesis considers the role of the metastatic microenvironment in UM pathology and progression and how this may be influenced by factors secreted by the UM. It studies the level and pattern of fibrosis in the liver in response to MUM cells, comparing the results with patient and tumour characteristics. It investigates the signalling pathways and biological functions associated with the total protein secretome of PUM and assesses the secretory mechanism of those proteins. It continues by demonstrating methods capable of isolating and characterising small exosome-like EVs from a panel of UM cell lines and assesses the biological functions and signalling pathways associated with their protein content.

7.1. Summary of results

A key feature of UM-related mortality is its prevalent organotropic metastasis to the liver (Singh, Durairaj and Yeung, 2018). An apparent fibrotic response has previously been demonstrated in MUM of the liver (Grossniklaus, 2013) and is a common characteristic of the liver metastases from other primary cancer types (Cox and Erler, 2014; Milette *et al.*, 2017). This fibrosis is characterised by excess ECM deposition and the activation of local resident fibroblasts. Chapter 3 investigated this fibrosis in the largest cohort of hepatic MUM to date. To my knowledge this is the first study to statistically assess the fibrotic response in the liver of patients with MUM and to compare this with other tumour/patient characteristics. Chapter 3 demonstrates that increased ECM deposition in hepatic MUM is a common occurrence. Two distinct patterns of ECM deposition were described;
(1) peritumoural ECM and (2) intratumoural ECM.

Peritumoural ECM deposition was shown to be statistically associated with co-localised αSMA positive cells, suggesting that peritumoural ECM deposition is a consequence of

activated HSCs (Brenner *et al.*, 2012). This phenomenon has previously been suggested to impact immune infiltration in UM (Krishna *et al.*, 2017) and the efficacy of chemotherapeutics in pancreatic cancer (Tanaka and Kano, 2018; Matsuda *et al.*, 2019).

A common pattern in the intratumoural ECM deposition was also apparent, presenting as interconnecting loops similar to PAS-positive loops seen in PUM (Folberg *et al.*, 1993) and cirrhotic nodules seen in the liver (Lo and Kim, 2017). Intratumoural αSMA positivity was also seen in looping patterns, similar to the ECM loops described; however, this relationship was not statistically significant. When statistically assessed, the fibrotic markers were not significantly related to any other tumour characteristic assessed.

The prevalent fibrotic microenvironment demonstrated in hepatic MUM in Chapter 3 offers an exciting therapeutic prospect. Previous research has investigated the treatment of cancer through targeting the associated fibrosis but has demonstrated contrasting results depending on the context. Targeting the fibroblasts directly in pancreatic cancer can increase the response to chemotherapy (Olive *et al.*, 2009; Ene-Obong *et al.*, 2013; Sherman *et al.*, 2014) but has also been associated with increase tumour progression and a more aggressive phenotype (Özdemir *et al.*, 2014; Rhim *et al.*, 2014). These studies both employed mouse models of pancreatic cancer and treated the mice with compounds known to mediate stellate cell activation. They measured efficacy and outcome with a variety of methods such as H&E or Sirius red staining, IHC for collagen I or fibronectin, metastatic count, measures of tumour volume, duration of survival, and qRT-PCR of genes known to represent pancreatic stellate cell activation. Similar research has not yet been conducted in UM and these methods could be used to investigate the effect of antifibrotic treatment in animal models of MUM (Burnier *et al.*, 2019). At present however, further

work is needed to determine whether the available animal models are representative of hepatic MUM and if they display the fibrotic response presented in this research.

Chapter 3 aimed to elucidate any relationship between the genetic profile of MUM and the pattern or level of fibrosis present. However, the cohort of UM sample employed harboured limited variation in the genetic profiles due to the method of sample collection. Similar research with a larger sample cohort, containing a more varied genetic profile, could highlight a relationship between fibrosis and UM genetics. Current clinical practice at the Royal Liverpool University Hospital employs a method for predicting metastatic risk in UM patients which incorporates the genetic profile of the PUM (Eleuteri *et al.*, 2007; Deparis *et al.*, 2016). Should a relationship between UM genetics and fibrotic response exist, this information could be used to predict the level of fibrosis in the MUM. If identified, it could impact the clinical management of patients with UM and open alternative therapeutic strategies such as targeting fibrosis as discussed above. It should be noted however, that differences in genetic profile between the PUM and MUM have been highlighted (McCarthy *et al.*, 2016), and so analysis of the MUM genetic profile through fine needle biopsy may be more appropriate. Additionally, While the present dataset contains limited variation of these genetic aberrations, it must be recognised that UM is a rare disease in which <10% of patients present with resectable MUM, making this one of the largest collections of MUM samples worldwide. The samples analysed were large, localised, resectable MUM and thus it is unclear whether similar patterns of the markers examined would be observed in hepatic MUM that present as non-resectable miliary lesions.

Following the results presented in Chapter 3, I hypothesised that the fibrotic microenvironment in hepatic MUM is a response to the secretion of biologically active proteins by the UM cells and that the proteins secreted from PUM cells promote tumour progression through autocrine signalling and education of the premetastatic niche in the

liver. To investigate this, chapter 4 assessed the proteomic profile of the secretome of patient-derived PUM cells from those patients at a HR or LR of developing metastasis and the secretome of cadaver-derived NCM. The study identifies the mechanism of secretion of each protein and performs GO-annotation and functional enrichment on the resulting proteome in order to predict biological functions and signalling pathways associated with the UM secretome.

Chapter four demonstrated that a large proportion of the UM secreted proteome may be of EV origin and GO-annotation of the cellular component demonstrated association with the terms 'Vesicle' and 'Extracellular exosome', among other similar terms. Functional enrichment highlighted an upregulation of functions associated with cellular adhesion, migration and invasion in UM compared with NCM, and in HR-UM compared with LR-UM. Upregulated pathways included Rho, Rac and actin signalling, mTOR/S6K signalling, and agrin, integrin, ILK, paxillin and ephrin pathways. Each of these signalling networks are involved in cellular adhesion and migration. Furthermore, pathways associated with proliferation were also demonstrated, such as an upregulation in PI3K/AKT, HGF, and glycolysis signalling and a down regulation in PTEN signalling.

Interestingly, hepatic fibrosis and HSC signalling demonstrated the highest association with the UM secretome. When considering the propensity of UM to metastasise to the liver and the fibrotic response to MUM in the liver described in chapter 3, this result suggests that proteins secreted by UM cells are likely to be involved in signalling that regulates the activation of the resident fibroblasts in the liver. Rho GTPase, mTOR, actin and integrin signalling dynamics are known to co-operatively regulate the cell's response to its surrounding ECM (Boyle and Samuel, 2016) and these pathways are not only important in cancer migration and metastasis, but also in the activation of fibroblasts (Thoen *et al.*,

2011; Shafiei and Rockey, 2012; Martin *et al.*, 2016). Unfortunately, while upregulation of the Rho GTPase, mTOR, actin and integrin signalling mechanisms were predicted in UM vs NCM and in HR-UM vs LR-UM, up or down regulation of hepatic fibrosis and HSC activation was not predicted by the software. This process and its associated signalling require further investigation in models of UM.

The UM patient samples employed in chapter 4 were stratified according to chromosome 3 status, a strong predictor of a patient's risk of developing metastases (Cassoux *et al.*, 2014). The dataset employed in this study contained a large number of M3 HR-UM as compared with D3 LR-UM due to the isolation of PUM cells from large tumours that were either enucleated or underwent local resection. The HR-UM group contained ten samples, the LR-UM contained only four samples and the NCM group contained only five samples. While this could cause a bias in the results towards the difference between HR-UM and NCM, limiting the impact of LR-UM, it could be addressed in future research by also isolating cells from more D3 UM undergoing biopsy rather than resection.

To my knowledge, this is the first study to perform functional enrichment and pathway analysis on the total secreted proteome of PUM and NCM cultures. The results align well with previously published literature on pathways associated with UM pathology. The consistency of the results throughout these analyses and their alignment with the literature strengthens their interpretation and points to an important role of these pathways in UM progression. These findings contribute considerably to the development of novel hypotheses and future research projects into the involvement of specific signalling pathways and proteins in the pathology and metastatic progression of UM. An important implication of these findings is the association with the MTORC2-RhoA signalling axis. MTORC2 and RhoA have previously been reported to have roles in cell motility, invasion

and metastasis (Huang and Zhou, 2011). These signalling pathways require further investigation in models of UM and are discussed in further detail later in this chapter. A striking outcome of this research was the high proportion of EV associated proteins, representing two thirds of the UM secretome. Chapters five and six investigated UM EVs further demonstrating their isolation, characterisation and an investigation of their proteome and predicted functions.

The research in chapter 4 highlighted EV release as a major factor contributing to the UM protein secretome. I hypothesised that the protein content of EVs released by UM cells plays an important role in intercellular signalling and may be involved in educating the metastatic niche. Chapter 5 brings together methods previously described in the literature for the isolation and characterisation of small exosome-like EVs and applies these for the first time to the secretome of 2D cultured UM cells. The results demonstrate EVs with appropriate size, in line with published values (Muller *et al.*, 2014; Xu *et al.*, 2016; Garcia-Contreras *et al.*, 2017), and a reduction in size distribution following UC. TEM micrographs of isolated UM EVs demonstrated characteristic 'cup-shaped' morphology of exosomes as previously described (Théry *et al.*, 2006). Assessment of protein expression identified varied expression of common 'exosomal markers'; however, also showed the presence of 'negative markers' that should be absent in exosomes (Lötvall *et al.*, 2014). Collectively, the results presented in chapter 5 demonstrate the successful isolation and characterisation of small exosome-like EVs from a panel of UM cell lines.

These results are broadly consistent with those produced by Eldh *et al.,* and Ragusa *et al.,* in their research into UM exosomes (Eldh *et al.*, 2014; Ragusa *et al.*, 2015). Both employed UC for the isolation of small exosome-like EVs from biofluid samples collected from patients with UM. Ragusa *et al.,* demonstrated small exosome-like EVs with an average diameter of

100 nm, isolated from the vitreous humor of patients with PUM (Ragusa *et al.*, 2015). Eldh *et al.,* isolated small exosome-like EVs from the liver perfusate of patients with MUM, demonstrating a diameter of 50 nm when measured by TEM (Eldh *et al.*, 2014). Similar to the results presented herein, both authors also demonstrated 'cup-shaped' morphology by TEM and highlighted varied expression of 'canonical' exosome markers by flow cytometry (Eldh *et al.*, 2014; Ragusa *et al.*, 2015).

As this research demonstrates the ability to isolate small exosome-like EVs from cultured UM cells, functional studies could be undertaken with isolated UM EVs to understand their role in UM pathology. These are discussed in further detail later in this chapter.

Several cell types are known to 'take up' EVs, which can modulate mechanisms in the recipient cell that have previously been described to aid metastatic progression and education of the pre-metastatic niche. For instance, EVs have been shown to be taken up by endothelial cells, promoting angiogenesis and tumour vascularisation (Chiba *et al.*, 2018). EVs can be taken up by immune cells such as T-cells and macrophages including Kupffer cells (Costa-Silva *et al.*, 2015; Hoshino *et al.*, 2015; Barros *et al.*, 2018), causing modulation of the immune response. They can also be taken up by fibroblasts/resident stellate cells impacting fibrosis and desmoplasia (Costa-Silva *et al.*, 2015; Yang *et al.*, 2019). The impact UM EVs have on these different cell types could be investigated in future studies employing UM models. In particular, the role PUM derived EVs play in the education of the pre-metastatic niche and their promotion of fibrosis requires investigation. Following the demonstration of the fibrotic microenvironment of MUM in chapter three and the functional enrichment of hepatic fibrosis/HSC activation signalling in the UM secretome demonstrated in chapter 4, the impact the UM EVs have on quiescent HSCs could be investigated in relevant UM models.

EVs also represent possible biomarkers of disease (Halvaei *et al.*, 2018; Zhang *et al.*, 2019). EVs isolated with the methods in chapter five could be investigated for the presence of biomarkers of UM stage, such as the development of MUM in the liver. They could also be a marker of therapy effectiveness during the treatment of MUM. In order to represent non-invasive biomarkers in liquid biopsies, any potential protein, lipid or genetic biomarker revealed in the EVs of cultured UM cells would require validation in patient biofluids, such as plasma.

Bioinformatic analysis of the total content of EVs can also reveal functions and mechanisms not immediately apparent in univariate investigations. EVs are known to contain several types of bioactive molecules, such as proteins, lipids RNAs and DNA (Jeppesen *et al.*, 2019). Research into the microRNA content of UM small exosome-like EVs (Eldh *et al.*, 2014; Ragusa *et al.*, 2015) has begun yet there are currently no published studies of their total protein content.

Chapter six investigates the protein content of EVs isolated from UM cell lines using nano-liquid chromatography tandem mass spectrometry for in-depth proteomic analysis. The generated proteome underwent bioinformatic analyses using a range of tools to define biological functions and signalling pathways associated with the dataset as undertaken in Chapter four. Similarities and differences between the two proteomic datasets were also investigated. I hypothesised that UM EVs contain proteins associated with UM growth and metastatic progression, and that these proteins may differ between PUM and MUM as well as UM harbouring different initiating mutations (*GNAQ vs GNA11*).

Similar to the bioinformatic analysis of the total secretome, presented in chapter four, functional enrichment of UM EV proteome highlighted an association with proliferation, adhesion and migration functions as well as mTOR, GTPase, integrin, paxillin, agrin and ephrin signalling networks.

The results presented are consistent with those of Eldh *et al.,* and Surman *et al.,*(Eldh *et al.*, 2014; Surman *et al.*, 2019). Eldh *et al.,* demonstrated the association of focal adhesion signalling with a cluster of mircoRNAs present in small exosome-like EVs isolated from the liver perfusate of patients with hepatic MUM and a cultured melanoma cell line. These microRNAs differentiated between the EVs from patients with MUM (plus one melanoma cell line) and EVs from unrelated cell lines, such as mast cells and other cancers (Eldh *et al.*, 2014). Surman *et al.,* investigated larger EVs considered ectosomes. Functional enrichment of their proteome highlighted an association with focal adhesion, translation initiation and GTPase signalling (Surman *et al.*, 2019). While the research methodologies differed to those presented herein, the similarities between the findings of these studies further highlight an important role of UM EVs in the regulation of cellular adhesion. These functions, the associated signalling pathways and the proteins or microRNAs involved require further investigation.

Functional enrichment identified pathways and functions associated with proliferation, adhesion and migration. These were predicted by the software to be downregulated in EVs isolated from cell lines of MUM as compared with EVs isolated from cell lines derived from PUM. This suggest that EVs secreted by PUM cells would promote metastasis more so than those from MUM cells.

It is important to consider however, that cells residing in 2D culture may produce EVs with a differing protein content when compared with that produced by cells in a more representative microenvironment. As more representative in vitro models of UM are developed, such as multicellular 3D spheroids, further investigation of EVs and their contents will be necessary for comparison with the data generated herein.

The grouping of cell lines also adds limitations to the conclusions drawn from the GNAQ-GNA11 comparison due to numerical imbalance in such a low samples number (2 vs 4). Due to this limited number of samples, there is limited genetic variability between samples. Increased numbers could allow comparisons between biologically relevant differences, such as EIF1AX mutant vs wild-type, SF3B1 mutant vs wild-type, BAP1 mutant vs wild-type etc. With the limited number of UM cell lines that appropriately represent the genetic landscape of UM (Amirouchene-Angelozzi *et al.*, 2014), a way to overcome this would be to culture primary tumour derived tissue as described by Angi *et al.,* (Angi *et al.*, 2016) and to isolate UM EVs as described in chapter 5 of this thesis. Chapter 4 compares the secretome of primary UM cells against that of cultured primary NCMs. Yet similar comparison was not possible in chapter 6 due to a lack of an NCM cell line. Primary NCM are slow growing with presumed limited EV production compared with cancer cell lines (Whiteside, 2016). EVs could be isolated from larger cultures of pooled NCM samples, and future studies could compare these to EVs isolated from PUM cultures grown as described by (Angi *et al.*, 2016).

Future larger studies hoping to demonstrate differences in these pathways between different UM genotypes should include greater numbers of different UM cell lines or large numbers of cultures from primary samples. Statistical analyses against an appropriate control could also improve the conclusions drawn from this research; EVs isolated from

several large NCM cultures from multiple donors could be pooled to generate enough material for this purpose.

Although this study examined for the first time the protein content of UM EVs, it has been well documented that EVs contain several different types of actively and selectively enriched biologically active molecules, such as mRNA, microRNA, lncRNA, double stranded DNA and lipids (Jeppesen *et al.*, 2019); all of which could impact downstream biological processes. By integrating information about all of these molecules secreted in EVs from UM cell lines a more comprehensive picture of their functional role in the disease may be obtained.

7.2. Consistent themes throughout the thesis

Throughout this thesis, the mTOR signalling axis was highlighted as an important pathway governed by the UM secretome and by UM EVs. MTORC1 signalling is known to govern amino acid metabolism, nucleotide metabolism, fatty acid and lipid metabolism, and glucose metabolism (Saxton and Sabatini, 2017; Mossmann, Park and Hall, 2018). The S6K and eIF4E signalling networks were also highlighted in the two datasets, both are downstream effectors of the MTORC1 pathway and known to increase the translation of metabolic enzymes and metabolism-related transcription factors (Saxton and Sabatini, 2017). MTORC2 signalling is known to impact cytoskeletal remodelling through PKCα and GTPases such as Rho, Rac and cdc42(Huang and Zhou, 2011). Cytoskeletal remodelling, GTPase signalling and multiple adhesion networks were frequently associated with the UM secretome and UM EVs. This suggests an integral role of MTORC2 signalling in UM through extracellular protein and EV transfer. MTORC2 is also known to modulate cell survival and proliferation through AKT and SGK1 (Sarbassov *et al.*, 2005; García-Martínez and Alessi, 2008). MTORC2 and AKT have both been shown to co-localize with newly assembled focal

adhesion complexes including the protein paxillin (Sen *et al.*, 2014). Both adhesion and paxillin signalling were highlighted in this thesis as associated with UM EVs and the UM secretome. Alongside these functions, both MTORC1 and MTORC2 were shown to impact cellular adhesion pathways, with MTORC1 functioning through S6K1 and 4E-BP1 pathways and MTORC2 through an undefined AKT-independent pathway (L. Chen *et al.*, 2015). These functional mechanisms are all highlighted in chapters 4 and 6 and have been linked with the progression of other cancers in the literature. These pathways have also been linked with the stimulation of fibrosis (Hillel and Gelbard, 2015; Lawrence and Nho, 2018; Woodcock *et al.*, 2019) and the activation of cancer associated fibroblasts (Conciatori *et al.*, 2018). Chapter three demonstrated hepatic fibrosis and the activation of HSCs in MUM and chapter 4 highlighted an association of hepatic fibrosis and HSCs activation with the proteins in the PUM secretome.

The results presented throughout this thesis correspond with those previously described in the UM literature. mTOR signalling has previously been shown to be important in UM, regulating cell viability in vitro and tumour growth in vivo (Ho *et al.*, 2012; Amirouchene-Angelozzi *et al.*, 2014; Carita *et al.*, 2016), while Feng *et al.,* demonstrated Rho and Rac GTPase signalling and their activation of YAP, downstream of the UM oncogene *GNAQ* (Feng *et al.*, 2014). Differential integrin expression has been demonstrated in invasive and non-invasive UM (Woodward *et al.*, 2005) and α6β1 has previously been suggested as a prognostic factor in UM (Elshaw *et al.*, 2001). The role of paxillin in UM was previously discussed at the 2014 annual ARVO meeting (Morales *et al.*, 2014) where the authors demonstrated significantly reduced cellular migration and proliferation through targeted inhibition of paxillin. Vukoja *et al.,* demonstrated that nuclear expression of the ephrin receptor EphA2 in PUM is associated with an increased rate of metastatic progression

Collectively, the prevalence of these pathways throughout this thesis and their previously reported roles in UM suggest an important role of the UM secretome and UM EVs in the pathological progression of UM. The findings presented herein can contribute considerably to the development and evaluation of further studies in UM. In order to determine if the signalling pathways highlighted by functional enrichment are active in UM and if they are stimulated by protein or EV transfer, functional studies that assess the downstream effects of these pathways could be employed in UM models, such as those previously described (Valyi-Nagy *et al.*, 2012; Angi *et al.*, 2016; Burnier *et al.*, 2019).

7.3. Future work

Dose dependent studies could employ UM EVs or the UM secretome to investigate their role in promoting cell proliferation, migration, adhesion or HSC activation through mTOR, GTPase, integrin, paxillin, ephrin and agrin signalling pathways. UM models could be challenged with increasing numbers of UM EVs or increasing quantities of the UM secretome, and downstream measures of these pathways assessed.

Signalling through MTORC1 could be assessed as described by Li *et al.,* who investigated its role in gastric cancer in response to dysregulated the long non-coding RNA urothelial carcinoma-associated 1 lncRNA-UCA1 (C. Li *et al.*, 2017). They employed western blotting and optical densitometry to assess fold change expression of downstream mTORC1 targets in response to different conditions.

The involvement of MTORC2 could be assessed with methods performed by Joly *et al.,* in their study in breast cancer (Joly *et al.*, 2016), where they used *in vitro* culture and *in vivo* xenograft models alongside IHC and western blotting to assess expression levels of key MTORC2 pathway components.

The activity of GTPases could be assessed similar to how Yan *et al.,* investigated its activity in endothelial cells in response to heparin sulphate and CXCL8 treatment (Yan *et al.*, 2016). The authors used western blotting, and a Rho GTPase activity assay and imaging of downstream morphological effects to assess GTPase activity.

Integrin activation during cell adhesion could be assessed with the methods used by (Du *et al.*, 2011). The authors used a combination of immunochemical analysis, imaging techniques and western blotting to assess integrin involvement in stem cell differentiation.

The involvement of paxillin signalling in UM could be assessed with the methods employed by German *et al.,* in their study into endothelial migration and angiogenesis in response to neuropilin-2 expression (German *et al.*, 2014). They used siRNA knockdown models alongside western blotting, immunocytochemistry and functional assays to assess paxillin levels and activity.

The ephrin signalling axis could be assessed in UM with the methods described by Youngblood *et al.* The authors employed micro array analysis and expression profiling of patients with breast cancer (Youngblood *et al.*, 2016). They assessed ephrin's functional role through siRNA knockdown and IHC, western blot, proliferation assays and spheroid size measures of *in vitro* cell lines, and tumour volume measures in mouse xenograft models.

Agrin involvement in YAP translocation and activity was investigated in hepatocellular carcinoma by Chakraborty *et al.,*(Chakraborty *et al.*, 2017). They employed siRNA and shRNA knockdown models with immunofluorescence imaging, IHC and western blotting, as

well as ECM stiffness, collagen gel contraction assays and transwell migration assays to assess the downstream effects of agrin depleted models.

The ability of UM EVs or the UM secretome to activate HSCs could be assessed *in vitro.* Human HSCs could be cultured according to methods described by Xu *et al.,*(Xu *et al.*, 2005), and their activation assessed with the methods discussed in Chapter 3. These methods could also be used in conjunction with 3D and organoid models of hepatic fibrosis (Mazza, Al-Akkad and Rombouts, 2017).

The prospect of these pathways being stimulated through local intercellular transfer of secreted biomolecules — as discussed in Chapter 4 — offers potential drug targets that could impact clinical pathways. Furthermore, the promotion of these intercellular signalling pathways through EV secretion — as demonstrated in Chapter 6 — suggests the possibility of more distal signalling with cells and tissues elsewhere in the body. This is because the packaging of biologically active materials into EVs prolongs their stability in the bloodstream (Akuma, Okagu and Udenigwe, 2019).

It should be noted that the presence of these proteins in UM EVs and the UM secretome may not mean they actively contribute to the functionally enriched pathways associated with their presence. It could simply mean that the proteins associated with those pathways are present in the given proteome. This could be true if the proteins overlapping with the given pathway are those downstream of the pathway rather than those stimulating it. In the context of this research, the HSC activation pathway — associated with the secretome in Chapter 4 — mainly overlapped the dataset through proteins produced by the pathway, rather than ligands stimulating it. The given signalling pathway may be active in the UM cells and the downstream products sequestered in EVs or secreted due to overproduction.

These proteins may not confer any relevant activity through horizontal transfer. Equally, this can be the case for EVs which contain functionally active proteins or proteins which may be able to stimulate a given pathway. EV uptake mechanisms can involve endosomal processing which may lead to lysosomal degradation of any protein transferred via EVs (McKelvey *et al.*, 2015), which would render their activity inert.

This thesis considers the proteome of UM EVs and the UM secretome; however, both of these sample types contain several other biologically active substances such as nucleic acids, lipids and metabolites, each of which can influence a recipient cells behaviour (Zhang *et al.*, 2019). Future research could employ the methods for UM secretome collection — described by Angi *et al.,*— and UM EV isolation — described in Chapter 5 — to further characterise the transcriptome, lipidome and metabolome of UM EVs, as previously described by Turchinovic *et al.,* Haraszti *et al.,* and Fellows *et al.,* respectively (Haraszti *et al.*, 2016; Fellows *et al.*, 2018; Turchinovich, Drapkina and Tonevitsky, 2019).

There have only been a limited number of previous studies investigating the role of small exosome-like EVs in UM, yet these have focused their research on UM EV micro-RNAs. Eldh *et al.,* previously described the microRNA content of small exosome-like EVs isolated directly from the liver circulation of patients with MUM (Eldh *et al.*, 2014). The authors demonstrated that a cluster of six microRNAs capable of differentiating the UM patient samples from cultured cell lines of other cancer types. Similar to the results herein, functional enrichment of these microRNAs showed association with focal adhesion signalling and mTOR signalling. They also demonstrated the presence of microRNA linked with TGF-β signalling (Eldh *et al.*, 2014). The TGF-β protein in a known regulator of cell morphology, growth and differentiation (Edlund *et al.*, 2002) and its role in hepatic fibrosis

has been extensively documented (Gressner *et al.*, 2002). These processes are stimulated through Rho GTPases signalling, including RhoA and Cdc42.

Ragusa *et al.,* examined the microRNA content of the vitreous humour of UM patients (Ragusa *et al.*, 2015), identifying 94 localised small microRNAs. While the majority of the identified microRNAs were thought to primarily function in the development of the eye, the microRNA mir146a is thought to have a role in angiogenesis and neovascularisation within the eye, and regulation of ECM deposition. Mir146a was expressed more highly in the vitreous humour of UM patients compared with other pathologies.

While the results presented in Chapters 3,4 and 6 all demonstrate a common theme suggesting the modulation of ECM and the promotion of related pathways. The ability to conflate the respective conclusion limited due to the different UM models employed. Each investigates biological processes in UM; Chapter 3 studies the activation of resident stellate cells in the liver and their promotion of MUM associated fibrosis, Chapter 4 enzymatically disaggregates primary UM tumours and grows them short-term in 2D culture for analysis of their protein secretome, while chapters 5 and 6 culture established UM cell lines for the isolation of small exosome-like EVs. While these all represent UM and have their own benefits and flaws, the cross-chapter comparison of the results and the conflation of conclusion derived drawn may be inappropriate. Future studies should be performed in one comparable *in vitro* model system that could then be validated *in vivo*.

7.4. Conclusions

This thesis provides statistically relevant rational in chapters 4 and 6 for the investigation of multiple signalling pathways in UM and their response to secreted UM proteins or EVs. The primary implications of these findings are that UM cells secrete proteins and EVs associated

with adhesion, cytoskeletal remodelling and migration. These functions may be governed by specific signalling networks associated with the proteins released. The molecular functions and signalling pathways highlighted in this research have been shown to contribute to tumour malignancy and metastatic progression in other cancers. These pathways have also been linked in the literature with the pathological progression of fibrosis through the activation of resident HSCs, a feature highlighted in the liver of patients with MUM in chapter 3. Hepatic fibrosis and HSC activation was also the pathway most associated with the UM secretome in chapter 4. Collectively, these results highlight a possible role of these molecular functions and signalling pathways in UM progression and metastasis, not only through autocrine promotion of cellular proliferation and migration but through advantageous communication with resident stromal cells in the metastatic niche. While the pathways highlighted in this thesis require functional validation in UM models, their modulation through EV transfer represents an unexplored therapeutic target. These pathways could be directly targeted through chemotherapeutic or immunotherapeutic inhibition and the release or uptake of EVs could also be targeted in conjunction with current therapeutic strategies.

REFERENCES

Abbott, A. (2003) 'Cell culture: Biology's new dimension', *Nature*, 424(8), pp. 870–872.

Abdel-Rahman, M. H., Pilarski, R., Cebulla, C. M., Massengill, J. B., Christopher, B. N., Boru, G., Hovland, P. and Davidorf, F. H. (2011) 'Germline BAP1 mutation predisposes to uveal melanoma, lung adenocarcinoma, meningioma, and other cancers', *Journal of Medical Genetics*, 48(12), pp. 856–859.

Acerbi, I., Cassereau, L., Dean, I., Shi, Q., Au, A., Park, C., Chen, Y. Y., Liphardt, J., Hwang, E. S. and Weaver, V. M. (2015) 'Human breast cancer invasion and aggression correlates with ECM stiffening and immune cell infiltration', *Integrative Biology (United Kingdom)*. Royal Society of Chemistry, 7(10), pp. 1120–1134.

Adachi, S. (2017) 'Rigid geometry solves "curse of dimensionality" effects in clustering methods: An application to omics data.', *PloS one*, 12(6), p. e0179180.

Affo, S., Yu, L.-X. and Schwabe, R. F. (2017) 'The Role of Cancer-Associated Fibroblasts and Fibrosis in Liver Cancer.', *Annual review of pathology*, 12, pp. 153–186.

Ah-Fat, F. G. and Damato, B. E. (1998) 'Delays in the diagnosis of uveal melanoma and effect on treatment', *Eye*. Royal College of Ophthalmologists, 12(5), pp. 781–782.

Ahmed, K. A. and Xiang, J. (2011) 'Mechanisms of cellular communication through intercellular protein transfer.', *Journal of cellular and molecular medicine*, 15(7), pp. 1458–73.

Akuma, P., Okagu, O. D. and Udenigwe, C. C. (2019) 'Naturally Occurring Exosome Vesicles as Potential Delivery Vehicle for Bioactive Compounds', *Frontiers in Sustainable Food Systems*, 3.

Amirouchene-Angelozzi, N., Nemati, F., Gentien, D., Nicolas, A., Dumont, A., Carita, G., Camonis, J., Desjardins, L., Cassoux, N., Piperno-Neumann, S., Mariani, P., Sastre, X., Decaudin, D. and Roman-Roman, S. (2014) 'Establishment of novel cell lines recapitulating the genetic landscape of uveal melanoma and preclinical validation of mTOR as a

therapeutic target', *Molecular Oncology*. John Wiley and Sons Ltd, 8(8), pp. 1508–1520.

Amirouchene-Angelozzi, N., Frisch-Dit-Leitz, E., Carita, G., Dahmani, A., Raymondie, C., Liot, G., Gentien, D., Némati, F., Decaudin, D., Roman-Roman, S. and Schoumacher, M. (2016) 'The mTOR inhibitor Everolimus synergizes with the PI3K inhibitor GDC0941 to enhance anti-tumor efficacy in uveal melanoma.', *Oncotarget*, 7(17), pp. 23633–46.

Angi, M., Damato, B., Kalirai, H., Dodson, A., Taktak, A. and Coupland, S. E. (2011) 'Immunohistochemical assessment of mitotic count in uveal melanoma.', *Acta ophthalmologica*, 89(2), pp. e155-60.

Angi, M., Kalirai, H., Prendergast, S., Simpson, D., Hammond, D. E., Madigan, M. C., Beynon, R. J. and Coupland, S. E. (2016) 'In-depth proteomic profiling of the uveal melanoma secretome', *Oncotarget*, 7(31).

Antonyak, M. A. and Cerione, R. A. (2015) 'Emerging picture of the distinct traits and functions of microvesicles and exosomes', *Proceedings of the National Academy of Sciences of the United States of America*. National Academy of Sciences, pp. 3589–3590.

Apte, R. S., Niederkorn, J. Y., Mayhew, E. and Alizadeh, H. (2001) 'Angiostatin produced by certain primary uveal melanoma cell lines impedes the development of liver metastases.', *Archives of ophthalmology (Chicago, Ill. : 1960)*, 119(12), pp. 1805–9.

Artinian, N., Cloninger, C., Holmes, B., Benavides-Serrato, A., Bashir, T. and Gera, J. (2015) 'Phosphorylation of the Hippo Pathway Component AMOTL2 by the mTORC2 Kinase Promotes YAP Signaling, Resulting in Enhanced Glioblastoma Growth and Invasiveness.', *The Journal of biological chemistry*, 290(32), pp. 19387–401.

Ashburner, M., Ball, C. A., Blake, J. A., Botstein, D., Butler, H., Cherry, J. M., Davis, A. P., Dolinski, K., Dwight, S. S., Eppig, J. T., Harris, M. A., Hill, D. P., Issel-Tarver, L., Kasarskis, A., Lewis, S., Matese, J. C., Richardson, J. E., Ringwald, M., Rubin, G. M. and Sherlock, G. (2000) 'Gene ontology: Tool for the unification of biology', *Nature Genetics*, pp. 25–29.

Atay, S. and Godwin, A. K. (2014) 'Tumor-derived exosomes: A message delivery system for

tumor progression.', *Communicative & integrative biology*, 7(1), p. e28231.

Atkin-Smith, G. K., Tixeira, R., Paone, S., Mathivanan, S., Collins, C., Liem, M., Goodall, K. J., Ravichandran, K. S., Hulett, M. D. and Poon, I. K. H. (2015) 'A novel mechanism of generating extracellular vesicles during apoptosis via a beads-on-a-string membrane structure.', *Nature communications*, 6, p. 7439.

Atkin-Smith, G. K., Paone, S., Zanker, D. J., Duan, M., Phan, T. K., Chen, W., Hulett, M. D. and Poon, I. K. H. (2017) 'Isolation of cell type-specific apoptotic bodies by fluorescence-activated cell sorting.', *Scientific reports*, 7, p. 39846.

Augsburger, J. J., Corrêa, Z. M. and Shaikh, A. H. (2009) 'Effectiveness of Treatments for Metastatic Uveal Melanoma', *American Journal of Ophthalmology*, 148(1), pp. 119–127.

Awad, R. M., De Vlaeminck, Y., Maebe, J., Goyvaerts, C. and Breckpot, K. (2018) 'Turn Back the TIMe: Targeting Tumor Infiltrating Myeloid Cells to Revert Cancer Progression.', *Frontiers in immunology*, 9, p. 1977.

Baixauli, F., López-Otín, C. and Mittelbrunn, M. (2014) 'Exosomes and autophagy: Coordinated mechanisms for the maintenance of cellular fitness', *Frontiers in Immunology*, 5(AUG).

Barak, V., Goike, H., Panaretakis, K. W. and Einarsson, R. (2004) 'Clinical utility of cytokeratins as tumor markers', *Clinical Biochemistry*, pp. 529–540.

Barczyk, M., Carracedo, S. and Gullberg, D. (2010) 'Integrins', *Cell and Tissue Research*, 339(1), pp. 269–280.

Barros, F. M., Carneiro, F., Machado, J. C. and Melo, S. A. (2018) 'Exosomes and immune response in cancer: Friends or foes?', *Frontiers in Immunology*. Frontiers Media S.A.

Bendtsen, J. D., Jensen, L. J., Blom, N., Von Heijne, G. and Brunak, S. (2004) 'Feature-based prediction of non-classical and leaderless protein secretion.', *Protein engineering, design & selection : PEDS*, 17(4), pp. 349–56.

Bendtsen, J. D., Nielsen, H., von Heijne, G. and Brunak, S. (2004) 'Improved prediction of

signal peptides: SignalP 3.0.', *Journal of molecular biology*, 340(4), pp. 783–95.

Bernard, S. and Eilers, M. (2006) 'Control of cell proliferation and growth by Myc proteins', *Results and Problems in Cell Differentiation*, 42, pp. 329–342.

Bianchi-Smiraglia, A., Bagati, A., Fink, E. E., Moparthy, S., Wawrzyniak, J. A., Marvin, E. K., Battaglia, S., Jowdy, P., Kolesnikova, M., Foley, C. E., Berman, A. E., Kozlova, N. I., Lipchick, B. C., Paul-Rosner, L. M., Bshara, W., Ackroyd, J. J., Shewach, D. S. and Nikiforov, M. A. (2017) 'Microphthalmia-associated transcription factor suppresses invasion by reducing intracellular GTP pools.', *Oncogene*, 36(1), pp. 84–96.

Bishop, A. L. and Hall, A. (2000) 'Rho GTPases and their effector proteins', *Biochemical Journal*, pp. 241–255.

Bissig, C. and Gruenberg, J. (2013) 'Lipid sorting and multivesicular endosome biogenesis.', *Cold Spring Harbor perspectives in biology*, 5(10), p. a016816.

Blanc, L. and Vidal, M. (2018) 'New insights into the function of Rab GTPases in the context of exosomal secretion.', *Small GTPases*, 9(1–2), pp. 95–106.

Bobrie, A., Colombo, M., Krumeich, S., Raposo, G. and Théry, C. (2012) 'Diverse subpopulations of vesicles secreted by different intracellular mechanisms are present in exosome preparations obtained by differential ultracentrifugation', *Journal of Extracellular Vesicles*. Co-Action Publishing, 1(1).

Böing, A. N., van der Pol, E., Grootemaat, A. E., Coumans, F. A. W., Sturk, A. and Nieuwland, R. (2014) 'Single-step isolation of extracellular vesicles by size-exclusion chromatography', *Journal of Extracellular Vesicles*. Co-Action Publishing, 3(1).

Bolm, L., Cigolla, S., Wittel, U. A., Hopt, U. T., Keck, T., Rades, D., Bronsert, P. and Wellner, U. F. (2017) 'The Role of Fibroblasts in Pancreatic Cancer: Extracellular Matrix Versus Paracrine Factors', *Translational Oncology*. Neoplasia Press, Inc., 10(4), pp. 578–588.

Borthwick, N. J., Thombs, J., Polak, M., Gabriel, F. G., Hungerford, J. L., Damato, B., Rennie, I. G., Jager, M. J. and Cree, I. A. (2011) 'The biology of micrometastases from uveal

melanoma.', *Journal of clinical pathology*, 64(8), pp. 666–71.

Boyle, S. T. and Samuel, M. S. (2016) 'Mechano-reciprocity is maintained between physiological boundaries by tuning signal flux through the Rho-associated protein kinase', *Small GTPases*. Taylor and Francis Inc., pp. 139–146.

Breitkopf, K., Godoy, P., Ciuclan, L., Singer, M. V and Dooley, S. (2006) 'TGF-beta/Smad signaling in the injured liver.', *Zeitschrift fur Gastroenterologie*, 44(1), pp. 57–66.

Brenner, D. A., Kisseleva, T., Scholten, D., Paik, Y. H., Iwaisako, K., Inokuchi, S., Schnabl, B., Seki, E., De Minicis, S., Oesterreicher, C. and Taura, K. (2012) 'Origin of myofibroblasts in liver fibrosis', *Fibrogenesis & Tissue Repair*, 5(S1), p. S17.

Breuza, L., Poux, S., Estreicher, A., Famiglietti, M. L., Magrane, M., Tognolli, M., Bridge, A., Baratin, D. and Redaschi, N. (2016) 'The UniProtKB guide to the human proteome', *Database*. Oxford University Press, 2016.

Brodt, P. (2016) 'Role of the Microenvironment in Liver Metastasis: From Pre- to Prometastatic Niches.', *Clinical cancer research : an official journal of the American Association for Cancer Research*, 22(24), pp. 5971–5982.

Brown, M. C. and Turner, C. E. (2004) 'Paxillin: Adapting to change', *Physiological Reviews*, pp. 1315–1339.

Brożyna, A. A., Jóźwicki, W., Roszkowski, K., Filipiak, J. and Slominski, A. T. (2016) 'Melanin content in melanoma metastases affects the outcome of radiotherapy.', *Oncotarget*, 7(14), pp. 17844–53.

Brzozowski, J. S., Jankowski, H., Bond, D. R., McCague, S. B., Munro, B. R., Predebon, M. J., Scarlett, C. J., Skelding, K. A. and Weidenhofer, J. (2018) 'Lipidomic profiling of extracellular vesicles derived from prostate and prostate cancer cell lines', *Lipids in Health and Disease*, 17(1), p. 211.

Burnier, J. V., Mastromonaco, C., Lasiste, J. M. and Burnier, M. N. (2019) 'Animal Models in Uveal Melanoma', in *Clinical Ophthalmic Oncology*. Springer International Publishing, pp.

135–154.

Buschow, S. I., Liefhebber, J. M. P., Wubbolts, R. and Stoorvogel, W. (2005) 'Exosomes contain ubiquitinated proteins', *Blood Cells, Molecules, and Diseases*, 35(3), pp. 398–403.

Bustelo, X. R. (2010) 'A transcriptional cross-talk between RhoA and c-Myc inhibits the RhoA/Rock-dependent cytoskeleton.', *Small GTPases*, 1(1), pp. 69–74.

Butcher, D. T., Alliston, T. and Weaver, V. M. (2009) 'A tense situation: Forcing tumour progression', *Nature Reviews Cancer*, pp. 108–122.

Caines, R., Eleuteri, A., Kalirai, H., Fisher, A. C., Heimann, H., Damato, B. E., Coupland, S. E. and Taktak, A. F. G. (2015) 'Cluster analysis of multiplex ligation-dependent probe amplification data in choroidal melanoma', *Molecular Vision*. Molecular Vision, 21, pp. 1–11.

Cam, H., Easton, J. B., High, A. and Houghton, P. J. (2010) 'mTORC1 signaling under hypoxic conditions is controlled by atm-dependent phosphorylation of HIF-1α', *Molecular Cell*, 40(4), pp. 509–520.

Campos, H., Blijlevens, E., McNamara, J. R., Ordovas, J. M., Posner, B. M., Wilson, P. W. F., Castelli, W. P. and Schaefer, E. J. (1992) 'LDL particle size distribution: Results from the Framingham Offspring Study', *Arteriosclerosis and Thrombosis*, 12(12), pp. 1410–1419.

Camussi, G., Deregibus, M. C., Bruno, S., Cantaluppi, V. and Biancone, L. (2010) 'Exosomes/microvesicles as a mechanism of cell-to-cell communication', *Kidney International*. Nature Publishing Group, pp. 838–848.

Canning, C. R. and Hungerford, J. (1988) 'Familial uveal melanoma.', *British Journal of Ophthalmology*, 72(4), pp. 241–243.

Carita, G., Frisch-Dit-Leitz, E., Dahmani, A., Raymondie, C., Cassoux, N., Piperno-Neumann, S., Némati, F., Laurent, C., De Koning, L., Halilovic, E., Jeay, S., Wylie, A., Emery, C., Roman-Roman, S., Schoumacher, M. and Decaudin, D. (2016) 'Dual inhibition of protein kinase C and p53-MDM2 or PKC and mTORC1 are novel efficient therapeutic approaches for uveal

melanoma', *Oncotarget*. Impact Journals LLC, 7(23), pp. 33542–33556.

Carmeliet, P. (2005) 'VEGF as a key mediator of angiogenesis in cancer.', *Oncology*, 69 Suppl 3, pp. 4–10.

Carubia, J. M., Yu, R. K., Macala, L. J., Kirkwood, J. M. and Varga, J. M. (1984) 'Gangliosides of normal and neoplastic human melanocytes.', *Biochemical and biophysical research communications*, 120(2), pp. 500–4.

Carvajal, R. D., Schwartz, G. K., Tezel, T., Marr, B., Francis, J. H. and Nathan, P. D. (2017) 'Metastatic disease from uveal melanoma: treatment options and future prospects.', *The British journal of ophthalmology*, 101(1), pp. 38–44.

Cassoux, N., Cayette, S., Plancher, C., Lumbroso-Le Rouic, L., Levy-Gabriel, C., Asselain, B., Sastre, X., Couturier, J., Arrufat, S., Piperno-Neumann, S., Dendale, R., Lehoang, P. and Desjardins, L. (2013) 'Choroidal Melanoma: Does endoresection prevent neovascular glaucoma in patient treated with proton beam irradiation?', *Retina*, 33(7), pp. 1441–1447.

Cassoux, N., Rodrigues, M. J., Plancher, C., Asselain, B., Levy-Gabriel, C., Lumbroso-Le Rouic, L., Piperno-Neumann, S., Dendale, R., Sastre, X., Desjardins, L. and Couturier, J. (2014) 'Genome-wide profiling is a clinically relevant and affordable prognostic test in posterior uveal melanoma', *British Journal of Ophthalmology*. BMJ Publishing Group, 98(6), pp. 769–774.

Cecconi, D., Carbonare, L. D., Mori, A., Cheri, S., Deiana, M., Brandi, J., Degaetano, V., Masiero, V., Innamorati, G., Mottes, M., Malerba, G. and Valenti, M. T. (2018) 'An integrated approach identifies new oncotargets in melanoma', *Oncotarget*. Impact Journals LLC, 9(14), pp. 11489–11502.

Chakraborty, S., Lakshmanan, M., Swa, H. L. F., Chen, J., Zhang, X., Ong, Y. S., Loo, L. S., Aklncllar, S. C., Gunaratne, J., Tergaonkar, V., Hui, K. M. and Hong, W. (2015) 'An oncogenic role of Agrin in regulating focal adhesion integrity in hepatocellular carcinoma', *Nature Communications*. Nature Publishing Group, 6.

Chakraborty, S., Njah, K., Pobbati, A. V., Lim, Y. B., Raju, A., Lakshmanan, M., Tergaonkar, V., Lim, C. T. and Hong, W. (2017) 'Agrin as a Mechanotransduction Signal Regulating YAP through the Hippo Pathway', *Cell Reports*. Elsevier B.V., 18(10), pp. 2464–2479.

Chang, M. Y. and McCannel, T. A. (2013) 'Local treatment failure after globe-conserving therapy for choroidal melanoma.', *The British journal of ophthalmology*, 97(7), pp. 804–11.

Chang, T.-C., Yu, D., Lee, Y.-S., Wentzel, E. A., Arking, D. E., West, K. M., Dang, C. V, Thomas-Tikhonenko, A. and Mendell, J. T. (2008) 'Widespread microRNA repression by Myc contributes to tumorigenesis.', *Nature genetics*, 40(1), pp. 43–50.

Chen, B. W., Chen, W., Liang, H., Liu, H., Liang, C., Zhi, X., Hu, L.-Q., Yu, X.-Z., Wei, T., Ma, T., Xue, F., Zheng, L., Zhao, B., Feng, X.-H., Bai, X.-L. and Liang, T.-B. (2015) 'Inhibition of mTORC2 Induces Cell-Cycle Arrest and Enhances the Cytotoxicity of Doxorubicin by Suppressing MDR1 Expression in HCC Cells.', *Molecular cancer therapeutics*, 14(8), pp. 1805–15.

Chen, G.-C., Turano, B., Ruest, P. J., Hagel, M., Settleman, J. and Thomas, S. M. (2005) 'Regulation of Rho and Rac Signaling to the Actin Cytoskeleton by Paxillin during Drosophila Development', *Molecular and Cellular Biology*. American Society for Microbiology, 25(3), pp. 979–987.

Chen, H. B., Chen, L., Zhung, J. K., Chow, V. W., Wu, B. Q., Wang, Z. H., Cheng, S. B. and Chew, E. C. (2001) 'Expression of laminin in metastatic melanoma cell lines with different metastatic potential.', *Anticancer research*, 21(1A), pp. 505–508.

Chen, L., Xu, B., Liu, L., Liu, C., Luo, Y., Chen, X., Barzegar, M., Chung, J. and Huang, S. (2015) 'Both mTORC1 and mTORC2 are involved in the regulation of cell adhesion', *Oncotarget*. Impact Journals LLC, 6(9), pp. 7136–7150.

Cheng, P., Jiang, F. H., Zhao, L. M., Dai, Q., Yang, W. Y., Zhu, L. M., Wang, B. J., Xu, C., Bao, Y. J. and Zhang, Y. J. (2010) 'Human macrophage metalloelastase correlates with angiogenesis and prognosis of gastric carcinoma', *Digestive Diseases and Sciences*, 55(11), pp. 3138–

3146.

Cheng, Y., Dai, X., Yang, T., Zhang, N., Liu, Z. and Jiang, Y. (2019) 'Low Long Noncoding RNA Growth Arrest-Specific Transcript 5 Expression in the Exosomes of Lung Cancer Cells Promotes Tumor Angiogenesis', *Journal of Oncology*. Hindawi Limited, 2019.

Cheng, Y. and Schorey, J. S. (2016) 'Targeting soluble proteins to exosomes using a ubiquitin tag.', *Biotechnology and bioengineering*, 113(6), pp. 1315–24.

Cheruvanky, A., Zhou, H., Pisitkun, T., Kopp, J. B., Knepper, M. A., Yuen, P. S. T. and Star, R. A. (2007) 'Rapid isolation of urinary exosomal biomarkers using a nanomembrane ultrafiltration concentrator', *American Journal of Physiology - Renal Physiology*, 292(5).

Cheung, C. H. Y. and Juan, H.-F. (2017) 'Quantitative proteomics in lung cancer.', *Journal of biomedical science*, 24(1), p. 37.

Chiba, M., Kubota, S., Sato, K. and Monzen, S. (2018) 'Exosomes released from pancreatic cancer cells enhance angiogenic activities via dynamin-dependent endocytosis in endothelial cells in vitro', *Scientific Reports*. Nature Publishing Group, 8(1).

Chowdhury, R., Webber, J. P., Gurney, M., Mason, M. D., Tabi, Z. and Clayton, A. (2015) 'Cancer exosomes trigger mesenchymal stem cell differentiation into pro-angiogenic and pro-invasive myofibroblasts', *Oncotarget*. Impact Journals LLC, 6(2), pp. 715–731.

Christensen, M. V., Høgdall, C. K., Umsen, K. M. J. and Høgdall, E. V. S. (2018) 'Annexin A2 and cancer: A systematic review', *International Journal of Oncology*. Spandidos Publications, pp. 5–18.

Chua, V., Lapadula, D., Randolph, C., Benovic, J. L., Wedegaertner, P. B. and Aplin, A. E. (2017) 'Dysregulated GPCR Signaling and Therapeutic Options in Uveal Melanoma.', *Molecular cancer research : MCR*, 15(5), pp. 501–506.

Cizmar, P. and Yuana, Y. (2017) 'Detection and Characterization of Extracellular Vesicles by Transmission and Cryo-Transmission Electron Microscopy', *Methods in molecular biology (Clifton, N.J.)*, 1660, pp. 221–232.

Clarijs, R., van Dijk, M., Ruiter, D. J. and de Waal, R. M. W. (2005) 'Functional and morphologic analysis of the fluid-conducting meshwork in xenografted cutaneous and primary uveal melanoma.', *Investigative ophthalmology & visual science*, 46(9), pp. 3013–20.

Clark, D. J., Fondrie, W. E., Liao, Z., Hanson, P. I., Fulton, A., Mao, L. and Yang, A. J. (2015) 'Redefining the Breast Cancer Exosome Proteome by Tandem Mass Tag Quantitative Proteomics and Multivariate Cluster Analysis.', *Analytical chemistry*, 87(20), pp. 10462–9.

Clayton, A., Court, J., Navabi, H., Adams, M., Mason, M. D., Hobot, J. A., Newman, G. R. and Jasani, B. (2001) 'Analysis of antigen presenting cell derived exosomes, based on immuno-magnetic isolation and flow cytometry', *Journal of Immunological Methods*, 247(1–2), pp. 163–174.

Coday, M. P., Warner, M. A., Jahrling, K. V and Rubin, P. A. D. (2002) 'Acquired monocular vision: functional consequences from the patient's perspective.', *Ophthalmic plastic and reconstructive surgery*, 18(1), pp. 56–63.

Cohen, P. (2000) 'The regulation of protein function by multisite phosphorylation - A 25 year update', *Trends in Biochemical Sciences*, pp. 596–601.

Coleman, M. L., Sahai, E. A., Yeo, M., Bosch, M., Dewar, A. and Olson, M. F. (2001) 'Membrane blebbing during apoptosis results from caspase-mediated activation of ROCK I', *Nature Cell Biology*, 3(4), pp. 339–345.

Conciatori, F., Bazzichetto, C., Falcone, I., Pilotto, S., Bria, E., Cognetti, F., Milella, M. and Ciuffreda, L. (2018) 'Role of mTOR signaling in tumor microenvironment: An overview', *International Journal of Molecular Sciences*. MDPI AG.

Del Conde, I., Shrimpton, C. N., Thiagarajan, P. and López, J. A. (2005) 'Tissue-factor-bearing microvesicles arise from lipid rafts and fuse with activated platelets to initiate coagulation.', *Blood*, 106(5), pp. 1604–11.

Cools-Lartigue, J., Marshall, J. C., Caissie, A. L., Saraiva, V. S. and Burnier, M. N. (2005)

'Secretion of hepatocyte growth factor and vascular endothelial growth factor during uveal melanoma-monocyte in vitro interactions.', *Melanoma research*, 15(3), pp. 141–5.

Costa-Silva, B., Aiello, N. M., Ocean, A. J., Singh, S., Zhang, H., Thakur, B. K., Becker, A., Hoshino, A., Mark, M. T., Molina, H., Xiang, J., Zhang, T., Theilen, T.-M., García-Santos, G., Williams, C., Ararso, Y., Huang, Y., Rodrigues, G., Shen, T.-L., Labori, K. J., Lothe, I. M. B., Kure, E. H., Hernandez, J., Doussot, A., Ebbesen, S. H., Grandgenett, P. M., Hollingsworth, M. A., Jain, M., Mallya, K., Batra, S. K., Jarnagin, W. R., Schwartz, R. E., Matei, I., Peinado, H., Stanger, B. Z., Bromberg, J. and Lyden, D. (2015) 'Pancreatic cancer exosomes initiate pre-metastatic niche formation in the liver.', *Nature cell biology*, 17(6), pp. 816–26.

Cottrell, J. S. (2011) 'Protein identification using MS/MS data.', *Journal of proteomics*, 74(10), pp. 1842–51.

Coupland, S. E., Vorum, H., Mandal, N., Kalirai, H., Honoré, B., Urbak, S. F., Lake, S. L., Dopierala, J. and Damato, B. (2010) 'Proteomics of uveal melanomas suggests HSP-27 as a possible surrogate marker of chromosome 3 loss', *Investigative Ophthalmology and Visual Science*, 51(1), pp. 12–20.

Coupland, S. E., Lake, S. L., Zeschnigk, M. and Damato, B. E. (2013) 'Molecular pathology of uveal melanoma', *Eye*, 27(2), pp. 230–242.

Coupland, S. E., Lake, S. L. and Damato, B. (2014) 'Molecular pathology of uveal melanoma', in *Clinical Ophthalmic Oncology: Uveal Tumors*. Springer Berlin Heidelberg, pp. 125–136.

Cox, T. R. and Erler, J. T. (2011) 'Remodeling and homeostasis of the extracellular matrix: implications for fibrotic diseases and cancer.', *Disease models & mechanisms*, 4(2), pp. 165–78.

Cox, T. R. and Erler, J. T. (2014) 'Molecular pathways: Connecting fibrosis and solid tumor metastasis', *Clinical Cancer Research*. American Association for Cancer Research Inc., 20(14), pp. 3637–3643.

Crabb, J. W., Hu, B., Crabb, J. S., Triozzi, P., Saunthararajah, Y., Tubbs, R. and Singh, A. D.

(2015) ‘iTRAQ quantitative proteomic comparison of metastatic and non-metastatic uveal melanoma tumors’, *PLoS ONE*. Public Library of Science, 10(8).

Craig, R. and Beavis, R. C. (2004) ‘TANDEM: matching proteins with tandem mass spectra’, *Bioinformatics*, 20(9), pp. 1466–1467.

Crescitelli, R., Lässer, C., Szabó, T. G., Kittel, A., Eldh, M., Dianzani, I., Buzás, E. I. and Lötvall, J. (2013) ‘Distinct RNA profiles in subpopulations of extracellular vesicles: apoptotic bodies, microvesicles and exosomes.’, *Journal of extracellular vesicles*, 2.

Cruess, A. F., Augsburger, J. J., Shields, J. A., Donoso, L. A. and Amsel, J. (1984) ‘Visual Results Following Cobalt Plaque Radiotherapy for Posterior Uveal Melanomas’, *Ophthalmology*, 91(2), pp. 131–136.

Cummings, T. J. (2013) *Ophthalmic pathology : a concise guide*. Springer.

Dalla-Favera, R., Bregni, M., Erikson, J., Patterson, D., Gallo, R. C. and Croce, C. M. (1982) ‘Human c-myc onc gene is located on the region of chromosome 8 that is translocated in Burkitt lymphoma cells’, *Proceedings of the National Academy of Sciences of the United States of America*, 79(24 I), pp. 7824–7827.

Damato, B., Groenewald, C., McGalliard, J. and Wong, D. (1998) ‘Endoresection of choroidal melanoma.’, *The British journal of ophthalmology*, 82(3), pp. 213–8.

Damato, B. (2001) ‘Detection of uveal melanoma by optometrists in the United Kingdom.’, *Ophthalmic & physiological optics : the journal of the British College of Ophthalmic Opticians (Optometrists)*, 21(4), pp. 268–71.

Damato, B., Kacperek, A., Chopra, M., Campbell, I. R. and Errington, R. D. (2005) ‘Proton beam radiotherapy of choroidal melanoma: the Liverpool-Clatterbridge experience.’, *International journal of radiation oncology, biology, physics*, 62(5), pp. 1405–11.

Damato, B., Duke, C., Coupland, S. E., Hiscott, P., Smith, P. A., Campbell, I., Douglas, A. and Howard, P. (2007) ‘Cytogenetics of uveal melanoma: a 7-year clinical experience.’, *Ophthalmology*, 114(10), pp. 1925–31.

Damato, B., Dopierala, J., Klaasen, A., van Dijk, M., Sibbring, J. and Coupland, S. E. (2009) 'Multiplex ligation-dependent probe amplification of uveal melanoma: correlation with metastatic death.', *Investigative ophthalmology & visual science*, 50(7), pp. 3048–55.

Damato, B. (2010) 'Does ocular treatment of uveal melanoma influence survival?', *British journal of cancer*, 103(3), pp. 285–90.

Damato, B. (2012a) 'Progress in the management of patients with uveal melanoma. the 2012 Ashton Lecture', *Eye (Basingstoke)*. Nature Publishing Group, 26(9), pp. 1157–1172.

Damato, B. (2012b) 'Treatment selection for uveal melanoma.', *Developments in ophthalmology*, 49, pp. 16–26.

Damato, B. and Coupland, S. E. (2009) 'Translating uveal melanoma cytogenetics into clinical care', *Archives of Ophthalmology*, 127(4), pp. 423–429.

Damato, B. and Foulds, W. S. (1996) 'Indications for trans-scleral local resection of uveal melanoma.', *The British journal of ophthalmology*, pp. 1029–1030.

Dang, C. V. (2012) 'MYC on the path to cancer', *Cell*, pp. 22–35.

Daniels, K. J., Boldt, H. C., Martin, J. A., Gardner, L. M., Meyer, M. and Folberg, R. (1996) 'Expression of type VI collagen in uveal melanoma: its role in pattern formation and tumor progression.', *Laboratory investigation; a journal of technical methods and pathology*, 75(1), pp. 55–66.

Daniels, M. P. (2012) 'The role of agrin in synaptic development, plasticity and signaling in the central nervous system', in *Neurochemistry International*, pp. 848–853.

Decaudin, D., El Botty, R., Diallo, B., Massonnet, G., Fleury, J., Naguez, A., Raymondie, C., Davies, E., Smith, A., Wilson, J., Howes, C., Smith, P. D., Cassoux, N., Piperno-Neumann, S., Roman-Roman, S. and Némati, F. (2018) 'Selumetinib-based therapy in uveal melanoma patient-derived xenografts.', *Oncotarget*, 9(31), pp. 21674–21686.

Deparis, S. W., Taktak, A., Eleuteri, A., Enanoria, W., Heimann, H., Coupland, S. E. and Damato, B. (2016) 'External validation of the liverpool uveal melanoma prognosticator

online', *Investigative Ophthalmology and Visual Science*. Association for Research in Vision and Ophthalmology Inc., 57(14), pp. 6116–6122.

Desgrosellier, J. S. and Cheresh, D. A. (2010) 'Integrins in cancer : therapeutic opportunities', *Nature Reviews Cancer*. Nature Publishing Group, 10(1), pp. 9–22.

Van Deun, J., Mestdagh, P., Sormunen, R., Cocquyt, V., Vermaelen, K., Vandesompele, J., Bracke, M., De Wever, O. and Hendrix, A. (2014) 'The impact of disparate isolation methods for extracellular vesicles on downstream RNA profiling', *J Extracell Vesicles*. Co-Action Publishing, 3(1).

Dey, A., Seshasayee, D., Noubade, R., French, D. M., Liu, J., Chaurushiya, M. S., Kirkpatrick, D. S., Pham, V. C., Lill, J. R., Bakalarski, C. E., Wu, J., Phu, L., Katavolos, P., LaFave, L. M., Abdel-Wahab, O., Modrusan, Z., Seshagiri, S., Dong, K., Lin, Z., Balazs, M., Suriben, R., Newton, K., Hymowitz, S., Garcia-Manero, G., Martin, F., Levine, R. L. and Dixit, V. M. (2012) 'Loss of the tumor suppressor BAP1 causes myeloid transformation.', *Science (New York, N.Y.)*, 337(6101), pp. 1541–6.

Diener-West, M., Reynolds, S. M., Agugliaro, D. J., Caldwell, R., Cumming, K., Earle, J. D., Hawkins, B. S., Hayman, J. A., Jaiyesimi, I., Jampol, L. M., Kirkwood, J. M., Koh, W.-J., Robertson, D. M., Shaw, J. M., Straatsma, B. R., Thoma, J. and Collaborative Ocular Melanoma Study Group (2005) 'Development of metastatic disease after enrollment in the COMS trials for treatment of choroidal melanoma: Collaborative Ocular Melanoma Study Group Report No. 26.', *Archives of ophthalmology (Chicago, Ill. : 1960)*, 123(12), pp. 1639–43.

Doherty, G. J. and Mcmahon, H. T. (2009) 'Mechanisms of Endocytosis'.

Dono, M., Angelini, G., Cecconi, M., Amaro, A., Esposito, A. I., Mirisola, V., Maric, I., Lanza, F., Nasciuti, F., Viaggi, S., Gualco, M., Bandelloni, R., Truini, M., Coviello, D. A., Zupo, S., Mosci, C. and Pfeffer, U. (2014) 'Mutation frequencies of GNAQ, GNA11, BAP1, SF3B1, EIF1AX and TERT in uveal melanoma: detection of an activating mutation in the TERT gene

promoter in a single case of uveal melanoma.', *British journal of cancer*, 110(4), pp. 1058–65.

Downward, J. (2003) 'Targeting RAS signalling pathways in cancer therapy.', *Nature reviews. Cancer*, 3(1), pp. 11–22.

Dragovic, R. A., Gardiner, C., Brooks, A. S., Tannetta, D. S., Ferguson, D. J. P., Hole, P., Carr, B., Redman, C. W. G., Harris, A. L., Dobson, P. J., Harrison, P. and Sargent, I. L. (2011) 'Sizing and phenotyping of cellular vesicles using Nanoparticle Tracking Analysis', *Nanomedicine: Nanotechnology, Biology, and Medicine*, 7(6), pp. 780–788.

Du, J., Chen, X., Liang, X., Zhang, G., Xu, J., He, L., Zhan, Q., Feng, X. Q., Chien, S. and Yang, C. (2011) 'Integrin activation and internalization on soft ECM as a mechanism of induction of stem cell differentiation by ECM elasticity', *Proceedings of the National Academy of Sciences of the United States of America*, 108(23), pp. 9466–9471.

Duan, F., Lin, M., Li, C., Ding, X., Qian, G., Zhang, H., Ge, S., Fan, X. and Li, J. (2014) 'Effects of inhibition of hedgehog signaling on cell growth and migration of uveal melanoma cells.', *Cancer biology & therapy*, 15(5), pp. 544–59.

Duijvesz, D., Burnum-Johnson, K. E., Gritsenko, M. A., Hoogland, A. M., Vredenbregt-van Den Berg, M. S., Willemsen, R., Luider, T., Paša-Tolić, L. and Jenster, G. (2013) 'Proteomic profiling of exosomes leads to the identification of novel biomarkers for prostate cancer', *PLoS ONE*, 8(12).

Dupont, S., Morsut, L., Aragona, M., Enzo, E., Giulitti, S., Cordenonsi, M., Zanconato, F., Le Digabel, J., Forcato, M., Bicciato, S., Elvassore, N. and Piccolo, S. (2011) 'Role of YAP/TAZ in mechanotransduction', *Nature*, 474(7350), pp. 179–184.

Eden, E., Navon, R., Steinfeld, I., Lipson, D. and Yakhini, Z. (2009) 'GOrilla: A tool for discovery and visualization of enriched GO terms in ranked gene lists', *BMC Bioinformatics*, 10.

Edlund, S., Landström, M., Heldin, C.-H. and Aspenström, P. (2002) 'Transforming growth

factor-beta-induced mobilization of actin cytoskeleton requires signaling by small GTPases Cdc42 and RhoA.', *Molecular biology of the cell*, 13(3), pp. 902–14.

Ekholm, S. V and Reed, S. I. (2000) 'Regulation of G(1) cyclin-dependent kinases in the mammalian cell cycle.', *Current opinion in cell biology*, 12(6), pp. 676–84.

Eldh, M., Olofsson Bagge, R., Lässer, C., Svanvik, J., Sjöstrand, M., Mattsson, J., Lindnér, P., Choi, D.-S., Gho, Y. S. and Lötvall, J. (2014) 'MicroRNA in exosomes isolated directly from the liver circulation in patients with metastatic uveal melanoma', *BMC cancer*, 14(1).

Eleuteri, A., Aung, M. S. H., Taktak, A. F. G., Damato, B. and Lisboa, P. J. G. (2007) 'Continuous and discrete time survival analysis: neural network approaches.', *Conference proceedings : ... Annual International Conference of the IEEE Engineering in Medicine and Biology Society. IEEE Engineering in Medicine and Biology Society. Annual Conference*, 2007, pp. 5420–3.

Elshaw, S. R., Sisley, K., Cross, N., Murray, A. K., MacNeil, S. M., Wagner, M., Nichols, C. E. and Rennie, I. G. (2001) 'A comparison of ocular melanocyte and uveal melanoma cell invasion and the implication of α1β1, α4β1 and α6β1 integrins', *British Journal of Ophthalmology*, 85(6), pp. 732–738.

Ene-Obong, A., Clear, A. J., Watt, J., Wang, J., Fatah, R., Riches, J. C., Marshall, J. F., Chin-Aleong, J., Chelala, C., Gribben, J. G., Ramsay, A. G. and Kocher, H. M. (2013) 'Activated pancreatic stellate cells sequester CD8+ T cells to reduce their infiltration of the juxtatumoral compartment of pancreatic ductal adenocarcinoma', *Gastroenterology*. W.B. Saunders, 145(5), pp. 1121–1132.

Eng, F. J. and Friedman, S. L. (2000) 'Fibrogenesis. I. New insights into hepatic stellate cell activation: The simple becomes complex', *American Journal of Physiology - Gastrointestinal and Liver Physiology*, 279(1 42-1).

Eng, J. K., McCormack, A. L. and Yates, J. R. (1994) 'An approach to correlate tandem mass spectral data of peptides with amino acid sequences in a protein database', *Journal of the*

American Society for Mass Spectrometry. Springer-Verlag, 5(11), pp. 976–989.

Enzmann, V., Faude, F., Kohen, L. and Wiedemann, P. (1998) 'Secretion of cytokines by human choroidal melanoma cells and skin melanoma cell lines in vitro.', *Ophthalmic research*, 30(3), pp. 189–94.

Erler, J. T., Bennewith, K. L., Cox, T. R., Lang, G., Bird, D., Koong, A., Le, Q.-T. and Giaccia, A. J. (2009) 'Hypoxia-induced lysyl oxidase is a critical mediator of bone marrow cell recruitment to form the premetastatic niche.', *Cancer cell*, 15(1), pp. 35–44.

Eskelin, S., Pyrhönen, S., Summanen, P., Prause, J. U. and Kivelä, T. (1999) 'Screening for metastatic malignant melanoma of the uvea revisited.', *Cancer*, 85(5), pp. 1151–9.

Ewens, K. G., Kanetsky, P. A., Richards-Yutz, J., Al-Dahmash, S., de Luca, M. C., Bianciotto, C. G., Shields, C. L. and Ganguly, A. (2013) 'Genomic profile of 320 uveal melanoma cases: Chromosome 8p-loss and metastatic outcome', *Investigative Ophthalmology and Visual Science*, 54(8), pp. 5721–5729.

Ewens, K. G., Kanetsky, P. A., Richards-Yutz, J., Purrazzella, J., Shields, C. L., Ganguly, T. and Ganguly, A. (2014) 'Chromosome 3 status combined with BAP1 and EIF1AX mutation profiles are associated with metastasis in uveal melanoma', *Investigative Ophthalmology and Visual Science*. Association for Research in Vision and Ophthalmology Inc., 55(8), pp. 5160–5167.

Fabregat, A., Jupe, S., Matthews, L., Sidiropoulos, K., Gillespie, M., Garapati, P., Haw, R., Jassal, B., Korninger, F., May, B., Milacic, M., Roca, C. D., Rothfels, K., Sevilla, C., Shamovsky, V., Shorser, S., Varusai, T., Viteri, G., Weiser, J., Wu, G., Stein, L., Hermjakob, H. and D'Eustachio, P. (2018) 'The Reactome Pathway Knowledgebase', *Nucleic Acids Research*. Oxford University Press, 46(D1), pp. D649–D655.

Faingold, D., Filho, V. B., Fernandes, B., Jagan, L., de Barros, A. M., Orellana, M. E., Antecka, E. and Burnier, M. N. (2014) 'Expression of focal adhesion kinase in uveal melanoma and the effects of Hsp90 inhibition by 17-AAG.', *Pathology, research and practice*, 210(11), pp.

739–45.

Farquhar, N., Thornton, S., Coupland, S. E., Coulson, J. M., Sacco, J. J., Krishna, Y., Heimann, H., Taktak, A., Cebulla, C. M., Abdel-Rahman, M. H. and Kalirai, H. (2018) 'Patterns of BAP1 protein expression provide insights into prognostic significance and the biology of uveal melanoma.', *The journal of pathology. Clinical research*, 4(1), pp. 26–38.

Feingold, K. R. and Grunfeld, C. (2000) *Introduction to Lipids and Lipoproteins*, *Endotext*.

Fellows, C., Quasnichka, H., Chowdhury, N. R., Budd, E., Skene, D. J. and Mobasheri, A. (2018) 'Metabolomics and metabolic function analysis of the secretome of articular cartilage and isolated chondrocytes in response to pro-inflammatory cytokines', *Osteoarthritis and Cartilage*. Elsevier BV, 26, p. S172.

Feng, L., Zhang, J., Zhu, N., Ding, Q., Zhang, X., Yu, J., Qiang, W., Zhang, Z., Ma, Y., Huang, D., Shen, Yujun, Fang, S., Yu, Y., Wang, H. and Shen, Yuxian (2017) 'Ubiquitin ligase SYVN1/HRD1 facilitates degradation of the SERPINA1 Z variant/α-1-antitrypsin Z variant via SQSTM1/p62-dependent selective autophagy', *Autophagy*. Taylor and Francis Inc., 13(4), pp. 686–702.

Feng, X., Degese, M. S., Iglesias-Bartolome, R., Vaque, J. P., Molinolo, A. A., Rodrigues, M., Zaidi, M. R., Ksander, B. R., Merlino, G., Sodhi, A., Chen, Q. and Gutkind, J. S. (2014) 'Hippo-independent activation of YAP by the GNAQ uveal melanoma oncogene through a trio-regulated rho GTPase signaling circuitry.', *Cancer cell*, 25(6), pp. 831–45.

Filipe, V., Hawe, A. and Jiskoot, W. (2010) 'Critical evaluation of nanoparticle tracking analysis (NTA) by NanoSight for the measurement of nanoparticles and protein aggregates', *Pharmaceutical Research*, 27(5), pp. 796–810.

Fingar, D. C., Richardson, C. J., Tee, A. R., Cheatham, L., Tsou, C. and Blenis, J. (2004) 'mTOR Controls Cell Cycle Progression through Its Cell Growth Effectors S6K1 and 4E-BP1/Eukaryotic Translation Initiation Factor 4E', *Molecular and Cellular Biology*. American Society for Microbiology, 24(1), pp. 200–216.

Fischer, E. R., Hansen, B. T., Nair, V., Hoyt, F. H. and Dorward, D. W. (2012) 'Scanning electron microscopy', *Current Protocols in Microbiology*, (SUPPL.25).

Flach, E. H., Rebecca, V. W., Herlyn, M., Smalley, K. S. M. and Anderson, A. R. A. (2011) 'Fibroblasts contribute to melanoma tumor growth and drug resistance', *Molecular Pharmaceutics*, 8(6), pp. 2039–2049.

Folberg, R., Pe'er, J., Gruman, L. M., Woolson, R. F., Jeng, G., Montague, P. R., Moninger, T. O., Yi, H. and Moore, K. C. (1992) 'The morphologic characteristics of tumor blood vessels as a marker of tumor progression in primary human uveal melanoma: A matched case-control study', *Human Pathology*, 23(11), pp. 1298–1305.

Folberg, R., Rummelt, V., Parys-Van Ginderdeuren, R., Hwang, T., Woolson, R. F., Pe'er, J. and Gruman, L. M. (1993) 'The prognostic value of tumor blood vessel morphology in primary uveal melanoma.', *Ophthalmology*, 100(9), pp. 1389–98.

Fong, M. Y., Zhou, W., Liu, L., Alontaga, A. Y., Chandra, M., Ashby, J., Chow, A., O'Connor, S. T. F., Li, S., Chin, A. R., Somlo, G., Palomares, M., Li, Z., Tremblay, J. R., Tsuyada, A., Sun, G., Reid, M. A., Wu, X., Swiderski, P., Ren, X., Shi, Y., Kong, M., Zhong, W., Chen, Y. and Wang, S. E. (2015) 'Breast-cancer-secreted miR-122 reprograms glucose metabolism in premetastatic niche to promote metastasis', *Nature Cell Biology*. Nature Publishing Group, 17(2), pp. 183–194.

Frank, K. and Sippl, M. J. (2008) 'High-performance signal peptide prediction based on sequence alignment techniques', *Bioinformatics*, 24(19), pp. 2172–2176.

Frantz, C., Stewart, K. M. and Weaver, V. M. (2010) 'The extracellular matrix at a glance.', *Journal of cell science*, 123(Pt 24), pp. 4195–200.

Frenkel, S., Nir, I., Hendler, K., Lotem, M., Eid, A., Jurim, O. and Pe'er, J. (2009) 'Long-term survival of uveal melanoma patients after surgery for liver metastases.', *The British journal of ophthalmology*, 93(8), pp. 1042–6.

Friedman, S. L. (2004) 'Mechanisms of disease: Mechanisms of hepatic fibrosis and

therapeutic implications.', *Nature clinical practice. Gastroenterology & hepatology*, 1(2), pp. 98–105.

Fujita, K., Kume, H., Matsuzaki, K., Kawashima, A., Ujike, T., Nagahara, A., Uemura, M., Miyagawa, Y., Tomonaga, T. and Nonomura, N. (2017) 'Proteomic analysis of urinary extracellular vesicles from high Gleason score prostate cancer', *Scientific Reports*. Nature Publishing Group, 7.

García-Campos, M. A., Espinal-Enríquez, J. and Hernández-Lemus, E. (2015) 'Pathway analysis: State of the art', *Frontiers in Physiology*. Frontiers Research Foundation.

Garcia-Contreras, M., Shah, S. H., Tamayo, A., Robbins, P. D., Golberg, R. B., Mendez, A. J. and Ricordi, C. (2017) 'Plasma-derived exosome characterization reveals a distinct microRNA signature in long duration Type 1 diabetes.', *Scientific reports*, 7(1), p. 5998.

García-Martínez, J. M. and Alessi, D. R. (2008) 'mTOR complex 2 (mTORC2) controls hydrophobic motif phosphorylation and activation of serum- and glucocorticoid-induced protein kinase 1 (SGK1)', *Biochemical Journal*, 416(3), pp. 375–385.

García-Silva, S. and Peinado, H. (2016) 'Melanosomes foster a tumour niche by activating CAFs', *Nature Cell Biology*. Nature Publishing Group, pp. 911–913.

Garraway, L. A., Widlund, H. R., Rubin, M. A., Getz, G., Berger, A. J., Ramaswamy, S., Beroukhim, R., Milner, D. A., Granter, S. R., Du, J., Lee, C., Wagner, S. N., Li, C., Golub, T. R., Rimm, D. L., Meyerson, M. L., Fisher, D. E. and Sellers, W. R. (2005) 'Integrative genomic analyses identify MITF as a lineage survival oncogene amplified in malignant melanoma.', *Nature*, 436(7047), pp. 117–22.

Geer, L. Y., Markey, S. P., Kowalak, J. A., Wagner, L., Xu, M., Maynard, D. M., Yang, X., Shi, W. and Bryant, S. H. (2004) 'Open Mass Spectrometry Search Algorithm', *Journal of Proteome Research*, 3(5).

Gene Ontology Consortium, Blake, J. A., Dolan, M., Drabkin, H., Hill, D. P., Westerfield, M., *et al.* (2013) 'Gene Ontology annotations and resources.', *Nucleic acids research*,

41(Database issue), pp. D530-5.

Gerdes, H.-H., Bukoreshtliev, N. V. and Barroso, J. F. V. (2007) 'Tunneling nanotubes: A new route for the exchange of components between animal cells', *FEBS Letters*, 581(11), pp. 2194–2201.

German, A. E., Mammoto, T., Jiang, E., Ingber, D. E. and Mammoto, A. (2014) 'Paxillin controls endothelial cell migration and tumor angiogenesis by altering neuropilin 2 expression', *Journal of Cell Science*. Company of Biologists Ltd, 127(8), pp. 1672–1683.

Ghossoub, R., Lembo, F., Rubio, A., Gaillard, C. B., Bouchet, J., Vitale, N., Slavík, J., Machala, M. and Zimmermann, P. (2014) 'Syntenin-ALIX exosome biogenesis and budding into multivesicular bodies are controlled by ARF6 and PLD2', *Nature Communications*. Nature Publishing Group, 5.

Gialeli, C., Theocharis, A. D. and Karamanos, N. K. (2011) 'Roles of matrix metalloproteinases in cancer progression and their pharmacological targeting', *FEBS Journal*, pp. 16–27.

Giatromanolaki, A. N., Charitoudis, G. S., Bechrakis, N. E., Kozobolis, V. P., Koukourakis, M. I., Foerster, M. H. and Sivridis, E. L. (2011) 'Autophagy patterns and prognosis in uveal melanomas.', *Modern pathology : an official journal of the United States and Canadian Academy of Pathology, Inc*, 24(8), pp. 1036–45.

Gilbert, J. A. (2014) 'MEK1/2 inhibition delays progression of uveal melanoma.', *The Lancet. Oncology*, 15(9), p. e366.

Di Girolamo, F., Lante, I., Muraca, M. and Putignani, L. (2013) 'The Role of Mass Spectrometry in the "Omics" Era.', *Current organic chemistry*, 17(23), pp. 2891–2905.

Gonin, H. T. (1936) ' XIV. The use of factorial moments in the treatment of the hypergeometric distribution and in tests for regression ', *The London, Edinburgh, and Dublin Philosophical Magazine and Journal of Science*. Informa UK Limited, 21(139), pp. 215–226.

Graveley, B. R. (2001) 'Alternative splicing: Increasing diversity in the proteomic world',

Trends in Genetics, pp. 100–107.

Green, J. A. and Yamada, K. M. (2007) 'Three-dimensional microenvironments modulate fibroblast signaling responses.', *Advanced drug delivery reviews*, 59(13), pp. 1293–8.

Greening, D. W., Xu, R., Ji, H., Tauro, B. J. and Simpson, R. J. (2015) 'A protocol for exosome isolation and characterization: Evaluation of ultracentrifugation, density-gradient separation, and immunoaffinity capture methods', in *Methods in Molecular Biology*. Humana Press Inc., pp. 179–209.

Gressner, A. M., Weiskirchen, R., Breitkopf, K. and Dooley, S. (2002) 'Roles of TGF-beta in hepatic fibrosis.', *Frontiers in bioscience : a journal and virtual library*.

Griffin, C. A., Long, P. P. and Schachat, A. P. (1988) 'Trisomy 6p in an ocular melanoma.', *Cancer genetics and cytogenetics*, 32(1), pp. 129–32.

Grossniklaus, H. E. (2013) 'Progression of ocular melanoma metastasis to the liver: the 2012 Zimmerman lecture.', *JAMA ophthalmology*, 131(4), pp. 462–9.

Grossniklaus, H. E., Zhang, Q., You, S., McCarthy, C., Heegaard, S. and Coupland, S. E. (2016) 'Metastatic ocular melanoma to the liver exhibits infiltrative and nodular growth patterns.', *Human pathology*, 57, pp. 165–175.

Gulhati, P., Bowen, K. A., Liu, J., Stevens, P. D., Rychahou, P. G., Chen, M., Lee, E. Y., Weiss, H. L., O'Connor, K. L., Gao, T. and Evers, B. M. (2011) 'mTORC1 and mTORC2 regulate EMT, motility, and metastasis of colorectal cancer via RhoA and Rac1 signaling pathways', *Cancer Research*, 71(9), pp. 3246–3256.

György, B., Szabó, T. G., Pásztói, M., Pál, Z., Misják, P., Aradi, B., László, V., Pállinger, É., Pap, E., Kittel, Á., Nagy, G., Falus, A. and Buzás, E. I. (2011) 'Membrane vesicles, current state-of-the-art: Emerging role of extracellular vesicles', *Cellular and Molecular Life Sciences*, pp. 2667–2688.

Ha, D., Yang, N. and Nadithe, V. (2016) 'Exosomes as therapeutic drug carriers and delivery vehicles across biological membranes: current perspectives and future challenges.', *Acta*

pharmaceutica Sinica. B, 6(4), pp. 287–96.

Halban, P. A. and Irminger, J. C. (1994) 'Sorting and processing of secretory proteins.', *The Biochemical journal*, 299 (Pt 1), pp. 1–18.

Hall, A. (1998) 'Rho GTpases and the actin cytoskeleton', *Science*, pp. 509–514.

Halvaei, S., Daryani, S., Eslami-S, Z., Samadi, T., Jafarbeik-Iravani, N., Bakhshayesh, T. O., Majidzadeh-A, K. and Esmaeili, R. (2018) 'Exosomes in Cancer Liquid Biopsy: A Focus on Breast Cancer', *Molecular Therapy - Nucleic Acids*. Cell Press, pp. 131–141.

Hamabe, W., Fukushima, N., Yoshida, A. and Ueda, H. (2000) 'Serum-free induced neuronal apoptosis-like cell death is independent of caspase activity', *Molecular Brain Research*, 78(1–2), pp. 186–191.

Hamidi, H. and Ivaska, J. (2018) 'Every step of the way: integrins in cancer progression and metastasis', *Nature Reviews Cancer*. Nature Publishing Group, pp. 1–16.

Hammond, D. E., Claydon, A. J., Simpson, D. M., Edward, D., Stockley, P., Hurst, J. L. and Beynon, R. J. (2016) 'Proteome dynamics: Tissue variation in the kinetics of proteostasis in intact animals', *Molecular and Cellular Proteomics*. American Society for Biochemistry and Molecular Biology Inc., 15(4), pp. 1204–1219.

Hanahan, D. and Weinberg, R. A. (2000) 'The hallmarks of cancer', *Cell*, pp. 57–70.

Hanahan, D. and Weinberg, R. A. (2011) 'Hallmarks of cancer: The next generation', *Cell*, pp. 646–674.

Hanash, S. M., Pitteri, S. J. and Faca, V. M. (2008) 'Mining the plasma proteome for cancer biomarkers.', *Nature*, 452(7187), pp. 571–9.

Hao, X., Sun, B., Zhang, S. and Zhao, X. (2003) '[Correlation between the expression of collgen IV, VEGF and vasculogenic mimicry].', *Zhonghua zhong liu za zhi [Chinese journal of oncology]*, 25(6), pp. 524–6.

Haraszti, R. A., Didiot, M. C., Sapp, E., Leszyk, J., Shaffer, S. A., Rockwell, H. E., Gao, F., Narain, N. R., DiFiglia, M., Kiebish, M. A., Aronin, N. and Khvorova, A. (2016) 'High-

resolution proteomic and lipidomic analysis of exosomes and microvesicles from different cell sources', *Journal of Extracellular Vesicles*. Taylor and Francis Ltd., 5(1).

Harbour, J. W., Onken, M. D., Roberson, E. D. O., Duan, S., Cao, L., Worley, L. A., Council, M. L., Matatall, K. A., Helms, C. and Bowcock, A. M. (2010) 'Frequent mutation of BAP1 in metastasizing uveal melanomas.', *Science (New York, N.Y.)*, 330(6009), pp. 1410–3.

Hartman, M. L. and Czyz, M. (2015) 'MITF in melanoma: mechanisms behind its expression and activity.', *Cellular and molecular life sciences : CMLS*, 72(7), pp. 1249–60.

Hartwell, L. H., Hopfield, J. J., Leibler, S. and Murray, A. W. (1999) 'From molecular to modular cell biology', *Nature*, 402(6761 SUPPL. 1).

Helwa, I., Cai, J., Drewry, M. D., Zimmerman, A., Dinkins, M. B., Khaled, M. L., Seremwe, M., Dismuke, W. M., Bieberich, E., Stamer, W. D., Hamrick, M. W. and Liu, Y. (2017) 'A Comparative Study of Serum Exosome Isolation Using Differential Ultracentrifugation and Three Commercial Reagents.', *PloS one*, 12(1), p. e0170628.

Hendrix, M. J., Seftor, E. A., Seftor, R. E., Kirschmann, D. A., Gardner, L. M., Boldt, H. C., Meyer, M., Pe'er, J. and Folberg, R. (1998) 'Regulation of uveal melanoma interconverted phenotype by hepatocyte growth factor/scatter factor (HGF/SF).', *The American journal of pathology*, 152(4), pp. 855–63.

Henne, W. M., Stenmark, H. and Emr, S. D. (2013) 'Molecular mechanisms of the membrane sculpting ESCRT pathway.', *Cold Spring Harbor perspectives in biology*, 5(9).

Hessvik, N. P. and Llorente, A. (2018) 'Current knowledge on exosome biogenesis and release.', *Cellular and molecular life sciences : CMLS*, 75(2), pp. 193–208.

Hikita, T., Miyata, M., Watanabe, R. and Oneyama, C. (2018) 'Sensitive and rapid quantification of exosomes by fusing luciferase to exosome marker proteins', *Scientific Reports*. Nature Publishing Group, 8(1).

Hillel, A. T. and Gelbard, A. (2015) 'Unleashing rapamycin in fibrosis', *Oncotarget*, pp. 15722–15723.

Hiller, K., Grote, A., Scheer, M., Munch, R. and Jahn, D. (2004) 'PrediSi: prediction of signal peptides and their cleavage positions', *Nucleic Acids Research*, 32(Web Server), pp. W375–W379.

Hiratsuka, S., Watanabe, A., Sakurai, Y., Akashi-Takamura, S., Ishibashi, S., Miyake, K., Shibuya, M., Akira, S., Aburatani, H. and Maru, Y. (2008) 'The S100A8-serum amyloid A3-TLR4 paracrine cascade establishes a pre-metastatic phase.', *Nature cell biology*, 10(11), pp. 1349–55.

Ho, A. L., Musi, E., Ambrosini, G., Nair, J. S., Deraje Vasudeva, S., de Stanchina, E. and Schwartz, G. K. (2012) 'Impact of combined mTOR and MEK inhibition in uveal melanoma is driven by tumor genotype', *PLoS ONE*, 7(7).

Hong, Y., Li, S., Wang, J. and Li, Y. (2018) 'In vitro inhibition of hepatic stellate cell activation by the autophagy-related lipid droplet protein ATG2A', *Scientific Reports*. Nature Publishing Group, 8(1).

Hood, J. L., Pan, H., Lanza, G. M. and Wickline, S. A. (2009) 'Paracrine induction of endothelium by tumor exosomes', *Laboratory Investigation*, 89(11), pp. 1317–1328.

Hood, J. L., San, R. S. and Wickline, S. A. (2011) 'Exosomes released by melanoma cells prepare sentinel lymph nodes for tumor metastasis.', *Cancer research*, 71(11), pp. 3792–801.

Hope-Stone, L., Brown, S. L., Heimann, H., Damato, B. and Salmon, P. (2015) 'Phantom Eye Syndrome: Patient Experiences after Enucleation for Uveal Melanoma.', *Ophthalmology*, 122(8), pp. 1585–90.

Horsman, D. E., Sroka, H., Rootman, J. and White, V. A. (1990) 'Monosomy 3 and isochromosome 8q in a uveal melanoma', *Cancer Genetics and Cytogenetics*, 45(2), pp. 249–253.

Hoshino, A., Costa-Silva, B., Shen, T.-L., Rodrigues, G., Hashimoto, A., Lyden, D., *et al.* (2015) 'Tumour exosome integrins determine organotropic metastasis.', *Nature*, 527(7578), pp.

329–35.

Hosseini-Beheshti, E., Pham, S., Adomat, H., Li, N. and Tomlinson Guns, E. S. (2012) 'Exosomes as biomarker enriched microvesicles: Characterization of exosomal proteins derived from a panel of prostate cell lines with distinct AR phenotypes', *Molecular and Cellular Proteomics*, 11(10), pp. 863–885.

Hu, J., Xu, Y., Hao, J., Wang, S., Li, C. and Meng, S. (2012) 'MiR-122 in hepatic function and liver diseases', *Protein and Cell*. Higher Education Press, pp. 364–371.

Hu, Z.-Z., Huang, H., Wu, C. H., Jung, M., Dritschilo, A., Riegel, A. T. and Wellstein, A. (2011) 'Omics-based molecular target and biomarker identification.', *Methods in molecular biology (Clifton, N.J.)*, 719, pp. 547–71.

Huang, D. W., Sherman, B. T. and Lempicki, R. A. (2009a) 'Bioinformatics enrichment tools: Paths toward the comprehensive functional analysis of large gene lists', *Nucleic Acids Research*, 37(1), pp. 1–13.

Huang, D. W., Sherman, B. T. and Lempicki, R. A. (2009b) 'Systematic and integrative analysis of large gene lists using DAVID bioinformatics resources', *Nature Protocols*, 4(1), pp. 44–57.

Huang, J., Ding, Z., Luo, Q. and Xu, W. (2019) 'Cancer cell-derived exosomes promote cell proliferation and inhibit cell apoptosis of both normal lung fibroblasts and non-small cell lung cancer cell through delivering alpha-smooth muscle actin', *American Journal of Translational Research*. E-Century Publishing Corporation, 11(3), pp. 1711–1723.

Huang, S. and Zhou, H. (2011) 'Role of mTOR Signaling in Tumor Cell Motility, Invasion and Metastasis', *Current Protein & Peptide Science*, 12(1), pp. 30–42.

Huber, V., Fais, S., Iero, M., Lugini, L., Canese, P., Squarcina, P., Zaccheddu, A., Colone, M., Arancia, G., Gentile, M., Seregni, E., Valenti, R., Ballabio, G., Belli, F., Leo, E., Parmiani, G. and Rivoltini, L. (2005) 'Human colorectal cancer cells induce T-cell death through release of proapoptotic microvesicles: Role in immune escape', *Gastroenterology*. W.B. Saunders,

128(7), pp. 1796–1804.

van Huizen, N. A., Coebergh van den Braak, R. R. J., Doukas, M., Dekker, L. J. M., IJzermans, J. N. M. and Luider, T. M. (2019) 'Up-regulation of collagen proteins in colorectal liver metastasis compared with normal liver tissue', *Journal of Biological Chemistry*. American Society for Biochemistry and Molecular Biology Inc., 294(1), pp. 281–289.

Hulkower, K. I. and Herber, R. L. (2011) 'Cell migration and invasion assays as tools for drug discovery.', *Pharmaceutics*, 3(1), pp. 107–24.

Hulsmans, M. and Holvoet, P. (2013) 'MicroRNA-containing microvesicles regulating inflammation in association with atherosclerotic disease.', *Cardiovascular research*, 100(1), pp. 7–18.

Huotari, J. and Helenius, A. (2011) 'Endosome maturation.', *The EMBO journal*, 30(17), pp. 3481–500.

Inagaki, Y. and Okazaki, I. (2007) 'Emerging insights into Transforming growth factor beta Smad signal in hepatic fibrogenesis.', *Gut*, 56(2), pp. 284–92.

Jacinto, E., Loewith, R., Schmidt, A., Lin, S., Rüegg, M. A., Hall, A. and Hall, M. N. (2004) 'Mammalian TOR complex 2 controls the actin cytoskeleton and is rapamycin insensitive', *Nature Cell Biology*, 6(11), pp. 1122–1128.

Jager, M. J., Magner, J. A. B., Ksander, B. R. and Dubovy, S. R. (2016) 'Uveal Melanoma Cell Lines: Where do they come from? (An American Ophthalmological Society Thesis)', *Transactions of the American Ophthalmological Society*, p. T5.

Jang, J.-Y., Lee, J.-K., Jeon, Y.-K. and Kim, C.-W. (2013) 'Exosome derived from epigallocatechin gallate treated breast cancer cells suppresses tumor growth by inhibiting tumor-associated macrophage infiltration and M2 polarization.', *BMC cancer*, 13, p. 421.

Jatho, A., Hartmann, S., Kittana, N., Mügge, F., Wuertz, C. M., Tiburcy, M., Zimmermann, W.-H., Katschinski, D. M. and Lutz, S. (2015) 'RhoA Ambivalently Controls Prominent Myofibroblast Characteritics by Involving Distinct Signaling Routes', *PLOS ONE*. Edited by D.

Gullberg, 10(10), p. e0137519.

Jeppesen, D. K., Fenix, A. M., Franklin, J. L., Higginbotham, J. N., Zhang, Q., Zimmerman, L. J., Liebler, D. C., Ping, J., Liu, Q., Evans, R., Fissell, W. H., Patton, J. G., Rome, L. H., Burnette, D. T. and Coffey, R. J. (2019) 'Reassessment of Exosome Composition', *Cell*. Cell Press, 177(2), pp. 428-445.e18.

Ji, H., Greening, D. W., Barnes, T. W., Lim, J. W., Tauro, B. J., Rai, A., Xu, R., Adda, C., Mathivanan, S., Zhao, W., Xue, Y., Xu, T., Zhu, H.-J. and Simpson, R. J. (2013) 'Proteome profiling of exosomes derived from human primary and metastatic colorectal cancer cells reveal differential expression of key metastatic factors and signal transduction components.', *Proteomics*, 13(10–11), pp. 1672–86.

Johnson, M. S., Lu, N., Denessiouk, K., Heino, J. and Gullberg, D. (2009) 'Integrins during evolution: evolutionary trees and model organisms.', *Biochimica et biophysica acta*, 1788(4), pp. 779–89.

Johnstone, R. M., Adam, M., Hammond, J. R., Orr, L. and Turbide, C. (1987) 'Vesicle formation during reticulocyte maturation. Association of plasma membrane activities with released vesicles (exosomes).', *Journal of Biological Chemistry*, 262(19), pp. 9412–9420.

Joly, M. M., Hicks, D. J., Jones, B., Sanchez, V., Estrada, M. V., Young, C., Williams, M., Rexer, B. N., Sarbassov, D. D., Muller, W. J., Brantley-Sieders, D. and Cook, R. S. (2016) 'Rictor/mTORC2 drives progression and therapeutic resistance of HER2-amplified breast cancers', *Cancer Research*. American Association for Cancer Research Inc., 76(16), pp. 4752–4764.

Jovanovic, P., Mihajlovic, M., Djordjevic-Jocic, J., Vlajkovic, S., Cekic, S. and Stefanovic, V. (2013) 'Ocular melanoma: An overview of the current status', *International Journal of Clinical and Experimental Pathology*, pp. 1230–1244.

Kalirai, H., Dodson, A., Faqir, S., Damato, B. E. and Coupland, S. E. (2014) 'Lack of BAP1 protein expression in uveal melanoma is associated with increased metastatic risk and has

utility in routine prognostic testing.', *British journal of cancer*, 111(7), pp. 1373–80.

Kalluri, R. and Zeisberg, M. (2006) 'Fibroblasts in cancer', *Nature Reviews Cancer*, pp. 392–401.

Kalpana, G., Figy, C., Yeung, M. and Yeung, K. C. (2019) 'Reduced RhoA expression enhances breast cancer metastasis with a concomitant increase in CCR5 and CXCR4 chemokines signaling', *Scientific Reports*, 9(1), p. 16351.

Kalra, H., Simpson, R. J., Ji, H., Aikawa, E., Altevogt, P., Mathivanan, S., *et al.* (2012) 'Vesiclepedia: a compendium for extracellular vesicles with continuous community annotation.', *PLoS biology*, 10(12), p. e1001450.

Kanchi Ravi, R., Khosroheidari, M. and DiStefano, J. K. (2015) 'A modified precipitation method to isolate urinary exosomes', *Journal of visualized experiments : JoVE*, (95), p. 51158.

Kaplan, R. N., Riba, R. D., Zacharoulis, S., Bramley, A. H., Vincent, L., Costa, C., MacDonald, D. D., Jin, D. K., Shido, K., Kerns, S. A., Zhu, Z., Hicklin, D., Wu, Y., Port, J. L., Altorki, N., Port, E. R., Ruggero, D., Shmelkov, S. V., Jensen, K. K., Rafii, S. and Lyden, D. (2005) 'VEGFR1-positive haematopoietic bone marrow progenitors initiate the pre-metastatic niche', *Nature*, 438(7069), pp. 820–827.

Karagiannis, G. S., Poutahidis, T., Erdman, S. E., Kirsch, R., Riddell, R. H. and Diamandis, E. P. (2012) 'Cancer-associated fibroblasts drive the progression of metastasis through both paracrine and mechanical pressure on cancer tissue.', *Molecular cancer research : MCR*, 10(11), pp. 1403–18.

Karantza, V. (2011) 'Keratins in health and cancer: More than mere epithelial cell markers', *Oncogene*, pp. 127–138.

Karin, M., Cao, Y., Greten, F. R. and Li, Z. W. (2002) 'NF-κB in cancer: From innocent bystander to major culprit', *Nature Reviews Cancer*, pp. 301–310.

Karousou, E., D'Angelo, M. L., Kouvidi, K., Vigetti, D., Viola, M., Nikitovic, D., De Luca, G. and

Passi, A. (2014) ‘Collagen VI and hyaluronan: the common role in breast cancer.’, *BioMed research international*, 2014, p. 606458.

Katsuda, T., Kosaka, N. and Ochiya, T. (2014) ‘The roles of extracellular vesicles in cancer biology: toward the development of novel cancer biomarkers.’, *Proteomics*, 14(4–5), pp. 412–25.

Keenan, T. D. L., Yeates, D. and Goldacre, M. J. (2012) ‘Uveal melanoma in England: Trends over time and geographical variation’, *British Journal of Ophthalmology*, 96(11), pp. 1415–1419.

Keerthikumar, S., Chisanga, D., Ariyaratne, D., Al Saffar, H., Anand, S., Zhao, K., Samuel, M., Pathan, M., Jois, M., Chilamkurti, N., Gangoda, L. and Mathivanan, S. (2016) ‘ExoCarta: A Web-Based Compendium of Exosomal Cargo’, *Journal of Molecular Biology*. Academic Press, 428(4), pp. 688–692.

Kerkelä, E., Ala-aho, R., Klemi, P., Grénman, S., Shapiro, S. D., Kähäri, V. M. and Saarialho-Kere, U. (2002) ‘Metalloelastase (MMP-12) expression by tumour cells in squamous cell carcinoma of the vulva correlates with invasiveness, while that by macrophages predicts better outcome’, *Journal of Pathology*, 198(2), pp. 258–269.

Khalili, A. A. and Ahmad, M. R. (2015) ‘A Review of cell adhesion studies for biomedical and biological applications’, *International Journal of Molecular Sciences*. MDPI AG, pp. 18149–18184.

Khan, S., Aspe, J. R., Asumen, M. G., Almaguel, F., Odumosu, O., Acevedo-Martinez, S., De Leon, M., Langridge, W. H. R. and Wall, N. R. (2009) ‘Extracellular, cell-permeable survivin inhibits apoptosis while promoting proliferative and metastatic potential’, *British Journal of Cancer*, 100(7), pp. 1073–1086.

Khan, S., Jutzy, J. M. S., Aspe, J. R., McGregor, D. W., Neidigh, J. W. and Wall, N. R. (2011) ‘Survivin is released from cancer cells via exosomes’, *Apoptosis*, 16(1), pp. 1–12.

Khoury, G. A., Baliban, R. C. and Floudas, C. A. (2011) ‘Proteome-wide post-translational

modification statistics: Frequency analysis and curation of the swiss-prot database', *Scientific Reports*. Nature Publishing Group, 1.

Kim, S. K., Lund, J., Kiraly, M., Duke, K., Jiang, M., Stuart, J. M., Eizinger, A., Wylie, B. N. and Davidson, G. S. (2001) 'A gene expression map for Caenorhabditis elegans', *Science*, 293(5537), pp. 2087–2092.

Kim, Y. C. and Guan, K. L. (2015) 'MTOR: A pharmacologic target for autophagy regulation', *Journal of Clinical Investigation*. American Society for Clinical Investigation, pp. 25–32.

King, O. D., Foulger, R. E., Dwight, S. S., White, J. V and Roth, F. P. (2003) 'Predicting gene function from patterns of annotation.', *Genome research*, 13(5), pp. 896–904.

Koga, K., Matsumoto, K., Akiyoshi, T., Kubo, M., Yamanaka, N., Tasaki, A., Nakashima, H., Nakamura, M., Kuroki, S., Tanaka, M. and Katano, M. (2005) 'Purification, characterization and biological significance of tumor-derived exosomes', in *Anticancer Research*, pp. 3703–3707.

Kondo, T., Okabayashi, K., Hasegawa, H., Tsuruta, M., Shigeta, K. and Kitagawa, Y. (2016) 'The impact of hepatic fibrosis on the incidence of liver metastasis from colorectal cancer', *British Journal of Cancer*. Nature Publishing Group, 115(1), pp. 34–39.

Konoshenko, M. Y., Lekchnov, E. A., Vlassov, A. V and Laktionov, P. P. (2018) 'Isolation of Extracellular Vesicles: General Methodologies and Latest Trends.', *BioMed research international*, 2018, p. 8545347.

Koopmans, A. E., Vaarwater, J., Paridaens, D., Naus, N. C., Kilic, E., de Klein, A. and Group, R. O. M. S. (2013) 'Patient survival in uveal melanoma is not affected by oncogenic mutations in GNAQ and GNA11.', *British journal of cancer*, 109(2), pp. 493–6.

Koopmans, A. E., Verdijk, R. M., Brouwer, R. W. W., Van Den Bosch, T. P. P., Van Den Berg, M. M. P., Vaarwater, J., Kockx, C. E. M., Paridaens, D., Naus, N. C., Nellist, M., Van Ijcken, W. F. J., Kiliç, E. and De Klein, A. (2014) 'Clinical significance of immunohistochemistry for detection of BAP1 mutations in uveal melanoma', *Modern Pathology*. Nature Publishing

Group, 27(10), pp. 1321–1330.

Kornilov, R., Puhka, M., Mannerström, B., Hiidenmaa, H., Peltoniemi, H., Siljander, P., Seppänen-Kaijansinkko, R. and Kaur, S. (2018) 'Efficient ultrafiltration-based protocol to deplete extracellular vesicles from fetal bovine serum', *Journal of Extracellular Vesicles*. Taylor and Francis Ltd., 7(1).

Kowal, J., Arras, G., Colombo, M., Jouve, M., Morath, J. P., Primdal-Bengtson, B., Dingli, F., Loew, D., Tkach, M. and Théry, C. (2016) 'Proteomic comparison defines novel markers to characterize heterogeneous populations of extracellular vesicle subtypes', *Proceedings of the National Academy of Sciences of the United States of America*. National Academy of Sciences, 113(8), pp. E968–E977.

Kowal, J., Tkach, M. and Thery, C. (2014) 'Biogenesis and secretion of exosomes', *Curr Opin Cell Biol*, 29, pp. 116–125.

Krämer, A., Green, J., Pollard, J. and Tugendreich, S. (2014) 'Causal analysis approaches in ingenuity pathway analysis', *Bioinformatics*, 30(4), pp. 523–530.

Krishna, Y., McCarthy, C., Kalirai, H. and Coupland, S. E. (2017) 'Inflammatory cell infiltrates in advanced metastatic uveal melanoma', *Human Pathology*. W.B. Saunders, 66, pp. 159–166.

Krishnamoorthy, G. P., Davidson, N. R., Leach, S. D., Zhao, Z., Lowe, S. W., Lee, G., Landa, I., Nagarajah, J., Saqcena, M., Singh, K., Wendel, H.-G., Dogan, S., Tamarapu, P. P., Blenis, J., Ghossein, R. A., Knauf, J. A., Rätsch, G. and Fagin, J. A. (2019) 'EIF1AX and RAS Mutations Cooperate to Drive Thyroid Tumorigenesis through ATF4 and c-MYC.', *Cancer discovery*, 9(2), pp. 264–281.

Kujala, E., Damato, B., Coupland, S. E., Desjardins, L., Bechrakis, N. E., Grange, J.-D. and Kivelä, T. (2013) 'Staging of ciliary body and choroidal melanomas based on anatomic extent.', *Journal of clinical oncology : official journal of the American Society of Clinical Oncology*, 31(22), pp. 2825–31.

Kullander, K. and Klein, R. (2002) 'Mechanisms and functions of Eph and ephrin signalling', *Nature Reviews Molecular Cell Biology*, pp. 475–486.

Kung, C. P., Budina, A., Balaburski, G., Bergenstock, M. K. and Murphy, M. E. (2011) 'Autophagy in tumor suppression and cancer therapy', *Critical Reviews in Eukaryotic Gene Expression*. Begell House Inc., pp. 71–100.

Kuzet, S.-E. and Gaggioli, C. (2016) 'Fibroblast activation in cancer: when seed fertilizes soil.', *Cell and tissue research*, 365(3), pp. 607–19.

Lai, K., Di Girolamo, N., Conway, R. M., Jager, M. J. and Madigan, M. C. (2007) 'The effect of ultraviolet radiation on choroidal melanocytes and melanoma cell lines: cell survival and matrix metalloproteinase production.', *Graefe's archive for clinical and experimental ophthalmology = Albrecht von Graefes Archiv fur klinische und experimentelle Ophthalmologie*, 245(5), pp. 715–24.

De Lange, M. J., Razzaq, L., Versluis, M., Verlinde, S., Dogrusöz, M., Böhringer, S., Marinkovic, M., Luyten, G. P. M., De Keizer, R. J. W., De Gruijl, F. R., Jager, M. J. and Van Der Velden, P. A. (2015) 'Distribution of GNAQ and GNA11 mutation signatures in uveal melanoma points to a light dependent mutation mechanism', *PLoS ONE*. Public Library of Science, 10(9).

Laplante, M. and Sabatini, D. M. (2009) 'An emerging role of mTOR in lipid biosynthesis.', *Current biology : CB*, 19(22), pp. R1046-52.

Lattman, J., Kroll, S., Char, D. H., Ghazvini, S., Frigillana, H., O'Brien, J. M. and Elbakri, H. R. (1995) 'Cell cycling and prognosis in uveal melanoma.', *Clinical cancer research : an official journal of the American Association for Cancer Research*, 1(1), pp. 41–7.

Lawrence, J. and Nho, R. (2018) 'The role of the mammalian target of rapamycin (mTOR) in pulmonary fibrosis', *International Journal of Molecular Sciences*. MDPI AG.

Lazar, I., Clement, E., Ducoux-Petit, M., Denat, L., Soldan, V., Dauvillier, S., Balor, S., Burlet-Schiltz, O., Larue, L., Muller, C. and Nieto, L. (2015) 'Proteome characterization of

melanoma exosomes reveals a specific signature for metastatic cell lines.', *Pigment cell & melanoma research*, 28(4), pp. 464–75.

Lee, J. and Kim, S. S. (2010) 'Current implications of cyclophilins in human cancers', *Journal of Experimental and Clinical Cancer Research*.

Lee, J. W., Stone, M. L., Porrett, P. M., Thomas, S. K., Komar, C. A., Li, J. H., Delman, D., Graham, K., Gladney, W. L., Hua, X., Black, T. A., Chien, A. L., Majmundar, K. S., Thompson, J. C., Yee, S. S., O'Hara, M. H., Aggarwal, C., Xin, D., Shaked, A., Gao, M., Liu, D., Borad, M. J., Ramanathan, R. K., Carpenter, E. L., Ji, A., de Beer, M. C., de Beer, F. C., Webb, N. R. and Beatty, G. L. (2019) 'Hepatocytes direct the formation of a pro-metastatic niche in the liver', *Nature*. Nature Publishing Group, pp. 249–252.

Levin, Y., Hradetzky, E. and Bahn, S. (2011) 'Quantification of proteins using data-independent analysis (MSE) in simple andcomplex samples: a systematic evaluation.', *Proteomics*, 11(16), pp. 3273–87.

Li, C., Liang, G., Yang, S., Sui, J., Yao, W., Shen, X., Zhang, Y., Peng, H., Hong, W., Xu, S., Wu, W., Ye, Y., Zhang, Z., Zhang, W., Yin, L. and Pu, Y. (2017) 'Dysregulated lncRNA-UCA1 contributes to the progression of gastric cancer through regulation of the PI3K-Akt-mTOR signaling pathway', *Oncotarget*. Impact Journals LLC, 8(55), pp. 93476–93491.

Li, H., Lin, J., Wang, X., Yao, G., Wang, L., Zheng, H., Yang, C., Jia, C., Liu, A. and Bai, X. (2012) 'Targeting of mTORC2 prevents cell migration and promotes apoptosis in breast cancer.', *Breast cancer research and treatment*, 134(3), pp. 1057–66.

Li, H., Alizadeh, H. and Niederkorn, J. Y. (2008) 'Differential expression of chemokine receptors on uveal melanoma cells and their metastases.', *Investigative ophthalmology & visual science*, 49(2), pp. 636–43.

Li, J., Lee, Y., Johansson, H. J., Mäger, I., Vader, P., Nordin, J. Z., Wiklander, O. P. B., Lehtiö, J., Wood, M. J. A. and Andaloussi, S. El (2015) 'Serum-free culture alters the quantity and protein composition of neuroblastoma-derived extracellular vesicles.', *Journal of*

extracellular vesicles, 4, p. 26883.

Li, L., Liu, D.-X., Zhang, N., Liang, Q., Feng, J., Yao, M., Liu, J., Li, X., Zhang, Y., Lu, J. and Huang, B. (2015) 'SHON, a novel secreted protein, regulates epithelial-mesenchymal transition through transforming growth factor-β signaling in human breast cancer cells.', *International journal of cancer*, 136(6), pp. 1285–95.

Li, M., Lu, Y., Xu, Y., Wang, J., Zhang, C., Du, Y., Wang, L., Li, L., Wang, B., Shen, J., Tang, J. and Song, B. (2018) 'Horizontal transfer of exosomal CXCR4 promotes murine hepatocarcinoma cell migration, invasion and lymphangiogenesis', *Gene*. Elsevier B.V., 676, pp. 101–109.

Li, P., Kaslan, M., Lee, S. H., Yao, J. and Gao, Z. (2017) 'Progress in exosome isolation techniques', *Theranostics*. Ivyspring International Publisher, 7(3), pp. 789–804.

Li, Y., Casey, S. C. and Felsher, D. W. (2014) 'Inactivation of MYC reverses tumorigenesis.', *Journal of internal medicine*, 276(1), pp. 52–60.

Lin, A. Y., Maniotis, A. J., Valyi-Nagy, K., Majumdar, D., Setty, S., Kadkol, S., Leach, L., Pe'er, J. and Folberg, R. (2005) 'Distinguishing fibrovascular septa from vasculogenic mimicry patterns.', *Archives of pathology & laboratory medicine*, 129(7), pp. 884–92.

Linge, A., Kennedy, S., O'Flynn, D., Beatty, S., Moriarty, P., Henry, M., Clynes, M., Larkin, A. and Meleady, P. (2012) 'Differential expression of fourteen proteins between uveal melanoma from patients who subsequently developed distant metastases versus those who did not', *Investigative Ophthalmology and Visual Science*, 53(8), pp. 4634–4643.

Liotta, L. A. and Kohn, E. C. (2001) 'The microenvironment of the tumour - Host interface', *Nature*, pp. 375–379.

Liu, D., Mei, X., Wang, L. and Yang, X. (2017) 'RhoA inhibits apoptosis and increases proliferation of cultured SPCA1 lung cancer cells', *Molecular Medicine Reports*. Spandidos Publications, 15(6), pp. 3963–3968.

Lo, R. C. and Kim, H. (2017) 'Histopathological evaluation of liver fibrosis and cirrhosis

regression.', *Clinical and molecular hepatology*, 23(4), pp. 302–307.

Lobb, R. J., Becker, M., Wen, S. W., Wong, C. S. F., Wiegmans, A. P., Leimgruber, A. and Möller, A. (2015) 'Optimized exosome isolation protocol for cell culture supernatant and human plasma', *Journal of Extracellular Vesicles*. Taylor and Francis Ltd., 4(1).

Lötvall, J., Hill, A. F., Hochberg, F., Buzás, E. I., Vizio, D. Di, Gardiner, C., Gho, Y. S., Kurochkin, I. V., Mathivanan, S., Quesenberry, P., Sahoo, S., Tahara, H., Wauben, M. H., Witwer, K. W. and Théry, C. (2014) 'Minimal experimental requirements for definition of extracellular vesicles and their functions: A position statement from the International Society for Extracellular Vesicles', *Journal of Extracellular Vesicles*. Co-Action Publishing.

Lu, P., Takai, K., Weaver, V. M. and Werb, Z. (2011) 'Extracellular Matrix degradation and remodeling in development and disease', *Cold Spring Harbor Perspectives in Biology*, 3(12).

Lubec, G. and Afjehi-Sadat, L. (2007) 'Limitations and pitfalls in protein identification by mass spectrometry.', *Chemical reviews*, 107(8), pp. 3568–84.

Ludwig, J. A. and Weinstein, J. N. (2005) 'Biomarkers in cancer staging, prognosis and treatment selection', *Nature Reviews Cancer*, pp. 845–856.

Lundholm, M., Schröder, M., Nagaeva, O., Baranov, V., Widmark, A., Mincheva-Nilsson, L. and Wikström, P. (2014) 'Prostate tumor-derived exosomes down-regulate NKG2D expression on natural killer cells and CD8+ T cells: Mechanism of immune evasion', *PLoS ONE*. Public Library of Science, 9(9).

Lundmark, R., Doherty, G. J., Howes, M. T., Cortese, K., Vallis, Y., Parton, R. G. and McMahon, H. T. (2008) 'The GTPase-Activating Protein GRAF1 Regulates the CLIC/GEEC Endocytic Pathway', *Current Biology*, 18(22), pp. 1802–1808.

Lydic, T. A., Townsend, S., Adda, C. G., Collins, C., Mathivanan, S. and Reid, G. E. (2015) 'Rapid and comprehensive "shotgun" lipidome profiling of colorectal cancer cell derived exosomes.', *Methods (San Diego, Calif.)*, 87, pp. 83–95.

Lyngholm, M., Vorum, H., Nielsen, K., Ehlers, N. and Honoré, B. (2011) 'Attempting to

distinguish between endogenous and contaminating cytokeratins in a corneal proteomic study', *BMC Ophthalmology*, 11(1).

Maji, S., Chaudhary, P., Akopova, I., Nguyen, P. M., Hare, R. J., Gryczynski, I. and Vishwanatha, J. K. (2016) 'Exosomal Annexin A2 Promotes Angiogenesis and Breast Cancer Metastasis', *Author Manuscript Published OnlineFirst*.

Mäkitie, T., Summanen, P., Tarkkanen, A. and Kivelä, T. (2001) 'Tumor-infiltrating macrophages (CD68+ cells) and prognosis in malignant uveal melanoma', *Investigative Ophthalmology and Visual Science*, 42(7), pp. 1414–1421.

Makridakis, M., Roubelakis, M. G., Bitsika, V., Dimuccio, V., Samiotaki, M., Kossida, S., Panayotou, G., Coleman, J., Candiano, G., Anagnou, N. P. and Vlahou, A. (2010) 'Analysis of secreted proteins for the study of bladder cancer cell aggressiveness.', *Journal of proteome research*, 9(6), pp. 3243–59.

Mallick, P. and Kuster, B. (2010) 'Proteomics: A pragmatic perspective', *Nature Biotechnology*. Nature Publishing Group, pp. 695–709.

Man, Y.-G. (2010) 'Aberrant leukocyte infiltration: a direct trigger for breast tumor invasion and metastasis.', *International journal of biological sciences*, 6(2), pp. 129–32.

Mariani, P., Piperno-Neumann, S., Servois, V., Berry, M. G., Dorval, T., Plancher, C., Couturier, J., Levy-Gabriel, C., Lumbroso-Le Rouic, L., Desjardins, L. and Salmon, R. J. (2009) 'Surgical management of liver metastases from uveal melanoma: 16 years' experience at the Institut Curie.', *European journal of surgical oncology : the journal of the European Society of Surgical Oncology and the British Association of Surgical Oncology*, 35(11), pp. 1192–7.

Martin, K., Pritchett, J., Llewellyn, J., Mullan, A. F., Athwal, V. S., Dobie, R., Harvey, E., Zeef, L., Farrow, S., Streuli, C., Henderson, N. C., Friedman, S. L., Hanley, N. A. and Hanley, K. P. (2016) 'PAK proteins and YAP-1 signalling downstream of integrin beta-1 in myofibroblasts promote liver fibrosis', *Nature Communications*. Nature Publishing Group, 7.

Martin, M., Maßhöfer, L., Temming, P., Rahmann, S., Metz, C., Bornfeld, N., van de Nes, J., Klein-Hitpass, L., Hinnebusch, A. G., Horsthemke, B., Lohmann, D. R. and Zeschnigk, M. (2013) 'Exome sequencing identifies recurrent somatic mutations in EIF1AX and SF3B1 in uveal melanoma with disomy 3.', *Nature genetics*, 45(8), pp. 933–6.

Matatall, K. A., Agapova, O. A., Onken, M. D., Worley, L. A., Bowcock, A. M. and Harbour, J. W. (2013) 'BAP1 deficiency causes loss of melanocytic cell identity in uveal melanoma.', *BMC cancer*, 13, p. 371.

Mathias, R. A., Wang, B., Ji, H., Kapp, E. A., Moritz, R. L., Zhu, H.-J. and Simpson, R. J. (2009) 'Secretome-based proteomic profiling of Ras-transformed MDCK cells reveals extracellular modulators of epithelial-mesenchymal transition.', *Journal of proteome research*, 8(6), pp. 2827–37.

Mathivanan, S., Lim, J. W. E., Tauro, B. J., Ji, H., Moritz, R. L. and Simpson, R. J. (2010) 'Proteomics analysis of A33 immunoaffinity-purified exosomes released from the human colon tumor cell line LIM1215 reveals a tissue-specific protein signature', *Molecular and Cellular Proteomics*, 9(2), pp. 197–208.

Mathivanan, S., Ji, H. and Simpson, R. J. (2010) 'Exosomes: Extracellular organelles important in intercellular communication', *Journal of Proteomics*, pp. 1907–1920.

Mathivanan, S. and Simpson, R. J. (2009) 'ExoCarta: A compendium of exosomal proteins and RNA', *Proteomics*, 9(21), pp. 4997–5000.

Matsuda, Y., Inoue, Y., Hiratsuka, M., Kawakatsu, S., Arai, T., Matsueda, K., Saiura, A. and Takazawa, Y. (2019) 'Encapsulating fibrosis following neoadjuvant chemotherapy is correlated with outcomes in patients with pancreatic cancer', *PLOS ONE*. Edited by F. X. Real, 14(9), p. e0222155.

Matsusue, R., Kubo, H., Hisamori, S., Okoshi, K., Takagi, H., Hida, K., Nakano, K., Itami, A., Kawada, K., Nagayama, S. and Sakai, Y. (2009) 'Hepatic stellate cells promote liver metastasis of colon cancer cells by the action of SDF-1/CXCR4 axis', *Annals of Surgical*

Oncology, 16(9), pp. 2645–2653.

Mazza, G., Al-Akkad, W. and Rombouts, K. (2017) 'Engineering in vitro models of hepatofibrogenesis', *Advanced Drug Delivery Reviews*. Elsevier B.V., pp. 147–157.

McCarthy, C., Kalirai, H., Lake, S. L., Dodson, A., Damato, B. E. and Coupland, S. E. (2016) 'Insights into genetic alterations of liver metastases from uveal melanoma.', *Pigment cell & melanoma research*, 29(1), pp. 60–7.

McKelvey, K. J., Powell, K. L., Ashton, A. W., Morris, J. M. and McCracken, S. A. (2015) 'Exosomes: Mechanisms of Uptake', *Journal of Circulating Biomarkers*. SAGE Publications Ltd.

McLean, I. W., Zimmerman, L. E. and Evans, R. M. (1978) 'Reappraisal of Callender's spindle a type of malignant melanoma of choroid and ciliary body.', *American journal of ophthalmology*, 86(4), pp. 557–64.

McLean, L., Hurst, J. L., Gaskell, C. J., Lewis, J. C. M. and Beynon, R. J. (2007) 'Characterization of cauxin in the urine of domestic and big cats', *Journal of Chemical Ecology*, 33(10), pp. 1997–2009.

Mears, R., Craven, R. A., Hanrahan, S., Totty, N., Upton, C., Young, S. L., Patel, P., Selby, P. J. and Banks, R. E. (2004) 'Proteomic analysis of melanoma-derived exosomes by two-dimensional polyacrylamide gel electrophoresis and mass spectrometry.', *Proteomics*, 4(12), pp. 4019–31.

Meehan, K. and Vella, L. J. (2016) 'The contribution of tumour-derived exosomes to the hallmarks of cancer', *Critical Reviews in Clinical Laboratory Sciences*. Taylor and Francis Ltd, pp. 121–131.

Meir, T., Dror, R., Yu, X., Qian, J., Simon, I., Pe'er, J. and Chowers, I. (2007) 'Molecular characteristics of liver metastases from uveal melanoma.', *Investigative ophthalmology & visual science*, 48(11), pp. 4890–6.

Meister, M. and Tikkanen, R. (2014) 'Endocytic trafficking of membrane-bound cargo: A

flotillin point of view', *Membranes*. MDPI AG, pp. 356–371.

Meyer, S., Hafner, C., Guba, M., Flegel, S., Geissler, E. K., Becker, B., Koehl, G. E., Orso, E., Landthaler, M. and Vogt, T. (2005) 'Ephrin-B2 overexpression enhances integrin-mediated ECM-attachment and migration of B16 melanoma cells', *International Journal of Oncology*, 27(5), pp. 1197–1206.

Mi, H., Muruganujan, A. and Thomas, P. D. (2013) 'PANTHER in 2013: modeling the evolution of gene function, and other gene attributes, in the context of phylogenetic trees.', *Nucleic acids research*, 41(Database issue), pp. D377-86.

Micallef, L., Vedrenne, N., Billet, F., Coulomb, B., Darby, I. A. and Desmoulière, A. (2012) 'The myofibroblast, multiple origins for major roles in normal and pathological tissue repair.', *Fibrogenesis & tissue repair*, 5(Suppl 1), p. S5.

Milette, S., Sicklick, J. K., Lowy, A. M. and Brodt, P. (2017) 'Molecular Pathways Molecular Pathways: Targeting the Microenvironment of Liver Metastases', *Clin Cancer Res*, 23(21).

Millodot, M. (2014) *Dictionary of Optometry and Visual Science E-Book*. Elsevier Health Sciences.

Mineo, M., Garfield, S. H., Taverna, S., Flugy, A., De Leo, G., Alessandro, R. and Kohn, E. C. (2012) 'Exosomes released by K562 chronic myeloid leukemia cells promote angiogenesis in a Src-dependent fashion.', *Angiogenesis*, 15(1), pp. 33–45.

Missotten, G. S., Beijnen, J. H., Keunen, J. E. and Bonfrer, J. M. (2003) 'Proteomics in uveal melanoma', *Melanoma Research*, 13(6), pp. 627–629.

Mitchell, P. J., Welton, J., Staffurth, J., Court, J., Mason, M. D., Tabi, Z. and Clayton, A. (2009) 'Can urinary exosomes act as treatment response markers in prostate cancer?', *Journal of translational medicine*, 7, p. 4.

Moore, R. F. (1930) 'CHOROIDAL SARCOMA TREATED BY THE INTRAOCULAR INSERTION OF RADON SEEDS', *British Journal of Ophthalmology*. BMJ, 14(4), pp. 145–152.

Mooy, C. M., De Jong, P. T. V. M., Van Der Kwast, T. H., Mulder, P. G. H., Jager, M. J. and

Ruiter, D. J. (1990) 'Ki-67 Immunostaining in Uveal Melanoma: The Effect of Pre-enucleation Radiotherapy', *Ophthalmology*, 97(10), pp. 1275–1280.

Morales, V. M., Yates, R., Toutounchian, J. J., Kibe, M. W., Miller, D., Jiang, Y., Steinle, J. J., Mendoza, P. R., Grossniklaus, H. E. and Wilson, M. W. (2014) 'Modulation of Cytoskeletal Adaptor Proteins in Uveal Melanoma to Control Metastasis', *Investigative Ophthalmology & Visual Science*. Investigative Ophthalmology & Visual Science, 55(13), p. 3578.

Morel, E. and Gruenberg, J. (2009) 'Annexin A2 Binding to endosomes and functions in endosomal transport are regulated by tyrosine 23 phosphorylation', *Journal of Biological Chemistry*, 284(3), pp. 1604–1611.

Morita, M., Sato, T., Nomura, M., Sakamoto, Y., Inoue, Y., Tanaka, R., Ito, S., Kurosawa, K., Yamaguchi, K., Sugiura, Y., Takizaki, H., Yamashita, Y., Katakura, R., Sato, I., Kawai, M., Okada, Y., Watanabe, H., Kondoh, G., Matsumoto, S., Kishimoto, A., Obata, M., Matsumoto, M., Fukuhara, T., Motohashi, H., Suematsu, M., Komatsu, M., Nakayama, K. I., Watanabe, T., Soga, T., Shima, H., Maemondo, M. and Tanuma, N. (2018) 'PKM1 Confers Metabolic Advantages and Promotes Cell-Autonomous Tumor Cell Growth', *Cancer Cell*. Cell Press, 33(3), pp. 355-367.e7.

Mormone, E., George, J. and Nieto, N. (2011) 'Molecular pathogenesis of hepatic fibrosis and current therapeutic approaches.', *Chemico-biological interactions*, 193(3), pp. 225–31.

Moss, D. K., Betin, V. M., Malesinski, S. D. and Lane, J. D. (2006) 'A novel role for microtubules in apoptotic chromatin dynamics and cellular fragmentation.', *Journal of cell science*, 119(Pt 11), pp. 2362–74.

Mossmann, D., Park, S. and Hall, M. N. (2018) 'mTOR signalling and cellular metabolism are mutual determinants in cancer', *Nature Reviews Cancer*. Nature Publishing Group, pp. 744–757.

Mousavi, S. A., Malerød, L., Berg, T. and Kjeken, R. (2004) 'Clathrin-dependent endocytosis', *Biochemical Journal*, pp. 1–16.

Mukaida, N. and Sasaki, S. (2016) 'Fibroblasts, an inconspicuous but essential player in colon cancer development and progression', *World Journal of Gastroenterology*. Baishideng Publishing Group Co., Limited, pp. 5301–5316.

Mulcahy, L. A., Pink, R. C. and Carter, D. R. F. (2014) 'Routes and mechanisms of extracellular vesicle uptake', *Journal of Extracellular Vesicles*. Co-Action Publishing.

Muller, L., Hong, C. S., Stolz, D. B., Watkins, S. C. and Whiteside, T. L. (2014) 'Isolation of biologically-active exosomes from human plasma', *Journal of Immunological Methods*. Elsevier, 411, pp. 55–65.

Muzny, D. M., Bainbridge, M. N., Chang, K., Dinh, H. H., Drummond, J. A., Thomson., E., *et al.* (2012) 'Comprehensive molecular characterization of human colon and rectal cancer', *Nature*, 487(7407), pp. 330–337.

Nakai, W., Yoshida, T., Diez, D., Miyatake, Y., Nishibu, T., Imawaka, N., Naruse, K., Sadamura, Y. and Hanayama, R. (2016) 'A novel affinity-based method for the isolation of highly purified extracellular vesicles', *Scientific Reports*. Nature Publishing Group, 6.

Nayman, T., Bostan, C., Logan, P. and Burnier, M. N. (2017) 'Uveal Melanoma Risk Factors: A Systematic Review of Meta-Analyses', *Current Eye Research*. Taylor and Francis Ltd, pp. 1085–1093.

Nickel, W. and Seedorf, M. (2008) 'Unconventional mechanisms of protein transport to the cell surface of eukaryotic cells.', *Annual review of cell and developmental biology*, 24, pp. 287–308.

Nielsen, H., Engelbrecht, J., Brunak, S. and Von Heijne, G. (1997) 'Identification of prokaryotic and eukaryotic signal peptides and prediction of their cleavage sites', *Protein Engineering*, 10(1), pp. 1–6.

Nolte-'t Hoen, E., Cremer, T., Gallo, R. C. and Margolis, L. B. (2016) 'Extracellular vesicles and viruses: Are they close relatives?', *Proceedings of the National Academy of Sciences of the United States of America*, 113(33), pp. 9155–61.

Nonnis, S., Maffioli, E., Zanotti, L., Santagata, F., Negri, A., Viola, A., Elliman, S. and Tedeschi, G. (2016) 'Effect of fetal bovine serum in culture media on MS analysis of mesenchymal stromal cells secretome.', *EuPA open proteomics*, 10, pp. 28–30.

O'Connor, K. L. and Chen, M. (2013) 'Dynamic functions of RhoA in tumor cell migration and invasion', *Small GTPases*.

Okazaki, Y., Ohno, H., Takase, K., Ochiai, T. and Saito, T. (2000) 'Cell surface expression of calnexin, a molecular chaperone in the endoplasmic reticulum', *Journal of Biological Chemistry*, 275(46), pp. 35751–35758.

Olaso, E., Salado, C., Egilegor, E., Gutierrez, V., Santisteban, A., Sancho-Bru, P., Friedman, S. L. and Vidal-Vanaclocha, F. (2003) 'Proangiogenic role of tumor-activated hepatic stellate cells in experimental melanoma metastasis', *Hepatology*. W.B. Saunders, 37(3), pp. 674–685.

Olive, K. P., Jacobetz, M. A., Davidson, C. J., Gopinathan, A., McIntyre, D., Honess, D., Madhu, B., Goldgraben, M. A., Caldwell, M. E., Allard, D., Frese, K. K., DeNicola, G., Feig, C., Combs, C., Winter, S. P., Ireland-Zecchini, H., Reichelt, S., Howat, W. J., Chang, A., Dhara, M., Wang, L., Rückert, F., Grützmann, R., Pilarsky, C., Izeradjene, K., Hingorani, S. R., Huang, P., Davies, S. E., Plunkett, W., Egorin, M., Hruban, R. H., Whitebread, N., McGovern, K., Adams, J., Iacobuzio-Donahue, C., Griffiths, J. and Tuveson, D. A. (2009) 'Inhibition of Hedgehog signaling enhances delivery of chemotherapy in a mouse model of pancreatic cancer', *Science*, 324(5933), pp. 1457–1461.

Olofsson, R., Cahlin, C., All-Ericsson, C., Hashimi, F., Mattsson, J., Rizell, M. and Lindnér, P. (2014) 'Isolated hepatic perfusion for ocular melanoma metastasis: registry data suggests a survival benefit.', *Annals of surgical oncology*, 21(2), pp. 466–72.

Ong, S. E., Blagoev, B., Kratchmarova, I., Kristensen, D. B., Steen, H., Pandey, A. and Mann, M. (2002) 'Stable isotope labeling by amino acids in cell culture, SILAC, as a simple and accurate approach to expression proteomics.', *Molecular & cellular proteomics : MCP*, 1(5),

pp. 376–386.

Onken, M. D., Worley, L. A., Ehlers, J. P. and Harbour, J. W. (2004) 'Gene expression profiling in uveal melanoma reveals two molecular classes and predicts metastatic death.', *Cancer research*, 64(20), pp. 7205–9.

Onken, M. D., Worley, L. A., Long, M. D., Duan, S., Council, M. L., Bowcock, A. M. and Harbour, J. W. (2008) 'Oncogenic mutations in GNAQ occur early in uveal melanoma.', *Investigative ophthalmology & visual science*, 49(12), pp. 5230–4.

Oskarsson, T. (2013) 'Extracellular matrix components in breast cancer progression and metastasis.', *Breast (Edinburgh, Scotland)*, 22 Suppl 2, pp. S66-72.

Oza, A. M. and Boyd, N. F. (1993) 'Mammographic parenchymal patterns: a marker of breast cancer risk.', *Epidemiologic reviews*, 15(1), pp. 196–208.

Özdemir, B. C., Pentcheva-Hoang, T., Carstens, J. L., Zheng, X., Wu, C. C., Simpson, T. R., Laklai, H., Sugimoto, H., Kahlert, C., Novitskiy, S. V., DeJesus-Acosta, A., Sharma, P., Heidari, P., Mahmood, U., Chin, L., Moses, H. L., Weaver, V. M., Maitra, A., Allison, J. P., LeBleu, V. S. and Kalluri, R. (2014) 'Depletion of carcinoma-associated fibroblasts and fibrosis induces immunosuppression and accelerates pancreas cancer with reduced survival', *Cancer Cell*. Cell Press, 25(6), pp. 719–734.

Paggetti, J., Haderk, F., Seiffert, M., Janji, B., Distler, U., Ammerlaan, W., Kim, Y. J., Adam, J., Lichter, P., Solary, E., Berchem, G. and Moussay, E. (2015) 'Exosomes released by chronic lymphocytic leukemia cells induce the transition of stromal cells into cancer-associated fibroblasts.', *Blood*, 126(9), pp. 1106–17.

Pap, E., Pállinger, E. and Falus, A. (2011) 'The role of membrane vesicles in tumorigenesis.', *Critical reviews in oncology/hematology*, 79(3), pp. 213–23.

Paquette, M., El-Houjeiri, L. and Pause, A. (2018) 'mTOR pathways in cancer and autophagy', *Cancers*. MDPI AG.

Pardo, M., García, Á., Thomas, B., Piñeiro, A., Akoulitchev, A., Dwek, R. A. and Zitzmann, N.

(2006) ‘The characterization of the invasion phenotype of uveal melanoma tumour cells shows the presence of MUC18 and HMG-1 metastasis markers and leads to the identification of DJ-1 as a potential serum biomarker’, *International Journal of Cancer*, 119(5), pp. 1014–1022.

Pardo, M., García, Á., Antrobus, R., Blanco, M. J., Dwek, R. A. and Zitzmann, N. (2007) ‘Biomarker discovery from uveal melanoma secretomes: Identification of gp100 and cathepsin D in patient serum’, *Journal of Proteome Research*, 6(7), pp. 2802–2811.

Parrella, P., Caballero, O. L., Sidransky, D. and Merbs, S. L. (2001) ‘Detection of c-myc amplification in uveal melanoma by fluorescent in situ hybridization.’, *Investigative ophthalmology & visual science*, 42(8), pp. 1679–84.

Pasquale, E. B. (2005) ‘Developmental Cell Biology: Eph receptor signalling casts a wide net on cell behaviour’, *Nature Reviews Molecular Cell Biology*, 6(6), pp. 462–475.

Patel, K., Sullivan, K., Berd, D., Mastrangelo, M. J., Shields, C. L., Shields, J. A. and Sato, T. (2005) ‘Chemoembolization of the hepatic artery with BCNU for metastatic uveal melanoma: Results of a phase II study’, *Melanoma Research*, 15(4), pp. 297–304.

Patel, M., Smyth, E., Chapman, P. B., Wolchok, J. D., Schwartz, G. K., Abramson, D. H. and Carvajal, R. D. (2011) ‘Therapeutic implications of the emerging molecular biology of uveal melanoma.’, *Clinical cancer research : an official journal of the American Association for Cancer Research*, 17(8), pp. 2087–100.

Patel, S., Ngounou Wetie, A. G., Darie, C. C. and Clarkson, B. D. (2014) ‘Cancer secretomes and their place in supplementing other hallmarks of cancer.’, *Advances in experimental medicine and biology*, 806, pp. 409–42.

Pe’er, J., Gnessin, H., Shargal, Y. and Livni, N. (1994) ‘PC-10 Immunostaining of Proliferating Cell Nuclear Antigen in Posterior Uveal Melanoma: Enucleadon versus Enucleation Posdrradiadon Groups’, *Ophthalmology*, 101(1), pp. 56–62.

Peinado, H., Alečković, M., Lavotshkin, S., Matei, I., Costa-Silva, B., Moreno-Bueno, G.,

Hergueta-Redondo, M., Williams, C., García-Santos, G., Ghajar, C. M., Nitadori-Hoshino, A., Hoffman, C., Badal, K., Garcia, B. A., Callahan, M. K., Yuan, J., Martins, V. R., Skog, J., Kaplan, R. N., Brady, M. S., Wolchok, J. D., Chapman, P. B., Kang, Y., Bromberg, J. and Lyden, D. (2012) 'Melanoma exosomes educate bone marrow progenitor cells toward a pro-metastatic phenotype through MET', *Nature Medicine*, 18(6), pp. 883–891.

Perkins, D. N., Pappin, D. J., Creasy, D. M. and Cottrell, J. S. (1999) 'Probability-based protein identification by searching sequence databases using mass spectrometry data.', *Electrophoresis*, 20(18), pp. 3551–67.

Pickup, M. W., Mouw, J. K. and Weaver, V. M. (2014) 'The extracellular matrix modulates the hallmarks of cancer', *EMBO reports*. EMBO, 15(12), pp. 1243–1253.

Piersma, S. R., Fiedler, U., Span, S., Lingnau, A., Pham, T. V, Hoffmann, S., Kubbutat, M. H. G. and Jiménez, C. R. (2010) 'Workflow comparison for label-free, quantitative secretome proteomics for cancer biomarker discovery: method evaluation, differential analysis, and verification in serum.', *Journal of proteome research*, 9(4), pp. 1913–22.

Piper, R. C. and Katzmann, D. J. (2007) 'Biogenesis and Function of Multivesicular Bodies', *Annual Review of Cell and Developmental Biology*. Annual Reviews, 23(1), pp. 519–547.

Pisitkun, T., Shen, R. F. and Knepper, M. A. (2004) 'Identification and proteomic profiling of exosomes in human urine', *Proceedings of the National Academy of Sciences of the United States of America*, 101(36), pp. 13368–13373.

Pluquet, O., Pourtier, A. and Abbadie, C. (2015) 'The unfolded protein response and cellular senescence. A Review in the Theme: Cellular Mechanisms of Endoplasmic Reticulum Stress Signaling in Health and Disease', *American Journal of Physiology-Cell Physiology*, 308(6), pp. C415–C425.

van der Pol, E., Böing, A. N., Harrison, P., Sturk, A. and Nieuwland, R. (2012) 'Classification, functions, and clinical relevance of extracellular vesicles', *Pharmacological Reviews*. American Society for Pharmacology and Experimental Therapy, 64(3), pp. 676–705.

Poon, Ivan K.H., Lucas, C. D., Rossi, A. G. and Ravichandran, K. S. (2014) 'Apoptotic cell clearance: Basic biology and therapeutic potential', *Nature Reviews Immunology*, pp. 166–180.

Poon, Ivan K H, Chiu, Y.-H., Armstrong, A. J., Kinchen, J. M., Juncadella, I. J., Bayliss, D. A. and Ravichandran, K. S. (2014) 'Unexpected link between an antibiotic, pannexin channels and apoptosis.', *Nature*, 507(7492), pp. 329–34.

Pópulo, H., Soares, P., Rocha, A. S., Silva, P. and Lopes, J. M. (2010) 'Evaluation of the mTOR pathway in ocular (uvea and conjunctiva) melanoma', *Melanoma Research*, 20(2), pp. 107–117.

Pospichalova, V., Svoboda, J., Dave, Z., Kotrbova, A., Kaiser, K., Klemova, D., Ilkovics, L., Hampl, A., Crha, I., Jandakova, E., Minar, L., Weinberger, V. and Bryja, V. (2015) 'Simplified protocol for flow cytometry analysis of fluorescently labeled exosomes and microvesicles using dedicated flow cytometer', *Journal of Extracellular Vesicles*. Co-Action Publishing, 4(2015), pp. 1–15.

Prescher, G., Bornfeld, N., Hirche, H., Horsthemke, B., Jöckel, K. H. and Becher, R. (1996) 'Prognostic implications of monosomy 3 in uveal melanoma', *Lancet*. Lancet Publishing Group, 347(9010), pp. 1222–1225.

Principe, M., Ceruti, P., Shih, N. Y., Chattaragada, M. S., Rolla, S., Conti, L., Bestagno, M., Zentilin, L., Yang, S. H., Migliorini, P., Cappello, P., Burrone, O. and Novelli, F. (2015) 'Targeting of surface alpha-enolase inhibits the invasiveness of pancreatic cancer cells', *Oncotarget*. Impact Journals LLC, 6(13), pp. 11098–11113.

Provenzano, P. P., Inman, D. R., Eliceiri, K. W., Knittel, J. G., Yan, L., Rueden, C. T., White, J. G. and Keely, P. J. (2008) 'Collagen density promotes mammary tumor initiation and progression.', *BMC medicine*, 6, p. 11.

Provenzano, P. P., Cuevas, C., Chang, A. E., Goel, V. K., Von Hoff, D. D. and Hingorani, S. R. (2012) 'Enzymatic Targeting of the Stroma Ablates Physical Barriers to Treatment of

Pancreatic Ductal Adenocarcinoma', *Cancer Cell*, 21(3), pp. 418–429.

Qu, J.-L., Qu, X.-J., Zhao, M.-F., Teng, Y.-E., Zhang, Y., Hou, K.-Z., Jiang, Y.-H., Yang, X.-H. and Liu, Y.-P. (2009) 'Gastric cancer exosomes promote tumour cell proliferation through PI3K/Akt and MAPK/ERK activation.', *Digestive and liver disease : official journal of the Italian Society of Gastroenterology and the Italian Association for the Study of the Liver*, 41(12), pp. 875–80.

Qu, Z., Jiang, C., Wu, J. and Ding, Y. (2015) 'Exosomes as potent regulators of HCC malignancy and potential bio-tools in clinical application.', *International journal of clinical and experimental medicine*, 8(10), pp. 17088–95.

Te Raa, G. D., Derks, I. A. M., Navrkalova, V., Skowronska, A., Moerland, P. D., van Laar, J., Oldreive, C., Monsuur, H., Trbusek, M., Malcikova, J., Lodén, M., Geisler, C. H., Hüllein, J., Jethwa, A., Zenz, T., Pospisilova, S., Stankovic, T., van Oers, M. H. J., Kater, A. P. and Eldering, E. (2015) 'The impact of SF3B1 mutations in CLL on the DNA-damage response.', *Leukemia*, 29(5), pp. 1133–42.

Van Raamsdonk, C. D., Bezrookove, V., Green, G., Bauer, J., Gaugler, L., O'Brien, J. M., Simpson, E. M., Barsh, G. S. and Bastian, B. C. (2009) 'Frequent somatic mutations of GNAQ in uveal melanoma and blue naevi.', *Nature*, 457(7229), pp. 599–602.

Van Raamsdonk, C. D., Griewank, K. G., Crosby, M. B., Garrido, M. C., Vemula, S., Wiesner, T., Obenauf, A. C., Wackernagel, W., Green, G., Bouvier, N., Sozen, M. M., Baimukanova, G., Roy, R., Heguy, A., Dolgalev, I., Khanin, R., Busam, K., Speicher, M. R., O'Brien, J. and Bastian, B. C. (2010) 'Mutations in GNA11 in uveal melanoma.', *The New England journal of medicine*, 363(23), pp. 2191–9.

Ragusa, M., Barbagallo, C., Statello, L., Caltabiano, R., Russo, A., Puzzo, L., Avitabile, T., Longo, A., Toro, M. D., Barbagallo, D., Valadi, H., Di Pietro, C., Purrello, M. and Reibaldi, M. (2015) 'miRNA profiling in vitreous humor, vitreal exosomes and serum from uveal melanoma patients: Pathological and diagnostic implications', *Cancer Biology and Therapy*.

Taylor and Francis Inc., 16(9), pp. 1387–1396.

Raposo, G. and Stoorvogel, W. (2013) 'Extracellular vesicles: Exosomes, microvesicles, and friends', *Journal of Cell Biology*, pp. 373–383.

Räsänen, K. and Vaheri, A. (2010) 'Activation of fibroblasts in cancer stroma.', *Experimental cell research*, 316(17), pp. 2713–22.

Repp, A. C., Mayhew, E. S., Apte, S. and Niederkorn, J. Y. (2000) 'Human Uveal Melanoma Cells Produce Macrophage Migration-Inhibitory Factor to Prevent Lysis by NK Cells', *The Journal of Immunology*. The American Association of Immunologists, 165(2), pp. 710–715.

Rhim, A. D., Oberstein, P. E., Thomas, D. H., Mirek, E. T., Palermo, C. F., Sastra, S. A., Dekleva, E. N., Saunders, T., Becerra, C. P., Tattersall, I. W., Westphalen, C. B., Kitajewski, J., Fernandez-Barrena, M. G., Fernandez-Zapico, M. E., Iacobuzio-Donahue, C., Olive, K. P. and Stanger, B. Z. (2014) 'Stromal elements act to restrain, rather than support, pancreatic ductal adenocarcinoma', *Cancer Cell*. Cell Press, 25(6), pp. 735–747.

Riches, A., Campbell, E., Borger, E. and Powis, S. (2014) 'Regulation of exosome release from mammary epithelial and breast cancer cells - a new regulatory pathway.', *European journal of cancer (Oxford, England : 1990)*, 50(5), pp. 1025–34.

Ridley, A. J. (2015) 'Rho GTPase signalling in cell migration', *Current Opinion in Cell Biology*. Elsevier Ltd, pp. 103–112.

Riedl, A., Schlederer, M., Pudelko, K., Stadler, M. and Walter, S. (2016) 'Comparison of cancer cells cultured in 2D vs 3D reveals differences in AKT / mTOR / S6- kinase signaling and drug response Journal of Cell Science • Advance article Abstract Journal of Cell Science • Advance article', *journal of cell science*, (September).

Robinson, J. L., Feizi, A., Uhlén, M. and Nielsen, J. (2019) 'A Systematic Investigation of the Malignant Functions and Diagnostic Potential of the Cancer Secretome.', *Cell reports*, 26(10), pp. 2622-2635.e5.

Rocha, S., Carvalho, J., Oliveira, P., Voglstaetter, M., Schvartz, D., Thomsen, A. R., Walter,

N., Khanduri, R., Sanchez, J.-C., Keller, A., Oliveira, C. and Nazarenko, I. (2019) '3D Cellular Architecture Affects MicroRNA and Protein Cargo of Extracellular Vesicles', *Advanced Science*, 6(4), p. 1800948.

Rockey, D. C., Boyles, J. K., Gabbiani, G. and Friedman, S. L. (1992) 'Rat hepatic lipocytes express smooth muscle actin upon activation in vivo and in culture.', *Journal of submicroscopic cytology and pathology*, 24(2), pp. 193–203.

Rodrigues, P., Macaya, I., Bazzocco, S., Mazzolini, R., Andretta, E., Dopeso, H., Mateo-Lozano, S., Bilić, J., Cartón-García, F., Nieto, R., Suárez-López, L., Afonso, E., Landolfi, S., Hernandez-Losa, J., Kobayashi, K., Ramón y Cajal, S., Tabernero, J., Tebbutt, N. C., Mariadason, J. M., Schwartz, S. and Arango, D. (2014) 'RHOA inactivation enhances Wnt signalling and promotes colorectal cancer.', *Nature communications*, 5, p. 5458.

Rodríguez, M., Silva, J., Herrera, A., Herrera, M., Peña, C., Martín, P., Gil-Calderón, B., Larriba, M. J., Coronado, M. J., Soldevilla, B., Turrión, V. S., Provencio, M., Sánchez, A., Bonilla, F. and García-Barberán, V. (2015) 'Exosomes enriched in stemness/metastatic-related mRNAS promote oncogenic potential in breast cancer.', *Oncotarget*, 6(38), pp. 40575–87.

Rosa-Fernandes, L., Rocha, V. B., Carregari, V. C., Urbani, A. and Palmisano, G. (2017) 'A perspective on extracellular vesicles proteomics', *Frontiers in Chemistry*. Frontiers Media S. A.

Rothberg, J., Merriman, B. and Higgs, G. (2012) 'Bioinformatics. Introduction.', *The Yale journal of biology and medicine*, 85(3), pp. 305–8.

Royds, J. A., Sharrard, R. M., Parsons, M. A., Lawry, J., Rees, R., Cottam, D., Wagner, B. and Rennie, I. G. (1992) 'C-myc oncogene expression in ocular melanomas.', *Graefe's archive for clinical and experimental ophthalmology = Albrecht von Graefes Archiv fur klinische und experimentelle Ophthalmologie*, 230(4), pp. 366–71.

Rustom, A., Saffrich, R., Markovic, I., Walther, P. and Gerdes, H. H. (2004) 'Nanotubular

Highways for Intercellular Organelle Transport', *Science*, 303(5660), pp. 1007–1010.

Sánchez, C. A., Andahur, E. I., Valenzuela, R., Castellón, E. A., Fullá, J. A., Ramos, C. G. and Triviño, J. C. (2016) 'Exosomes from bulk and stem cells from human prostate cancer have a differential microRNA content that contributes cooperatively over local and pre-metastatic niche.', *Oncotarget*, 7(4), pp. 3993–4008.

Sandvig, K., Pust, S., Skotland, T. and van Deurs, B. (2011) 'Clathrin-independent endocytosis: mechanisms and function.', *Current opinion in cell biology*, 23(4), pp. 413–20.

Sarbassov, D. D., Guertin, D. A., Ali, S. M. and Sabatini, D. M. (2005) 'Phosphorylation and regulation of Akt/PKB by the rictor-mTOR complex', *Science*, 307(5712), pp. 1098–1101.

Sato-Kuwabara, Y., Melo, S. A., Soares, F. A. and Calin, G. A. (2015) 'The fusion of two worlds: non-coding RNAs and extracellular vesicles--diagnostic and therapeutic implications (Review).', *International journal of oncology*, 46(1), pp. 17–27.

Saxton, R. A. and Sabatini, D. M. (2017) 'mTOR Signaling in Growth, Metabolism, and Disease', *Cell*. Cell Press, pp. 960–976.

Schäfer, M. and Werner, S. (2008) 'Cancer as an overhealing wound: an old hypothesis revisited.', *Nature reviews. Molecular cell biology*, 9(8), pp. 628–38.

Schatz, G. and Dobberstein, B. (1996) 'Common principles of protein translocation across membranes', *Science*. American Association for the Advancement of Science, 271(5255), pp. 1519–1526.

Schey, K. L., Luther, J. M. and Rose, K. L. (2015) 'Proteomics characterization of exosome cargo.', *Methods (San Diego, Calif.)*, 87, pp. 75–82.

Schmidt, A., Forne, I. and Imhof, A. (2014) 'Bioinformatic analysis of proteomics data.', *BMC systems biology*, 8 Suppl 2, p. S3.

Sen, B., Xie, Z., Case, N., Thompson, W. R., Uzer, G., Styner, M. and Rubin, J. (2014) 'MTORC2 regulates mechanically induced cytoskeletal reorganization and lineage selection in marrow-derived mesenchymal stem cells', *Journal of Bone and Mineral Research*, 29(1),

pp. 78–89.

Shafiei, M. S. and Rockey, D. C. (2012) 'The function of integrin-linked kinase in normal and activated stellate cells: Implications for fibrogenesis in wound healing', *Laboratory Investigation*, 92(2), pp. 305–316.

Sharma, S., Rasool, H. I., Palanisamy, V., Mathisen, C., Schmidt, M., Wong, D. T. and Gimzewski, J. K. (2010) 'Structural-mechanical characterization of nanoparticle exosomes in human saliva, using correlative AFM, FESEM, and force spectroscopy.', *ACS nano*, 4(4), pp. 1921–6.

Shelke, G. V., Lässer, C., Gho, Y. S. and Lötvall, J. (2014) 'Importance of exosome depletion protocols to eliminate functional and RNA-containing extracellular vesicles from fetal bovine serum.', *Journal of extracellular vesicles*, 3.

Sherman, M. H., Yu, R. T., Engle, D. D., Ding, N., Atkins, A. R., Tiriac, H., Collisson, E. A., Connor, F., Van Dyke, T., Kozlov, S., Martin, P., Tseng, T. W., Dawson, D. W., Donahue, T. R., Masamune, A., Shimosegawa, T., Apte, M. V., Wilson, J. S., Ng, B., Lau, S. L., Gunton, J. E., Wahl, G. M., Hunter, T., Drebin, J. A., O'Dwyer, P. J., Liddle, C., Tuveson, D. A., Downes, M. and Evans, R. M. (2014) 'Vitamin D receptor-mediated stromal reprogramming suppresses pancreatitis and enhances pancreatic cancer therapy', *Cell*. Cell Press, 159(1), pp. 80–93.

Shi, Z. and Rockey, D. C. (2010) 'Interferon-gamma-mediated inhibition of serum response factor-dependent smooth muscle-specific gene expression.', *The Journal of biological chemistry*, 285(42), pp. 32415–24.

Shields, C. L., Kaliki, S., Shah, S. U., Luo, W., Furuta, M. and Shields, J. A. (2012) 'Iris melanoma: Features and prognosis in 317 children and adults', *Journal of AAPOS*, 16(1), pp. 10–16.

Shoushtari, A. N. and Carvajal, R. D. (2014) 'GNAQ and GNA11 mutations in uveal melanoma.', *Melanoma research*. Lippincott Williams and Wilkins, 24(6), pp. 525–34.

Simons, M. and Raposo, G. (2009) 'Exosomes--vesicular carriers for intercellular

communication', *Curr Opin Cell Biol*, 21(4), pp. 575–581.

Simpson, E. R., Gallie, B., Laperrierre, N., Beiki-Ardakani, A., Kivelä, T., Raivio, V., Heikkonen, J., Desjardins, L., Dendale, R., Mazal, A., Bornfeld, N., Sauerwein, W., Flüehs, D., Brualla, L., Honavar, S. G., Reddy, V. A., Suzuki, S., Murakami, N., Saakyan, S., Valskiy, V., Amiryan, A., Seregard, S., All-Eriksson, C., Hjelmqvist, L., Lundell, G., Sinclair, G., Lundell, M., Damato, B., Errington, R. D., Mayles, P., Mayles, H., Bergstrom, C., Grossniklaus, H., Crocker, I., Butker, E., Wilson, M., Haik, B., Geischen, H., Patra, P., Duker, J., Mignano, J., Rivard, M., Finger, P. T., Semenova, E., Choi, W. and Kalach, N. I. (2014) 'The American Brachytherapy Society consensus guidelines for plaque brachytherapy of uveal melanoma and retinoblastoma', *Brachytherapy*. Elsevier Inc., 13(1), pp. 1–14.

Simpson, R. J., Lim, J. W., Moritz, R. L. and Mathivanan, S. (2009) 'Exosomes: proteomic insights and diagnostic potential.', *Expert review of proteomics*, 6(3), pp. 267–83.

Singh, A. D., Turell, M. E. and Topham, A. K. (2011) 'Uveal melanoma: Trends in incidence, treatment, and survival', *Ophthalmology*, 118(9), pp. 1881–1885.

Singh, M., Durairaj, P. and Yeung, J. (2018) 'Uveal Melanoma: A Review of the Literature', *Oncology and Therapy*. Springer Science and Business Media LLC, 6(1), pp. 87–104.

Sisley, K., Rennie, I. G., Andrew Parsons, M., Jacques, R., Hammond, D. W., Bell, S. M., Potter, A. M. and Rees, R. C. (1997) 'Abnormalities of chromosomes 3 and 8 in posterior uveal melanoma correlate with prognosis', *Genes Chromosomes and Cancer*, 19(1), pp. 22–28.

Sódar, B. W., Kittel, Á., Pálóczi, K., Vukman, K. V., Osteikoetxea, X., Szabó-Taylor, K., Németh, A., Sperlágh, B., Baranyai, T., Giricz, Z., Wiener, Z., Turiák, L., Drahos, L., Pállinger, É., Vékey, K., Ferdinandy, P., Falus, A. and Buzás, E. I. (2016) 'Low-density lipoprotein mimics blood plasma-derived exosomes and microvesicles during isolation and detection', *Scientific Reports*. Nature Publishing Group, 6.

Song, H., Wang, L., Lyu, J., Wu, Y., Guo, W. and Ren, G. (2017) 'Loss of nuclear BAP1

expression is associated with poor prognosis in oral mucosal melanoma.', *Oncotarget*, 8(17), pp. 29080–29090.

Song, Y., Luo, Q., Long, H., Hu, Z., Que, T., Zhang, X., Li, Z., Wang, G., Yi, L., Liu, Z., Fang, W. Y. and Qi, S. (2014) 'Alpha-enolase as a potential cancer prognostic marker promotes cell growth, migration, and invasion in glioma', *Molecular Cancer*. BioMed Central Ltd., 13(1).

Sørensen, R. B., Junker, N., Kirkin, A., Voigt, H., Svane, I. M., Becker, J. C., Thor Straten, P. and Andersen, M. H. (2009) 'The immunodominant HLA-A2-restricted MART-1 epitope is not presented on the surface of many melanoma cell lines', *Cancer Immunology, Immunotherapy*, 58(5), pp. 665–675.

de Sousa Abreu, R., Penalva, L. O., Marcotte, E. M. and Vogel, C. (2009) 'Global signatures of protein and mRNA expression levels.', *Molecular bioSystems*, 5(12), pp. 1512–26.

Sporn, M. B. and Todaro, G. J. (1980) 'Autocrine secretion and malignant transformation of cells.', *The New England journal of medicine*, 303(15), pp. 878–80.

Srivastava, R. K., Li, C., Khan, J., Banerjee, N. S., Chow, L. T. and Athar, M. (2019) 'Combined mTORC1/mTORC2 inhibition blocks growth and induces catastrophic macropinocytosis in cancer cells', *Proceedings of the National Academy of Sciences*, p. 201911393.

Struckhoff, A. P., Rana, M. K. and Worthylake, R. A. (2011) 'RhoA can lead the way in tumor cell invasion and metastasis.', *Frontiers in bioscience (Landmark edition)*, 16, pp. 1915–26.

Su, K. H. and Dai, C. (2017) 'mTORC1 senses stresses: Coupling stress to proteostasis', *BioEssays*. John Wiley and Sons Inc.

Supek, F., Bošnjak, M., Škunca, N. and Šmuc, T. (2011) 'REVIGO summarizes and visualizes long lists of gene ontology terms.', *PloS one*, 6(7), p. e21800.

Surman, M., Hoja-łukowicz, D., Szwed, S., Kędracka-Krok, S., Jankowska, U., Kurtyka, M., Drożdż, A., Lityńska, A., Stępień, E. and Przybyło, M. (2019) 'An insight into the proteome of uveal melanoma-derived ectosomes reveals the presence of potentially useful biomarkers', *International Journal of Molecular Sciences*. MDPI AG, 20(15).

Swan, A. L., Mobasheri, A., Allaway, D., Liddell, S. and Bacardit, J. (2013) 'Application of machine learning to proteomics data: classification and biomarker identification in postgenomics biology.', *Omics : a journal of integrative biology*, 17(12), pp. 595–610.

Szalai, E., Wells, J. R., Ward, L. and Grossniklaus, H. E. (2018) 'Uveal Melanoma Nuclear BRCA1-Associated Protein-1 Immunoreactivity Is an Indicator of Metastasis.', *Ophthalmology*, 125(2), pp. 203–209.

Szatanek, R., Baj-Krzyworzeka, M., Zimoch, J., Lekka, M., Siedlar, M. and Baran, J. (2017) 'The Methods of Choice for Extracellular Vesicles (EVs) Characterization.', *International journal of molecular sciences*, 18(6).

Szklarczyk, D., Morris, J. H., Cook, H., Kuhn, M., Wyder, S., Simonovic, M., Santos, A., Doncheva, N. T., Roth, A., Bork, P., Jensen, L. J. and von Mering, C. (2017) 'The STRING database in 2017: quality-controlled protein–protein association networks, made broadly accessible', *Nucleic Acids Research*, 45(D1), pp. D362–D368.

Tadeo, I., Berbegall, A. P., Castel, V., García-Miguel, P., Callaghan, R., Påhlman, S., Navarro, S. and Noguera, R. (2016) 'Extracellular matrix composition defines an ultra-high-risk group of neuroblastoma within the high-risk patient cohort.', *British journal of cancer*, 115(4), pp. 480–9.

Tanaka, H. Y. and Kano, M. R. (2018) 'Stromal barriers to nanomedicine penetration in the pancreatic tumor microenvironment.', *Cancer science*, 109(7), pp. 2085–2092.

Tang, Y.-T., Huang, Y.-Y., Zheng, L., Qin, S.-H., Xu, X.-P., An, T.-X., Xu, Y., Wu, Y.-S., Hu, X.-M., Ping, B.-H. and Wang, Q. (2017) 'Comparison of isolation methods of exosomes and exosomal RNA from cell culture medium and serum.', *International journal of molecular medicine*, 40(3), pp. 834–844.

Tauro, B. J., Greening, D. W., Mathias, R. A., Ji, H., Mathivanan, S., Scott, A. M. and Simpson, R. J. (2012) 'Comparison of ultracentrifugation, density gradient separation, and immunoaffinity capture methods for isolating human colon cancer cell line LIM1863-

derived exosomes.', *Methods (San Diego, Calif.)*, 56(2), pp. 293–304.

Taylor, D. D., Zacharias, W. and Gercel-Taylor, C. (2011) 'Exosome isolation for proteomic analyses and RNA profiling', *Methods in Molecular Biology*, 728, pp. 235–246.

Taylor, J. and Bebawy, M. (2019) 'Proteins Regulating Microvesicle Biogenesis and Multidrug Resistance in Cancer.', *Proteomics*, 19(1–2), p. e1800165.

Taylor, R. C., Cullen, S. P. and Martin, S. J. (2008) 'Apoptosis: Controlled demolition at the cellular level', *Nature Reviews Molecular Cell Biology*, pp. 231–241.

Théry, C., Amigorena, S., Raposo, G. and Clayton, A. (2006) 'Isolation and Characterization of Exosomes from Cell Culture Supernatants and Biological Fluids', *Current Protocols in Cell Biology*. Wiley, 30(1), pp. 3.22.1-3.22.29.

Théry, C., Zitvogel, L. and Amigorena, S. (2002) 'Exosomes: Composition, biogenesis and function', *Nature Reviews Immunology*. European Association for Cardio-Thoracic Surgery, pp. 569–579.

Thippabhotla, S., Zhong, C. and He, M. (2019) '3D cell culture stimulates the secretion of in vivo like extracellular vesicles', *Scientific Reports*. Nature Publishing Group, 9(1).

Thoen, L. F. R., Guimarães, E. L. M., Dollé, L., Mannaerts, I., Najimi, M., Sokal, E. and Van Grunsven, L. A. (2011) 'A role for autophagy during hepatic stellate cell activation', *Journal of Hepatology*, 55(6), pp. 1353–1360.

Tjalsma, H., Bolhuis, A., Jongbloed, J. D. H., Bron, S. and van Dijl, J. M. (2000) 'Signal Peptide-Dependent Protein Transport in Bacillus subtilis: a Genome-Based Survey of the Secretome', *Microbiology and Molecular Biology Reviews*. American Society for Microbiology, 64(3), pp. 515–547.

Tominaga, N., Hagiwara, K., Kosaka, N., Honma, K., Nakagama, H. and Ochiya, T. (2014) 'RPN2-mediated glycosylation of tetraspanin CD63 regulates breast cancer cell malignancy', *Molecular Cancer*, 13(1), p. 134.

Torsvik, A., Stieber, D., Enger, P. O., Golebiewska, A., Molven, A., Svendsen, A., Westermark,

B., Niclou, S. P., Olsen, T. K., Chekenya Enger, M. and Bjerkvig, R. (2014) 'U-251 revisited: Genetic drift and phenotypic consequences of long-term cultures of glioblastoma cells', *Cancer Medicine*. Blackwell Publishing Ltd, 3(4), pp. 812–824.

Trams, E. G., Lauter, C. J., Norman Salem, J. and Heine, U. (1981) 'Exfoliation of membrane ecto-enzymes in the form of micro-vesicles', *BBA - Biomembranes*, 645(1), pp. 63–70.

Tricarico, C., Clancy, J. and D'Souza-Schorey, C. (2017) 'Biology and biogenesis of shed microvesicles.', *Small GTPases*, 8(4), pp. 220–232.

Tschentscher, F., Prescher, G., Zeschnigk, M., Horsthemke, B. and Lohmann, D. R. (2000) 'Identification of chromosomes 3, 6, and 8 aberrations in uveal melanoma by microsatellite analysis in comparison to comparative genomic hybridization', *Cancer Genetics and Cytogenetics*, 122(1), pp. 13–17.

Tsuchida, T. and Friedman, S. L. (2017) 'Mechanisms of hepatic stellate cell activation', *Nature Reviews Gastroenterology and Hepatology*. Nature Publishing Group, pp. 397–411.

Tucher, C., Bode, K., Schiller, P., Claßen, L., Birr, C., Souto-Carneiro, M. M., Blank, N., Lorenz, H.-M. and Schiller, M. (2018) 'Extracellular Vesicle Subtypes Released From Activated or Apoptotic T-Lymphocytes Carry a Specific and Stimulus-Dependent Protein Cargo.', *Frontiers in immunology*. Frontiers Media S.A., 9(MAR), p. 534.

Turchinovich, A., Drapkina, O. and Tonevitsky, A. (2019) 'Transcriptome of extracellular vesicles: State-of-the-art', *Frontiers in Immunology*. Frontiers Media S.A., 10(FEB).

Turner, C. E. (2000) 'Paxillin and focal adhesion signalling', *Nature Cell Biology*.

Ulianich, L., Garbi, C., Treglia, A. S., Punzi, D., Miele, C., Raciti, G. A., Beguinot, F., Consiglio, E. and Di Jeso, B. (2008) 'ER stress is associated with dedifferentiation and an epithelial-to-mesenchymal transition-like phenotype in PC C13 thyroid cells', *Journal of Cell Science*. Company of Biologists Ltd, 121(4), pp. 477–486.

Väisänen, A., Kallioinen, M., von Dickhoff, K., Laatikainen, L., Höyhtyä, M. and Turpeenniemi-Hujanen, T. (1999) 'Matrix metalloproteinase-2 (MMP-2) immunoreactive

protein--a new prognostic marker in uveal melanoma?', *The Journal of pathology*, 188(1), pp. 56–62.

Valadi, H., Ekström, K., Bossios, A., Sjöstrand, M., Lee, J. J. and Lötvall, J. O. (2007) 'Exosome-mediated transfer of mRNAs and microRNAs is a novel mechanism of genetic exchange between cells', *Nature Cell Biology*, 9(6), pp. 654–659.

Valvezan, A. J., Turner, M., Belaid, A., Lam, H. C., Miller, S. K., McNamara, M. C., Baglini, C., Housden, B. E., Perrimon, N., Kwiatkowski, D. J., Asara, J. M., Henske, E. P. and Manning, B. D. (2017) 'mTORC1 Couples Nucleotide Synthesis to Nucleotide Demand Resulting in a Targetable Metabolic Vulnerability.', *Cancer cell*, 32(5), pp. 624-638.e5.

Valyi-Nagy, K., Kormos, B., Ali, M., Shukla, D. and Valyi-Nagy, T. (2012) 'Stem cell marker CD271 is expressed by vasculogenic mimicryforming uveal melanoma cells in three-dimensional cultures', *Molecular Vision*, 18, pp. 588–592.

La Vecchia, C., Negri, E., Cavalieri d'Oro, L. and Franceschi, S. (1998) 'Liver cirrhosis and the risk of primary liver cancer.', *European journal of cancer prevention : the official journal of the European Cancer Prevention Organisation (ECP)*, 7(4), pp. 315–20.

Vidal-Vanaclocha, F. (2008) 'The prometastatic microenvironment of the liver.', *Cancer microenvironment : official journal of the International Cancer Microenvironment Society*, 1(1), pp. 113–29.

Vidulescu, C., Clejan, S. and O'Connor, K. C. (2004) 'Vesicle traffic through intercellular bridges in DU 145 human prostate cancer cells', *Journal of Cellular and Molecular Medicine*. Journal of Cellular and Molecular Medicine, 8(3), pp. 388–396.

Villarreal, L., Méndez, O., Salvans, C., Gregori, J., Baselga, J. and Villanueva, J. (2013) 'Unconventional secretion is a major contributor of cancer cell line secretomes.', *Molecular & cellular proteomics : MCP*, 12(5), pp. 1046–60.

Villarroya-Beltri, C., Gutiérrez-Vázquez, C., Sánchez-Cabo, F., Pérez-Hernández, D., Vázquez, J., Martin-Cofreces, N., Martinez-Herrera, D. J., Pascual-Montano, A., Mittelbrunn, M. and

Sánchez-Madrid, F. (2013) ‘Sumoylated hnRNPA2B1 controls the sorting of miRNAs into exosomes through binding to speVillarroya-Beltri, C., Gutiérrez-Vázquez, C., Sánchez-Cabo, F., Pérez-Hernández, D., Vázquez, J., Martin-Cofreces, N., … Sánchez-Madrid, F. (2013). Sumoylated hnRNPA2B’, *Nature communications*. Nature Publishing Group, 4, p. 2980.

De Visser, K. E., Eichten, A. and Coussens, L. M. (2006) ‘Paradoxical roles of the immune system during cancer development’, *Nature Reviews Cancer*, pp. 24–37.

Vogel, R., Willmott, G., Kozak, D., Roberts, G. S., Anderson, W., Groenewegen, L., Glossop, B., Barnett, A., Turner, A. and Trau, M. (2011) ‘Quantitative sizing of nano/microparticles with a tunable elastomeric pore sensor.’, *Analytical chemistry*, 83(9), pp. 3499–506.

Wang, L., Lawrence, M. S., Wan, Y., Stojanov, P., Sougnez, C., Stevenson, K., Werner, L., Sivachenko, A., DeLuca, D. S., Zhang, L., Zhang, W., Vartanov, A. R., Fernandes, S. M., Goldstein, N. R., Folco, E. G., Cibulskis, K., Tesar, B., Sievers, Q. L., Shefler, E., Gabriel, S., Hacohen, N., Reed, R., Meyerson, M., Golub, T. R., Lander, E. S., Neuberg, D., Brown, J. R., Getz, G. and Wu, C. J. (2011) ‘SF3B1 and other novel cancer genes in chronic lymphocytic leukemia.’, *The New England journal of medicine*, 365(26), pp. 2497–506.

Wang, L., Cao, L., Wang, H., Liu, B., Zhang, Q., Meng, Z., Wu, X., Zhou, Q. and Xu, K. (2017) ‘Cancer-associated fibroblasts enhance metastatic potential of lung cancer cells through IL-6/STAT3 signaling pathway’, *Oncotarget*. Impact Journals LLC, 8(44), pp. 76116–76128.

Wang, N., Song, Xingguo, Liu, L., Niu, L., Wang, X., Song, Xianrang and Xie, L. (2018) ‘Circulating exosomes contain protein biomarkers of metastatic non-small-cell lung cancer’, *Cancer Science*. Blackwell Publishing Ltd, 109(5), pp. 1701–1709.

Wang, S., Li, M., Xing, L. and Yu, J. (2019) ‘High expression level of peptidylprolyl isomerase A is correlated with poor prognosis of liver hepatocellular carcinoma’, *Oncology Letters*. Spandidos Publications, 18(5), pp. 4691–4702.

Wang, Xiaoxia, Jiang, W., Kang, J., Liu, Q. and Nie, M. (2015) ‘Knockdown of RhoA expression alters ovarian cancer biological behavior in vitro and in nude mice’, *Oncology*

Reports. Spandidos Publications, 34(2), pp. 891–899.

Wang, Xiaogang, Dong, H., Li, Q., Li, Y. and Hong, A. (2015) 'Thioredoxin induces Tregs to generate an immunotolerant tumor microenvironment in metastatic melanoma.', *Oncoimmunology*, 4(9), p. e1027471.

Wang, Y., Bao, X., Zhang, Z., Sun, Y. and Zhou, X. (2017) 'FGF2 promotes metastasis of uveal melanoma cells via store-operated calcium entry', *OncoTargets and Therapy*. Dove Medical Press Ltd., 10, pp. 5317–5328.

Weber, A., Hengge, U. R., Urbanik, D., Markwart, A., Mirmohammadsaegh, A., Reichel, M. B., Wittekind, C., Wiedemann, P. and Tannapfel, A. (2003) 'Absence of Mutations of the BRAF Gene and Constitutive Activation of Extracellular-Regulated Kinase in Malignant Melanomas of the Uvea', *Laboratory Investigation*, 83(12), pp. 1771–1776.

Welinder, C., Pawøowski, K., Szasz, A. M., Yakovleva, M., Sugihara, Y., Malm, J., Jönsson, G., Ingvar, C., Lundgren, L., Baldetorp, B., Olsson, H., Rezeli, M., Laurell, T., Wieslander, E. and Marko-Varga, G. (2017) 'Correlation of histopathologic characteristics to protein expression and function in malignant melanoma', *PLoS ONE*. Public Library of Science, 12(4).

Welton, J. L., Khanna, S., Giles, P. J., Brennan, P., Brewis, I. A., Staffurth, J., Mason, M. D. and Clayton, A. (2010) 'Proteomics analysis of bladder cancer exosomes.', *Molecular & cellular proteomics : MCP*, 9(6), pp. 1324–38.

Werfel, T. A., Wang, S., Jackson, M. A., Kavanaugh, T. E., Joly, M. M., Lee, L. H., Hicks, D. J., Sanchez, V., Ericsson, P. G., Kilchrist, K. V., Dimobi, S. C., Sarett, S. M., Brantley-Sieders, D. M., Cook, R. S. and Duvall, C. L. (2018) 'Selective mTORC2 inhibitor therapeutically blocks breast cancer cell growth and survival', *Cancer Research*. American Association for Cancer Research Inc., 78(7), pp. 1845–1858.

De Wever, O. and Mareel, M. (2003) 'Role of tissue stroma in cancer cell invasion.', *The Journal of pathology*, 200(4), pp. 429–47.

Whatcott, C. J., Diep, C. H., Jiang, P., Watanabe, A., LoBello, J., Sima, C., Hostetter, G.,

Shepard, H. M., Von Hoff, D. D. and Han, H. (2015) 'Desmoplasia in Primary Tumors and Metastatic Lesions of Pancreatic Cancer.', *Clinical cancer research : an official journal of the American Association for Cancer Research*, 21(15), pp. 3561–8.

White, J. S., Becker, R. L., McLean, I. W., Director-Myska, A. E. and Nath, J. (2006) 'Molecular cytogenetic evaluation of 10 uveal melanoma cell lines', *Cancer Genetics and Cytogenetics*, 168(1), pp. 11–21.

Whiteside, T. L. (2016) 'Tumor-Derived Exosomes and Their Role in Cancer Progression', in *Advances in Clinical Chemistry*. Academic Press Inc., pp. 103–141.

Williams, D. B. (2006) 'Beyond lectins: The calnexin/calreticulin chaperone system of the endoplasmic reticulum', *Journal of Cell Science*, pp. 615–623.

Willms, E., Cabañas, C., Mäger, I., Wood, M. J. A. and Vader, P. (2018) 'Extracellular vesicle heterogeneity: Subpopulations, isolation techniques, and diverse functions in cancer progression', *Frontiers in Immunology*. Frontiers Media S.A.

Wöll, E., Bedikian, A. and Legha, S. S. (1999) 'Uveal melanoma: natural history and treatment options for metastatic disease.', *Melanoma research*, 9(6), pp. 575–81.

Woodcock, H. V., Eley, J. D., Guillotin, D., Platé, M., Nanthakumar, C. B., Martufi, M., Peace, S., Joberty, G., Poeckel, D., Good, R. B., Taylor, A. R., Zinn, N., Redding, M., Forty, E. J., Hynds, R. E., Swanton, C., Karsdal, M., Maher, T. M., Bergamini, G., Marshall, R. P., Blanchard, A. D., Mercer, P. F. and Chambers, R. C. (2019) 'The mTORC1/4E-BP1 axis represents a critical signaling node during fibrogenesis', *Nature Communications*. Nature Publishing Group, 10(1).

Woodward, J. K. L., Rennie, I. G., Elshaw, S. R., Burn, J. L. and Sisley, K. (2005) 'Invasive and noninvasive uveal melanomas have different adhesive properties', *Eye*. Nature Publishing Group, 19(3), pp. 342–348.

Worley, L. A., Long, M. D., Onken, M. D. and Harbour, J. W. (2008) 'Micro-RNAs associated with metastasis in uveal melanoma identified by multiplexed microarray profiling',

Melanoma Research, 18(3), pp. 184–190.

Wynn, T. A. (2008) 'Cellular and molecular mechanisms of fibrosis', *Journal of Pathology*, pp. 199–210.

Xu, L., Hui, A. Y., Albanis, E., Arthur, M. J., O'Byrne, S. M., Blaner, W. S., Mukherjee, P., Friedman, S. L. and Eng, F. J. (2005) 'Human hepatic stellate cell lines, LX-1 and LX-2: New tools for analysis of hepatic fibrosis', *Gut*, 54(1), pp. 142–151.

Xu, R., Greening, D. W., Zhu, H. J., Takahashi, N. and Simpson, R. J. (2016) 'Extracellular vesicle isolation and characterization: Toward clinical application', *Journal of Clinical Investigation*. American Society for Clinical Investigation, pp. 1152–1162.

Yadav, L., Puri, N., Rastogi, V., Satpute, P. and Sharma, V. (2015) 'Tumour Angiogenesis and Angiogenic Inhibitors: A Review.', *Journal of clinical and diagnostic research : JCDR*, 9(6), pp. XE01–XE05.

Yamada, K. M., Pankov, R. and Cukierman, E. (2003) 'Dimensions and dynamics in integrin function', *Brazilian Journal of Medical and Biological Research*. Associacao Brasileira de Divulgacao Cientifica, pp. 959–966.

Yamasaki, S., Yagishita, N., Nishioka, K. and Nakajima, T. (2007) 'The roles of synoviolin in crosstalk between endoplasmic reticulum stress-induced apoptosis and p53 pathway', *Cell Cycle*. Taylor and Francis Inc., pp. 1319–1323.

Yan, G., Zou, R., Chen, Z., Fan, B., Wang, Z., Wang, Y., Yin, X., Zhang, D., Tong, L., Yang, F., Jiang, W., Fu, W., Bergo, M. O., Dalin, M., Zheng, J., Chen, S. and Zhou, J. (2014) 'Silencing RhoA inhibits migration and invasion through Wnt/β-catenin pathway and growth through cell cycle regulation in human tongue cancer', *Acta Biochimica et Biophysica Sinica*. Oxford University Press, 46(8), pp. 682–690.

Yan, Z., Liu, J., Xie, L., Liu, X. and Zeng, Y. (2016) 'Role of heparan sulfate in mediating CXCL8-induced endothelial cell migration', *PeerJ*. PeerJ Inc., 2016(2).

Yáñez-Mó, M., Siljander, P. R.-M., Andreu, Z., Bedina Zavec, A., Borràs, F. E., De Wever, O.,

et al. (2015) 'Biological properties of extracellular vesicles and their physiological functions', *Journal of Extracellular Vesicles*, 4(1), p. 27066.

Yang, L., Wu, X.-H., Wang, D., Luo, C.-L. and Chen, L.-X. (2013) 'Bladder cancer cell-derived exosomes inhibit tumor cell apoptosis and induce cell proliferation in vitro.', *Molecular medicine reports*, 8(4), pp. 1272–8.

Yang, W., Arii, S., Gorrin-Rivas, M. J., Mori, A., Onodera, H. and Imamura, M. (2001) 'Human macrophage metalloelastase gene expression in colorectal carcinoma and its clinicopathologic significance.', *Cancer*, 91(7), pp. 1277–83.

Yang, X., Li, Y., Zou, L. and Zhu, Z. (2019) 'Role of Exosomes in Crosstalk Between Cancer-Associated Fibroblasts and Cancer Cells', *Frontiers in Oncology*, 9.

Yavuzyigitoglu, S., Koopmans, A. E., Verdijk, R. M., Vaarwater, J., Eussen, B., van Bodegom, A., Paridaens, D., Kiliç, E., de Klein, A. and Rotterdam Ocular Melanoma Study Group (2016) 'Uveal Melanomas with SF3B1 Mutations: A Distinct Subclass Associated with Late-Onset Metastases.', *Ophthalmology*, 123(5), pp. 1118–28.

Yoshioka, Y., Konishi, Y., Kosaka, N., Katsuda, T., Kato, T. and Ochiya, T. (2013) 'Comparative marker analysis of extracellular vesicles in different human cancer types', *Journal of Extracellular Vesicles*, 2(1), p. 20424.

Youngblood, V. M., Kim, L. C., Edwards, D. N., Hwang, Y., Santapuram, P. R., Stirdivant, S. M., Lu, P., Ye, F., Brantley-Sieders, D. M. and Chen, J. (2016) 'The ephrin-A1/EPHA2 signaling axis regulates glutamine metabolism in HER2-positive breast cancer', *Cancer Research*. American Association for Cancer Research Inc., 76(7), pp. 1825–1836.

Yuana, Y., Levels, J., Grootemaat, A., Sturk, A. and Nieuwland, R. (2014) 'Co-isolation of extracellular vesicles and high-density lipoproteins using density gradient ultracentrifugation', *Journal of Extracellular Vesicles*. Co-Action Publishing, 3(1).

Zhang, H. G., Kim, H., Liu, C., Yu, S., Wang, J., Grizzle, W. E., Kimberly, R. P. and Barnes, S. (2007) 'Curcumin reverses breast tumor exosomes mediated immune suppression of NK

cell tumor cytotoxicity', *Biochimica et Biophysica Acta - Molecular Cell Research*, 1773(7), pp. 1116–1123.

Zhang, H. J., Yao, D. F., Yao, M., Huang, H., Wang, L., Yan, M. J., Yan, X. Di, Gu, X., Wu, W. and Lu, S. L. (2013) 'Annexin A2 silencing inhibits invasion, migration, and tumorigenic potential of hepatoma cells', *World Journal of Gastroenterology*, 19(24), pp. 3792–3801.

Zhang, J., Hawari, F. I., Shamburek, R. D., Adamik, B., Kaler, M., Islam, A., Liao, D.-W., Rouhani, F. N., Ingham, M. and Levine, S. J. (2008) 'Circulating TNFR1 exosome-like vesicles partition with the LDL fraction of human plasma.', *Biochemical and biophysical research communications*, 366(2), pp. 579–84.

Zhang, Y., Song, H., Guo, T., Zhu, Y., Tang, H., Qi, Z., Zhao, P. and Zhao, S. (2016) 'Overexpression of Annexin II Receptor-Induced Autophagy Protects Against Apoptosis in Uveal Melanoma Cells', *Cancer Biotherapy and Radiopharmaceuticals*. Mary Ann Liebert Inc., 31(4), pp. 145–151.

Zhang, Y., Liu, Y., Liu, H. and Tang, W. H. (2019) 'Exosomes: Biogenesis, biologic function and clinical potential', *Cell and Bioscience*. BioMed Central Ltd.

Zhang, Z., Zhu, S., Yang, Y., Ma, X. and Guo, S. (2015) 'Matrix metalloproteinase-12 expression is increased in cutaneous melanoma and associated with tumor aggressiveness', *Tumor Biology*. Springer Netherlands, 36(11), pp. 8593–8600.

Zhou, H., Yuen, P. S., Pisitkun, T., Gonzales, P. A., Yasuda, H., Dear, J. W., Gross, P., Knepper, M. A. and Star, R. A. (2006) 'Collection, storage, preservation, and normalization of human urinary exosomes for biomarker discovery', *Kidney Int*, 69(8), pp. 1471–1476.

Zou, Z., Chen, J., Liu, A., Zhou, X., Song, Q., Jia, C., Chen, Z., Lin, J., Yang, C., Li, M., Jiang, Y. and Bai, X. (2015) 'mTORC2 promotes cell survival through c-Myc-dependent up-regulation of E2F1.', *The Journal of cell biology*, 211(1), pp. 105–22.

Zuidervaart, W., van Nieuwpoort, F., Stark, M., Dijkman, R., Packer, L., Borgstein, A.-M., Pavey, S., van der Velden, P., Out, C., Jager, M. J., Hayward, N. K. and Gruis, N. A. (2005)

‘Activation of the MAPK pathway is a common event in uveal melanomas although it rarely occurs through mutation of BRAF or RAS.’, *British journal of cancer*, 92(11), pp. 2032–8.

Zuidervaart, W., Hensbergen, P. J., Wong, M. C., Deelder, A. M., Tensen, C. P., Jager, M. J. and Gruis, N. A. (2006) ‘Proteomic analysis of uveal melanoma reveals novel potential markers involved in tumor progression’, *Investigative Ophthalmology and Visual Science*, 47(3), pp. 786–793.

Zylbersztejn, K. and Galli, T. (2011) ‘Vesicular trafficking in cell navigation - role of SNAREs.’, *The FEBS journal*.